Hurricane Field Program
2016

2016 Hurricane Field Program Plan

Hurricane Research Division
National Oceanographic and Atmospheric Administration
Atlantic Oceanographic and Meteorological Laboratory
4301 Rickenbacker Causeway
Miami, FL 33149

Prepared by:

Robert Rogers, Sim Aberson, Altug Aksoy, Ghassan Alaka, Robert Black, Lisa Bucci, Hua Chen, Hui Christophersen, Joe Cione, Peter Dodge, Jason Dunion, John Gamache, Evan Kalina, John Kaplan, Brad Klotz, Frank Marks, Shirley Murillo, Paul Reasor, Kelly Ryan, Jun Zhang, Mark Bourassa, Luca Centurioni, Paul Chang, Klaus Dolling, Dave Emmitt, Chris Fairall, Gustavo Goni, George Halliwell, Heather Holbach, Rick Lumpkin, Michael Riemer, Nick Shay, and Jon Zawislak
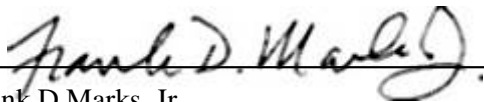
13 May 2016

Frank D Marks, Jr   Date
Director, Hurricane Research Division

TABLE OF CONTENTS

2016 HURRICANE FIELD PROGRAM PLAN

INTRODUCTION

National Oceanic and Atmospheric Administration Atlantic Oceanographic and Meteorological Laboratory
Hurricane Research Division
Miami, Florida. USA

1. Description of Intensity Forecasting Experiment (IFEX)

One of the key activities in the NOAA Strategic Plan Mission Goal 3 (Reduce Society's Risks from Weather and Water Impacts) is to improve the understanding and prediction of tropical cyclones (TCs). The National Centers for Environmental Prediction (NCEP) National Hurricane Center (NHC) is responsible for forecasting TCs in the Atlantic and East Pacific basins, while the Environmental Modeling Center (EMC) provides NWP guidance for the forecasters. Together they have made great strides in improving forecasts of TC track. With support from the research community, forecast errors of TC track have decreased by about 50% over the past 30 years. However, there has been much less improvement in forecasts of TC intensity, structure, and rainfall. This lack of improvement is largely the result of deficiencies in routinely collecting inner-core data and assimilating it into the modeling system, limitations in the numerical models themselves, and gaps in understanding of the physics of TCs and their interaction with the environment. Accurate forecasts will rely heavily on the use of improved numerical modeling systems, which in turn will rely on accurate observational datasets for assimilation and validation.

The operational Hurricane Weather Research and Forecasting (HWRF) model is run at 2 km grid length using an assortment of physical parameterizations intended to represent subgrid-scale processes important in TC evolution. Such a modeling system holds the potential of improving understanding and forecasting of TC track, intensity, structure, and rainfall. In order to realize such improvements, however, new data assimilation techniques must be developed and refined, physical parameterizations must be improved and adapted for TC environments, and the models must be reliably evaluated against detailed observations from a variety of TCs and their surrounding environments.

To conduct the research necessary to address the issues raised above, since 2005 NOAA has been conducting an experiment designed to improve operational forecasts of TC intensity, called the Intensity Forecasting EXperiment (IFEX; Rogers et al., BAMS, 2006, 2013). The IFEX goals, developed through a partnership involving the NOAA Hurricane Research Division (HRD), NHC, and EMC, are to improve operational forecasts of TC intensity, structure, and rainfall by providing data to improve the operational numerical modeling system (i.e., HWRF) and by improving understanding of the relevant physical processes. These goals will be accomplished by satisfying a set of requirements and recommendations guiding the collection of the data:

- **Goal 1**: Collect observations that span the TC life cycle in a variety of environments for model initialization and evaluation;
- **Goal 2**: Develop and refine measurement technologies that provide improved real-time monitoring of TC intensity, structure, and environment;
- **Goal 3**: Improve understanding of the physical processes important in intensity change for a TC at all stages of its lifecycle.

A unique, and critical, aspect of IFEX is the focus on providing measurements of TCs at all stages of their life cycle. The focus of hurricane research flights during the past 30 years has been on mature storms, leading to a dataset biased toward these types of systems. The strategy of observing the entire life cycle of a TC is new and unique, and will provide invaluable information, particularly in sparsely observed environments.

2. Experiment and module summaries

The field program aircraft missions presented in this document are separated into three distinct sections, corresponding to the primary IFEX goal being addressed (note that most experiments address multiple IFEX goals). The flight patterns that comprise these research and operational missions address various aspects of the TC lifecycle, and they all specifically address the main goals of IFEX. A detailed description of each research or operational mission follows, including clarification of the scientific objectives and details of the associated flight patterns.

In this document, reference is made to either "experiments" or "modules." For this discussion, "experiments" refer to missions in which research scientists (i.e., from HRD) set the flight pattern for the duration of the mission. Operational needs take priority in this scenario. "Modules" refer to short patterns that can be flown as a part of a larger experiment (either operational- or research-oriented). Modules generally take 1 h or less for completion.

IFEX GOAL 1: *Collect observations that span the TC life cycle in a variety of environments for model initialization and evaluation*

(1) <u>P-3 Three-Dimensional Doppler Winds Experiment</u>: This is a multi-option, single-aircraft operational mission designed to use the NOAA P-3 to sample TCs ranging in intensity from tropical depression to major hurricane. The definition is intended to separate this category from tropical waves and disturbances that have yet to develop a well-defined warm-core circulation. The main goals of these missions are: 1) to improve understanding of the factors leading to TC intensity and structure changes, 2) to provide a comprehensive data set for the initialization (including data assimilation) and validation of numerical hurricane simulations (in particular HWRF), 3) to improve and evaluate technologies for observing TCs, and 4) to develop rapid real-time communication of these observations to NCEP.

(2) <u>G-IV Tail Doppler Radar Experiment:</u> This experiment uses the G-IV aircraft. The goals are to 1) to evaluate the G-IV as a platform for observing the cores of TCs, 2) to improve understanding of the factors leading to TC structure and intensity changes, 3) to provide a comprehensive data set for the initialization (including data assimilation) and validation of numerical hurricane simulations (in particular HWRF), and 4) to develop rapid real-time communication of these observations to NCEP.

IFEX GOAL 2: *Develop and refine measurement technologies that provide improved real-time monitoring of TC intensity, structure, and environment*

(3) <u>Doppler Wind Lidar (DWL) Experiment:</u> This is a multi-option, single-aircraft missions designed to use the DWL to sample dust and winds in dry air. The main objectives of the P-3 DWL Experiment are to: 1) sample winds in a TC with an asymmetric distribution of precipitation, where this is little or no precipitation on one side of the storm; 2) characterize the suspended Saharan dust and mid-level (~600-800 hPa) easterly jet that are associated with the Saharan Air Layer (SAL) with a particular focus on SAL-TC interactions; 3) sample the kinematic structure of the hurricane boundary layer with a focus on investigating the characteristics of the boundary layer height and coherent structures; 4) characterize the upper level subsidence and boundary layer kinematics within the region between two concentric eyewalls and/or within a rainband moat.

(4) <u>Small Unmanned Aerial Vehicle Experiment (SUAVE):</u> The primary objective of this experiment is to further demonstrate and utilize the unique capabilities of a low latitude UAS platform in order to better document areas of the tropical cyclone environment that would otherwise be either impossible or impractical to observe. In addition, inter-comparisons of these unique data with comparable output from NOAA's coupled operational modeling system will be explored.

(5) <u>NESDIS Ocean Winds and Rain Experiment:</u> This will be executed by NESDIS and aims to improve understanding of microwave scatterometer retrievals of the ocean surface wind and to test new remote sensing techniques. The NESDIS/Center for Satellite Research and Applications in conjunction with the University of Massachusetts (UMASS) Microwave Remote Sensing Laboratory and AOC have been conducting flights as part this experiment for the past several years. Collecting the raw data allows spectral processing to be done which will allow the rain and surface contributions in the AWRAP data to be decoupled. This is critical in understanding the impacts of rain on the measurements, and thus, the ocean surface wind vector retrievals.

(6) <u>SFMR High-Incidence Angle Measurements Module:</u> The objective of this module is to determine the relationship between the SFMR measured surface brightness temperature and the ocean surface wave field characteristics.

(7) <u>Offshore Wind Module</u>: This module is designed as a multi-agency (NOAA, Department of Energy, Department of the Interior) supplemental data collection effort to gather hurricane environmental information in the vicinity of proposed offshore wind farms.

IFEX GOAL 3: *Improve understanding of the physical processes important in intensity change for a TC at all stages of its lifecycle*

(8) <u>Easterly Wave Genesis Experiment:</u> This is a multi-option, multi-aircraft experiment that is designed to sample the conditions of the environment and the inner-core structure of disturbances associated with easterly waves in the central Atlantic This experiment can use the G-IV aircraft in conjunction with the P-3 and/or Global Hawk.

(9) <u>East Pacific Easterly Wave Genesis Experiment:</u> This is a multi-option, single aircraft (G-IV) experiment designed to examine the kinematic and thermodynamic structure of convection in the Panama Bight area and evolution of easterly waves and potential tropical cyclone development downstream in the Eastern Pacific basin.

(10) <u>Rapid Intensity Change Experiment (RAPX):</u> This multi-option, multi-aircraft experiment is designed to collect datasets that encompass multiple scales with the overarching goal of improving our ability to predict the timing and magnitude of RI events. The goal of the RAPX experiment is to employ NOAA aircraft to collect oceanic, kinematic, and thermodynamic observations both within the inner-core (i.e., radius < 220 km) and in the surrounding large-scale environment (i.e., 220 km < radius < 440 km) for systems that have the potential to undergo RI within ~96 h.

(11) <u>TC in Shear Experiment:</u> The objective of this multi-aircraft experiment is to sample the TC at distinct phases of its interaction with vertical wind shear, measuring the kinematic and thermodynamic fields with the azimuthal and radial coverage necessary to test structure and intensity change hypotheses motivated by recent theoretical and numerical studies.

(12) <u>TC Diurnal Cycle Experiment:</u> This multi-option, multi-aircraft experiment employs both NOAA P-3 and G-IV aircraft to collect kinematic and thermodynamic observations both within the inner-core (i.e., radius < 200 km) and in the surrounding large- scale environment (i.e., 200 km < radius < 600 km) for systems that have exhibited signs of diurnal pulsing in the previous 24 hours.

(13) <u>TC-Ocean Interaction Experiment:</u> This is a multi-option, single aircraft experiment designed to address questions regarding the general role of various upper-ocean processes on TC intensification. It consists of: i) Pre-storm and post-storm expendable probe surveys associated with TC passage; and ii) Support of upper ocean and air-sea flux measurements made by oceanic floats and drifters. Specifically,

one to three float and drifter arrays will be deployed into one or two mature storms by an AFRC C-130J and provide real-time ocean data, and, a NOAA P-3 will deploy dropwindsondes and make SFMR and Scanning Radar Altimeter (SRA) measurements within the float and drifter array as the storm passes over it.

(14) Tropical Cyclone Landfall Experiment: This is a multi-option, single-aircraft experiment designed to study the changes in TC surface wind structure near landfall. It has several modules that could also be incorporated into operational surveillance or reconnaissance missions. An accurate description of the TC surface wind field is important for warning, preparedness, and recovery efforts.

(15) Rapid Weakening Experiment: This is a single-option, mutti-aircraft experiment intended to sample the environmental and inner-core thermodynamic and kinematic structure of tropical cyclones leading up to and during rapid weakening.

(16) Convective Burst Module: This is a multi-option, single-aircraft module whose objective is to sample the wind, temperature, and moisture fields within and around an area of deep convection at high time frequency and to use them in high-resolution data assimilation experiments.

(17) Eye-eyewall Mixing Module: This single-aircraft module is designed to sample meso- and miso-vortices along the interface of the eye and eyewall, which are thought to impact the structure and intensity of tropical cyclones.

(18) Secondary Eyewall Formation/Eyewall Replacement Cycle Module: This multi-aircraft, multi-option module is designed to sample the kinematic and thermodynamic structure of rainbands outside the primary eyewall of mature hurricanes (generally category 2 or stronger) to determine precursor signals to secondary eyewall formation, and to sample these structures once a secondary eyewall has formed to document an eyewall replacement cycle.

(19) TC Warm Core Module: By using the Global Hawk, P3, and G-IV aircraft, this module aims to sample the thermodynamic structure and evolution of the warm core, an important aspect in understanding the physical mechanisms that govern tropical cyclone intensity.

(20) Hurricane Planetary Boundary Layer Module: This is a multi-option, single or multiple-aircraft experiment that is designed to measure both the mean and turbulent structure of the hurricane boundary layer. A combination of data sources from GPS sondes, AXBTs, high frequency turbulence sensors, Doppler Wind Lidar (DWL), on NOAA P3s and COYOTE unmanned aircraft are applied to determine the quantities listed in the above objectives. This experiment includes 3 modules: 1) stepped-descent module, 2) DWL boundary-layer module, 3) boundary layer inflow module.

(21) Saharan Air Layer Experiment (SALEX): Arc Cloud Module: This is a single-aircraft module, designed to investigate how the thermodynamics and kinematics in the environment surrounding a TC are modified when low to mid-level dry air interacts with convection in the TC periphery. Objectives include improving our understanding of how arc clouds and the processes leading to arc cloud formation relate to TC intensity change. Observations could be made using either the P-3 aircraft conducting another experiment, or the G- IV during a synoptic surveillance mission.

OPERATIONS

1. Locations
Starting on 01 June, the N43RF aircraft will be available with two flight crews available for back to back missions. The Gulfstream IV-SP (N49RF) aircraft will be available 01 June with two flight crews available for back to back missions. Operations for all aircraft will primarily base out of Tampa, Florida and deployments to U.S. coastal locations in the western Gulf of Mexico for suitable Gulf storms, as well as other locations along the U.S. East Coast, St. Croix, Barbados, Bermuda, and La Paz, Acapulco, and Tapachula, Mexico. Occasionally, post-mission recovery may be accomplished elsewhere.

2. Field Program Duration
The hurricane field research program will be conducted from 01 June through 31 October 2016.

3. Research Mission Operations
The decision and notification process for hurricane research missions is shown, in flow chart form, in Appendix A (Figs. A-1, A-2, and A-3). The names of those who receive primary notification at each decision or notification point are shown in Figs. A-1, A-2, and A-3, and are also listed in Appendix A. Contacts are also maintained each weekday among the directors of HRD, NHC, EMC, and AOC.

Research operations must consider that the research aircraft are required to be placed in the National Hurricane Operations Plan of the Day (POD) 24 h before a mission. If operational requirements are accepted, the research aircraft must follow the operational constraints described in Section 7.

4. Task Force Configuration
The NOAA P-3 aircraft, equipped as shown in Appendix G, will be available for research missions on a non-interference basis with tasked operational missions from 01 June to 31 October 2015. Also, the G-IV aircraft should be available, on a non-interference basis with tasked operational missions from 01 June to 31 October 2015.

5. Field Operations
5.1 Scientific Leadership Responsibilities
The implementation of the Hurricane Field Program Plan is the responsibility of the Field Program Director, who in turn, reports directly to the HRD director. In the event of deployment, the Field Program Director may assign a ground team manager to assume overall responsibility for essential ground support logistics, site communications, and site personnel who are not actively engaged in flight. Designated lead project scientists are responsible to the Field Program Director or designated assistants. While in flight, lead project scientists are in charge of the scientific aspects of the mission.

5.2 Aircraft Scientific Crews
Tables B-2.1 through B-2.4 (Appendix B) list the NOAA scientific crewmembers needed to conduct the experiments. Actual named assignments may be adjusted on a case-by-case basis. Operations will include completion of detailed records by each scientific member while on the aircraft. General checklists of NOAA science-related functions are included in Appendix E.

5.3 Principal Duties of the Scientific Personnel
A list of primary duties for each NOAA scientific personnel position is given in Appendix D.

5.4 HRD Communications
All field program activities are communicated via our web blog and emails. When field activities are occurring, an internal email will be sent out daily to HRD. The internal email will include up-to-date crew, hotel, storm status and schedules. The blog is our main forum where we will provide field

operation status, including deployment information of aircraft and personnel for operations outside Miami.

NHC will serve as the communications center for information and will provide interface between AOC, NHC, and CARCAH (Chief, Aerial Reconnaissance Coordinator, All Hurricanes). Personnel who have completed a flight will provide information to the Field Program Director, as required.

6. Data Management
Data management and dissemination will be according to the HRD data policy that can be viewed at:
http://www.aoml.noaa.gov/hrd/data2.html

A brief description of the primary data types and contact information may be found at:
http://www.aoml.noaa.gov/hrd/data/products.html

Raw data are typically available to all of NOAA-sponsored personnel and co-investigators immediately after a flight, subject to technical and quality assurance limitations. Processed data or other data that has undergone further quality control or analyses are normally available to the principal and co-investigators within a period of several months after the end of the Hurricane Field Program.

All requests for NOAA data gathered during the Hurricane Field Program should be forwarded by email to the associated contact person in the HRD data products description (link above) or in writing to: Director, Hurricane Research Division/AOML, 4301 Rickenbacker Causeway, Miami, Florida 33149.

7. Operational Constraints
NOAA P-3 aircraft are routinely tasked by NHC and/or EMC through CARCAH (Chief, Aerial Reconnaissance Coordinator, All Hurricanes) to perform operational missions that always take precedence over research missions. Research objectives can frequently be met, however, through these operational missions. Occasionally, HRD may request, through NHC and CARCAH, slight modifications to the flight plan on operational missions. These requests must not deter from the basic requirements of the operational flight as determined by NHC and coordinated through CARCAH.

Hurricane research missions are routinely coordinated with hurricane reconnaissance operations. As each research mission is entered into the planned operation, a block of time is reserved for that mission and operational reconnaissance requirements are assigned. A mission, once assigned, *must be flown in the time period allotted and the tasked operational fixes met.* Flight departure times are critical. Scientific equipment or personnel not properly prepared for the flight at the designated pre-take-off time will remain inoperative or be left behind to insure meeting scheduled operational fix requirements. Information on delays to, or cancellations of, research flights must be relayed to CARCAH.

8. Calibration of Aircraft Systems
Calibration of aircraft systems is described in Appendix B (B.1 en-route calibration of aircraft systems). True airspeed (TAS) calibrations are required for each NOAA flight, both to and from station and should be performed as early and as late into each flight as possible (Fig. B-1).

EXPERIMENT AND MODULE DESCRIPTIONS

1. P-3 Three-Dimensional Doppler Winds Experiment

Principal Investigator(s): John Gamache, Paul Reasor, Altug Aksoy, Peter Dodge, Vijay Tallapragada (EMC), Mingjing Tong (EMC), and Jason Sippel (EMC)

Primary IFEX Goal: 1 - Collect observations that span the TC life cycle in a variety of environments for model initialization and evaluation

Program significance: This experiment is a response to the requirement listed as Core Doppler Radar in Section 5.4.2.9 of the National Hurricane Operations Plan. The goal of that particular mission is to gather airborne-Doppler wind measurements that permit an accurate initialization of HWRF, and also provide three- dimensional wind analyses for forecasters.

There are five main goals: 1) to provide a comprehensive data set for the initialization (including data assimilation) and validation of numerical hurricane simulations (in particular HWRF), 2) to improve understanding of the factors leading to TC intensity and structure changes by examining as much of the life cycle as possible, 3) to improve and evaluate technologies for observing TCs, 4) to develop rapid real-time communication of these observations to NCEP, and 5) to contribute to a growing tropical-cyclone database that permits the analysis of statistics of quantities within tropical cyclones of varying intensity.

The ultimate requirement for EMC is to obtain the three-dimensional wind field of Atlantic TCs from airborne Doppler data every 6 h to provide an initialization of HWRF through assimilation every 6 h. The maximum possible rotation of missions is two per day or every 12 h. A "poor man's" version of the 6 h data collection is to collect data in the last half of one 6-h observing period, and in the first half of the next 6-h observing period. In hurricanes, coordination will be required between HRD, NCEP, and NESDIS, to effectively collect observations for both the Three- Dimensional Doppler Winds Experiment and the Ocean Winds and Rain Experiment, a NESDIS program designed to improve understanding of satellite microwave surface scatterometry in high-wind conditions over the ocean by collecting surface scatterometry data and Doppler data in the boundary layer of hurricanes.

The highest vertical resolution is needed in the boundary and outflow layers. This is assumed to be where the most vertical resolution is needed in observations to verify the initialization and model. For this reason it is desirable that if sufficient dropwindsondes are available, they should be deployed in the radial penetrations in the Three-Dimensional Doppler Winds experiment to verify that the boundary-layer and surface wind forecasts produced by HWRF resemble those in observations. These observations will also supplement airborne Doppler observations, particularly in sectors of the storm without sufficient precipitation for radar reflectivity. If sufficient dropwindsondes are not available, a combination of SFMR, Advanced Wind and Rain Airborne Profiler (AWRAP), and airborne Doppler data will be used for verification.

Links to IFEX: The P-3 Tail Doppler Radar experiment supports the following NOAA IFEX goals:

Goal 1: Collect observations that span the TC lifecycle in a variety of environments
Goal 2: Develop and refine measurement technologies that provide improved real-time monitoring of TC intensity, structure, and environment
Goal 3: Improve understanding of the physical processes important in intensity change for a TC at all stages of its lifecycle

Mission Descriptions: (The NESDIS Ocean Winds and Rain Experiment will be executed by NESDIS. Specific details regarding these NESDIS missions are not included here)

Three-Dimensional Doppler Winds: Several different options are possible: i) the lawnmower pattern (Fig. 1-1); ii) the box-spiral pattern (Figs. 1-2 and 1-3); iii) the rotating figure-4 pattern (Fig. 1-4); iv) the butterfly pattern that consists of 3 penetrations across the storm center at 60-degree angles with respect to each other (Fig. 1-5); and v) the single figure-4 (Fig. 1-6). These patterns provide the maximum flexibility in planning, in which the need for dense Doppler-radar coverage must be balanced against the need to sample the entire vortex.

Single-aircraft option only: Temporal resolution (here defined as data collected as close as possible to a 6-h interval) is important, for both initialization and verification of HWRF. This has been verified in communication with EMC. To obtain the maximum temporal resolution feasible, this mission is expected to be a single-P-3 mission, to allow another crew to operate 12 h later, and to continue in a 12-h cycle of single sorties. The type of flight pattern will be determined from the organization, strength and radial extent of the circulation. Take-off times will be coordinated to provide quality-controlled Doppler radar observations to NCEP Central Operations (NCO) in every 6-h observing period, by observing the end of one period, and the beginning of the next. This will result generally in a takeoff time at or shortly before 0, 6, 12, or 18 UTC.

Lawnmower pattern: This pattern will be chosen for systems with small, generally asymmetric, weak, newly developed circulations, namely tropical depressions and weak tropical storms. If the system is small enough, lawnmower pattern A (Fig. 1-1) will be chosen, to permit complete coverage of all reflectors within the developing circulation. Otherwise pattern B will be flown. Pattern B permits a larger area to be sampled, at the expense of some gaps in the Doppler coverage. A specific flight level is not required for this mission. It is likely that the Air Force will be flying at an investigation level at this time, and the Three-Dimensional Doppler Winds Experiment can be flown anywhere from 5,000 ft to 12,000 ft. If detailed thermodynamic data from dropwindsondes is desirable, or the distribution of Doppler winds is highly asymmetric, then the preferred level would be 12,000 ft to allow the deepest observation of the thermodynamic and wind structure from the dropwindsondes, while reducing the likelihood of lightning strikes and graupel damage by staying below the melting level. Any orientation of the long and short flight legs may be flown, to permit the location of the initial and final points to be closest to the base(s) of operations.

Box-spiral pattern: As the weak, developing, poorly organized circulations become larger, it will be necessary to spread out the pattern to cover a larger area at the expense of complete Doppler coverage. Pattern A, as shown in Fig. 1-2, is designed to cover a box 280 nm x 280 nm with radial gaps in the coverage. As long as the circulation is still weak, but covers a larger area, this pattern will be considered; however, lack of symmetric coverage at all radii renders this a less viable option as the system organizes. Pattern B has denser coverage within the outside box, and it will be considered in smaller systems. Any orientation of the flight legs may be flown, to permit the location of the initial and final points to be closest to the base(s) of operations.

Rotating figure-4 pattern: As the system intensity and/or organization increases, and a circulation center becomes clearly defined, a rotating figure-4 pattern may be preferred (Fig. 1-4). The advantage of this pattern over the larger versions of the lawnmower pattern is symmetric wind coverage, and the advantage over the box-spiral pattern is good definition of the wind field at all radii within the pattern. This pattern is obviously preferable to the lawnmower pattern in the event there is any operational fix responsibility for the aircraft. Any orientation of the flight legs may be flown, to permit the location of the initial and final points to be closest to the base(s) of operations. See discussion of "lawnmower pattern"

regarding flight altitude and use of dropwindsondes.

Butterfly pattern: This pattern (Fig. 1-5) should be flown in larger, well-organized TCs, generally in hurricanes. As the hurricane circulation becomes larger, it will be necessary to get the full radial coverage at the expense of full azimuthal coverage. As an example, a butterfly pattern out to 100 nm could be flown in
3.3 h, compared to a similar lawnmower coverage that would take 4.8 h. This pattern is obviously preferable to the lawnmower pattern in the event there is any operational fix responsibility for the aircraft. Any orientation of the flight legs may be flown, to permit the location of the initial and final points to be closest to the base(s) of operations. See discussion of "lawnmower pattern" regarding flight altitude and use of dropwindsondes.

Single figure-4 pattern: This pattern (Fig. 1-6) will be flown in very large circulations, or when little time is available in storm, such as during ferries from one base of operations to another. It still provides wavenumber 0 and 1 coverage with airborne Doppler data, which should be sufficient in strong, organized systems. Radial coverage out to 240 and 300 nm (4 and 5 degrees) is possible in 5.4 and 6.8 h in pattern. Any orientation of the flight legs may be flown, to permit the location of the initial and final points to be closest to the base(s) of operations. See discussion of "lawnmower pattern" regarding flight altitude and use of dropwindsondes.

Three-Dimensional Doppler Winds Experiment Flight Planning Approach: NOAA will conduct a set of flights during several consecutive days, encompassing as much of a particular storm life cycle as possible. This would entail using the two available P-3s on back-to-back flights on a 12-h schedule when the system is at depression, tropical storm, or hurricane strength.

At times when more than one system could be flown, one may take precedence over others depending on factors such as storm strength and location, operational tasking, and aircraft availability. All other things being equal, the target will be an organizing tropical depression or weak tropical storm, to increase the observations available in these systems. One scenario could likely occur that illustrates how the mission planning is determined: an incipient TC, at depression or weak tropical storm stage is within range of an operational base and is expected to develop and remain within range of operational bases for a period of several days. Here, the highest priority would be to start the set of Three-Dimensional Doppler Winds flights, with single-P-3 missions, while the TC is below hurricane strength (preferably starting at depression stage), with continued single-P-3 missions at 12-h intervals until the system is out of range or makes landfall. During the tropical depression or tropical-storm portion of the vortex lifetime, higher azimuthal resolution of the wind field is preferred over radial extent of observations, while in the hurricane portion, the flight plan would be designed to get wavenumber 0 and 1 coverage of the hurricane out to the largest radius possible, rather than the highest temporal resolution of the eyewall. In all cases adequate spatial coverage is preferred over increased temporal resolution during one sortie.
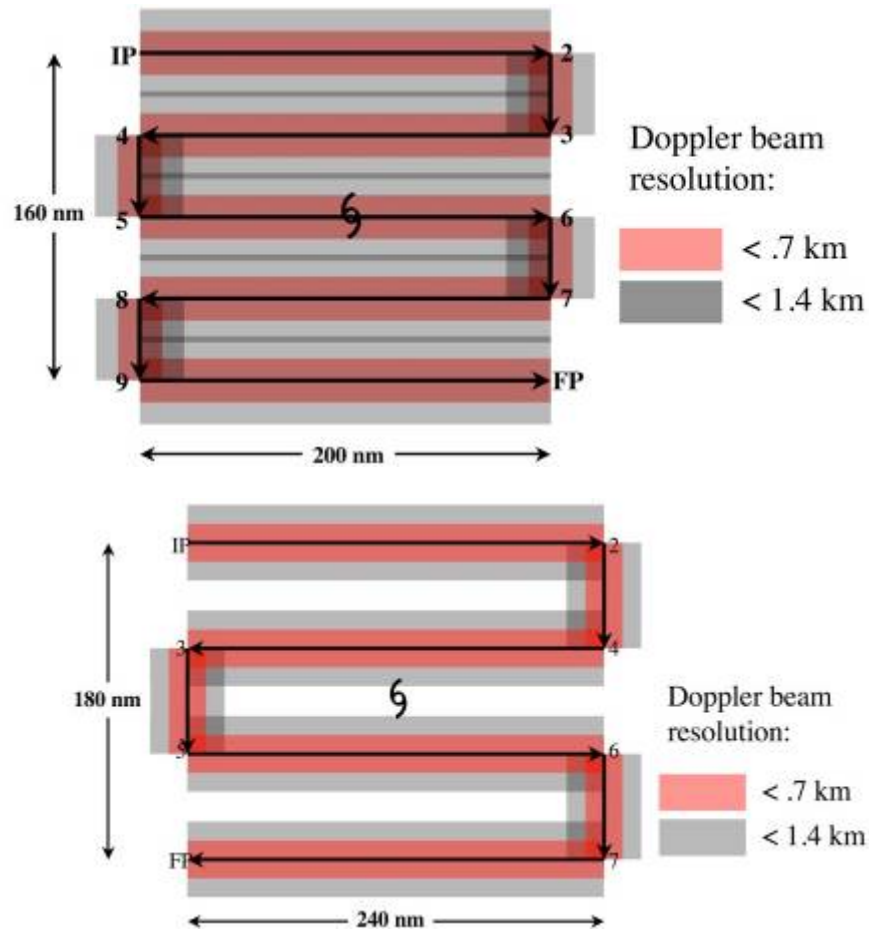
Figure 1-1: Display of Doppler coverage for A (upper panel) and B (lower panel) lawnmower patterns. Pink region shows areas where vertical beam resolution is better than 0.7 km and gray regions delineate areas where vertical beam resolution is better than 1.4 km. Maximum extent of gray area is approximately 40 km from flight track, generally the maximum usable extent of reliable airborne Doppler radar coverage. Total flight distance is 1160 nm for A and 1140 nm for B, and flight times are 4.8 and 4.75 hours, respectively.

Note 1. This is to be flown where even coverage is required, particularly in tropical depressions and tropical storms. Aircraft flies IP-2-3-4-5-6-7-FP. No attempt should be made to fix a center of circulation unless it is an operational request.
Note 2. Doppler radars should be operated in single-PRF mode, at a PRF of 2100. Radar scientist should verify this mode of operation with AOC engineers. If there is no assigned radar scientist, LPS should verify. *This is crucial for the testing and implementation of real-time quality control.*
Note 3. Assure that transmitter is switching between fore and aft antennas, by examining the real time display.
Note 4. IP can be at any desired heading relative to storm center
Note 5. To maximize dropwindsonde coverage aircraft should operate at highest altitudes that still minimize icing
Note 6. If dropwindsondes are not deployed, aircraft can operate at any level below the melting level, with 10,000 ft preferred. Aircraft might also fly lower, if circulation not evident at 10,000 ft.
Note 7. Dropwindsondes are not a required part of this flight plan and are optional.

Figure 1-2: Doppler radar coverage for box-spiral pattern A. Pink region shows areas where vertical beam resolution is better than 0.7 km and gray regions delineate areas where vertical beam resolution is better than

1.4 km. Maximum extent of gray area is approximately 40 km from flight track, approximately the maximum usable extent of reliable airborne Doppler radar coverage. Flight distance in pattern above is 1280 nm, and flight time is 5.33 hours.

Note 1. This is to be flown where even coverage is required, particularly in tropical depressions and tropical storms. Aircraft flies IP-2-3-4-5-6-7-8-FP. No attempt should be made to fix a center of circulation unless it is an operational request.
Note 2. Doppler radars should be operated in single-PRF mode, at a PRF of 2100. Radar scientist should verify this mode of operation with AOC engineers. If there is no assigned radar scientist, LPS should verify. *This is crucial for the testing and implementation of real-time quality control.*
Note 3. Assure that transmitter is switching between fore and aft antennas, by examining the real time display.
Note 4. IP can be at any desired heading relative to storm center
Note 5. To maximize dropwindsonde coverage aircraft should operate at highest altitudes that still minimize icing
Note 6. If dropwindsondes are not deployed, aircraft can operate at any level below the melting level, with 10,000 ft preferred. Aircraft might also fly lower, if circulation not evident at 10,000 ft.
Note 7. Dropwindsondes are not a required part of this flight plan and are optional.

Figure 1-3: Doppler radar coverage for box-spiral pattern with 200- (top) and 240- (bottom) nm legs. Pink region shows areas where vertical beam resolution is better than 0.7 km and gray regions delineate areas where vertical beam resolution is better than 1.4 km. Maximum extent of gray area is approximately 40 km from flight track, approximately the maximum usable extent of reliable airborne Doppler radar coverage. Upper pattern is 1500 nm and uses 6.25 hours, while lower pattern is 1250 nm and uses 5.2 hours.

Note 1. Pattern flown where even coverage is required, particularly in tropical depressions and tropical storms. Doppler radars should be operated in single-PRF mode, at a PRF of 2100. Radar scientist should verify this mode of operation with AOC engineers. If there is no assigned radar scientist, LPS should verify. *This is crucial for the testing and implementation of real-time quality control.*
Note 2. Assure that transmitter is switching between fore and aft antennas, by examining the real time display.
Note 3. IP can be at any desired heading relative to storm center
Note 4. To maximize dropwindsonde coverage aircraft should operate at highest altitudes that still minimize icing.
Note 5. Maximum radius may be decreased or increased within operational constraints.
Note 6. Dropwindsondes are not a required part of this flight plan and are optional.
Note 7. Maximum radius may be changed to meet operational needs while conforming to flight-length constraints.
Note 8. If dropwindsondes are not deployed, aircraft can operate at any level below the melting level, with 10,000 ft preferred. Aircraft might also fly lower, if circulation not evident at 10,000 ft.
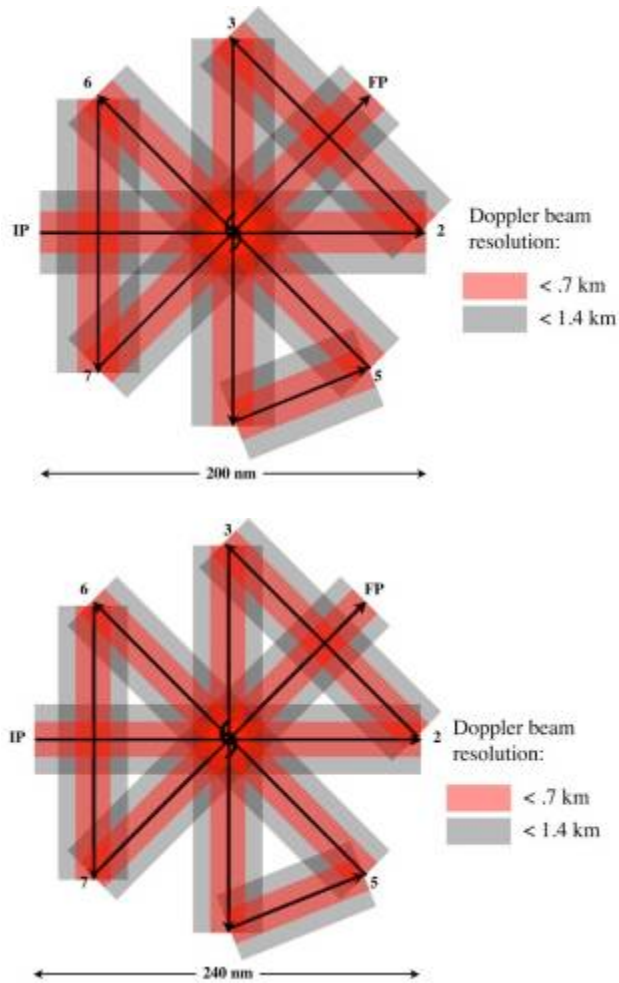
Figure 1-4: Doppler radar coverage for radial extents of 100 (top) and 120 (bottom) nm of the rotating figure-4 patterns. Pink region shows areas where vertical beam resolution is better than 0.7 km and gray regions delineate areas where vertical beam resolution is better than 1.4 km. Maximum extent of gray area is approximately 40 km from flight track, approximately the maximum usable extent of reliable airborne Doppler radar coverage. Flight distances for 100, 120 and 150 nm radial extents are 1160, 1395, and 1745 nm. Corresponding flight times are: 4.8, 5.8, and 7.3 h.
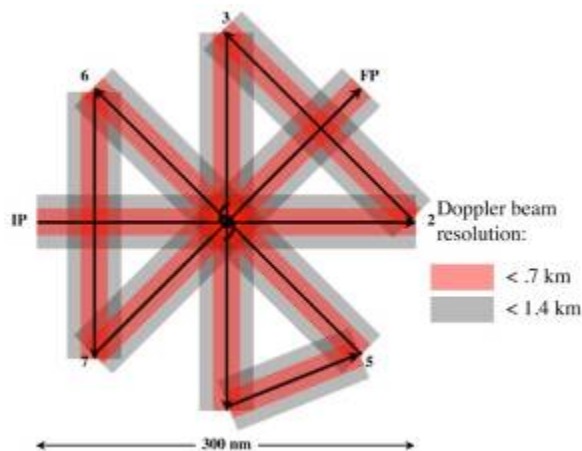
Figure 1-4 (continued): Doppler radar coverage for 150-nm legs for a rotating figure-4. Flight distances for 100, 120 and 150 nm radial extents are 1160, 1395, and 1745 nm. Corresponding flight times are: 4.8, 5.8, and 7.3 h.

Note 1. This pattern should be flown in strong tropical storms and hurricanes, where the circulation extends from 100 nm to 150 nm from the center. Doppler radars should be operated in single-PRF mode, at a PRF of 2100. Radar scientist should verify this mode of operation with AOC engineers. If there is no assigned radar scientist, LPS should verify. *This is crucial for the testing and implementation of real-time quality control.*
Note 2. Assure that transmitter is switching between fore and aft antennas, by examining the real time display.
Note 3.   IP can be at any desired heading relative to storm center
Note 4. To maximize dropwindsonde coverage aircraft should operate at highest altitudes that still minimize icing
Note 5.   Maximum radius may be decreased or increased within operational constraints
Note 6.   Dropwindsondes shown are not a required part of this flight plan and are optional.
Note 7.   Flight pattern should be centered around either the 03, 09, 15, or 21 UTC so Doppler observations are available for both surrounding observation periods.
Note 8. Maximum radius may be changed to meet operational needs while conforming to flight-length constraints.
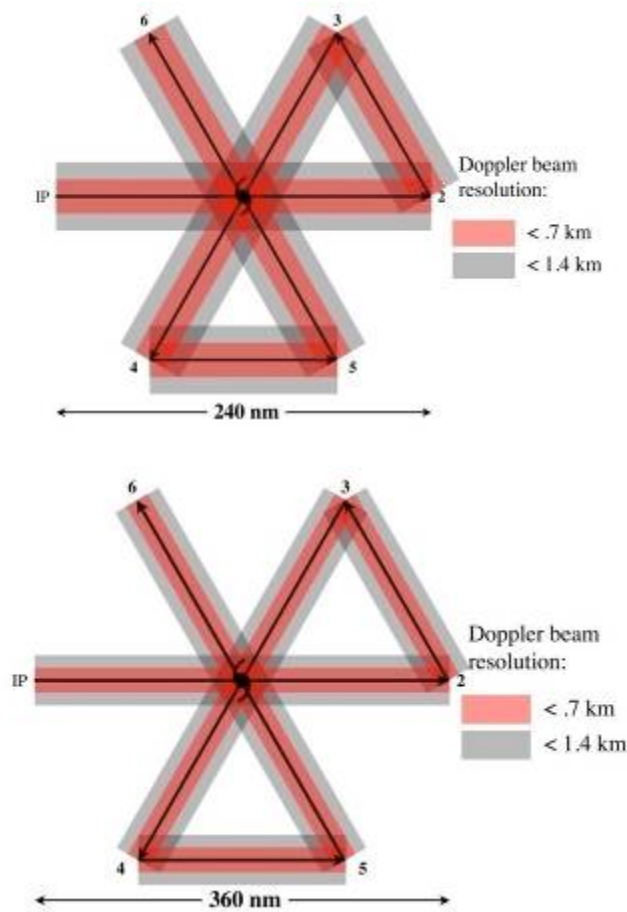
Figure 1-5: Doppler radar coverage for 120- (top) and 180- (bottom) nm legs for the Butterfly pattern. Pink region shows areas where vertical beam resolution is better than 0.75 km and gray regions delineate areas where vertical beam resolution is better than 1.5 km. Maximum extent of gray area is approximately 40 km from flight track, approximately the maximum usable extent of reliable airborne Doppler radar coverage. Flight distances for the patterns with 120 and 180 nm radials legs are 960 and 1440 nm. Corresponding flight durations are 4 and 6 h.

Note 1. This pattern will be flown in large tropical storms, as well as hurricanes. Doppler radars should be operated in single-PRF mode, at a PRF of 2100. Radar scientist should verify this mode of operation with AOC engineers. If there is no assigned radar scientist, LPS should verify. *This is crucial for the testing and implementation of real-time quality control.*
Note 2. Assure that transmitter is switching between fore and aft antennas, by examining the real time display.
Note 3. IP can be at any desired heading relative to storm center
Note 4. To maximize dropwindsonde coverage aircraft should operate at highest altitudes that still minimize icing
Note 5. Maximum radius may be decreased or increased within operational constraints
Note 6. Dropwindsondes are not a required part of this flight plan and are optional.
Note 7. Flight pattern should be centered around either 03, 09, 15, or 21 UTC so Doppler observations are available for both surrounding observation periods.
Note 8. Maximum radius may be changed to meet operational needs while conforming to flight-length constraints.

Three-Dimensional Doppler Winds
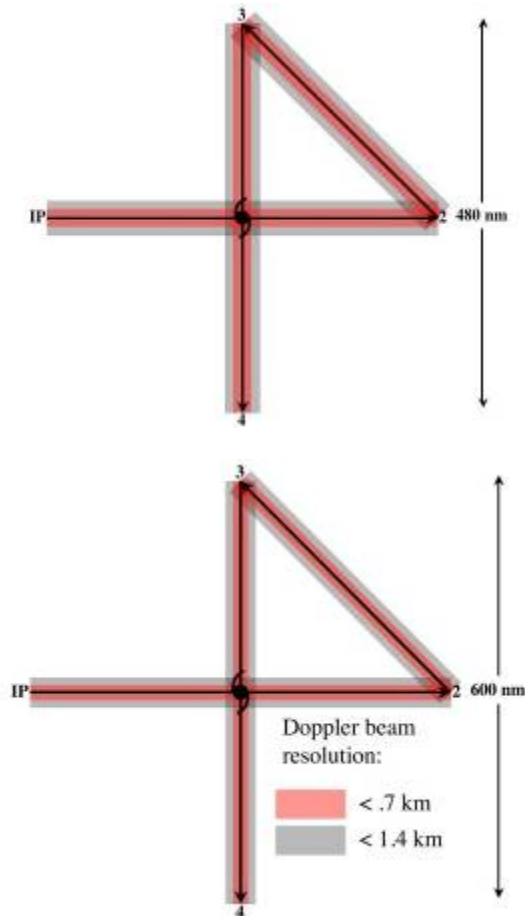
Figure 1-6: Doppler radar coverage for 300-nm legs for a single figure-4 pattern. Pink region shows areas where vertical beam resolution is better than 0.75 km and gray regions delineate areas where vertical beam resolution is better than 1.5 km. Maximum extent of gray area is approximately 40 km from flight track, approximately the maximum usable extent of reliable airborne Doppler radar coverage. Flight distances for radial extents of 240 and 300 nm are 1300 and 1645 nm, respectively. Corresponding flight times are 5.4 and 6.8 h.

Note 1. Pattern for large storms, to obtain as full a radial extent of observations of the full storm circulation as possible. Doppler radars should be operated in single-PRF mode, at a PRF of 2100. Radar scientist should verify this mode of operation with AOC engineers. If there is no assigned radar scientist, LPS should verify. *This is crucial for the testing and implementation of real-time quality control.*
Note 2. Assure that transmitter is switching between fore and aft antennas, by examining the real time display.
Note 3. IP can be at any desired heading relative to storm center
Note 4. To maximize dropwindsonde coverage aircraft should operate at highest altitudes that still minimize icing
Note 5. Maximum radius may be decreased or increased within operational constraints
Note 6. Dropwindsondes are not a required part of this flight plan and are optional.
Note 7. Flight pattern should be centered around either the 03, 09, 15, or 21 UTC so Doppler observations are available for both surrounding observation periods.
Note 8. Maximum radius may be changed to meet operational needs while conforming to flight-length constraints.

2. G-IV Tail Doppler Radar Experiment

Principal Investigator(s): John Gamache, Peter Dodge, Paul Reasor, Altug Aksoy,, Vijay Tallapragada (EMC), Mingjing Tong (EMC), and Jason Sippel (EMC)

Primary IFEX Goal: 1 - Collect observations that span the TC life cycle in a variety of environments for model initialization and evaluation.

Program significance: This experiment is a response to the requirement listed as Core Doppler Radar in Section 5.4.2.9 of the National Hurricane Operations Plan. The goal of that particular mission is to gather airborne-Doppler wind measurements that permit an accurate initialization of HWRF, and also provide three-dimensional wind analyses for forecasters. This experiment is similar to the P-3 Three-Dimensional Winds experiment, but employs the G-IV platform and tail Doppler radar.

There are four main goals: 1) to evaluate the G-IV as a platform for observing the cores of TCs, 2) to improve understanding of the factors leading to TC structure and intensity changes, 3) to provide a comprehensive data set for the initialization (including data assimilation) and validation of numerical hurricane simulations (in particular HWRF), and 4) to develop rapid real-time communication of these observations to NCEP.

The ultimate requirement for EMC is to obtain the three-dimensional wind field of Atlantic TCs from airborne Doppler data every 6 h to provide an initialization of HWRF through assimilation every 6 h. In 2016, the maximum possible rotation of missions is two per day or every 12 h. The G-IV platform is currently used by NHC for synoptic surveillance until approximately 36 h prior to TC landfall. In 2016 the flight modules described here are likely to be limited to cases within this landfall window or not of NHC operational interest. In anticipation of future operational use of the G-IV Doppler data, a preliminary flight pattern is introduced which attempts to satisfy the combined need for synoptic surveillance and optimal collection of Doppler data for assimilation. This flight pattern, as well as other proposed G-IV patterns, will be refined through experiments using the Hurricane Ensemble Data Assimilation System (HEDAS) and consultation with NHC.

Following the spring 2012 NOAA acceptance of the G-IV tail Doppler radar, the experiment will focus initially on documenting data coverage in TCs, in particular resolution of the outflow layer (via the central dense overcast). These observations will supplement those collected by the P-3 aircraft, and through HEDAS, their added value in TC initialization will be investigated. Flight patterns will also explore the viability of the G-IV as a substitute for the P-3 aircraft in terms of Doppler radar sampling of the TC core region. Coordinated flights with the P-3 aircraft will be required as part of this assessment.

Links to IFEX: The G-IV Tail Doppler Radar experiment supports the following NOAA IFEX goals:

Goal 1: Collect observations that span the TC lifecycle in a variety of environments
Goal 2: Develop and refine measurement technologies that provide improved real-time monitoring of TC intensity, structure, and environment
Goal 3: Improve understanding of the physical processes important in intensity change for a TC at all stages of its lifecycle

G-IV Three-Dimensional Doppler Winds: Several different options are possible: i) the square-spiral pattern (Figs. 2-1 and 2-2); ii) the rotating figure-4 pattern (Fig. 2-3); iii) the butterfly pattern that consists of 3 penetrations across the storm center at 60-degree angles with respect to each other (Fig. 2-4); iv) the single figure-4 (Fig. 2-5); and v) the surveillance/TDR combination pattern (Fig. 2-6). These patterns provide the maximum flexibility in planning, in which the need for dense date coverage must be balanced against the need to sample the entire vortex.

Square-spiral pattern: As the weak, developing, poorly organized circulations become larger, it will be necessary to spread out the pattern to cover a larger area at the expense of complete Doppler coverage. The pattern, as shown in Figs. 2-1 and 2-2, is designed to cover a box 300 nm x 300 nm with radial gaps in the coverage. As long as the circulation is still weak, but covers a larger area, this pattern will be considered; however, lack of symmetric coverage at all radii renders this a less viable option as the system organizes. Fig. 2-1 (2-2) shows the option of an outward (inward) spiral from (into) the center. Any orientation of the flight legs may be flown to permit the initial and final points to be closest to the base of operations.

Rotating figure-4 pattern: As the system intensity and/or organization increases, and a circulation center becomes clearly defined, a rotating figure-4 pattern may be preferred (Fig. 2-3). The advantage of this pattern over the square-spiral pattern is good definition of the wind field at all radii within the pattern. Any orientation of the flight legs may be flown to permit the initial and final points to be closest to the base of operations.

Butterfly pattern: This pattern (Fig. 2-4) should be flown in larger, well-organized TCs, generally in hurricanes. As the hurricane circulation becomes larger, it will be necessary to get the full radial coverage at the expense of full Doppler coverage. As an example, a butterfly pattern out to 100 nm could be flown in 3.3 h. Any orientation of the flight legs may be flown to permit the initial and final points to be closest to the base of operations.

Single figure-4 pattern: This pattern (Fig. 2-5) will be flown in very large circulations. It still provides wavenumber 0 and 1 coverage with airborne Doppler data, which should be sufficient in strong, organized systems. Radial coverage out to 240 and 300 nm (4 and 5 degrees) is possible in 5.4 and 6.8 h in pattern. Any orientation of the flight legs may be flown to permit the initial and final points to be closest to the base of operations.

Surveillance/TDR combination pattern: This pattern (Fig. 2-6) will be flown to test the ability of the G-IV platform to satisfy both NHC-tasked surveillance requirements (i.e., sampling the TC environment with GPS dropsondes) and the EMC-tasked requirement for tail Doppler radar sampling of the TC core region. The environmental sampling consists of a cyclonic circumnavigation of the TC at a fixed radius of 150 nm. This is followed by core region sampling using a rotating figure-4 pattern out to 75 nm. The duration of this pattern is approximately 6 h. Any orientation of the flight legs may be flown to permit the initial and final points to be closest to the base of operations.

G-IV Tail Doppler Radar Experiment Flight Planning Approach: Ideally, for initial experiments following the NOAA acceptance of the G-IV radar this would entail coordination with a P-3 aircraft conducting a Three-Dimensional Doppler Winds flight when the system is at depression, tropical storm, or hurricane strength. This initial coordination is necessary for 1) comparing and synthesizing storm structure derived from the two radar platforms and 2) the most thorough testing of HEDAS with this new data source. Subsequent flights may relax this requirement for P-3 coordination so as to test the Surveillance/TDR Combination Pattern (Fig. 2-6). It is not anticipated that the Combination Pattern will be flown during NHC tasking of the G-IV in 2015.

The likely scenarios in which this experiment would be carried out are as follows: 1) at the conclusion of NHC tasking for a landfalling TC, likely coordinated with the P-3 aircraft; 2) prior to NHC tasking for a TC of interest to EMC (priority is coordination with P-3 aircraft); 3) a recurving TC (priority is coordination with P-3 aircraft). Since coordination with the P-3 aircraft is an early requirement, this experiment would have to be weighed against other experiments (e.g., Rapid Intensification) which stagger the P-3 and G-IV flight times.

FP

Duration: 5.75 h

300 nm

IP
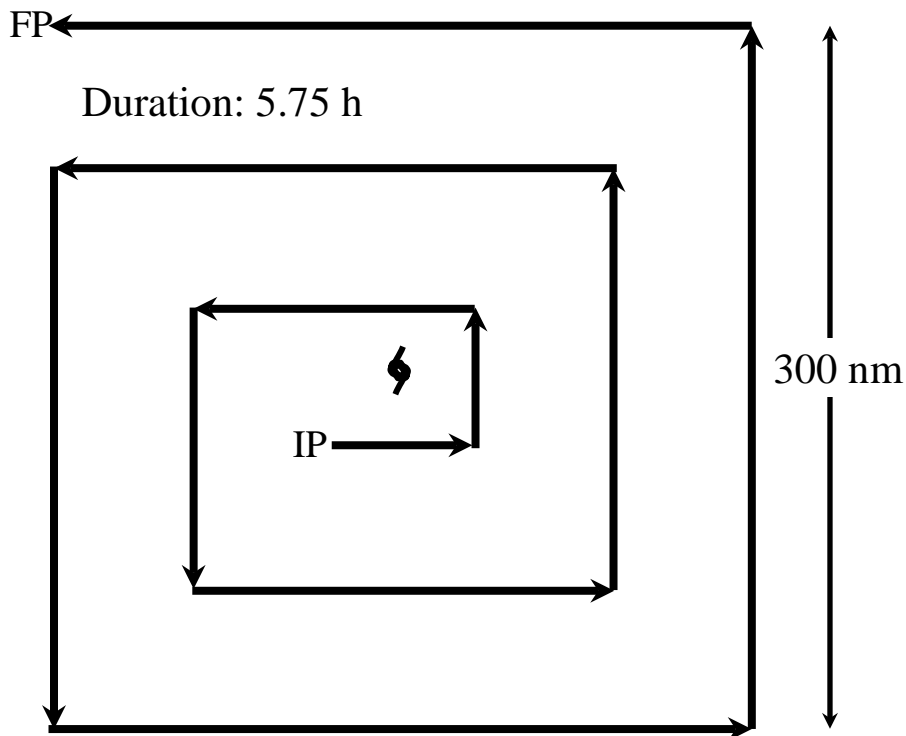
Figure 2-1: G-IV tail Doppler radar pattern – Square Spiral (outward)

Note 1. G-IV begins 30 nm to south and west of estimated circulation center (with proper rotation starting point can be NE, NW, SW, or SE of center)

Note 2. Fly 60 nm due east (due north, west, south, for IP SE, NE, or NW of center, respectively)--left turn--60 nm--left turn--120 nm--left turn--120 nm--left turn--180 nm--left turn--180 nm--left turn--240 nm--left turn--240 nm--left turn--300 nm--left turn--300 nm--left turn--300 nm

Note 3. Duration: 2100 nm, or 4.75 hour + 1 hour for deviations--covers 150 nm (2.5 deg) in each cardinal direction from center

Note 4. Aircraft should operate at its maximum cruising altitude of ~40-45 kft

Note 5. On all legs, deviate to avoid weather deemed to pose possible hazard

Note 6. As flight duration and ATC allow, attempt to sample as much of regions that require deviation

Note 7. Tail Doppler radar should be run in single PRF mode, 3000, since dual PRF is often in error when there is a strong vertical gradient of tangential wind.

Note 8. If flying above 40,000 ft, pattern may be flown clockwise, if preferred.
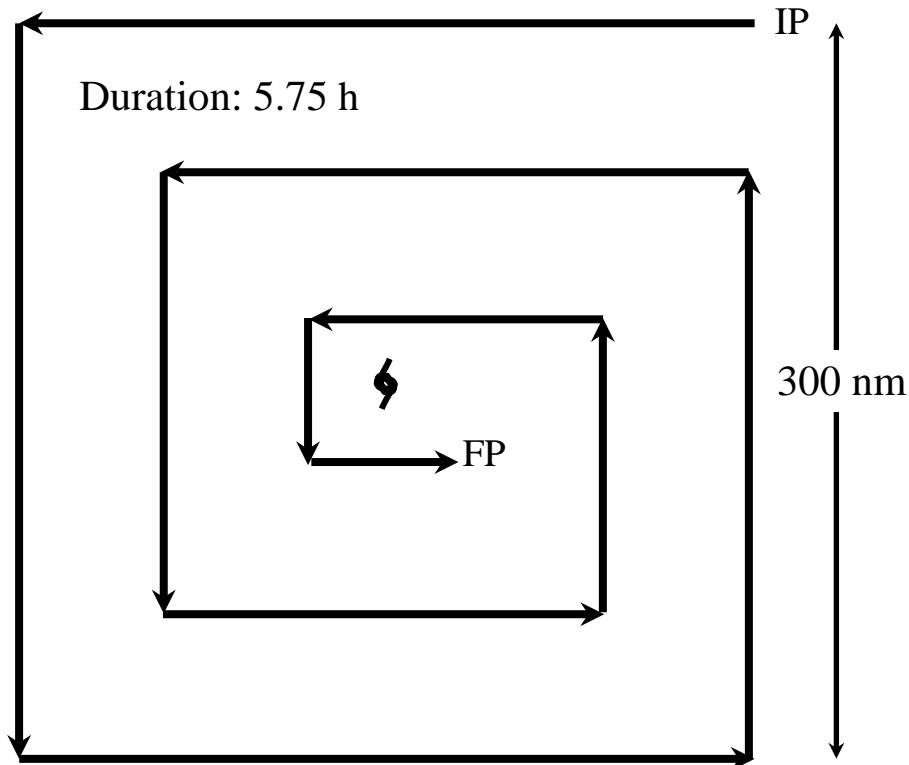
Figure 2-2: G-IV tail Doppler radar pattern – Square Spiral (inward)

Note 1. G-IV begins 150 nm to north and east of estimated circulation center (with proper rotation starting point can be NE, NW, SW, or SE of center)

Note 2. Fly 300 nm due west (due south, east, north, for IP NW, SW, or SE of center, respectively)--left turn--300 nm--left turn--300 nm--left turn--240 nm--left turn--240 nm--left turn--180 nm--left turn--180 nm--left turn--120 nm--left turn--120 nm--left turn--60 nm--left turn--60 nm

Note 3. Duration: 2100 nm, or 4.75 hour + 1 hour for deviations--covers 150 nm (2.5 deg) in each cardinal direction from center

Note 4. Aircraft should operate at its maximum cruising altitude of ~40-45 kftNote 5. On all legs, deviate to avoid weather deemed to pose possible hazard

Note 6. As flight duration and ATC allow, attempt to sample as much of regions that require deviation

Note 7. Tail Doppler radar should be run in single PRF mode, 3000, since dual PRF is often in error when there is a strong vertical gradient of tangential wind.

Note 8. If flying above 40,000 ft, pattern may be flown clockwise, if preferred.
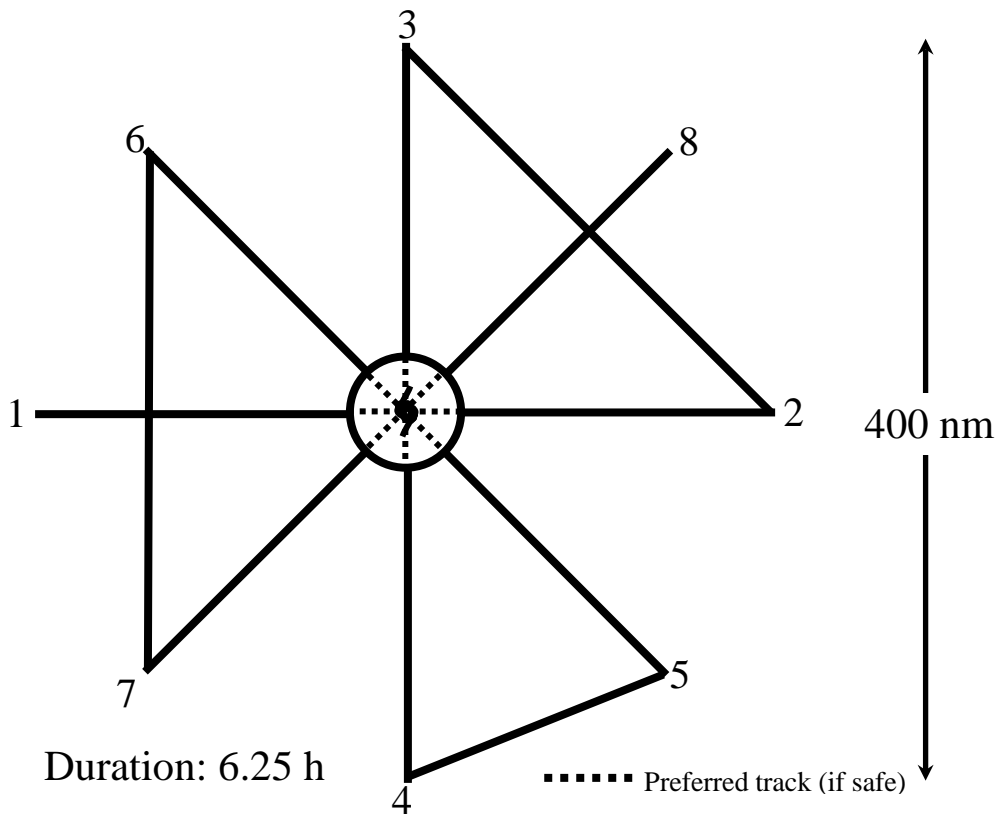
Figure 2-3: G-IV Doppler radar pattern – Rotating Figure-4

Note 1. IP is 200 nm from storm center
Note 2. Fly 1-2, deviating around eyewall if conditions require (eyewall assumed to extend 20 nm from center). If deviation is required, fly to right of convection if possible. If conditions permit, fly through center of circulation.
Note 3. Fly 2-3, deviating around convection if necessary
Note 4. Fly 3-4, as described in Note 2.
Note 5. Fly 4-5, deviating around convection, if necessary
Note 6. Fly 5-6-7-8 in the same manner as 1-2-3-4
Note 7. Duration: 2317 nm, or 5.25 hours + 1 hour for deviations
Note 8. Aircraft should operate at its maximum cruising altitude of ~40-45 km
Note 9. As flight duration and ATC allow, attempt to sample with TDR as much of regions that require deviations as possible.
Note 10. Tail Doppler radar should be operated in single PRF at 3000 per second
Note 11. If flying above 40,000 ft, pattern may be flown clockwise, if preferred.

Duration: 5.35 h

480 nm

■ ■ ■ ■ ■ ■ ■ Preferred track (if safe)
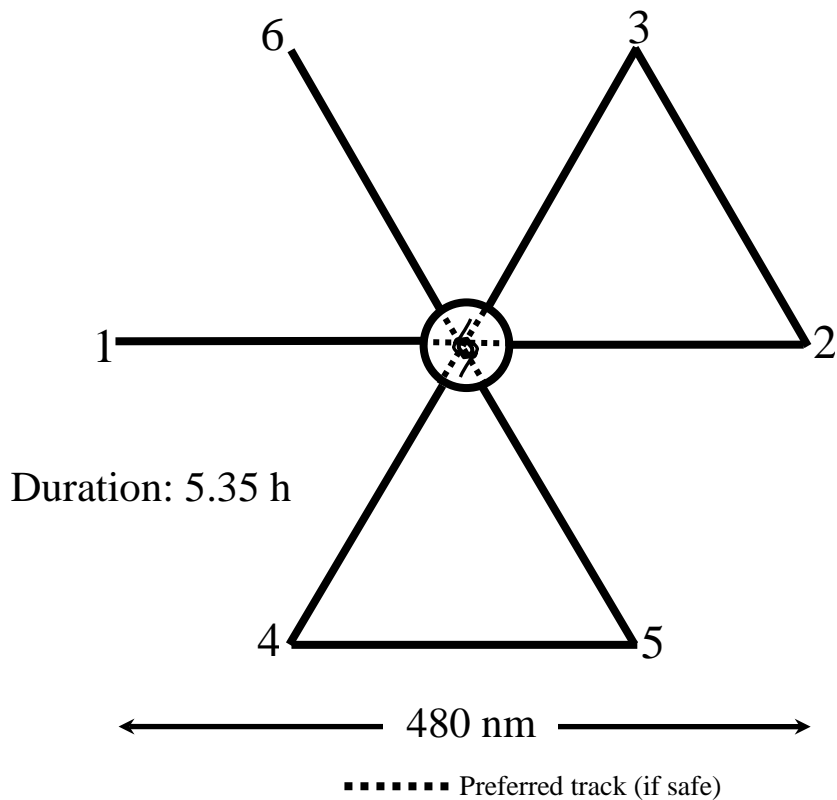
Figure 2-4: G-IV tail Doppler radar pattern – Butterfly

Note 1. IP is 240 nm from storm center at desired heading from storm center
Note 2. Fly 1-2, deviating around eyewall if conditions require (eyewall assumed to extend 20 nm from center in the figure). If deviation is required fly to right of convection if possible. If conditions permit, fly through center of circulation
Note 3. Fly 2-3, deviating around convection, if necessary.
Note 4. Fly 3-4, as described in Note 2.
Note 5. Fly 4-5, deviating around convection if necessary.
Note 6. Fly 5-6, as describe in Note 2.
Note 7. Aircraft should operate at its maximum cruising altitude of ~40-45 kft
Note 8. Duration: 1920 nm, or 4.35 hours + 1 hour for devations
Note 9. As flight duration and ATC allow, attempt to sample with TDR, as much of regions missed by deviations.
Note 10. Tail Doppler radar should be operated in single PRF, 3000 per second.
Note 11. If flying above 40,000 ft., pattern may be flown clockwise, if preferred.
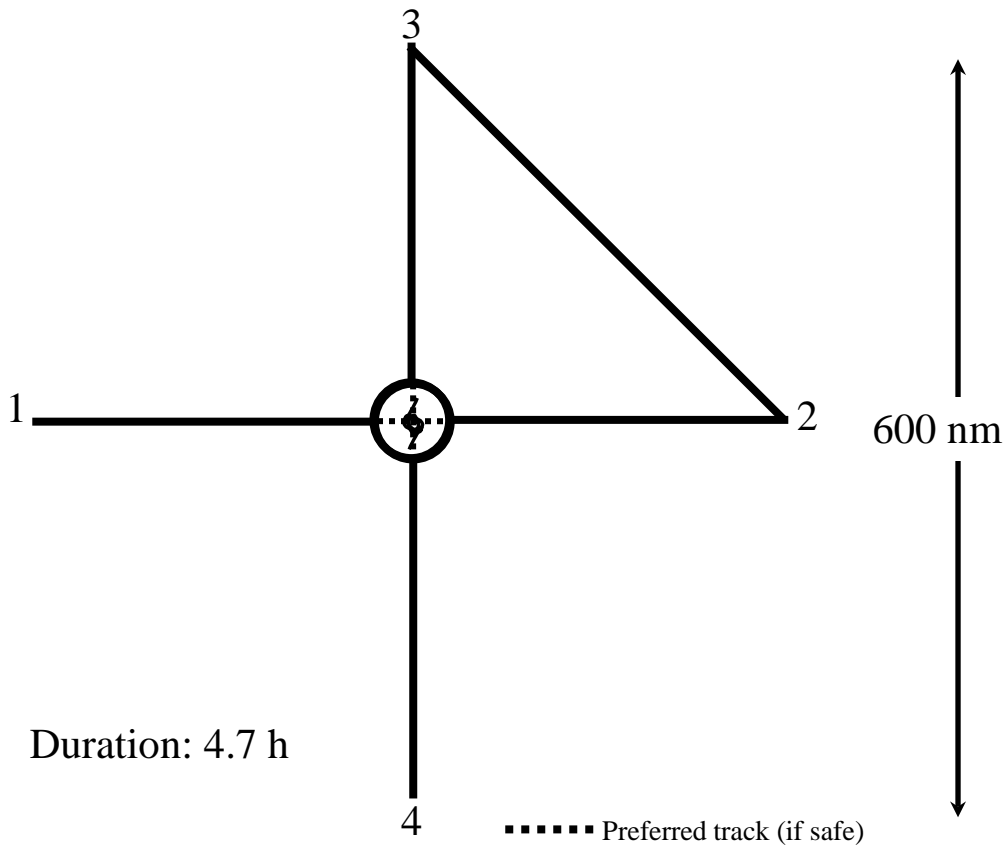
Figure 2.5: G-IV tail Doppler radar pattern – Single Figure 4.

Note 1. IP is 300 nm from storm center
Note 2. Fly 1-2, deviating around eyewall if conditions required (eyewall assume to extend 20 nm from center in this figure). If deviation is required, fly 1.5 circles around eyewall before continuing to point 2. Otherwise if conditions permit, fly directly through circulation center.
Note 3. Fly 2-3, deviating around convection, if necessary.
Note 4. Fly 3-4, as describe in segment 1-2; however if full circle done in first pass, only half circle is required.
Note 5. Duration 1624 nm, or 3.7 hours + 1 hour for deviations—pattern could be extended if time allows for greater radial coverage
Note 6. Aircraft should operate at its maximum cruising altitude of ~40-45 kft
Note 7. As flight duration and ATC allow, attempt to sample with TDR, as much of regions missed by deviations.
Note 8. Tail Doppler radar should be operated in single PRF, 3000 per second.
Note 9. If flying above 40,000 ft., pattern may be flown clockwise, if preferred.
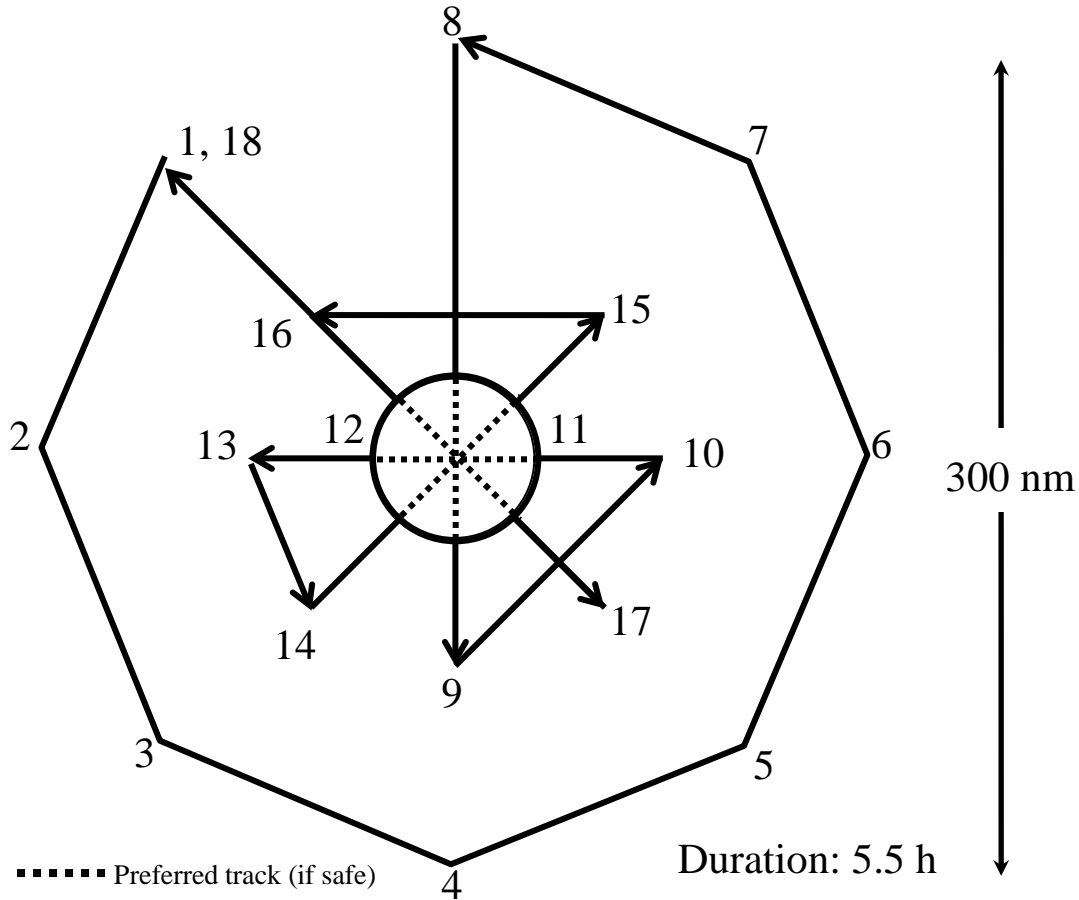
Figure 2-6: G-IV tail Doppler radar pattern – Surveillance/TDR combination

Note 1. IP is 150 nm from storm center
Note 2. Fly 1-2-3-4-5-6-7-8-9-10-11-12-13-14-15-16-17-18, deviating around eyewall if conditions require (eyewall assumed to extend 30 nm from center). If deviation is required, fly to right of convection if possible. If conditions permit, fly through center of circulation.
Note 3. Dropsondes should be launched at all numbered points (except 11 and 12). If the aircraft is able to cross the center, a sonde should be dropped there. Extra sondes may be requested.
Note 4. On-station duration: ~1933 nm, or about 4.5 hours + 1 hour for deviations.
Note 5. Aircraft should operate at its maximum cruising altitude of ~40-45 kft
Note 6. As flight duration and ATC allow, attempt to sample with TDR, as much of regions missed by deviations.
Note 7. Tail Doppler radar should be operated in single PRF, 3000 per second.
Note 8. If flying above 40,000 ft., pattern may be flown clockwise, if preferred.

24

3. Doppler Wind Lidar (DWL) Experiment

Principal Investigators: Lisa Bucci (HRD), Kelly Ryan (HRD), Jun Zhang (HRD), G. David Emmitt (SWA), Jason Dunion (HRD), and Robert Atlas (AOML)

Links to IFEX:

This experiment supports the following NOAA IFEX goals:

Goal 1: Collect observations that span the TC lifecycle in a variety of environments for model initialization and evaluation;

Goal 2: Develop and refine measurement technologies that provide improved real-time monitoring of TC intensity, structure, and environment;

Goal 3: Improve our understanding of the physical processes important in intensity change for a TC at all stages of its lifecycle;

Program Significance:

Currently there are limited continuous high-resolution wind observations in the TC boundary layer and in regions of low or no precipitation. A coherent-detection Doppler wind profile (P3DWL) system will be available for the 2016 hurricane season onboard NOAA-43. P3DWL can collect wind profiles through the detection of aerosol scatters in areas of optically thin or broken clouds or where aerosols are ~1 micron or larger. It is capable of performing a variety of scanning patterns, both above and below the aircraft. Depending on the scanning pattern, the vertical resolution of the wind profiles is 25-50m and the horizontal resolution is 1-2km. Below the aircraft, the instrument can observe winds at or near the surface (~25m). When sampling above the aircraft, it can observe as high as ~14km (in the presence of high cirrus). However, in the presence of optically thick convection or within ~400m of the instrument, P3DWL is unable to collect measurements.

This instrument was previously used in the West Pacific field campaign THORPEX in 2008 for typhoon research (Pu et al. 2010). The study showed P3DWL data collected in the near storm environment improved both the track and intensity of a TC forecast. The main goal of this experiment is to build upon those results and collect both near storm and inner core observations. The observations will be used in Observing System Experiments (OSEs) to assess the impact of P3DWL data on TC track and intensity forecasts. A secondary goal is to use the data to understand physical processes in data sparse regions such as in the boundary layer, Saharan Air Layer (SAL), regions in-between rainbands, and in the ambient tropical environment in and around the TC. Each module describes the observations the P3DWL should collect given the location of the plane and the structure of the TC. The P3DWL will require an onboard operator during each mission.

Objectives:

- Collect P3DWL observations in a variety of regions both in and near different types of TCs;
- Validate P3DWL observations against dropsonde and Tail Doppler Radar data;
- Evaluate P3DWL measurements on numerical analyses and forecasts for TC track, intensity and structure;
- Observe and characterize various features in the TC near environment and inner core (listed below):
o The Saharan Air Layer (SAL) and mid-level easterly jet (~600-800 hPa)
o Boundary layer (BL) heights and rolls
o Kinematic structure in region between two concentric eyewalls or the moat region between two rainbands

Model Evaluation Component:

OSEs will be performed using both the line of sight (LOS) data and the post-processed vector wind data product to determine the impact of P3DWL observations on the analyses of TC structures, track, and intensity forecasts.

Observations collected from the P3DWL in conjunction with other observing platforms will be used to evaluate the model representation of different aspects of a TC, such as the boundary layer, SAL intrusions, and sheared TCs. Multiple modeling frameworks are expected to be used. Options include the operational HWRF model, the latest Observing System Simulation Experiment (OSSE) system, and the HEDAS-HWRF setup.

OSSE Component:

Observing System Simulation Experiments (OSSEs) can provide useful information regarding the potential impact of P3DWL observations on TC structure, track, and intensity forecasts. OSSEs will be performed during the 2016 Atlantic hurricane season to investigate the suggested flight pattern and P3DWL observing plans for each module. Results from the OSSEs will be compared to averaged result from the OSEs (described in the previous section) after the conclusion of the season. Analysis work will include comparisons of 1) simulated to real observations, 2) track and intensity errors, and 3) impact of P3DWL on TC structure. Calibration of the OSSE system may occur after the analysis work is complete. The latest hurricane OSSE framework will be used in both the OSSEs and OSEs.

Mission Description:

While this experiment is presented as a standalone activity, the following modules may be performed during any of the following HRD research missions: TC Genesis, TC Shear Experiment, Rapid Intensity Experiment, or as part of operational NHC-EMC-HRD Tail Doppler Radar (TDR) missions. This experiment includes 4 types of modules: 1) asymmetric TC module, 2) SAL/Transit module, 3) boundary layer module, and 4) rainband moat module. Each module describes what region(s) of the TC to target with the P3DWL in different types of TCs.

Module 1- Asymmetric TC

The objective of this module is to provide symmetric coverage of the kinematic field in an asymmetric storm. The P3DWL will provide observations in low/no precipitation regions of a TC to complement the observations collected by the TDR. The combination of observations from these two platforms will be used to improve the initial structure of the TC in model analyses.

This module can be combined with other experiments such as TC Shear or TDR missions. The only pattern requirement is a symmetric coverage of an asymmetric TC (either a rotated Figure-4 or butterfly pattern). The preferred flight-level altitude is 8,000-10,00 feet and GPS dropsondes should be deployed at the end, mid, RMW, and center points of the flight pattern. Dropsonde data will be used to validate and develop quality control measures for the P3DWL vector wind product. Dropsonde observations will also be used to provide information in the boundary layer of the low/no precipitation portion of the TC.

In the regions of higher convection/precipitation, the P3DWL should be operated in the downward looking direction. The scanning mode should repeat a 20° conical pattern followed by a 1 second nadir stare. In the regions of the TC where there is low/no precipitation, the P3DWL should be placed in an upward looking direction. The scanning mode should be a 20° conical pattern, with a 1 second vertical stare after completing the pattern. Sufficient signal strength with the upward scan is important. If signal strength is poor due to lack of aerosols/high cirrus clouds, then return the P3DWL to the downward scanning mode. The scanning mode should not be switched from upward to downward often. Ideally this module should be chosen if half the storm is covered with convection, while the other half lacks precipitation.

Module 2- SAL/Transit Module

The objective of this module is to characterize the suspended Saharan dust and mid-level (~600-800 hPa) easterly jet that are associated with the SAL with a particular focus on SAL-TC interactions. Observations should target the possible impingement of the SAL mid-level jet and suspended dust along the edges of the storm inner core region. It can be conducted between the edges of the storm's (African Easterly Wave's (AEW)) inner core convection

(deep convection) to points well outside (several hundred kilometers) of the TC environment during the commute to/from the storm. There are no minimum leg lengths required. The aircraft should fly at the maximum allowable flight-level (~19,000 feet).

The P3DWL should be placed in a downward looking scanning mode. The preferred scanning mode is a conical pattern with an elevation angle of 10°. If that pattern is not collecting the necessary observations, a down and forward sweeping pattern can be used (elevation 20°, sweep -10° to +10° with 5° intervals). GPS dropsonde sampling along the transect will be used to observe the SAL's thermodynamics and winds as well as to validate the P3DWL's wind retrievals. Drop points should be spaced at ~25-50 nm increments near the region where the SAL is impinging on the storm/AEW and spaced at 50-75 nm increments farther from the storm (Fig. 3-1). GPS dropsonde spacing will be determined on a case by case basis at the lead project scientist's (LPS's) discretion.

If no SAL is present, the P3DWL should still collect observations during the transit to/from the TC. It should be placed in the downward scanning mode, with the preferred scanning mode being a 10° conical pattern. The operator should ensure the P3DWL is returning a signal from the surface. No GPS dropsondes are necessary, however, one may be dropped for the purpose of validating the P3DWL observations.
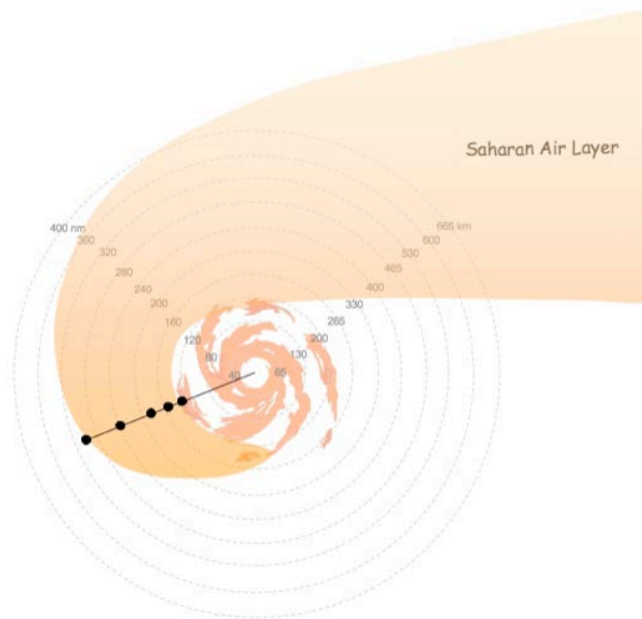
Fig. 3-1: Sample WP-3D flight track during the ferry to/from the storm and GPS dropsonde points for the P-3DWL SAL module.

Module 3- Boundary Layer Module

This module will target sampling of the kinematic structure of the boundary layer with focus on investigating the characteristics of the boundary layer height and coherent structures. The purpose of this data will be to improve the initial state of the HWRF model and validate the boundary layer structures represented in the model.

This module can be combined with other experiments and modules as it does not require a specific flight track. A symmetric coverage of the TC is preferred and TCs of all intensities should be sampled. The P3DWL should be placed in a downward scanning pattern. The preferred scanning mode is conical with an elevation angle of 10° and a 1 second stare at nadir.   If that pattern is not collecting the necessary data, a down and forward sweeping pattern can be used (elevation 20°, sweep -10° to +10° with 5° intervals). It is important optically thick convective be avoided as often as possible and the operator should ensure the P3DWL is returning a signal from the sea surface.

Module 4- Eyewall Replacement/Rainband Moat Module

This module will characterize the upper level subsidence and boundary layer kinematics within the region between two concentric eyewalls and/or within a rainband moat. It should only be performed in a stronger, more organized TC that contains either classic rainband structures (including a moat) or during an eyewall replacement cycle. The P3DWL should target the moat region and collect observations to complement data from the TDR.

This module does require a circumnavigation flight pattern, which will take ~1 hour to perform (depending on the size of the TC). It can be flown in conjunction with other experiments, such as TDR missions, as was done in Hurricane Arthur (2014). The aircraft should fly in an octagon pattern within the moat region, avoiding the optically thick deep convection in the eyewall and rainbands (Fig. 3-2; also see the SEF/ERC Experiment write-up). The P3DWL should be placed in an upward scanning pattern. The preferred scanning mode is a repeating conical pattern with an elevation angle 20° off vertical and a 1 second stare in the vertical. Sufficient signal strength with the upward scan is important. If signal strength is poor due to lack of aerosols/high cirrus clouds, then the P3DWL should be placed in the downward scanning mode. A GPS dropsonde should be deployed in each quadrant of the storm during the pattern. Quadrants should be defined based on the storm motion vector, and drops should be centered with the quadrant.

If there is opportunity to do a second circumnavigation, the P3DWL should be placed in a downward scanning pattern. GPS dropsondes may again be deployed for validation purposes of the P3DWL observation, however, they should be staggered 45° relative to the storm center from the previous deployed dropsondes.
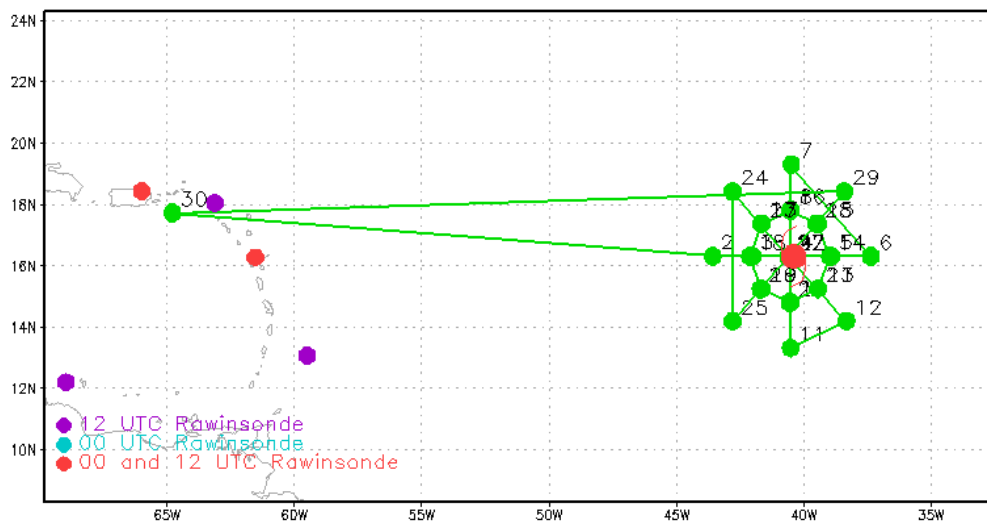
Fig. 3-2: Sample WP-3D flight track during a Moat Module. Pattern shows an initial Figure-4 pattern, followed by a circumnavigation that leads in a second Figure-4.

4. Small Unmanned Aerial Vehicle Experiment (SUAVE)

Primary IFEX Goal: 2 - Develop and refine measurement technologies that provide improved real-time monitoring of TC intensity, structure, and environment

Link to the model evaluation activities:: Conducting the UAS modules listed in this experiment (stand alone or as part of other HFP efforts) will enable enhanced high resolution comparisons between tropical cyclone boundary observations of temperature, moisture and wind with similar thermodynamic and kinematic output from NOAA's regional and global operational models.

Principal Investigator(s): J. Cione (HRD)

Co-Investigators: Module 1a: S. Aberson (HRD); Module 2: J. Zhang (HRD), G Barnes (UH); Module 3: J. Zhang; Module 4: C. Landsea (NHC); M DeMaria (NHC); Module 5: E. Kalina (HRD/PSD), G. Bryan (NCAR), C. Fairall (PSD)

Coyote UAS

Coyote is an aircraft platform that is built by the Raytheon Company (formerly Sensintel Corporation and British Aerospace Engineering (BAE)) and is currently being used by the US NAVY. The intended deployment vehicle for the Coyote is the P-3 Orion. The Coyote is a small electric-powered unmanned aircraft with 1-3 hour endurance and is capable of carrying a 1-2lb payload. The Coyote can be launched from a P-3 sonobuoy tube in flight, and terrain-permitting, is capable of autonomous landing and recovery. The Coyote is supported by BAE's integrated control station, which is capable of supporting multiple aircraft operations via touch screens that simultaneously show real-time video. This control station can also be incorporated onto the deployment aircraft (i.e. P-3), allowing for in-air command and control after launch. The Coyote, when deployed from NOAA's P-3's within a hurricane environment, provide a unique observation platform from which the low level atmospheric boundary layer environment can be diagnosed in great detail. In many ways, this UAS platform be considered a 'smart GPS dropsonde system' since it is deployed in similar fashion and currently utilizes a comparable meteorological payload (i.e. lightweight sensors for P, T, RH, V) similar to systems currently used by NOAA on the GIV and P-3 dropsonde systems. Unlike the GPS dropsonde however, the Coyote UAS can be directed from the NOAA P-3 to specific areas within the storm circulation (both in the horizontal and in the vertical). Also unlike the GPS dropsonde, Coyote observations are continuous in nature and give scientists an extended look into important thermodynamic and kinematic physical processes that regularly occur within the near-surface boundary layer environment. Coyote UAS operations also represent a potentially significant upgrade relative to the more traditional "deploy, launch and recover" low altitude UAS hurricane mission plan used in the past (e.g. Aerosonde). By leveraging existing NOAA manned aircraft assets, Coyote operations significantly reduce the need for additional manpower. The Coyote concept of operations also reduces overall mission risk since there is no flight ingress/egress. This fact should also help simplify the airspace regulatory approval process. Specifications associated with the Coyote UAS are illustrated in Figure 4-1.

Coyote Specifications

Parameter	Value (U.S.)	Value (Metric)
Maximum Gross Takeoff Weight (MGTW)	14 lbs	6.4 kg
Nominal Mission Takeoff Weight (NMTW)	12 lbs	5.4 kg
Nominal Mission Endurance	1.5 Hours	
Motor	Brushless Electric Motor	
Airspeed (Cruise @ NMTW)	50 kts	93 kph
Airspeed (Dash - level flight @ NMTW)	75 kts	140kph
Airspeed (Max. Endurance @ NMTW)	45 kts	83kph
Airspeed (Stall @ NMTW)	38 kts	70kph
Airspeed (VNE @ NMTW)	100 kts	185kph
Navigation	GPS	
Service Ceiling	25,000 feet	7,610 meters
Payload (EO)	Sony FCB-IX10A EO Camera	
Payload (IR)	BAE SCC500, Uncooled IR	
Command and Control Radio (C2)	Up to 2 Watt, Discrete/Frequency Agile, Military Band / ISM Band Radio Modem (TX/RX)	
Command and Control Radio Range	20 nm, Line of Sight (LOS)	36 km, Line of Sight (LOS)
Video Transmitter	2 Watt (optional 5W), S-Band FM Video TX With Optional 19.2kbps Data Carrier	
Video Transmission Frequency Range	2.20-2.39 GHz	
Video System Range	20 nm, LOS	36 km, LOS
Payload Capacity	Up to 5 lbs	Up to 2.25 kg
Onboard Power	12V, 200Wh	
Propulsion	13x13 Foldable Propeller	

3292 East Hemisphere Loop · Tucson, Arizona 85706
T: 520.573.6300 · F: 520.573.2057 · www.acrtucson.com

Figure 4-1. Coyote Unmanned Aerial System Specifications (Courtesy: Raytheon)

Relevance to NOAA

In recent years, an increasing number of hurricanes have impacted the United States with devastating results, and many experts expect this trend to continue in the years ahead. In the wake of Hurricane Sandy (2012), NOAA is being looked at to provide improved and highly accurate hurricane-related forecasts over a longer time window prior to landfall. NOAA is therefore challenged to develop a program that will require applying the best science and technology available to improve hurricane prediction without placing NOAA personnel at increased risk. UAS are an emerging technology in the civil and research arena capable of responding to this need.

In late February 2006, a meeting was held between NOAA, NASA and DOE partners (including NOAA NCEP and NHC representatives) to discuss the potential for using UAS in hurricanes to take measurements designed to improve intensity forecasts. The group came to a consensus around the need for a UAS demonstration project focused on observing low-level (<200 meters) hurricane winds for the following reasons:

- Hurricane intensity and track forecasts are critical at sea level (where coastal residents live)

- The hurricane's strongest winds are observed within the lowest levels of the atmosphere

- The air-sea interface is where the ocean's energy is directly transferred to the atmosphere

- Low-level observations will help improve operational model initialization and verification (especially boundary layer observations of temperature and moisture which are especially sparse)

- The low-level hurricane environment is too dangerous for manned aircraft

The potential importance of low-level UAS missions in hurricanes is further emphasized by the findings of the Hurricane Intensity Research Working Group established by the NOAA Science Advisory Board. Their recommendation is that:

"Low and Slow" Unmanned Aircraft Systems (UAS) have demonstrated a capacity to operate in hurricane conditions in 2005 and in 2007. Continued resources for low altitude UAS should be allocated in order to assess their ability to provide in situ observations in a critical region where manned aircraft satellite observations are lacking.

This effort is in direct support of NOAA's operational requirements and research needs. Such a project will directly assist NOAA's National Hurricane and Environmental Modeling Centers better meet several of their operational requirements by helping to assess:

> The strength and location of the storm's strongest winds

> The radius of maximum winds

The storm's minimum sea level pressure *(potentially give forecasters advanced warning as it relates to dangerous episodes of tropical cyclone rapid intensification)*

Thermodynamic conditions (particularly low level moisture) within the lower troposphere

In addition to these NOAA operational requirements, developing the capability to regularly fly low altitude UAS into tropical cyclones will also help advance NOAA research by allowing scientists to sample and analyze a region of the storm that would otherwise be impossible to observe in great detail (due to the severe safety risks associated with manned reconnaissance). It is believed that such improvements in basic understanding are likely to improve future numerical forecasts of tropical cyclone intensity change. Reducing the uncertainty associated with tropical cyclone intensity forecasts remains a top priority of the National Hurricane Center. Over time, projects such as this, which explore the utilization of unconventional and innovative technologies in order to more effectively sample critical regions of the storm environment should help reduce this inherent uncertainty.

This HRD field program module is designed to build on the successes from earlier NOAA UAS missions conducted in 2005 (Ophelia) and 2007 (Noel) while also fulfilling objectives from the recently funded Sandy Supplemental project entitled: *The Impact of Emerging Observing Technologies on Future Predictions of*

Hurricane Structure and Intensity Change. As part of this NOAA supported effort, all UAS data collected will be made available to NOAA's National Hurricane and Environmental Modeling Centers.

General Coyote UAS Mission Description:

The primary objective of this experiment is further demonstrate and utilize the unique capabilities of a low altitude UAS platform in order to better document areas of the tropical cyclone environment that would otherwise be either impossible or impractical to observe. For this purpose, NOAA is proposing to use the Coyote UAS. Since the Coyote will be deployed from the manned P-3 aircraft, no UAS-specific forward deployment teams will be required. Furthermore, since the Coyote is launched using existing AXBT launch infrastructure, no special equipment is required beyond a 'ground' control station that Coyote operators will have onboard the P-3.

Module/Option 1a: UAS Eye/Eyewall with P-3 loiter-

For this module the target candidate storm is a mature hurricane (likely strong category 2 or more) with a well-defined eye. Furthermore, since the P-3 will have to operate within the eye, daylight missions will be required so as to maintain P-3 visual contact with the eyewall at all times. In addition, other less restrictive Coyote-P3 modules are being developed and considered (see Module 1b). A 350-MHz communication stream between the UAS and the P-3 will be used to control the UAS flight characteristics and to receive data back from the Coyote. This capability will have the dual positive effect of minimizing risk to both science and safety, since the 350-MHz stream will permit communication over a range of at least 50 km. The immediate focus of this experimental module will be to test the operational capabilities of the Coyote UAS within a hurricane environment. Besides maintaining continuous command and control links with the P-3, these flights will test the accuracy of the new ITRI METOC payload by comparing UAS measurements with coincident observations taken from dropsondes released from the P-3. The UAS will be tested to see if it can maintain altitudes according to command. In addition, the Coyote UAS will attempt to fly at extreme altitudes (as low as 200 ft) in low (eye) and high (eyewall) wind conditions within the hurricane environment. The longer term goal for this UAS platform is to assist scientists so they can better document and ultimately improve their understanding of the rarely-observed tropical cyclone boundary layer. To help accomplish this, the UAS will make detailed observations of pressure, temperature, humidity, wind speed and wind direction (PTHU) at low altitudes within the hurricane eye and eyewall that will then be compared with multiple in-situ and remote-sensing observations obtained from manned aircraft (NOAA P-3 and as opportunities arise AFRES C-130, Global Hawk UAS) as well as select satellite-based remote sensor platforms. In addition, a primary objective (but not an immediate requirement) for this effort will be to provide real-time, near-surface wind observations to the National Hurricane and Environmental Modeling Centers in direct support of NOAA operational requirements. These unique data will also be used in a 'post storm' analysis framework in order to potentially assist in the numerical and NHC verification process.

For this experiment, the NOAA P-3 will descend to just above the top of the cloud layer in the eye (Fig. 4-2), and return to the previous altitude when the module is concluded. Assuming multiple UAS are available, both (~1.5h duration) modules could be conducted on the same mission. The eye-only module would be conducted first, followed by the eye-eyewall UAS module. The P-3 flight pattern is identical for both eye and eye-eyewall UAS modules. GPS dropsonde and AXBT drop locations are also identical for each UAS module. AXBT and GPS drop locations are explicitly illustrated in the flight plan below. UAS deployment on leg 3-4 is also identical for both modules. UAS operational altitude will be entirely below 5000ft. UAS motor will not be activated until an altitude of 5000ft is met. The UAS will be conducting a controlled, spiral glide (un-powered) descent from 10000ft to 5000ft.

Coyote UAS - P3 Mature Hurricane Eye/Eyewall Module
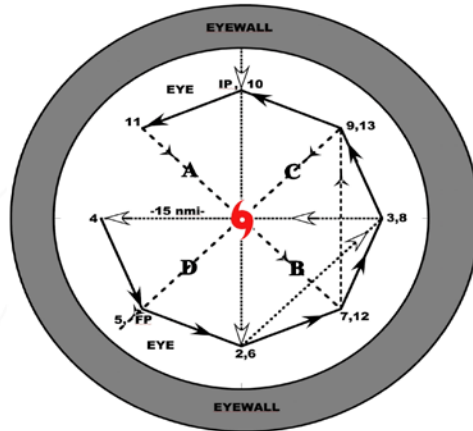
P-3 FLIGHT PATTERN

The P-3 approaches from the north at an altitude of 10,000ft, penetrates the eyewall into the eye, and performs a figure-4 (dotted line) in the eye. **Midway during leg 3-4 the Coyote UAS is released.** The P-3, remaining at 10,000ft, circumnavigates the eye in an octagon pattern and conducts another figure-4 rotated 45 degrees from the original (dashed line). Flight duration for this module should be close to 1 hour. An add-on ~45 minute duration module may also be conducted. This optional module would initiate where the preceding module ended (point 'FP'). The P-3 would proceed counterclockwise, repeating points 6-13 and completing the pattern once again at point 'FP'. **14 Dropsonde releases** should be conducted during the primary 1h module at the following locations: IP;2-5;7;9;11;A-D and midway during legs IP-2 and 13-FP. In addition, **9 AXBT launches** should be conducted at points 4 through 11 and midway during leg 11-12. (Note: except for AXBT drop at point 4, it is acceptable to launch all remaining 8 AXBT probes during the optional 45 minute second module.)
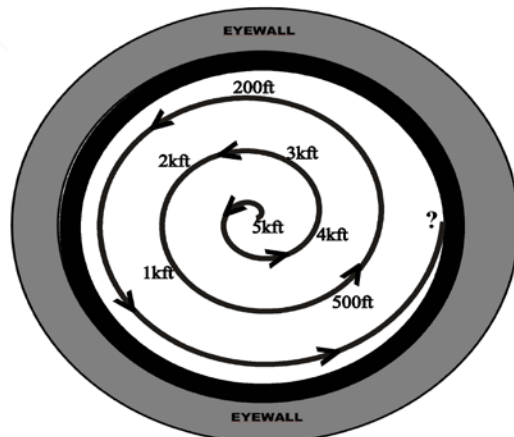
COYOTE UAS FLIGHT PATTERN (EYE ONLY)

Midway during P-3 leg 3-4, the Coyote UAS is released at 10,000ft altitude. The Coyote UAS proceeds to glide (unpowered) in a downward counterclockwise spiral to an altitude of 5,000ft. **At 5000ft, the UAS motor is started and the Coyote continues its counterclockwise descent in 1000ft increments.** At each interval (4kft,3kft,2kft,1kft), the UAS maintains altitude for 3 minutes prior continuing its counterclockwise, radially expanding with decreasing altitude, spiral descent. After 3 minutes at 1000ft, the Coyote descends to 500ft and remains at this altitude for 3 minutes. **The UAS continues to descend in 100ft increments down to 200ft, maintaining altitude for 3 minutes at each level.** The remainder of the flight is conducted at 200ft until battery power is fully expended and the UAS reaches the ocean surface. (Note: If full descent to 200ft is achieved and the UAS has sufficient battery power to continue, **an optional 'eyewall penetration' module may be considered** if conditions present themselves. Prior to any attempted UAS eye-eyewall penetration, the Coyote should ascend from 200ft to a (minimum) altitude of 500ft.)

Coyote UAS - P3 Mature Hurricane Eye/Eyewall Module
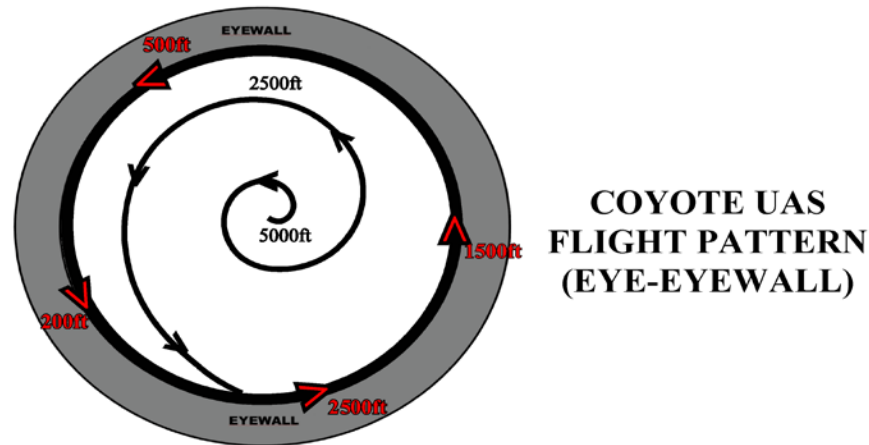
Midway during P-3 leg 3-4, the Coyote UAS is released at 10,000ft altitude. The Coyote UAS proceeds to glide (unpowered) in a downward counterclockwise spiral to an altitude of 5,000ft. At 5000ft, the UAS motor is started and the Coyote continues its counterclockwise descent to 2500ft. **The UAS maintains 2500 ft altitude and continues its outward counterclockwise spiral until it reaches the hurricane eyewall.** Once the Coyote penetrates and stabilizes **within the hurricane eyewall, the UAS begins a step-decent pattern from 2500ft down to 500ft** (while maintaining altitude for 3 minutes at each level). After reaching and maintaining 500ft for 5 minutes begin a steady decent down to 200ft within the eyewall. **Maintain 200ft altitude within the hurricane eyewall until battery power is fully expended and the UAS reaches the ocean surface.**

Figures 4-2a-c. (P-3 eye, UAS eye, UAS eyewall)

Module/Option 1b: UAS Eye/Eyewall *without* P-3 loiter-

This module is identical to Module 1a with the notable exception that the P-3 does not loiter in the eye. For this module, the target storm can be weaker than in Module 1a (e.g. Category 1) since the P-3 will not loiter in the eye after releasing the UAS at altitude near the TC center of circulation. This module can be conducted in the day time or at night. The UAS patterns identified in Module 1a remain the same for Module 1b. However, the P-3 pattern for Module 1b would include repeated eyewall penetrations using a rotating figure 4 pattern (see Figure 4-3 below). So as to maximize the ability to compare P-3 based observations with UAS observations (primarily PTHU from GPS dropsondes and winds from Doppler radar) the radial legs for the P-3 aircraft should be kept to a minimum in order to maximize the number of eye/eyewall penetrations. For this reason legs $\leq$ 40nm (measured from the IP to TC center) are preferred. Default P-3 penetration altitude is set to 10,000ft but can be adjusted as mission or storm specific conditions dictate.

For this module, GPS sondes will be released at all leg endpoints, directly in the eyewall and within the eye. This translates to 5 GPS when measured from leg end point to leg end point. In addition, AXBTs will be launched at all end points and for each eyewall penetration, which equates to 4 AXBTs per 'end point to end point' leg flown. The total number of GPS and AXBT deployed will depend upon how many penetrating legs are conducted. Based on the P-3 leg configuration described above, and assuming a 1hr UAS flight duration, 3 full penetrations should be possible.

34
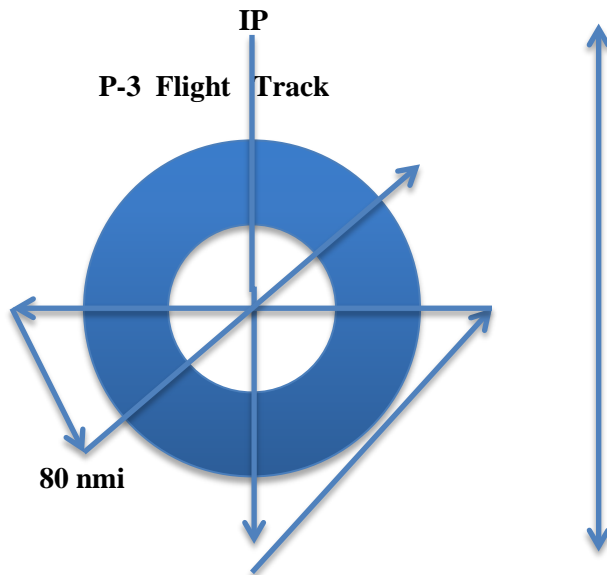
Figure 4-3. (P-3 'short leg' figure 4 pattern)

Module/Option 2: Boundary Layer Entrainment/Convective Downdraft module-

This module builds upon and complements the existing 'Boundary Layer Entrainment' (see HFP 2013, experiment 14 for additional details). No modifications to the existing P-3 patterns are required for this module. Instead, the low flying Coyote UAS will conduct very low (down to 100m) stepped descents in addition to patterns flown by the P-3 manned aircraft (see Figure 4-4). These very low altitude UAS patterns should allow for (a more direct) estimation of surface fluxes. In turn, the UAS-derived estimates can then be compared with surface fluxes computed by sampling the top of the boundary layer (residual method). In addition, it is also possible to conduct a UAS box pattern at 100-120m to complement the P-3 1-2km box pattern (not shown) that was designed to estimate divergence in precipitation-free areas.

It should also be noted that an additional goal of this module is to see how vertical mixing occurs above and within the boundary/surface layer just outside areas of active convection (e.g. near rainbands and radially outward of the TC's primary convective envelop). A goal of this module is to compare observational details from these convectively driven processes with comparable output from high-resolution operational regional and global model simulations.
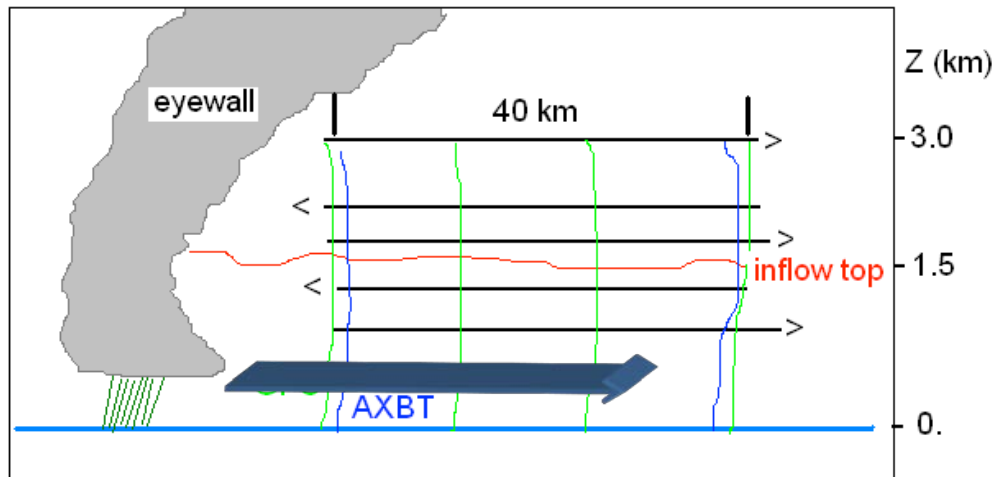
Figure 4-4. (From HFP Boundary Layer Entrainment Module) Vertical cross-section of the stepped-descent module. P3 pattern is in black, low altitude Coyote UAS in heavy blue.

Module/Option 3: Enhanced Boundary Layer Inflow Sampling-

This module builds upon the existing 'Boundary Layer Inflow experiment (see HFP 2012, experiment 16 for additional details). As in Modules 1-2, the P-3 pattern remains unchanged. At the IP the Coyote is released and slowly step descends down to 100m as it spirals inward (See Figure 4-5 below). Once at 100m the UAS step ascends up to an altitude just above the inflow layer (~1.5km). Then again descends to 100m. This process continues until eyewall penetration occurs at 500m. Once in the eyewall the UAS step descends in 50m increments every 5 minutes until it reaches 50m and maintains altitude until battery failure.

This module extends work originally conducted by Cione et al. in 2000. It also expands the capabilities associated with the original BLI experiment by providing continuous (vs. instantaneous) data at altitudes, radii and azimuths not previously sampled by GPS sonde deployments. In addition, these UAS data will help capture additional vertical variability associated with the inflow layer as a function of radius from the storm center. Once in the eyewall, UAS observations will provide wind and thermodynamic data utilizing a highly unique step descent eyewall orbiting sampling strategy.

Depending on storm conditions and other factors, it may be possible to combine portions of UAS Modules 2 and 3 into one UAS mission.
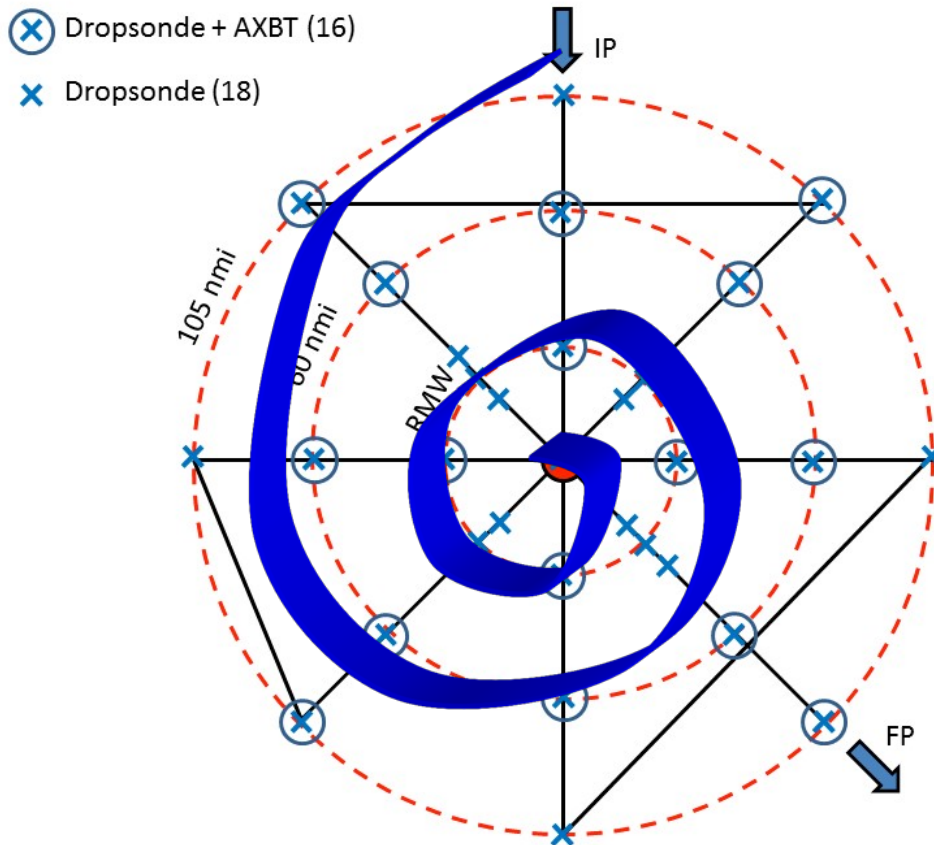
Figure 4-5 *(from the HFP Boundary Layer Inflow Experiment): Boundary Layer Inflow Module. GPS dropwindsondes (34 total) are deployed at 105 nmi and 60 nmi radii and at the radius of maximum wind along each of 8 radial legs (rotated alpha/Figure-4 pattern). On 4 of the 8 passes across the RMW, rapid deployment (~1 min spacing) of 3 sondes is requested. Center drops are requested on the initial and final pass through the eye. AXBT (16 total) deployments are paired with dropsondes at the indicated locations. Flight altitude is as required for the parent TDR mission, and initial and final points of the pattern are dictated by these same TDR mission requirements. Projected Coyote UAS spiral inflow pattern (in heavy blue) is overlayed.*

Module/Option 4: Radius of Maximum Wind (RMW) Mapping-

As in Modules 1-3, the P-3 pattern remains unchanged. After Coyote launch in the eye, the UAS would descend to as low a level as feasible (300 m would be ideal, but 500 to 1000 m would still be of interest) and head outward toward the eyewall and radius of maximum wind (Fig. 4-6). After reaching the RMW, the Coyote would continue outbound and downwind until the winds drop off by 10-20%, perhaps 20-40 nm outside the RMW. Then the UAS would turn inbound and downwind crossing the RMW and reaching the eye. This sequence would continue for the duration of the mission.

One difficulty with this plan may be in fighting the strong boundary layer inflow while trying to fly outbound across the eyewall/RMW. Flying the mission higher (closer to 1000 m vs 30 m) may be required. Mapping out the

low-level RMW all the way around a hurricane would be a unique capability, which would be of considerable use in operations.
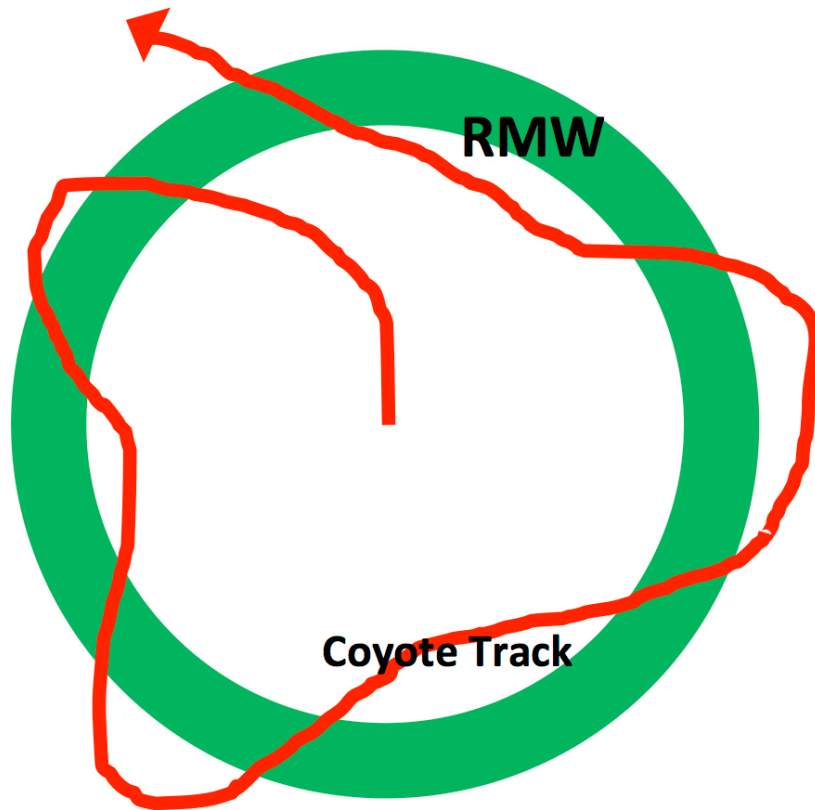
Figure 4-6: *Radius of Maximum Wind (RMW) Mapping. For this module the NOAA P3 pattern is shown in Figure 4-2a. P3 would not be required to continuously loiter. However, P3-UAS range considerations would need to be taken into consideration. Optimally up to 10 GPS/IR sondes would be deployed along with 5 AXBTs. These data would be used to compare with similar ocean/atmospheric data collected by the Coyote UAS. Coyote UAS track is shown in red while the hurricane RMW is denoted by a green ring. Once the UAS is deployed from the P3 within the eye, the Coyote descends to the desired altitude of 300m. Once at this level, the UAS proceeds to the eyewall and begins a counter clockwise flight path. Once the RMW is reached, the UAS continues radially outward and downwind until the maximum wind attained by the platform decreases by ~10-20%. Once this is level is achieved, the Coyote heads inbound and downwind until it enters the storm eye. This sequence would continue for the duration of the mission.*

Module/Option 5: Eddy Dissipation Rate Measurements

For this module, the target storm is a hurricane of any intensity, since low-altitude measurements of eddy dissipation rate and other turbulent quantities are rare in winds of 35 m s^{-1} and greater. To complete this module, approximately 30 minutes of battery life are required. Therefore, this experiment does not need to be the sole focus of a particular Coyote flight. Instead, the eddy dissipation rate measurements can be made following a Coyote eyewall penetration (Module 1) or at the conclusion of the Boundary Layer Inflow experiment (Module 3) or the Radius of Maximum Wind Mapping experiment (Module 4), both of which terminate with the Coyote near or in the eyewall.

The objective is to collect measurements of eddy dissipation rate in strong wind conditions (35 m s^{-1} or greater), with a focus on how the dissipation rate changes with altitude in the lower portion of the tropical cyclone boundary layer and in the surface layer. It is therefore preferable for the Coyote to remain at a constant radius from the tropical cyclone center (ideally at the radius of maximum wind) throughout the experiment. This will prevent the height-dependence of eddy dissipation from being confused with any dependence on distance from the tropical cyclone center.

Figure 4-7 is a schematic of the experimental design. The experiment will begin with the Coyote at a height of 350 m, in the eyewall and/or at the radius of maximum wind. The Coyote then will initiate and maintain a constant descent rate of $1/6 = 0.167$ m s^{-1}. This descent rate was chosen because it will allow the Coyote to descend to a height of 50 m at the end of the 30-minute period. At this point, the Coyote may continue to descend at the constant rate, but errors in the GPS vertical position of up to 30 m and waves up to 20 m tall could end the Coyote flight shortly thereafter.

The only requirement of the P-3 flight pattern for this module is that the P-3 remains within 50 km of the Coyote position during the experiment (to prevent loss of communication between the two platforms). This proximity requirement can be satisfied either by the P-3 loitering within the eye (see Module 1a; Fig. 2a) or by the P-3 completing multiple passes through the eye and eyewall using a rotated figure-four pattern with shortened legs (see Module 1b; Fig. 3). The second option may only be feasible in storms with a small radius of maximum wind (15 km or less), since the distance between the P-3 and the Coyote will at times exceed twice the radius of maximum wind when the P-3 samples the opposite side of the storm.
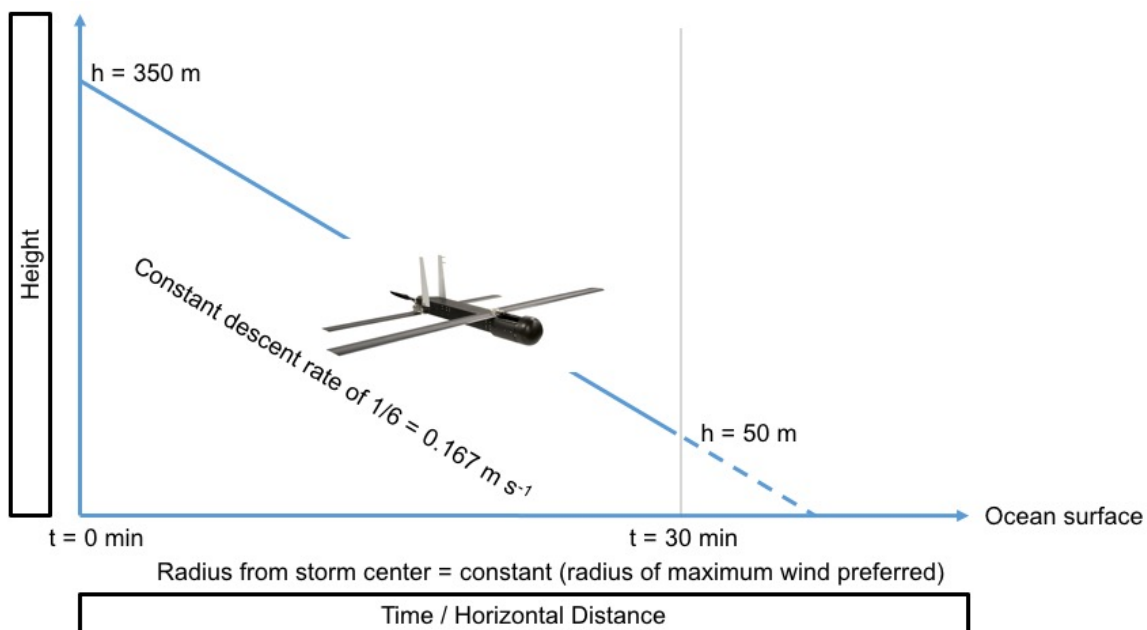
Figure 4-7: *Eddy dissipation measurements. The Coyote begins the experiment at a height of 350 m, descends at a constant rate of $1/6 = 0.167$ m s^{-1}, and reaches a height of 50 m after 30 minutes. The entire descent is conducted at a constant radius from the storm center (preferably at the radius of maximum wind).*

<center>**5. NESDIS Ocean Winds and Rain Experiment**</center>

Principal Investigator: Paul Chang (NESDIS)

Primary IFEX Goal: 2 - Develop and refine measurement technologies that provide improved real-time monitoring of TC intensity, structure, and environment

Motivation: This effort aims to improve our understanding of microwave scatterometer retrievals of the ocean surface wind field and to evaluate new remote sensing techniques/technologies. The NOAA/NESDIS/Center for Satellite Applications and Research in conjunction with the University of Massachusetts (UMASS) Microwave Remote Sensing Laboratory, the NOAA Hurricane Research Division, and the NOAA Aircraft Operations Center have been conducting flight experiments during hurricane season for the past several years. The Ocean Winds experiment is part of an ongoing field program whose goal is to further our understanding of microwave scatterometer and radiometer retrievals of the ocean surface winds in high wind speed conditions and in the presence of rain for all wind speeds. This knowledge is used to help improve and interpret operational wind retrievals from current and future satellite-based sensors. The hurricane environment provides the adverse atmospheric and ocean surface conditions required.

The Imaging Wind and Rain Airborne Profiler (IWRAP), which is also known as the Advanced Wind and Rain Airborne Profiler (AWRAP), was designed and built by UMass and is the critical sensor for these experiments. IWRAP/AWRAP consists of two dual-polarized, dual-incidence angle radar profilers operating at Ku-band and at C-band, which measure profiles of reflectivity and Doppler velocity of precipitation in addition to the ocean surface backscatter. The Stepped-Frequency Microwave Radiometer (SFMR) and GPS dropsonde system are also essential instrumentation on the NOAA-P3 aircraft for this effort. The NASA GORE (GNSS reflection) system is also desired to provide measurements to support the NASA CYGNSS mission.

The Ocean Winds P-3 flight experiment program has several objectives:
- Calibration and validation of satellite-based ocean surface vector wind (OSVW) sensors such as ASCAT and OSCAT.
- Product improvement and development for current and planned satellite-based sensors (ASCAT, RapidScat, ScatSat, CYGNSS and SCA)
- Testing of new remote sensing technologies for possible future satellite missions (risk reduction) such as the dual-frequency scatterometer concept. A key objective for this year will be the collection of cross-polarized data at C-band to support ESA and EUMETSAT studies for the ASCAT follow- on (SCA), which will be part of EPS-SG.
- Advancing our understanding of broader scientific questions such as:
o   Rain processes in tropical cyclones and severe storms: the coincident dual-polarized, dual- frequency, dual-incidence measurements would enable us to improve our understanding of precipitation processes in these moderate to extreme rainfall rate events.
o   Atmospheric boundary layer (ABL) wind fields: the conical scanning sampling geometry and the Doppler capabilities of this system provide a unique source of measurements from which the ABL winds can be derived. The raw data system will enable us to use spectral techniques to retrieve the wind field all the way down to the surface.
o   Analysis of boundary layer rolls: linearly organized coherent structures are prevalent in tropical cyclone boundary layers, consisting of an overturning "roll" circulation in the plane roughly perpendicular to the mean flow direction. IWRAP has been shown to resolve the kilometer-scale roll features, and the vast quantity of data this instrument has already collected offers a unique opportunity to study them.
o   Drag coefficient, Cd: extending the range of wind speeds for which the drag coefficient is known is of paramount importance to further our understanding of the coupling between the wind and surface waves under strong wind forcing, and has many important implications for hurricane and climate modeling. The new raw data capability, which allows us to retrieve wind profiles closer to the ocean surface, can also be exploited to derive drag coefficients by extrapolating the derived wind profiles down to 0 m altitude.

Flight Profiles:

Altitude:
The sensitivity of the IWRAP/AWRAP system defines the preferred flight altitude to be below 10,000 ft to enable the system to still measure the ocean surface in the presence of rain conditions typical of tropical systems. With the Air Force typically flying at 10,000 ft pressure this, we have typically ended up with an operating altitude of 7,000 ft radar. Operating at a constant radar altitude is desired to minimize changes in range and thus measurement footprint on the ground. Higher altitudes would limit the ability of IWRAP/AWRAP consistently see the surface during precipitation, but these altitudes would provide useful data, such as measurements through the melting layer, to study some of the broader scientific questions.

Maneuvers:
Straight and level flight with a nominal pitch offset unique to each P-3 is desired during most flight legs. Constant bank circles of 10-30 degrees have been recently implemented, as a method to obtain measurements at incidence angles greater than the current antenna was design for. These would be inserted along flight legs where the desired environmental conditions were present. Generally it would be a region of no rain and where we might expect the winds to be consistent over a range of about 6-10 miles, about the diameter of a circle. This would not be something we would want to do in a high gradient region where the conditions would change significantly while we did the circle.

Patterns:
Typically an ideal ocean winds flight pattern would include a survey pattern (figure 4 or butterfly) that extended 20-50 nm from the storm center. The actual distance would be dictated by the storm size and safety of flight considerations. Dependent upon what was observed during the survey pattern a racetrack or lawnmower pattern would be setup over a feature of interest such as a rain band or wind band.

Storm types:
The ideal ocean winds storm would typically be a developed hurricane (category 1 and above) where a large range of wind speeds and rain rates would be found. However, data collected within tropical depressions and tropical storms would still provide very useful observations of rain impacts.

6. SFMR High-Incidence Angle Measurements

Principal Investigator(s): Heather Holbach (FSU/HRD), Brad Klotz (HRD), and Dr. Mark Bourassa (FSU)

Primary IFEX Goal: 2 - Develop and refine measurement technologies that provide improved real-time monitoring of TC intensity, structure, and environment

Motivation: Surface winds in a tropical cyclone are essential for determining its intensity. Currently, the Stepped-Frequency Microwave Radiometer (SFMR) is used for obtaining surface wind measurements. Due to poor knowledge about sea surface microwave emission at large incidence angles and high wind speeds, SFMR winds are only retrieved when the antenna is pointed directly downward from the aircraft. Understanding the relationship between the SFMR measured brightness temperatures, which are used to obtain a surface wind speed, wind direction, and the ocean surface wave field at off-nadir incidence angles would potentially allow for the retrieval of wind speed measurements when the aircraft is in turns. It is hypothesized that at off-nadir incidence angles the distribution of foam on the ocean surface from breaking waves impacts the SFMR measurements differently than at nadir. Therefore, by analyzing the excess brightness temperature at various wind speeds and locations within the tropical cyclone environment at off-nadir incidence angles, the relationship between the ocean surface characteristics and the SFMR measurements will be quantified as a function of wind direction relative to the look angle.

Objective: Determine the relationship between the SFMR measured surface brightness temperature and the ocean surface wave field characteristics.

Module overview: These modules are designed to obtain SFMR measurements in various locations of the tropical cyclone environment for several different wind speeds during constant banked aircraft turns at several different roll angles, specified below. A full pattern for each module consists of three complete circles for each specified roll angle (Figure 6-1). It is important to maintain a constant roll angle. A dropwindsonde and AXBT pair should be released at the beginning of the pattern. The wide swath radar altimeter (WSRA) should also be obtaining measurements during the pattern for analysis of the ocean surface characteristics. The wave spectra obtained by the WSRA will allow for a more accurate investigation of the sensitivity of the SFMR to the surface wave characteristics. It is ideal to fly these modules in rain-free areas as to reduce the impact of the atmospheric emission on the SFMR measurements and to obtain measurements in regions of moderate to heavy precipitation, as deemed safe by the aircraft pilots, in order to understand the impact of varying the path length of the precipitation. Coordinating measurements with HIRad overpasses would also be ideal if possible.

Modules:

1.   Zero wind, high incidence angle response
o   This module is designed to determine the antenna pattern corrections and possible impacts of sun glint
o   Fly circles at roll angles of 15, 30, 45, and 60 degrees

2.   Moderate wind response (~15 m/s, 30 kts)
o   This module is designed to understand the mixed "phase" (i.e., foam vs roughness contributions to brightness temperature)
o   Fly circles at roll angles of 15, 30, and 45 degrees

3.   Moderate winds (~15 m/s, 30 kts) and substantial swell or varying fetch length response
o   This module is designed to determine the sensitivity to stress
o   This can be performed on the way to the storm or in different sectors of the storm
o   Fly circles at roll angles of 15, 30, and 45 degrees
o   It would be ideal to coincide with a WindSat overpass if cloud free

4.	Strong wind response (>30 m/s, 60 kts)
o	This module should be flown in multiple storm quadrants (motion relative)
o	Fly circles at roll angles of 15, 30, and 45 degrees

•	Other things to consider
o	Possibility for V-pol measurements (i.e., rotate SFMR antenna 90 deg)

Data Analysis: The SFMR data from these flights will be analyzed to determine if a double harmonic oscillation is evident in the excess brightness temperatures as was found in data collected from Hurricane Gustav (2008). The WSRA data will then be used to analyze the differences in the ocean surface characteristics to reveal any possible relationships between the double harmonic oscillation found in the SFMR measurements and the ocean surface characteristics. Wind speed and direction from the dropwindsondes will be used to verify the SFMR wind speed. SST from the AXBTs will be used as input to the brightness temperature algorithm. If coinciding measurements are retrieved from HIRad it will be possible to do a comparison with the SFMR measurements to gain a further understanding of the SFMR data.
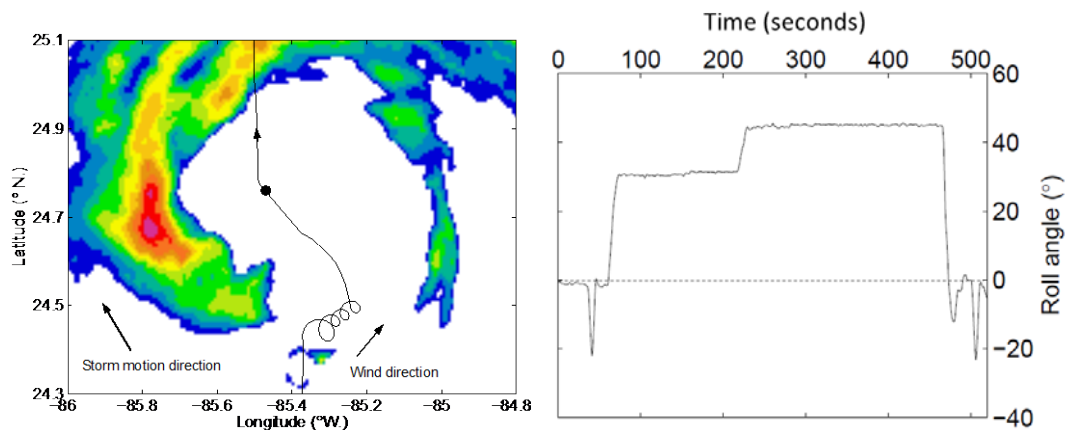
Figure 6-1: Flight pattern for module flown in Hurricane Gustav (2008) in a rain-free portion of the eyewall experiencing approximately 35 ms^{-1} surface winds (left panel). Time series of P-3 roll angle during period of turns in Gustav (right panel).

Thus far, measurements have been obtained primarily on the right side of storms (Figure 6-2). To develop a more complete composite picture, we are particularly interested in obtaining measurements on the left side of storms (motion relative) this season. We would also like to focus on regions with wind speeds greater than 20 m/s.
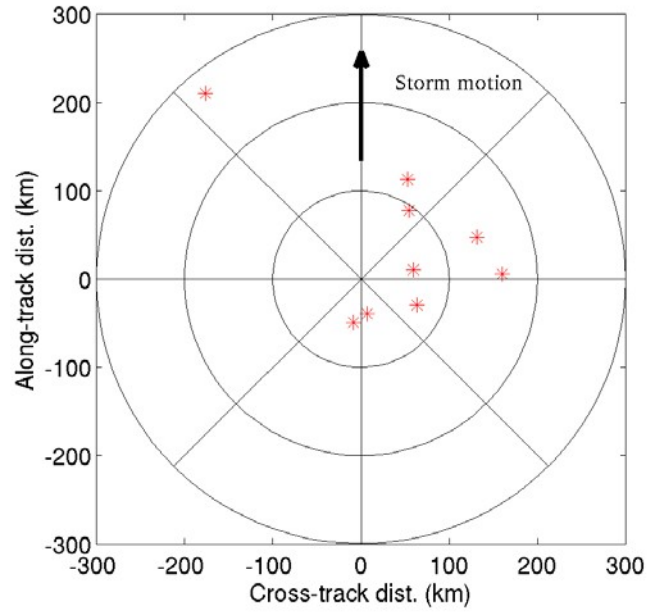
Figure 6-2: Storm-relative locations of high-incidence SFMR observations obtained to date.

7. Offshore Wind Module

HRD Point of Contact: Shirley Murillo

This module is designed as a multi-agency (NOAA, Department of Energy, Department of the Interior) supplemental data collection effort to gather hurricane environmental information in the vicinity of proposed offshore wind farms. Offshore wind energy is seen as an important component in President Obama's goal of the U.S. supplying 80% of energy needs from clean energy by the year 2030. The Bureau of Ocean Energy Management (BOEM) has identified several wind energy and lease areas in federal waters off the Atlantic coast (Fig. 7-1, Table 7-1) and the Department of Energy has identified additional areas as demonstration projects for offshore wind power development. For offshore wind energy to develop into a new industry, the turbines must be designed to withstand extreme environmental conditions that occur during hurricanes.

Modern offshore turbines are huge structures with masts near 100 m above the surface and rotor zones extending to near 180 m. Conventional offshore turbines are erected upon foundations constructed in shallow (<40 m) water but new designs for deep water turbines are in operation off Norway and Portugal and expected off the coast of Maine as part of a DOE funded program to get demonstration projects in the water. Current standards for the design of tall offshore structures are governed by power law wind profiles specified with constant roughness or wind profiles based on Norwegian Sea that are unrepresentative when compared to GPS sonde based hurricane wind profiles. Turbulence intensity specifications used for the design of offshore wind turbines specified according to a marine roughness that increases with wind speed. To better document design wind profiles in hurricane conditions, additional GPS sonde and airborne Doppler wind profiles are needed in relatively shallow water areas in the vicinity of the proposed wind farm locations. In addition, wave height and directional wave spectrum measurements from NOAA's wide-swath radar altimeter are needed to determine wave loading.

Samples of the mean wind profile, wave heights and spectrum, and profiles of air density, temperature, humidity, and rainfall will assist design engineers in specifying materials and construction that will allow wind farms to survive hurricane conditions. Since this module is generally a "piggyback" mission, we request additional GPS sonde launches in the vicinity of the wind farm location. The PI will provide data collection coordinates to the Lead Project Scientist of the primary mission. This module is requested whenever a NOAA aircraft is flying and the hurricane is projected to be within 150 nm of an identified offshore wind development site (Table 7-2).

As an example, we show a "fly-by" pattern in Fig. 7-2 in which the wind farm location is near the route to or from the storm or near an existing leg of the primary experiment flown that day. In this case 4 GPS sondes are dropped in succession. It would be preferable to repeat the pattern and collect these measurements on the inbound or outbound routes to the storm, or as part of the pattern in the storm.

Since the Hurricane Field Program will already be in operation and experiments flown, the offshore wind module is a cost effective solution for participating federal agencies and industry partners to collect critical data relevant to the design risk. Since flight hours have already been dedicated to existing HFP experiments, those experiments have priority. The opportunity to fly the offshore mission as a piggy-back module is at the discretion of the Field Program Director. In order to fly the module, support for expendables is required. In addition, collection of data from many of the specialized data and analysis systems (e.g. Doppler radar, Scanning radar altimeter) depends on availability and may require additional support.

Figure 7-1: *Potential offshore wind farm and Atlantic Wind Connection subsurface transmission line locations in federal waters off the U. S. Atlantic coast. Additional areas include state waters off Nantucket Sound MA, Block Island RI, Atlantic City NJ, Virginia Beach VA and Georgia. (Table 1).*

Offshore Wind Farm	Location	State or Federal
Fisherman's Energy	Atlantic City, NJ (3 miles offshore)	State
Dominion Virginia Power	Virginia Beach	Federal
Statoil North America (Hywind Maine)	Boothbay Harbor	State
University of Maine (DeepCwind)	Monhegan Island	State
Deepwater Wind	Block Island (5 mi SE)	State
Cape Wind	Nantucket Sound (Horseshoe shoal)	State
Maryland Wind Energy Area	See Fig. 7-1	Federal
Rhode Island Wind Energy Area	See Fig. 7-1	Federal
New Jersey Wind Energy area	See Fig. 7-1	Federal
Maryland Wind Energy Area	See Fig. 7-1	Federal
Virginia Wind Energy Area	See Fig. 7-1	Federal
Delaware	See Fig. 7-1	Federal
North Carolina	See Fig. 7-1	Federal
South Carolina	See Fig. 7-1	Federal
Georgia	Lease request for a MET mast off Tybee Island	Federal

Table 7-1: *Listing of DOE funded demonstration projects and other offshore wind developments planned or projected in state and federal waters.*
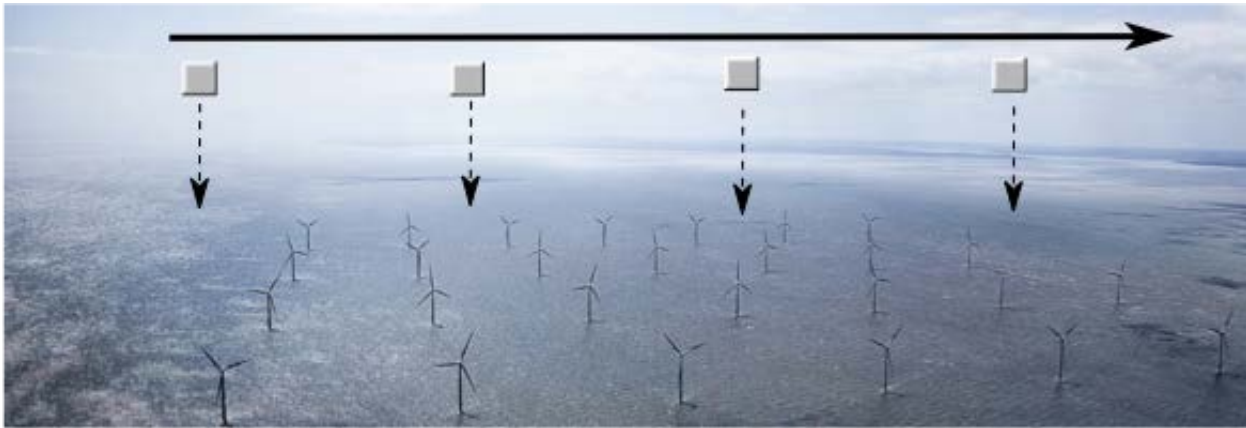
Figure 7-2: Schematic of piggyback pattern showing hypothetical wind farm fly-by with expendable launches at a 2-4 km interval. No U.S. wind farms are yet in operation. (Dong Energy Gunfleet Sands 1farm off SE England)

Table 7-2: Expendables (Ex) and aircraft (A/C) measurement systems required for conducting offshore wind experiment

Observing system	Measurement	Number	Type
GPS sonde	Pressure, Temperature, Humidity, Velocity	4-10	Ex
Stepped Frequency Microwave Radiometer (SFMR)	Surface wind speed rain rate		A/C
NOAA wide-swath radar altimeter	wave height and directional wave spectrum		A/C
Airborne Doppler radar	3D wind velocity, rain rate		A/C
Lower fuselage radar	reflectivity		A/C

8. Easterly Wave Genesis Experiment

Principle Investigators: Ghassan Alaka (HRD)   Alan Brammer (U. Albany)
                                Chris Thorncroft (U. Albany) Mark Boothe (NPS)
                                Jason Dunion (HRD)   Yuan-Ming Cheng (U. Albany)

Significance & Background:

As early as the 1930s, westward propagating disturbances in the lower troposphere were identified as seed circulations for most tropical cyclones (TCs) in the North Atlantic Ocean (Dunn 1940). The origins of these disturbances were traced back to North Africa and are now known as African easterly waves (AEWs; Riehl 1945). About 70% of all TCs and, more impressively, 85% of major hurricanes in the North Atlantic Ocean have been found to initiate from AEWs (Landsea 1993). On average, sixty AEWs exit the West African coast each year. However, determining which of these AEWs will develop into TCs has proven to be a forecasting challenge. For example, over 50% of TC genesis events in the Atlantic main development region predicted by the Global Forecast System (GFS) from 2004-2011 were false alarms (Halperin et al. 2013).

Recent research has shed some light on the relationship between AEWs and TC genesis in the North Atlantic Ocean. The AEW-relative flow around an incipient disturbance has been hypothesized to be an important factor in protecting the disturbance from environmental intrusions and thus creating or maintaining a favorable environment for TC genesis to occur (Dunkerton et al. 2009). Brammer and Thorncroft (2015) have shown that, as AEWs leave West Africa, the troughs are sensitive to the low-level environment to their west and northwest (Fig. 8-1). Although the vortex at 700 hPa typically has closed circulation in the wave-relative reference frame, the AEW troughs are still cold-core in the lower troposphere and, therefore, there is relative westerly flow under the vortex and through the lower levels of the trough. In a composite analysis, significant differences in the moisture of the low-level environment to the northwest of the troughs were found between developing and non-developing waves. Favorable developing waves had significantly higher moisture content in the lower troposphere to the northwest of the trough as they exited the West African coast compared to favorable non-developing waves. Trajectory analysis for all the waves revealed that as the AEWs transition over the West African coast the troughs are typically open to the environment ahead and to the northwest of the trough. For developing waves this means that moist air (e.g. moist tropical sounding, Dunion 2011) is ingested into the lower levels of the system, while for non-developing waves dry air (e.g. SAL or mid-latitude dry air intrusion soundings) is ingested. At this stage in the AEW life cycle, moisture differences may be fundamental in determining whether a favorable wave will develop or not.

The depth and the integrity of the closed circulation around the pre-genesis disturbance is an important consideration for providing a convectively favorable environment for TC genesis. Freismuth *et al.* (2016) argue that the vortex of ex-Gaston (2010) was susceptible to dry air above the vortex maxima, which hindered deep convection and led to a weakening of the vortex.

In addition, non-developing disturbance (AL90 2014) encountered lower tropospheric dry air to its west and northwest, which was ingested by the disturbance and was likely a major contributor in the failed genesis (Fig. 8-2). Preliminary results by Brammer (2015) suggest that as AEWs leave the West African coast, these troughs typically possess closed circulations at 700-600 hPa. Yet, these troughs remain open to the environment both above and below the 700-600-hPa layer. As AEWs propagate across the North Atlantic, the troughs are more likely to exhibit closed circulations at low-levels due to either increased vorticity within the trough or the changing background shear profile over the central Atlantic. It was
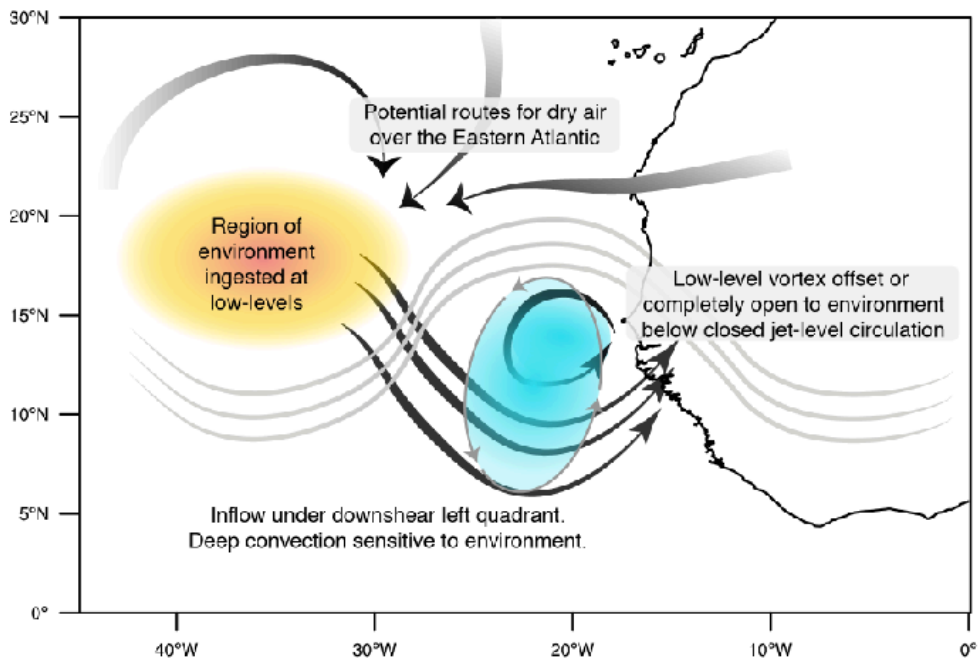
Figure 8-1*. Schematic of the ingestion of dry environmental air by an African easterly wave.*
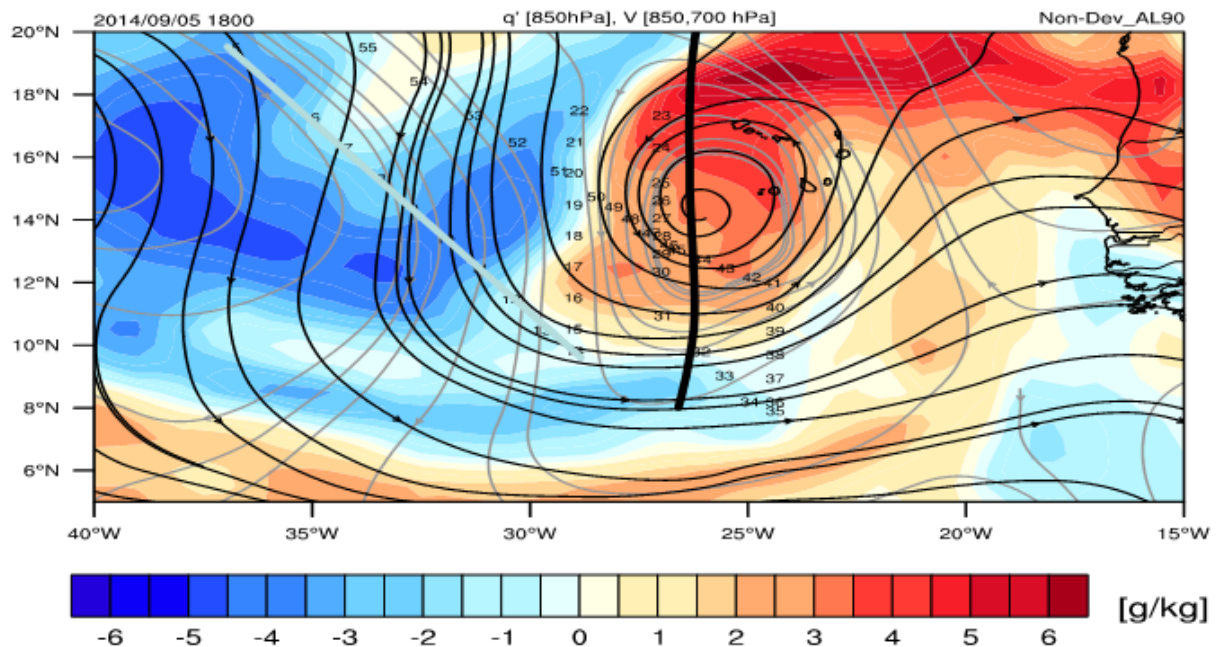
Figure 8-2*. 850 hPa specific humidity anomalies (shading), 850 hPa streamflow (black contours) and 700 hPa streamflow (gray contours) are shown for a non-developing case (AL90) at 18Z 5 Sept 2014.*

therefore hypothesized that AEWs are especially sensitive to the low-level environment to the west and northwest of the trough during the first three days after leaving the West African coast. Since AEWs typically propagate at 7.5 m s^{-1} over the Atlantic (Kiladis et al. 2006), these waves are typically located near 35°W after three days.

Objectives: (List form)

- Collect NOAA G-IV GPS dropwindsonde and flight level data in the environment to the west of an invest to improve model biases in temperature and humidity. This is known as the Environmental Survey option (Fig. 8-3). The invest should be an AEW that is expected to develop located at 35°W or further west. The target environment should be 5°-10° to the west of the approximate invest center.
- Collect NOAA G-IV and/or NOAA P-3 Doppler radar, GPS dropwindsonde and flight level data to assess the dynamic and thermodynamic structure of the invest to determine if environmental air was ingested into the disturbance once it has reached 40°W. This is known as the AEW Survey option (Fig. 8-4). Precise flight patterns will depend upon the developmental status of the invest. Two flight options are provided in Fig. 8-4.

Hypotheses: (List form)

- Environmental air to the west and northwest of an AEW is ingested by an AEW, before the low-level circulation is closed, as it traverses the Atlantic Ocean.
- Environmental air to the west and northwest of an AEW (i.e., TC seed) is vital to determine whether or not the disturbance will develop.
- Dynamical models (e.g., GFS) are consistently too moist in the inflow layer to the west of the AEW, which incorrectly encourages genesis.

OSSE Evaluation:
Time and resource permitting, an OSSE will be performed to determine optimal flight patterns in order to maximize the impact of these observations on the GFS and HWRF systems. With the high genesis false alarm rate in the GFS, this data may be especially useful to that system in order to reduce the model bias for over-predicting TC genesis.

Modeling Evaluation Component:
Halerpin et al. (2013) found that over 50% of TC genesis events in the main development region are false alarms for the GFS. Given the importance of the west and northwest environment identified by Brammer and Thorncroft (2015), reducing model biases in this region could be critical to improving TC genesis forecasts. Since the HWRF system is initialized from the GFS, these improvements could extend to both models. Model evaluation will primarily focus on specific humidity, which will be used to determine if the models are too wet or too dry compared to observations. Another important point to consider is whether or not this environmental air to the west and northwest of the invest is actually ingested into the system in models. GFS and Basin-Scale HWRF dividing streamlines and multi-level radial profiles of Lagrangian Okubo-Weiss produced by the Montgomery Research Group (NPS) will provide initial real-time assessments of the robustness of pouch boundaries. Backwards trajectories will be leveraged to determine the source of the air that makes it to the core of the AEW.

Links to IFEX Goals:
Goal 1: Collect observations that span the TC life cycle in a variety of environments for model initialization and evaluation;
Goal 3: Improve understanding of the physical processes important in intensity change for a TC at all stages of its lifecycle.

Mission Description:
This is a **multi-plane**, **multi-option** experiment. The target of this experiment is an AEW that is deemed an "invest" (i.e., a disturbance that has a chance to become a TC) by the National Hurricane Center (NHC). In particular, priority will be given to AEW invests that have a high chance of development based on NHC probabilities and model forecasts. This experiment relies on the balance between sampling as far to the east as possible and optimizing on-station time. This balance highlights a region between 35°W ad 40°W as the optimal location to sample the AEW environment and the AEW itself. The NOAA G-IV is the primary aircraft for this experiment. However, the NOAA P-3 becomes an option for this experiment if the AEW approaches 45°W (~2.5

hr on-station time). When possible, the G-IV and P-3 will coordinate with NOAA Sensing Hazards with Operational Unmanned Technology (SHOUT) Global Hawk missions to optimize sampling of environmental targets of interest (see section: *Coordination with Supplemental Aircraft*).

This experiment will be broken up into two options:

1) **Environmental Survey**
This option will sample the environment to the west of the AEW starting when the disturbance is near 35°W with the NOAA G-IV (Fig. 8-3). This experiment can be shifted to the west to accommodate AEWs that have propagated further without developing. Research shows that the disturbances typically close off in the low-levels by 35°W-40°W, so the number of candidates for this experiment decreases west of 40°W. This experiment will utilize GPS dropwindsonde and flight level data to document the thermodynamic properties of the AEW inflow region. In order to sample as much environmental moisture as possible, a lawn mower pattern with long meridional legs will be employed. The lawn mower pattern should be centered on the latitude of the approximate AEW center and should extend at least 3° to the north and to the south of that center. The zonal legs of this lawn mower pattern should be about 1°-2° (150 nm), while the meridional legs should be about 6°-10° (600-1000 nm). GPS dropwindsondes should be administered every 150-250 nm on each meridional leg, but this spacing is flexible based on dropwindsonde availability.

Importantly, the Environmental Survey option may be administered stand-alone experiment or may be included as a module in other experiments. For example, the AEW Survey option, which highlights the sampling of the actual AEW, may be altered to include the Environmental Survey as a module. In addition, the Environmental Survey may be added as a module within other NOAA P-3 and/or NOAA G-IV experiments or operational tasked missions. The proposed far-field sampling can often be performed during P-3 and G-IV aircraft ferries to and from the tropical disturbance. If a Saharan Air Layer outbreak is present in the far field environment, the DWL Experiment SAL module can be conducted.

This option will sample a developing AEW to determine if environmental air has been ingested and assess impacts on the structure and organization of the tropical disturbance. Once the AEW reaches 40°W, the disturbance may be investigated with the NOAA G-IV (Fig. 8-4). If the AEW reaches 45°W and has still not developed, the NOAA P-3 may also be used to carry out this experiment. The *AEW Survey* experiment may incorporate the *Environmental Survey* as a module, as shown by the dashed line in Fig. 8-4.
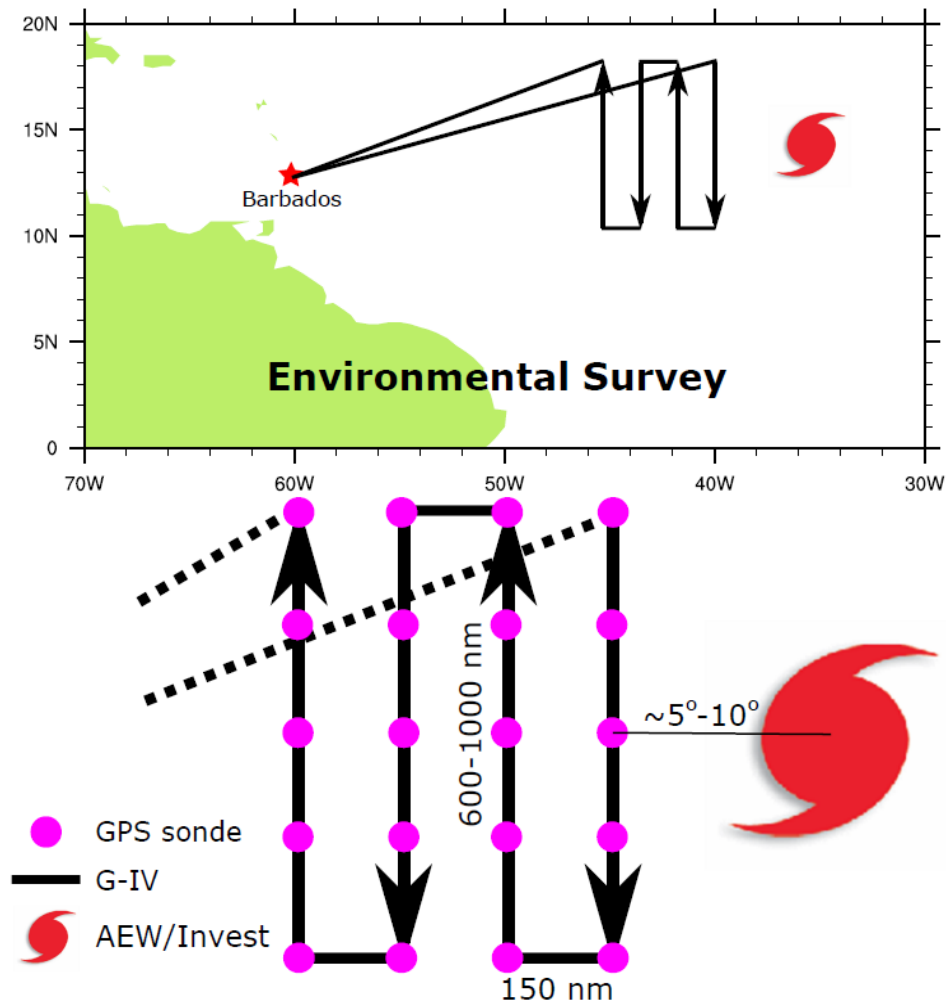
Figure 8-3.   *The Environmental Survey pattern.*

Analysis Strategy: NOAA G-IV (and, if applicable, NOAA P-3) GPS dropwindsonde and flight level data will be analyzed to determine the thermodynamic environment to the west of the AEW. NASA Global Hawk GPS dropwindsondes, if available, will be used in conjunction with NOAA aircraft data to observe the structure and evolution of the to-be-ingested environmental air. The vertical structure of specific humidity will be especially important in this environmental survey. These specific humidity measurements will be used to determine HWRF and GFS biases in the environment ahead of AEWs.

2) **AEW Survey**

If the AEW is showing signs of genesis, the *AEW Survey* will focus on center fixes, as shown in the top of Fig. 8-4. If the AEW is disorganized, the *AEW Survey* will focus on a general survey pattern around the disturbance, as shown in the bottom of Fig. 8-4. Regardless of the AEW developmental status, this experiment will employ Doppler radar, GPS dropwindsondes and flight level data to create a full picture of the dynamic and thermodynamic structure of the AEW. The strategy for GPS dropwindsonde sampling should be consistent with other survey or figure-four flight patterns.
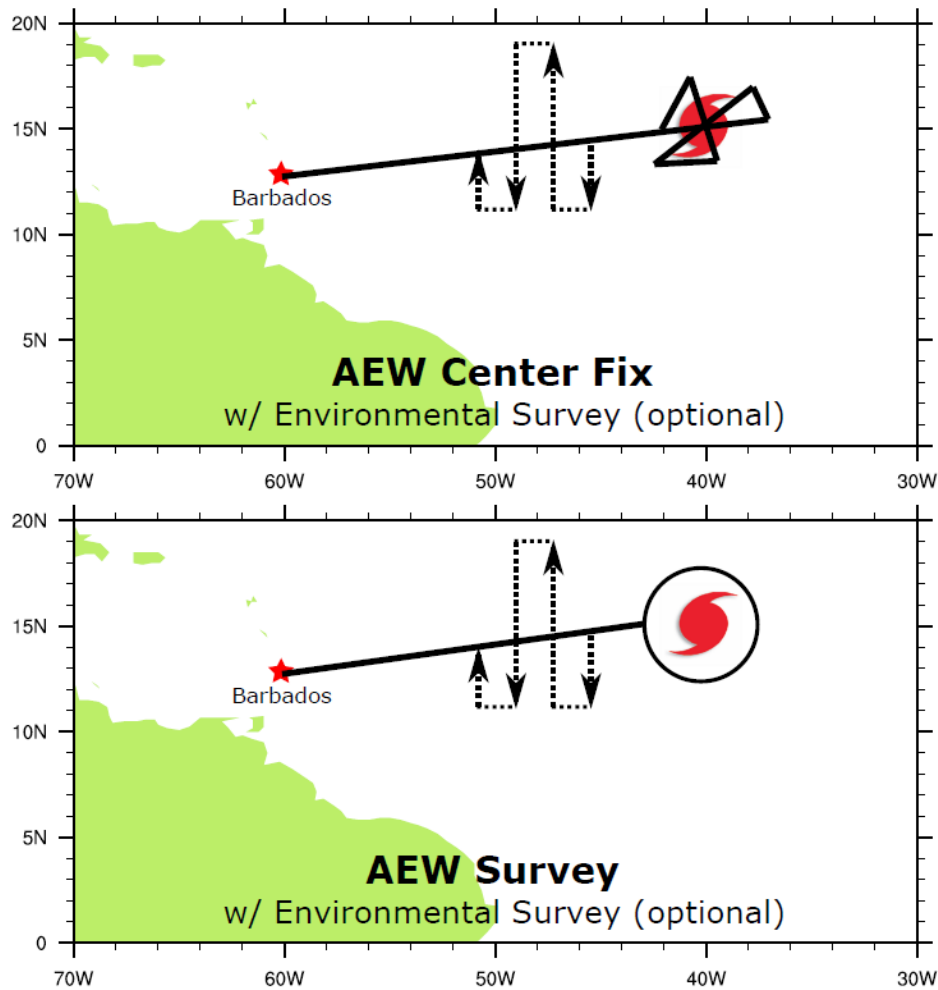
Figure 8-4. *The AEW Survey experiment. (Top) AEW Center Fix option with optional Environmental Survey module. (Bottom) AEW Survey option with Environmental Survey module.*

Analysis Strategy: NOAA G-IV and NOAA P-3 Doppler radar, GPS dropwindsonde and flight level data will be synthesized to assess the dynamic and thermodynamic structure of the AEW, with a focus on whether or not the previously-observed environmental air was ingested into the disturbance. In addition to searching for signs of development, evidence for the ingestion of environmental air observed in the previous flight will be sought out. In particular, the impact of this environmental air on the organization and the intensity of the system will be the focal point of this experiment. If the AEW is interacting with a Saharan Air Layer outbreak, GPS dropwindsonde sampling of the SAL's low to mid-level dry air (~500-850 hPa) and mid-level easterly jet (25-50 kt near 600-800 hPa) should also be prioritized and the P-3 DWL Experiment SAL module can be conducted.

Coordination with Supplemental Aircraft:
NOAA is planning to conduct the SHOUT field campaign during the 2016 hurricane season. The SHOUT campaign will utilize one unmanned Global Hawk (GH) aircraft, flying at approximately 55-60,000 ft. altitude with mission durations of ~24 h. The GH will be equipped with a GPS dropwindsonde system capable of deploying 88 dropwindsondes per mission, the JPL HAMSR microwave sounder for analyzing 3-D distributions of temperature (e.g. the TC warm core), water vapor, and cloud liquid water, and the NASA HIWRAP dual frequency Doppler radar for observing 3-D winds, ocean vector winds, and precipitation. The primary science goals of SHOUT include: i) improving model forecasts of TC track and intensity by designing optimal GPS dropwindsonde sampling strategies for the Global Hawk using a real-time ensemble data assimilation and forecasting system; and ii) gaining a better understanding of both the inner-core and environmental processes that are important to TC intensity change.

Figure 8-5. *Sample GH flight patterns for the 2016 NOAA SHOUT field campaign. (Left) sequence of small-large-small butterflies. The small butterfly patterns have 120 nm (220 km) radial legs and take ~3-hr to complete while the large butterfly pattern has 240 nm (450 km) legs and takes ~6.5-hr to complete. (Right) rotated butterfly pattern with 30 degree rotated radials that are 240 nm (450 km) in length from the storm center. Both GH patterns would be flown in a storm relative framework.*

When possible, it will be desirable to fly patterns with the NOAA P-3 and/or G-IV aircraft that are coordinated with the GH. For the NOAA P-3, "coordinated" means optimizing sampling strategies that target the AEW environment and optimize sampling of the thermodynamics (e.g. low to mid-level moisture) and kinematics (e.g. vertical wind shear and SAL's mid-level easterly jet). For the G-IV, "coordinated" means optimizing far field and AEW sampling either concurrently or on alternating days (to attain nearly continuous 2-plane coverage of both the AEW and peripheral environment). The details of these coordinated missions will be handled on a case-by-case basis.

References

Brammer A., (2015): Evolution of African easterly waves and their relationship to tropical cyclogenesis., Ph.D. thesis, SUNY at Albany. url: http://gradworks.umi.com/37/38/3738908.html

Brammer A., and C. D. Thorncroft, 2015: Variability and Evolution of African Easterly Wave Structures and Their Relationship with Tropical Cyclogenesis over the Eastern Atlantic.
Mon. Wea. Rev. 143(12), 4975-4995.

Dunion, J.P., 2011: Re-writing the climatology of the tropical North Atlantic and Caribbean Sea atmosphere. *J. Climate*, **24 (3)**, 893-908.

Dunkerton, T. J., M. T. Montgomery, and Z. Wang, 2009: Tropical cyclogenesis in a tropical wave critical layer: Easterly waves. *Atmos. Chem. Phys.*, **9**, 5587–5646.

Dunn, G. E., 1940: Cyclogenesis in the tropical Atlantic. *Bull. Amer. Meteor. Soc.*, 21, 215-229.

Freismuth, T. M., Rutherford, B., Boothe, M. A., and Montgomery, M. T, 2016: Why did the storm ex-Gaston (2010) fail to redevelop during the PREDICT experiment?, Atmos. Chem. Phys. Discuss., doi:10.5194/acp-2015-692, in review.

Halperin, D. J., H. E. Fuelberg, R. E. Hart, J. H. Cossuth, P. Sura, and R. J. Pasch, 2013: An evaluation of tropical cyclone genesis forecasts from global numerical models. *Wea. Forecasting*, **28**, 1423–1445, doi:10.1175/WAF-D-13-00008.1

Landsea, C. W., 1993: A climatology of intense (or major) Atlantic hurricanes. *Mon. Wea. Rev.*, **121**, 1703-1713.

Riehl, H., 1945: "Waves in the easterlies and the polar front in the tropics" Misc. Rep. No. 17, Department of Meteorology, University of Chicago, 79 pp.

9. East Pacific Easterly Wave Genesis Experiment

Principle Investigators: Ghassan Alaka (HRD)   Adam Rydbeck (NRL)

                                            Eric Maloney (CSU)

Significance & Background:

Many studies have hypothesized that African easterly waves (EWs) serve as seed disturbances for East Pacific tropical cyclones (TCs) (e.g., Avila and Pasch 1992). However, it is often difficult to track African EWs crossing Central America and entering the East Pacific basin. In addition, African EWs may not be necessary to initiate EWs in the East Pacific. Several mechanisms for the in situ generation of EWs in the East Pacific have been proposed: 1) breakdown of the inter-tropical convergence zone (Ferriera and Schubert 1997), 2) barotropically unstable gap jets (Mozer and Zehnder 1996), 3) inertial instabilities from cross-equatorial pressure gradients (Toma and Webster 2010), 4) growth of vorticity noise by barotropic conversion in favorable basic states (Maloney and Hartmann 2001, Hartmann and Maloney 2001), and 5) upscale vorticity organization from diurnal convection in the Panama Bight (Rydbeck et al. 2016). This last mechanism for EW generation, proposed by Rydbeck et al. (2016), is the focus of this experiment.

East Pacific EW initiation can occur near the coasts of Panama and Colombia, with little or no preceding signal propagating from the Atlantic Ocean (Rydbeck and Maloney 2014). The Panama Bight has the highest occurrence of organized deep convection on the planet based on the NOAA Highly Reflective Cloud dataset (Kilonsky and Ramage 1976). Accordingly, mesoscale convective systems (and often mesoscale convective complexes) are initiated diurnally and propagate westward in boreal summer (Mapes et al. 2003). Previous studies have removed topography near the Panama Bight to demonstrate its vitality to the formation of convection in this region (e.g., Mapes et al. 2003, Rydbeck et al. 2016). Without the strong diurnal variability in Panama Bight convection, EW vorticity variance decreased by an order of magnitude in the Weather Research and Forecasting (WRF) model (Fig. 9-1).

Mesoscale convective systems in the Panama Bight are hypothesized to contribute to the initiation and intensification of EWs in the East Pacific through a process of upscale vorticity organization. When serial mesoscale convective systems are generated in the Panama Bight, precipitating regions are associated with positive vorticity anomalies and dry regions are associated with negative vorticity anomalies. In the middle troposphere, vertical stretching has been shown to increase the positive vorticity and decrease the negative vorticity in the region. Over successive mesoscale convective systems, the pattern of preferentially aggregating positive vorticity and dispersing negative vorticity in the vicinity of the Panama Bight leads to the development of long-lived cyclonic vorticity at mid levels that serves as the seed for an EW. These seeds are often referred to as "invests" in the hurricane forecast community.

In the very active 2015 East Pacific hurricane season, the Global Forecast System (GFS) under-predicted TC genesis in 120 h forecasts. This experiment aims to investigate a mechanism (i.e., convection in the Panama Bight) by which EWs form and from which TCs may develop in the East Pacific. A better representation of convection in the Panama Bight may improve EW initiation and growth in dynamical models, such as the GFS, thereby providing more realistic seed disturbances for TC genesis forecasts.
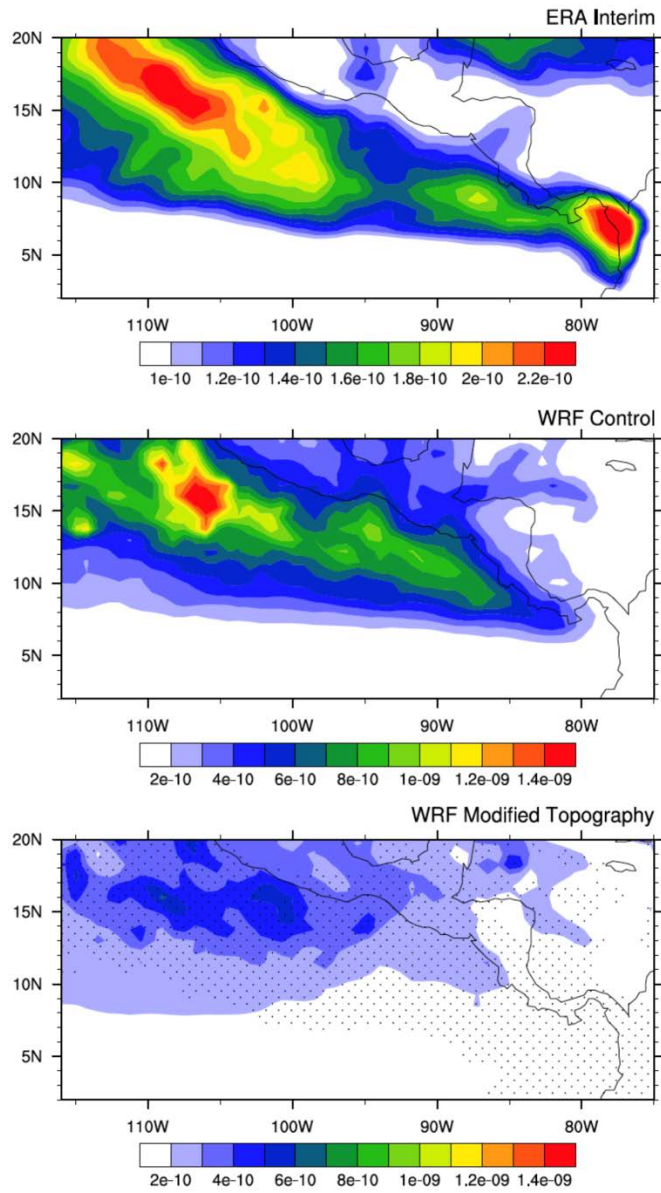
Figure 9-1. *2.5 – 12 day bandpass filtered 550-hPa relative vorticity variance (s-2, color contours) is shown for ERA-Interim (top), WRF control (middle), and WRF modified topography (bottom) for May-Nov. of 2000-2009. Figure from Rydbeck et al. (2016).*

Objectives: (List form)
- Collect NOAA G-IV Doppler radar, GPS dropwindsondes and flight level data in the Panama Bight.
- Document the dynamic and thermodynamic structure and evolution of diurnal convection, especially focusing on the aggregation of convection and vorticity.
- Differentiate between dynamic and thermodynamic structures that lead to TCs, invests and non-developers.

Hypotheses: (List form)
- East Pacific EWs can develop in situ near the Panama Bight without a pre-existing disturbance from the Atlantic Ocean.
- Panama Bight convection can reinvigorate a pre-existing disturbance that crosses into the East Pacific Ocean from the Atlantic Ocean.
- Westward propagating diurnal convection originating near the Panama Bight grows upscale via vertical vorticity stretching.

Links to IFEX Goals:
Goal 1: Collect observations that span the TC life cycle in a variety of environments for model initialization and evaluation;
Goal 3: Improve understanding of the physical processes important in intensity change for a TC at all stages of its lifecycle.

OSSE Evaluation:
Time and resource permitting, an OSSE will be performed to determine optimal flight patterns in order to maximize the impact of these observations on the GFS and HWRF systems.

Modeling Evaluation Component:
The data collected through this experiment will be used to evaluate biases in dynamical models, (e.g., GFS, HWRF). In 2015, the GFS under-predicted TC genesis in the East Pacific for 120 h forecasts. As demonstrated by earlier studies, the misrepresentation of convection (both timing and intensity) in the Panama Bight could have negative implications for EW initiation in the East Pacific. It is not clear if Panama Bight convection and its multiscale interactions are well represented in these dynamical models. Further, the upscale growth of vorticity anomalies (particularly through vertical vorticity stretching) associated with Panama Bight convection appears to be important for EW initiation. It is not clear how well dynamical models capture the growth of vorticity anomalies within mesoscale convective features via vortex stretching. The HWRF system, with its convection-permitting high-resolution nests, may be especially insightful into the dynamical and thermodynamical evolution of convection in the Panama Bight. An experimental uniform 3 km version of HWRF could be used to test the importance of horizontal grid spacing on convection and vorticity tendency biases in the Panama Bight.

Mission Description:
This is a **single-plane**, **multi-option** experiment. The target of this experiment is a developing East Pacific easterly wave, especially in the Panama Bight region. Priority will be given to disturbances that the National Hurricane Center (NHC) identifies as having a chance for development in the next 120 h. However, due to the typically disorganized state of convection in the Panama Bight, candidate disturbances may be identified via model forecasts and/or observations of an Atlantic Ocean EW about to propagate into the East Pacific. The NOAA G-IV is the only aircraft that will be employed for this experiment. NOAA G-IV flights that depart from Tapachula, Mexico will allow for the most on-station time in the Panama Bight. However, the Panama Bight may also be sampled if the NOAA G-IV departs from St. Croix. The range rings for Tapachula and St. Croix are provided in Fig. 9-2. Tampa and Barbados remain options, but should be considered last resorts since neither offers more than 2 hours of on-station time in the Panama Bight. The Panama Bight and surrounding areas are out of range for the NOAA P-3, so this aircraft should not be considered for this experiment.

This experiment is broken up into three (3) modules. The approximate location of each module is shown in Fig. 9-2. At least one (1) module must be chosen for this experiment to run, with the option for two (2) modules depending on the scenario, flight time and departure point. The three (3) modules are as follows:
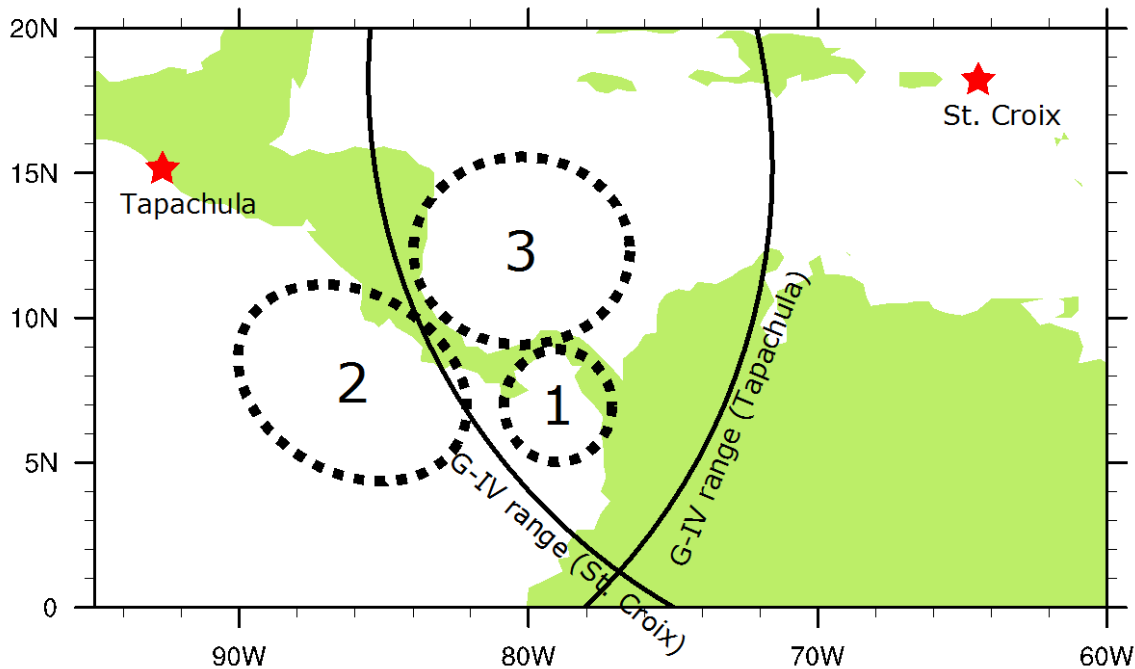
***Figure 9-2**.   Location of the three modules described in the East Pacific Easterly Wave Genesis Experiment. Tapachula, Mexico and St. Croix are shown along with NOAA G-IV range rings (assuming 2 hrs of on-station time).*

1) Panama Bight Convection Module

This module samples convection in the Panama Bight through a general survey of that region. The *Panama Bight Convection Module* is at the core of this experiment, which seeks to understand EW genesis or re-invigoration in the East Pacific. Convection is typically disorganized in the Panama Bight, which allows for a lot of flexibility in the flight plan to optimize sampling. This module will utilize tail Doppler radar, GPS dropwindsondes and flight level data to create an accurate picture of the dynamic and thermodynamic structure. A general survey pattern around the Panama Bight and the convection of interest is shown in Fig. 9-3. In general, GPS dropwindsondes should be deployed every 100 km along this general survey pattern, but this number can be adjusted based on dropwindsonde availability. Detours to circle/box around features of interest are encouraged, provided they can be done so safely. For example, the mesoscale convective system (MCS) depicted near 80.5°W would be a prime target for such a detour. GPS dropwindsondes should be deployed every 25-50 km, but this number can be adjusted based on dropwindsonde availability. This module can be combined with the *East Pacific Development Module* or the *Easterly Wave Transition Module* in order to maximize the data collected per flight.   Note that, while all flight patterns below depict a smoothly-varying rounded pattern, in fact all efforts should be made to conduct turns with a series of straight and level segments, to minimize loss of radar data from aircraft banks.
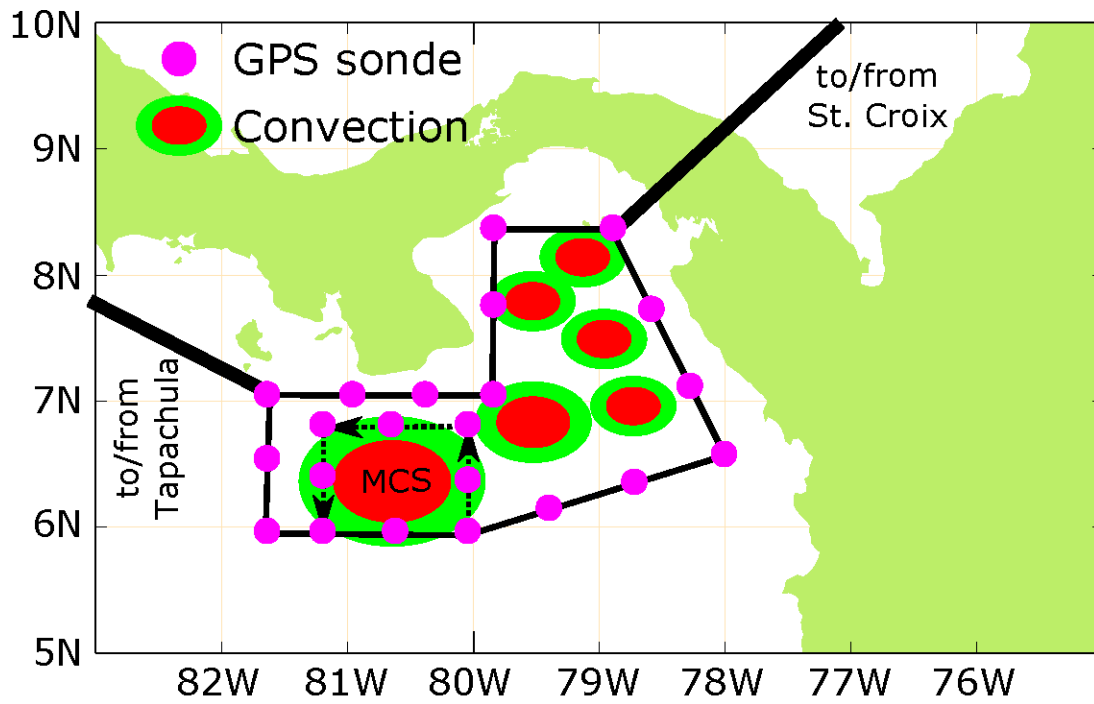
Figure 9-3.　　*The Panama Bight Convection Module.*

2) East Pacific Development Module

This module surveys an EW in the East Pacific (southeast of Tapachula, Mexico) that is showing signs of development. Ideally, this module will be useful to continue tracking a disturbance that originates and grows from the Panama Bight region. To maintain this connection in the analysis, candidate EWs should be located east of 90°W. This module is only available for flights departing from Tapachula. It is out of range for the NOAA G-IV from every other base. Rydbeck et al. (2016) found evidence that Panama Bight convection to the east of a developing EW is responsible for increasing vorticity on the backside of the EW and slowing the propagation speed of this disturbance. Therefore, the *East Pacific Development Module* pairs well with the *Panama Bight Convection Module*. These two modules may be completed in the same flight, in any order.

Two general flight pattern options exist for this module (Fig. 9-4). The precise flight plan will depend on the situation. If the disturbance is still disorganized (very likely), then a general survey pattern around the storm is recommended. However, if the disturbance is organized, a figure-four flight pattern is recommended, anchored to the estimated center location. Please note that if no discernable disturbance can be identified, this module should be skipped in order to maximize on-station time in the Panama Bight. This module will utilize tail Doppler radar, GPS dropwindsondes and flight level data to create an accurate picture of the dynamic and thermodynamic structure of the developing disturbance. For the figure-4 pattern, dropsondes should be released at the turn points, midpoints, and one center pass. For the survey flight path, GPS dropwindsondes should be deployed every 100 km, but this number may be changed based on availability.
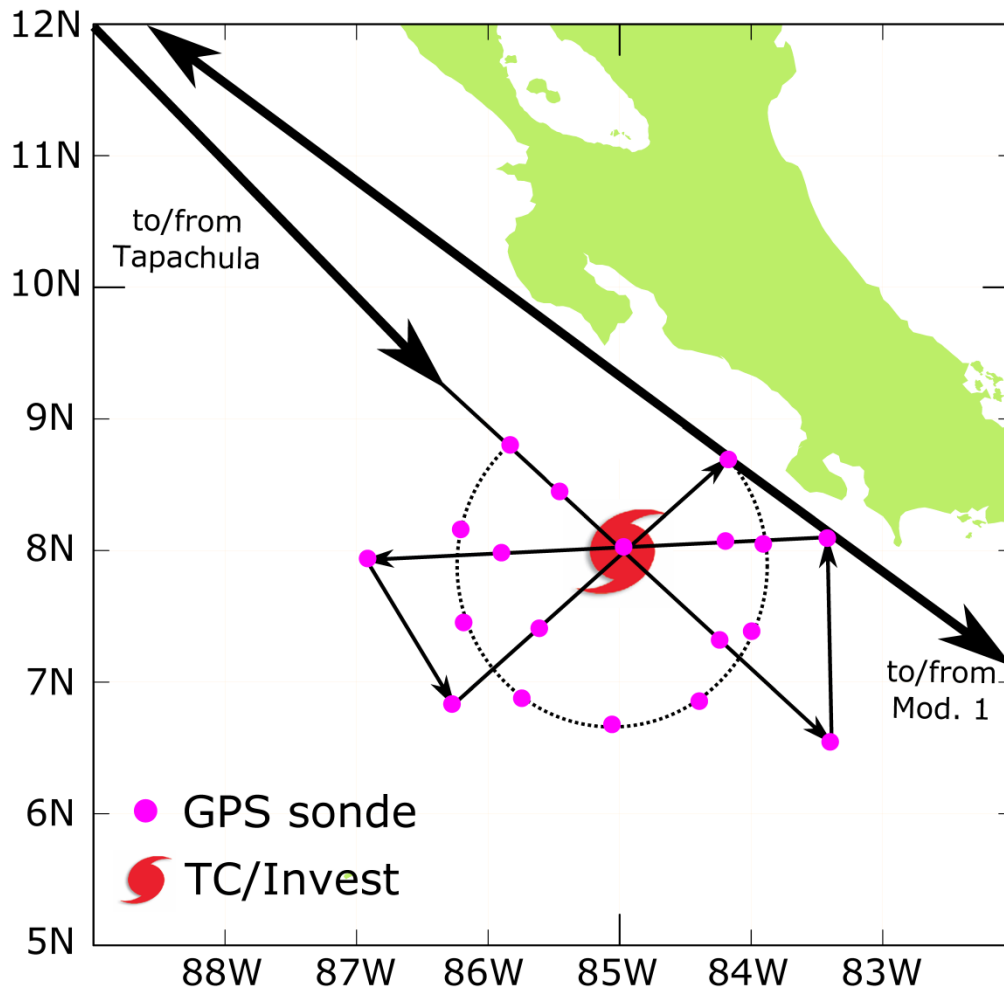
Figure 9-4. The East Pacific Development Module.

3) Easterly Wave Transition Module

This module surveys an EW that is transitioning from the Atlantic basin to the East Pacific basin. While recent work has highlighted the in situ generation of EWs in the East Pacific, many studies have shown evidence supporting the propagation of robust EWs from the Atlantic into the East Pacific. Convection in the Panama Bight may be important for the maintenance, or re-invigoration, of these EWs as they cross Central America. EWs that are north of 15°N should not be considered for this module since these disturbances are too far from the Panama Bight and are less likely to propagate into the East Pacific. In addition, candidate EWs should be located at and to the west of 78°W (longitude of Panama Bight). A broad survey around the EW while in the extreme western Caribbean Sea is recommended (Fig. 9-5). GPS dropwindsondes should be deployed every 100 km, but this number may be changed based on availability. Combination with the *Panama Bight Convection Module* is encouraged.
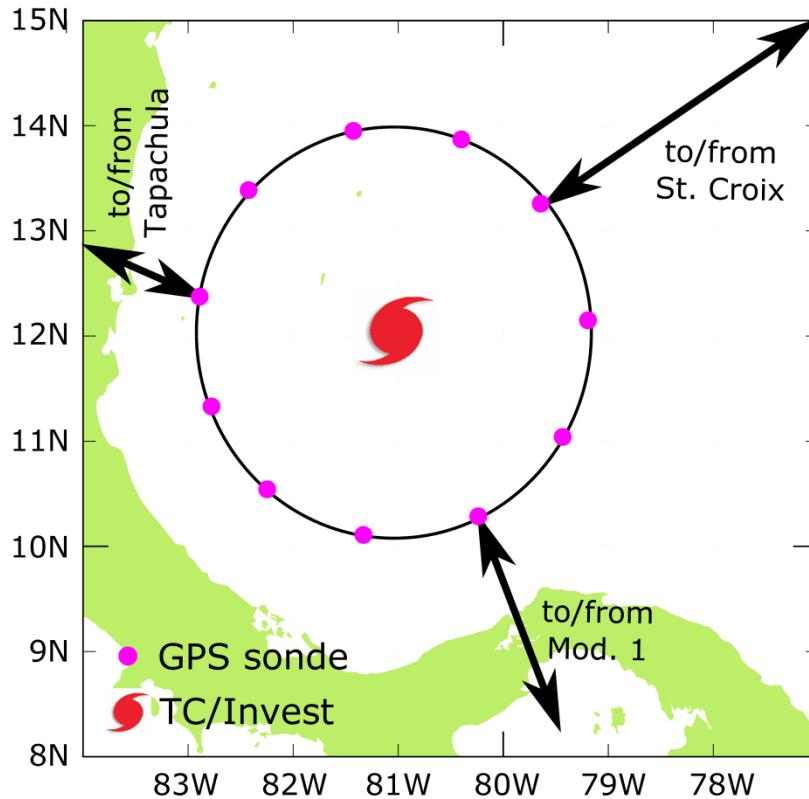
Figure 9-5. *The Easterly Wave Transition Module.*

Analysis Strategy:

The analysis strategy is the same for all three modules. Winds and vorticity are the most important fields to retrieve to compare with previous work on the importance of Panama Bight convection. Tail Doppler radar will be especially useful to reconstruct a three-dimensional wind field structure for convective cells, which will be vital in the calculation of vertical vorticity stretching. Vertical vorticity stretching has been hypothesized to be key for the upscale growth of vorticity in the Panama Bight region. Thermodynamic fields, such as temperature and moisture, will be leveraged to identify thresholds necessary for convection in the Panama Bight as well as back out vertical profiles of Q1, the apparent heat source, and Q2, the apparent moisture sink. In a regional model and global reanalysis these profiles have been shown to evolve over time as mesoscale convective systems and EWs intensify in the Panama Bight region (Rydbeck et al. 2016). In a regional model, Q1 evolves into a robust stratiform heating profile consistent with the local generation of mid level vorticity, a result we hope to validate with this experiment. In addition, biases related to the dynamic and thermodynamic structure of Panama Bight convection will be identified in the GFS and other dynamical models.

Coordination with Supplemental Aircraft:

NOAA is planning to conduct the SHOUT field campaign during the 2016 hurricane season. The SHOUT campaign will utilize one unmanned Global Hawk (GH) aircraft, flying at approximately 55-60,000 ft. altitude with mission durations of ~24 h (Fig. 9-6). The GH will be equipped with a GPS dropwindsonde system capable of deploying 88 dropwindsondes per mission, the JPL HAMSR microwave sounder for analyzing 3-D distributions of temperature (e.g. the TC warm core), water vapor, and cloud liquid water, and the NASA HIWRAP dual frequency Doppler radar for observing 3-D winds, ocean vector winds, and precipitation. The primary science goals of SHOUT include: i) improving model forecasts of TC track and intensity by designing optimal GPS dropwindsonde sampling strategies for the Global Hawk using a real-time ensemble data assimilation and forecasting system; and ii) gaining a better understanding of both the inner-core and environmental processes that are important to TC intensity change.

When possible, it will be desirable to fly patterns with the NOAA P-3 and/or G-IV aircraft that are coordinated with the GH. For the NOAA G-IV, "coordinated" means optimizing far field and AEW sampling either concurrently or on alternating days (to attain nearly continuous 2-plane coverage of both the EW and peripheral environment). The details of these coordinated missions will be handled on a case-by-case basis.
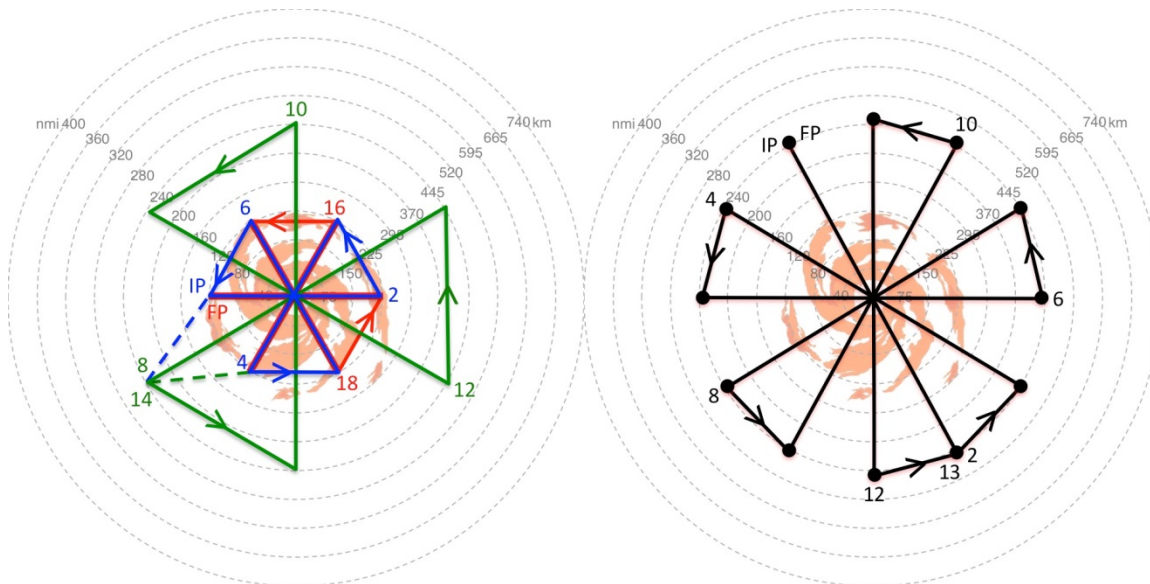
Figure 9-6. Sample GH flight patterns for the 2016 NOAA SHOUT field campaign. (Left) sequence of small-large-small butterflies. The small butterfly patterns have 120 nm (220 km) radial legs and take ~3-hr to complete while the large butterfly pattern has 240 nm (450 km) legs and takes ~6.5-hr to complete. (Right) rotated butterfly pattern with 30 degree rotated radials that are 240 nm (450 km) in length from the storm center. Both GH patterns would be flown in a storm relative framework.

References:

Avila, L. A., and R. J. Pasch, 1992: Atlantic tropical systems of 1991. *Mon. Wea. Rev.*, **120**, 2688–2696.

Ferreira, R. N., and W. H. Schubert, 1997: Barotropic aspects of ITCZ breakdown. *J. Atmos. Sci.*, **54**, 261–285.

Hartmann, D. L., and E. D. Maloney, 2001: The Madden–Julian oscillation, barotropic dynamics, and North Pacific tropical cyclone formation. Part II: Stochastic barotropic modeling. *J. Atmos. Sci.*, **58**, 2559–2570.

Kilonsky, B. J. and C. S. Ramage, 1976: A technique for estimating tropical open-ocean rainfall from satellite observations. J. Appl. Meteor., **15**, 972-976.

Maloney, E. D., and D. L. Hartmann, 2001: The Madden–Julian oscillation, barotropic dynamics, and North Pacific tropical cyclone formation. Part I: Observations. *J. Atmos. Sci.*, **58**, 2545–2558.

Mapes, B. E., T. T. Warner, and M. Xu, 2003: Diurnal patterns of rainfall in northwestern South America. Part III: Diurnal gravity waves and nocturnal convection offshore. *Mon. Wea. Rev.*, **131**, 830–844.

Mozer, J. B., and J. A. Zehnder, 1996: Lee vorticity production by large-scale tropical mountain ranges. Part I: Eastern North Pacific tropical cyclogenesis. *J. Atmos. Sci.*, **53**, 521–538.

Rydbeck, A. V. and E. D. Maloney, 2014: Energetics of East Pacific Easterly Waves during Intraseasonal Events. *J. Climate*, **27**, 7603–7621.

Rydbeck, A. V., E. D. Maloney, and G. J. Alaka, 2016: In Situ Initiation of East Pacific Easterly Waves in a Regional Model. *J. Atmos Sci.*, submitted.

Toma, V. and P. J. Webster, 2010: Oscillations of the intertropical convergence zone and the genesis of easterly waves. I Theory and diagnostics. *Clim. Dyn.,* **34**, 587-604.

10. Rapid Intensification Experiment (RAPX)

Co-Principal Investigators: Robert F. Rogers (HRD), John Kaplan (HRD), and Jason P. Dunion (HRD)

Motivation:

While some improvements in operational tropical cyclone intensity forecasting have been made in recent years (DeMaria et al. 2014), predicting changes in tropical cyclone intensity (as defined by the 1-min. maximum sustained wind) remains problematic. In particular, the operational prediction of rapid intensification (RI) has proven to be especially difficult (Kaplan et al. 2010) and given the significant impact of such episodes, has prompted the Tropical Prediction Center/National Hurricane Center (TPC/NHC) (Rappaport 2012) to declare it as its top forecast priority. The difficulty of forecasting RI stems from a general lack of understanding of the physical mechanisms that are responsible for these rare events. Generally speaking researchers have attributed RI to a combination of inner-core, oceanic, and large-scale processes.

To date, statistically-based prediction schemes such as the SHIPS rapid intensification index (SHIPS-RII) (Kaplan et al. 2010) and the more recently developed Bayesian and logistic regression RI models (Rozoff and Kossin 2011) have generally been shown to provide the most skillful objective RI guidance (Kaplan et al. 2015).   The aforementioned models employ predictors derived from large-scale fields and GOES infrared satellite imagery. These models include such predictors as the environmental vertical wind shear and moisture, the departure of the vortex's present intensity from its empirical maximum potential and the symmetry of the inner-core convection around the storm center as deduced utilizing GOES infrared imagery. Kaplan et al. (2015) showed that the statistical models, such as the SHIPS-RII, are capable of explaining roughly 20% of the skill of Atlantic basin RI forecasts at a lead-time of 24-h. Thus, the remaining 80% of the skill not explained by the statistical models is assumed to be attributable either to processes not explicitly accounted for by those models or by limitations in the predictability of RI events. Rogers et al. (2013b; 2015) used airborne Doppler measurements to identify several characteristics of the inner-core structure of tropical cyclones that were associated with intensification, though many questions were raised from this work related to the mechanisms responsible for the formation of these structures. In particular, the interaction of the vortex with vertical shear, the role of vortex tilt and alignment, and the distribution, structure, and evolution of deep convection (and other modes of precipitation) prior to and during RI are all outstanding questions. The goal of this experiment is to collect datasets that can be used both to initialize 3-D numerical models and to improve our understanding of RI processes across multiple scales, with the overarching goal of improving our ability to predict the timing and magnitude of RI events.

Objective:

To employ both NOAA P-3 and G-IV aircraft to collect oceanic, kinematic, and thermodynamic observations both within the inner-core (i.e., radius < 220 km) and in the surrounding large-scale environment (i.e., 220 km < radius < 440 km) for systems that have been identified as having the potential to undergo RI within ~96 h. Both the probabilistic statistical RI guidance (i.e., SHIPS-RII, Bayesian, logistic regression) and numerical models will be used to assist with selection of candidate systems for the short-term time periods (lead times $\leq$ 48 h) while both the statistical and numerical models will be used at the longer lead times (i.e., beyond 48 h). The datasets collected from this experiment will aid in the quantification of the current capabilities of the operational coupled model forecast system to adequately distinguish the environmental, vortex, and convective-scale structures of tropical cyclones that undergo RI from those that do not.

Hypotheses:

- By gathering observations that span spatial scales from 10s to 100s of kilometers it is possible to improve our understanding of the atmospheric and oceanic conditions that precede RI, particularly within the less observed inner-core region.

- Characteristics of the tropical cyclone inner core, both on the vortex- and convective-scale, contribute a non-negligible amount to the predictability of RI.
- The aforementioned multi-scale RAPX data sets can be used both to initialize and evaluate numerical model forecasts made for episodes of RI and successful completion of these tasks will lead to improved numerical and statistical model predictions of RI.

Links to IFEX goals:

- **Goal 1**: Collect observations that span the TC lifecycle in a variety of environments
- **Goal 3**: Improve understanding of the physical processes important in intensity change for a TC at all stages of its lifecycle

Model Evaluation Component: Recent analysis of global and airborne Doppler data have shown that statistically significant differences exist in the environmental and the inner-core structures of steady-state and rapidly intensifying TCs. In addition to the differences in the large-scale variables utilized by the statistical RI models described above, variations in such structures as the inner- and outer-core vorticity field, inflow depth and strength, and number, radial, and azimuthal distribution of deep convection have been found to exist for RI and non-RI TCs. Since the data collected as a part of this experiment will span scales ranging from the environmental down to the convective and PBL scale, it should provide a means of evaluating the various features of the operational modeling system, including the sufficiency (or lack thereof) of the horizontal resolution, and the microphysical and planetary boundary layer parameterization schemes.

Mission Description:

Missions will be targeted for systems that have a reasonable chance of undergoing RI, based on the guidance indicated above. When possible (i.e., subject to range, timing, and other logistical constraints), missions will begin as much as 24 h prior to the expected onset of RI, even if the storm is still only a tropical depression or storm, to capture the structure during the time leading up to RI onset. Ideally missions will continue every 12 h, as long as feasible. The P-3 aircraft will dispense AXBTs and GPS dropsondes and collect Doppler radar data while flying a rotating figure-4 pattern (see sample pattern shown in Fig. 1) in the inner-core with leg lengths of ~90-180 km at the maximum safe altitude (~8k-12k feet) for avoiding graupel. The AXBTs and GPS dropsondes should be dispensed on each leg with a spacing of ~30-40 km to provide adequate coverage for deducing the radial variations in kinematic and thermodynamic storm properties. Particular efforts should be made to release expendables outside the flight-level radius of maximum winds (RMW); i.e., between ~1xRMW and 3xRMW. The desired AXBT/GPS dropsonde deployment strategy is for both an AXBT and GPS dropsonde to be dispensed in tandem at both the endpoints and midpoint of each leg of the figure-4 pattern so that a total of 12 AXBT/GPS pairs are dropped during the course of each completed figure-4 leg (pattern) as shown in Fig. 10-1. Additional dropsondes (no AXBTs) can be dropped at the discretion of the LPS to increase the radial and/or azimuthal coverage, particularly outside the RMW. The P-3 may also fly a Convective Burst Module (similar to that flown for the tropical cyclone genesis experiment) or an Arc Cloud Module if the opportunity to conduct such flight patterns presents itself.

The G-IV should fly the environmental pattern shown in Fig. 10-2 at an altitude of ~41-45 K ft. dispensing dropsondes at radii of 220, 330, and 440 km to measure the thermodynamic and kinematic fields in the near storm environment. These particularly radii were chosen since collecting data in this region is crucial for computing the vertical shear and upper-level divergence, both of which have been shown to be strongly correlated with RI. The radii of the innermost ring of G-IV drops shown in Fig. 10-2 can be adjusted outward if necessitated by safety considerations. However, the radii of the other rings of drops should then also be adjusted to maintain the specified 1-deg spacing. Depending on the time of day, aircraft duration limitations, and safety considerations, the lengths of the G-IV inner (outer) points could be shortened (extended) to ~200 km (~500 km) if an opportunity to sample a diurnal pulse "IR cool ring" presents itself (see TC Diurnal Cycle Experiment).

As noted above, this experiment requires that both the P-3 and G-IV be utilized. In addition, it is highly desirable that the P-3 aircraft fly a rotating figure-4 pattern (see Fig. 10-1) in the inner-core while the G-IV simultaneously flies the environmental surveillance pattern shown in Fig. 2a every 12 h. Although this mission can still be conducted if the G-IV aircraft flies a synoptic surveillance pattern instead of the one depicted in Fig. 10-2a, such a flight pattern should only be flown in the event that the G-IV has been tasked by the NHC to conduct an operational synoptic surveillance mission and thus would otherwise be unavailable for use in research missions. Furthermore, if either the P-3 or G-IV aircraft cannot fly every 12 h the experiment can still be conducted provided that the gap between missions for any one of the two aircraft does not exceed 24 h. Alternatively, an octagonal survey pattern like that depicted in Fig. 10-2b can also be flown by the G-IV aircraft. Such a pattern will allow Doppler radar measurements to be effectively collected from the G-IV, and would be particularly desirable if the P-3 were not available.
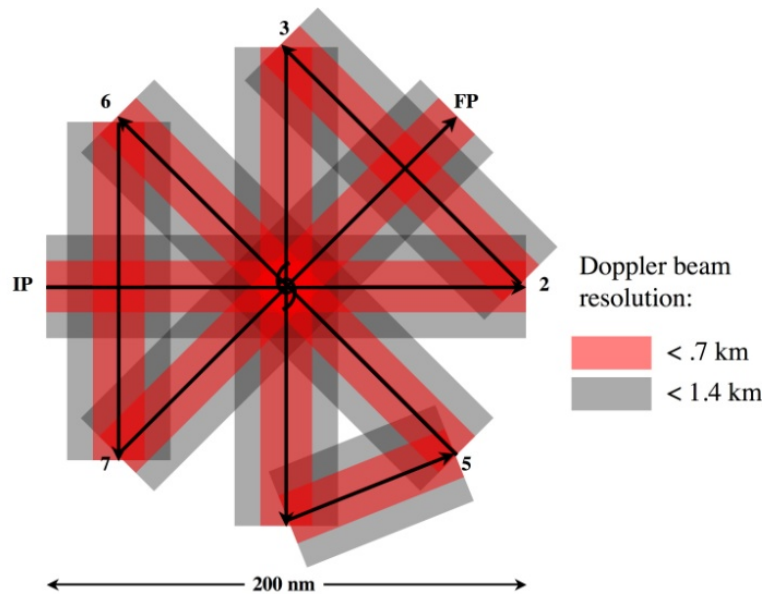
Figure 10-1. *Sample rotated figure-4 flight pattern for RAPX mission. The red shading denotes locations where vertical spacing of Doppler beam < 0.7 km, grey shading where vertical spacing < 1.4 km. GPS dropsondes should be released at all turn points (past the turn after the aircraft has leveled), at midpoints of inbound/outbound legs, and at center point between IP/2 and 5/6. An additional dropsonde should be released between the midpoint and turn points for each radial pass. If available, release AXBT's coincident with dropsondes at turn points, midpoints, and center points. Note that the above in-storm P-3 flight pattern requires about 3-4 hours to complete.*
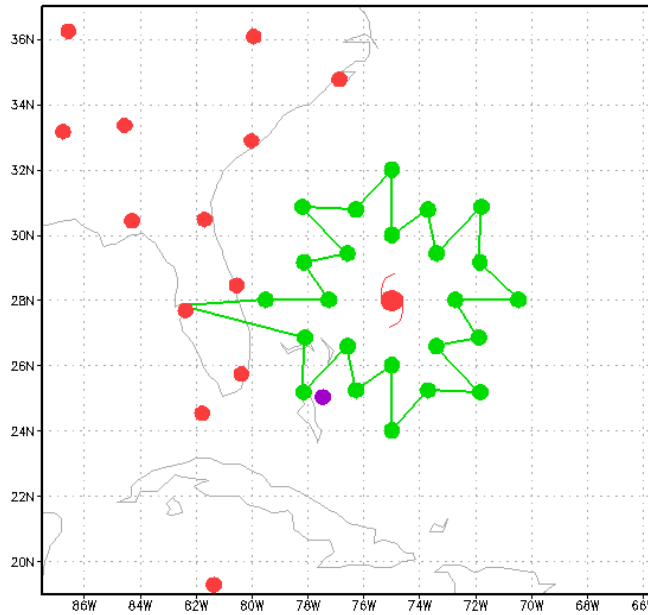
Figure 10-2a. *A sample G-IV flight pattern for the RAPX mission. The green dots denote the desired dropsonde locations at 220, 330, and 440 km radius from the storm center. Note that the end oints of each leg can be rounded slightly as required for aircraft flight considerations. The flight pattern shown in Fig. 2a (excluding ferry time to and from the storm) requires about 6 hours to complete.*

It is worth noting that there exists the potential to perform the RAPX experiment in the eastern North Pacific basin while operating out of Mexico during the upcoming 2016 Hurricane Season. Finally, when possible this experiment may also make use of the NASA Global Hawk aircraft that will be employed during the upcoming 2016 Hurricane season as part of the SHOUT program.
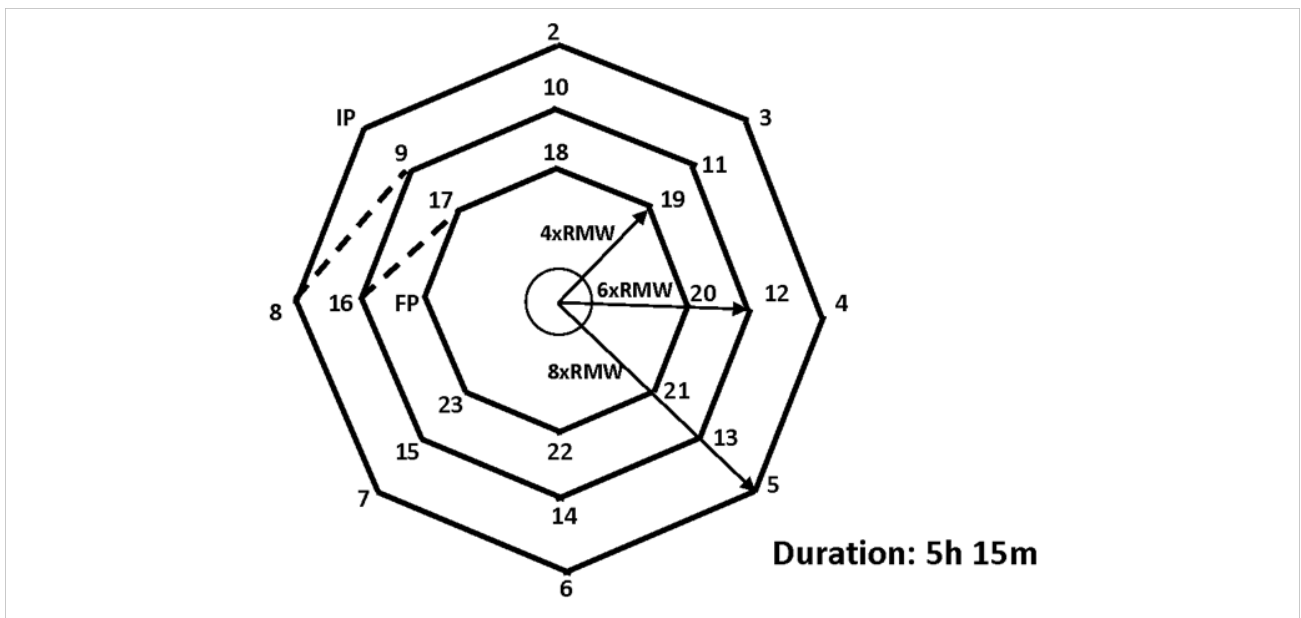
Figure 10-2b: G-IV outer-core survey pattern.

- Altitude: 40-45 kft
- Expendables: Deploy dropsondes at all turn points. No more than 24 GPS drops needed.
- Pattern: The pattern is flown with respect to the surface storm center. Three concentric octagons are flown clockwise at decreasing radii of 8xRMW, 6xRMW, and 4xRMW, where RMW is the estimated radius of maximum azimuthal-mean tangential wind (estimated from flight-level observations). For example, if RMW=18 nm, the maximum radial extent of the pattern is 144 nm. Dashed lines show transitions between rings.
- Instrumentation: Set airborne Doppler radar to scan F/AST on all legs.

Analysis Strategy

This experiment seeks to perform a multi-scale analysis of the conditions both before and during RI. Specifically, we will use GFS, GPS dropsonde, and ocean buoy observations to analyze the changes in energy transfer at the ocean-atmosphere interface during the time period of the experiment. Also, changes in the inner-core (i.e., radius <220 km) kinematic and thermodynamic structure will be examined using NOAA P-3 Doppler radar, flight-level, and GPS dropsonde data. Inner-core analyses will include an analysis of the symmetric and asymmetric vortex structure, vortex tilt, and inner-core vertical shear derived from airborne Doppler and dropsonde data and statistics of vertical velocity, vorticity, and reflectivity from airborne Doppler. Finally, an analysis of the near-storm large-scale environment (i.e., radius < 440 km) will be conducted using the high-resolution GFS analyses that contain the assimilated GPS dropsonde data deployed from NOAA G-IV aircraft. This near storm sampling effort will aid in the evaluation of many of the predictors being used in the current operational SHIPS RII including the vertical shear and a new predictor that employs microwave-derived total precipitable water imagery to detect dry air in the upshear TC environment. The overarching hypothesis of this analysis strategy is that by performing similar analyses for multiple RAPX data sets collected during both RI and non-RI events it will be possible to determine the conditions that are triggers for RI and to evaluate numerical model performance during such events.

Coordination with Supplemental Aircraft

NOAA is planning to conduct the SHOUT field campaign during the 2016 hurricane season. The SHOUT campaign will utilize one unmanned Global Hawk (GH) aircraft, flying at approximately 55-60,000 ft. altitude with mission durations of ~24 h. The GH will be equipped with a GPS dropsonde system capable of deploying 88 dropsondes per mission, the JPL HAMSR microwave sounder for analyzing 3-D distributions of temperature (e.g. the TC warm core), water vapor, and cloud liquid water, and the NASA HIWRAP dual frequency Doppler radar for observing 3-D winds, ocean vector winds, and precipitation. The primary science goals of SHOUT include: i) improving model forecasts of TC track and intensity by designing optimal GPS dropwindsonde sampling strategies for the Global Hawk using a real-time ensemble data assimilation and forecasting system; and ii) gaining a better understanding of both the inner-core and environmental processes that are important to TC intensity change.

When possible, it will be desirable to fly patterns with the NOAA P-3 and G-IV aircraft that are coordinated with the GH. For the NOAA P-3, "coordinated" means flying radial penetrations where the P-3 when the GH are vertically-stacked for at least a portion of the flight leg, preferably when the aircraft are approaching the center of the TC. The across-track displacement during such coordination should be kept as small as practicable, e.g., no greater than 5-10 km. In practice, the NOAA P-3 will likely fly its planned figure-4/butterfly/rotating figure-4 patterns as indicated in Fig. 10-1. The GH can fly patterns that are similar in geometry to the NOAA P-3 patterns (see Fig. 10-3). To achieve coordination the P-3 would align its legs such that the GH will be stacked with the P-3. Given the relatively long turn around of the NASA GH (~24-hr), the NOAA P-3 could also coordinate with the NOAA G-IV and GH on alternating days to attain nearly continuous 2-plane coverage of both the TC inner core and peripheral environment. The details of these coordinated missions would be handled on a case-by-case basis.
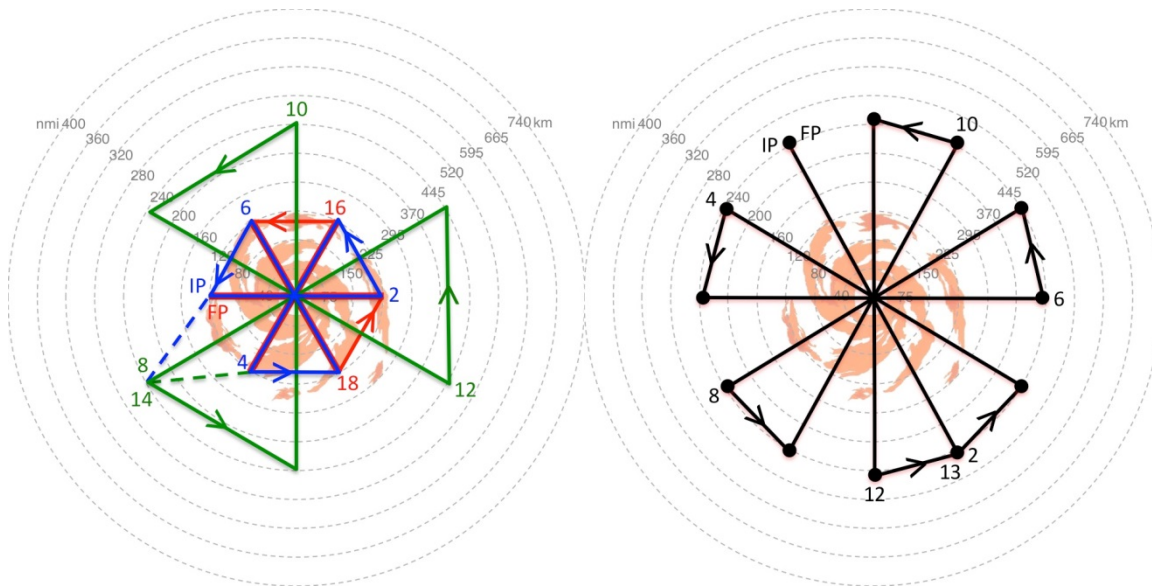
Figure10-3. Sample GH flight patterns for the 2016 NOAA SHOUT field campaign. (Left) sequence of small-large-small butterflies. The small butterfly patterns have 120 nm (220 km) radial legs and take ~3-hr to complete while the large butterfly pattern has 240 nm (450 km) legs and takes ~6.5-hr to complete. (Right) rotated butterfly pattern with 30 degree rotated radials that are 240 nm (450 km) in length from the storm center. Both GH patterns would be flown in a storm relative framework.

11. Tropical Cyclone in Shear Experiment

Principal Investigator(s): Paul Reasor (lead), Sim Aberson, Jason Dunion, John Kaplan, Rob Rogers, Jun Zhang, Michael Riemer (Johannes Gutenberg-Universität)

Links to IFEX:

- **Goal 1:** Collect observations that span the TC lifecycle in a variety of environments
- **Goal 3:** Improve understanding of the physical processes important in intensity change for a TC at all stages of its lifecycle

Motivation:

Forecasting of TC intensity remains a great challenge in which the gains in skill over the past decade have significantly lagged those of track at most forecast intervals (Rogers et al. 2006, DeMaria et al. 2005). As a multiscale atmospheric and oceanic problem, one of the constraints on TC intensity change is the vortex's interaction with the evolving environmental flow. Vertically-sheared flow in particular is generally acknowledged to limit storm intensity, especially when combined with other environmental factors like low sea-surface temperature and mid-tropospheric dry air (e.g., Tang and Emanuel 2012). In observation-based statistical models of intensity prediction (Kaplan and DeMaria 2003; DeMaria et al. 2005), the vertical wind shear (VWS) is an important predictor.

Although most TCs in HRD's data archive experience some degree of VWS, the timing of flights with respect to the shear evolution and the spatial sampling of kinematic and thermodynamic variables have not always been carried out in an optimal way for testing hypotheses regarding shear-induced modifications of TC structure and their impact on intensity change (see below). This experiment will sample the TC at distinct phases of its interaction with VWS and measure kinematic and thermodynamic fields with the azimuthal and radial coverage necessary to test existing hypotheses.

In addition to enhancing basic understanding, the dataset collected will guide improvements in initial conditions and the representation of moist physical processes in models. These improvements are likely necessary to increase the accuracy of short-term (<24 h) numerical intensity guidance for vertically sheared TCs. Initial conditions within the core region are important because the resilience of a TC (i.e., its ability to maintain a vertically-coherent structure under differential advection by the VWS) is sensitive to the strength, depth, and radial profile of the vortex (Reasor et al. 2004; Reasor and Montgomery 2015). Properly representing the flow outside the core region is also important since the flow topology there is critical to the thermodynamic interaction of the TC with surrounding dry environmental air (Riemer and Montgomery 2011). Physical processes in the model must also be well-represented so that 1) the structure on which the vortex resilience depends is not errantly transformed over short periods (< 6 h), 2) the convective response of the TC to vertical shearing and its feedback on vortex resilience are properly simulated, and 3) the shear-induced intensity modification mechanisms are permitted to operate as in nature.

Background:

Vertical wind shear impacts TC structure directly through vertical tilting of the vortex wind field and indirectly through modulation of the convective field (Black et al. 2002; Reasor et al., 2009; Reasor and Eastin 2012; Reasor et al. 2013). The impact of VWS on TC intensity is less certain and depends, in part, upon the timescale over which one considers the response (Frank and Ritchie 2001; Wang et al. 2004; Wong and Chan 2004; Riemer et al. 2010). The view of VWS as a generally negative influence on TC formation and intensification is supported by observational studies (e.g., Gray 1968) and observation-based statistical models of intensity prediction (Kaplan and DeMaria 2003; DeMaria et al. 2005). During the early stages of TC development, however, VWS can play a potentially positive role by organizing deep convection and vorticity production in the downshear region of the weak, pre-existing vortex (Molinari et al. 2004, 2006).

Early studies of shear-induced intensity change mechanisms focused on the role of VWS in ventilating the warm core (Simpson and Riehl 1958). Frank and Ritchie (2001) simulated the development of pronounced convective asymmetry in a vertically-sheared TC and argued that weakening occurs through the hydrostatic response to outward fluxes of upper-level potential vorticity (PV) and equivalent potential temperature. An alternative explanation by DeMaria (1996) focused on the balance-dynamics response of the vortex to vertical tilting. To maintain thermal wind balance as the wind structure is tilted, static stability must increase at low levels in the eyewall region. The negative impact on intensity was then hypothesized to arise through suppression of eyewall convection. Using a multi-level adiabatic primitive equation model, Jones (1995, 2000) demonstrated that low-level static stability evolves in a manner consistent with balance dynamics but does so asymmetrically within the eyewall. An asymmetrically balanced thermal anomaly develops in phase with the distortion of the wind field caused by vertical tilting, resulting in anomalously low (high) values of static stability located downtilt (uptilt). Thus, while convection might be suppressed on one side of the eyewall, it can be enhanced on the other. Jones additionally implicated the mesoscale transverse circulation (required to maintain asymmetric balance) in the development of convective asymmetry in the eyewall (see also Braun et al. 2006; Davis et al. 2008). The net impact of such static stability and vertical motion asymmetry on convective asymmetry and intensity change remains unclear.

Recently, Riemer et al. (2010) and Riemer et al. (2013) have proposed an intensity modification mechanism also rooted in a balance-dynamics framework. They argue that balanced vorticity asymmetry at low levels, generated outside the core through shear forcing, organizes convection outside the eyewall into a wavenumber-1 pattern through frictional convergence. Downdrafts associated with this vortex-scale convective asymmetry arise as precipitation generated by the convective updrafts falls into unsaturated air below. In their simulations, the downdrafts led to a vortex-scale transport of low equivalent potential temperature (θ_e) air into the inflow layer and disruption of the TC heat engine (Emanuel 1986, 1991). If particularly low θ_e air at lower to middle levels of the environment is able to reach the core region where convective enhancement occurs, the thermodynamic impacts of the downward transport of low θ_e air would be enhanced. Riemer and Montgomery (2011) proposed a simple kinematic model for this environmental interaction, quantifying the shear-induced distortion of the "moist envelope" surrounding the TC core as a function of shear strength, vortex size, and vortex intensity.

In the simulations of Riemer et al. (2010), the TC core region developed vertical tilt following its initial encounter with VWS, but then realigned, i.e., the vortex was resilient. The problem of dynamic resilience focuses on the ability of the TC to maintain a vertically-coherent vortex structure as it experiences vertical shearing. Jones (1995) found that coupling between vertical layers, and the tendency for the upper- and lower-level potential vorticity (PV) of the cyclonic core to precess upshear, restricts the development of vertical tilt that would otherwise occur through differential advection. For small-amplitude tilt, Reasor et al. (2004) developed a balance theory for the shear forcing of vortex tilt in which the tilt asymmetry behaves as a vortex-Rossby wave. In this vortex-Rossby wave framework, they developed a heuristic model for the TC in shear which predicts a left-of-shear tilt equilibrium. Furthermore, they demonstrated that the evolution towards this equilibrium tilt state depends not only on intrinsic scales of the flow (e.g., Rossby number and Rossby deformation radius), but also on the radial distribution of (potential) vorticity in the core region. Reasor and Montgomery (2015) have recently evaluated this heuristic model. The model is capable of predicting the enhancement of resilience that arises as the PV gradient outside the core increases. Even when moist neutral conditions exist within the eyewall, the model still describes the long-time evolution of the tilt asymmetry outside the eyewall.

Hypotheses: (Regarding a TC encountering a large increase in environmental VWS over a short period of time)

1) **Structure evolution:** The vertically-tilted vortex structure which develops following a significant increase in VWS is governed by balance-dynamics theory. [There are two components here: 1) determine whether the wavenumber-1 vorticity and thermodynamic structures of the tilt asymmetry within the eyewall region are consistent with the expectations of asymmetric balance (see **Background**); and 2) document, to the extent

possible, the structural evolution of the tilt asymmetry on the timescale of a vortex circulation period (~1 h) and over the longer timescale dictated by the mission frequency (~12 h), and then compare the observed evolution with expectations from idealized modeling (Reasor et al. 2004; Reasor and Montgomery 2015). Core-region kinematic structure is sampled out to 4-5xRMW with Doppler radar at specific times relative to the VWS evolution. Thermodynamic structure is sampled with flight-level instruments and closely-spaced dropsondes.]

2) **Convective asymmetry:** Eyewall convective asymmetry is organized by shear-forced, balanced mesoscale ascent. [Several explanations have been proposed for shear-forced convective asymmetry, including balanced ascent associated with vortex tilting, vorticity budget balance, and interaction of mesovortices with the flow outside the eyewall. While it may not be possible (given our current limited understanding of shear-forced eyewall convective asymmetry) to determine the predominance of one mechanism over another using only observed data, at a minimum we may assess whether each mechanism is plausible in a given case. This data will aid future theoretical and numerical investigations designed to understand why convection is preferred in shear-relative locations of the TC eyewall. Core kinematic and precipitation structures are sampled with Doppler radar during a period when VWS is the dominant forcing of low-wavenumber asymmetry. Thermodynamic structure is sampled with flight-level instruments and closely-spaced dropsondes. Satellite observations of convective activity should also be archived during the observation periods.]

3) **Intensity modification:** As stated in Riemer et al. (2010), VWS inhibits intensification through the downward transport of low-θ_e air into the inflow layer outside the core, brought on by the wavenumber-1 organization of convection outside the core via balance-dynamics mechanisms. [The proposed link between balance-dynamics mechanisms and weakening, through modification of inflow layer thermodynamic properties, has not been demonstrated in the observational context. Core-region kinematic structure of the vortex (e.g., the tilt asymmetry) must be sampled out to 4-5xRMW with Doppler radar at specific times relative to the VWS evolution. Reflectivity data collected during the flight will also provide insight into the convective structure outside the eyewall. Thermodynamic structure of the inflow layer is sampled with closely-spaced dropsondes. Near-core thermodynamic structure of the lower to middle troposphere is sampled by flight-level and dropsonde measurements, especially before and during the period of increasing VWS.]

4) **TC isolation:** As stated in Riemer and Montgomery (2011), the shape of the moist envelope (i.e., high-θ_e air) surrounding the eyewall above the inflow layer (and below the outflow layer) is at first approximation closely related to the horizontal flow topology, and is distorted by VWS; for environmental air to impact eyewall convection, time-dependent and/or vertical motions outside the core (see Hypothesis 3) are generally necessary for all but the weakest TCs in VWS. [For a strong hurricane in VWS, the closest approach of environmental air is expected to be well-removed from the eyewall. If low- to mid-level low-θ_e air intrudes far enough into the core region, and undercuts near-core convection, the mechanism identified in Hypothesis 3 may operate in an amplified manner. The moist envelope is defined using P-3 flight-level and P-3/G-IV dropsonde data within and surrounding the eyewall out to about 150 nmi, before and after the shear increase. Similarly, the low- to mid-level storm-relative horizontal flow topology outside the core is examined using flight-level, dropsonde, and Doppler radar measurements.]

Experiment Description:

The experiment design is motivated through the use of fields from an example sheared hurricane simulated by HWRF. These fields will be treated as atmospheric observations for the purpose of the discussion below. The mission details at each stage of the experiment are also described below.

The optimal experiment is one in which the VWS increases significantly over a short period of time, approximating the canonical idealized numerical experiment of a TC in VWS (e.g., Bender 1997; Frank and Ritchie 2001; Riemer et al. 2010, 2013). A *hurricane-strength* TC encounters an instantaneous increase in VWS and undergoes an immediate structural change in response to sustained shear forcing. Figure 11-1 illustrates the large-scale, deep-layer VWS evolution in a case (Hurricane Michael, initialized at 00Z on 7 Sept., 2012) that would constitute an acceptable target for this experiment. The VWS increases approximately

30 kts over 24 h, or at a rate of 1.25 kts/h.
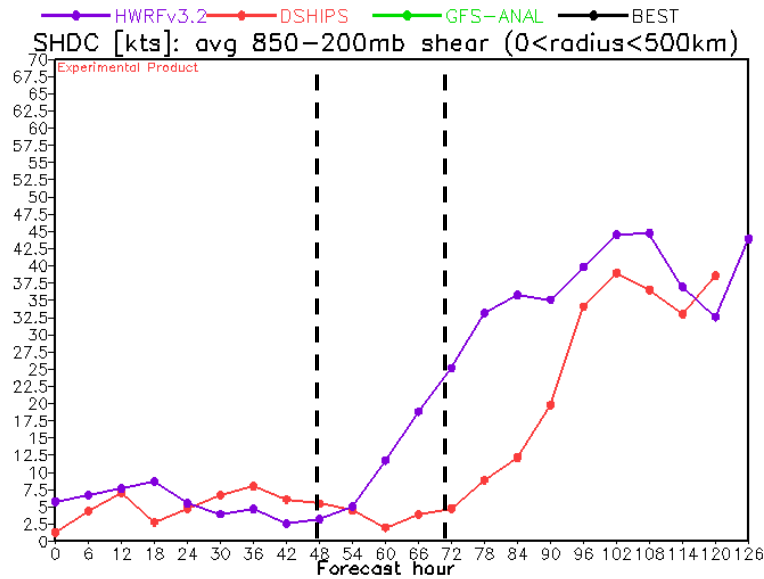
Figure 11-1: *Ideal shear evolution from HWRF (purple).*

Pre-shear sampling:

The TC is sampled prior to increasing shear (~48 h in Fig. 11-1) to obtain a reference vortex and environmental structure. Figure 11-2 shows a vertically aligned vorticity structure through a deep layer near this time.

Mission 1: The G-IV aircraft performs storm-relative environmental TDR and dropsonde sampling (Fig. 11-6) through clockwise circumnavigation, starting at 150 nmi, moving inward to 90 nmi, and finishing at 60 nmi. A coordinated P-3 aircraft performs a Figure-4 pattern (orientation chosen for efficiency) with TDR to obtain the TC core structure (Fig. 11-7). Radial legs are standard length for TDR missions, from 90-105 nmi. As time permits, the aircraft executes a second, rotated Figure-4 pattern. A primary objective of the P-3 and G-IV dropsonde sampling is to document the initial "pre-shear" moist envelope surrounding the core.
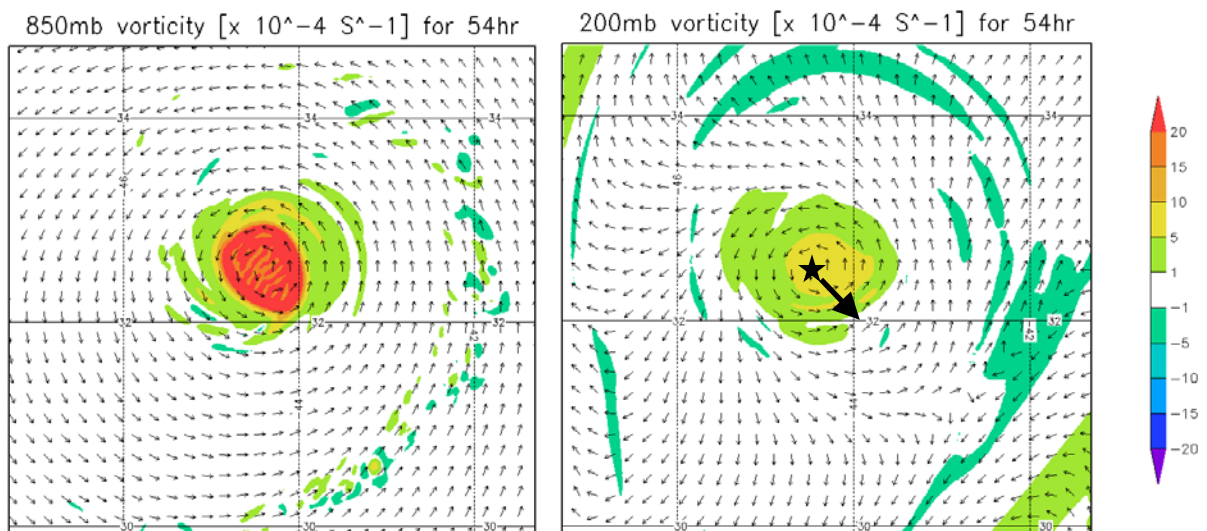
Figure 11-2: *Anticipated "pre-shear" vortex structure from HWRF.*

<u>Threshold shear and large tilt sampling:</u>

The TC's kinematic structure responds to increasing VWS in one of three ways: 1) maintain a vertically upright vortex core throughout the troposphere, 2) develop significant tilt of the vortex core, but then realign into a steady-state tilt configuration (esp. if the shear is sustained), and 3) exhibit continuous and irreversible separation of the upper- and lower-level vortex cores, resulting in a shallow low-level circulation usually void of deep convection.

If a sufficiently high threshold value of VWS is employed, scenario 1) is least likely. For a TC that follows scenario 2), determining the target time of maximum tilt is critical. If the TC is sampled after realignment has already completed, the structural changes we wish to document may be greatly diminished. Furthermore, it would not be possible to fully test the intensity modification Hypothesis 3. For a TC that follows scenario 3), 12-h sampling of the TC until the low-level circulation becomes completely exposed (and void of deep convection) is adequate.

Since the possibility of scenario 2), and the precise timing of maximum tilt, depend on a variety of factors, as discussed in the **Background**, time series of forecast shear from a number of different sources (e.g., SHIPS, HWRF coarse grid, etc.) should be used in conjunction with a threshold shear value to guide the timing of flights subsequent to the pre-shear sampling. For the Category 2-3 hurricane in the example, a noticeable tilt of the circulation center with height becomes evident 18-24 h after the first mission, or when the shear approaches a value of 20 kts (not shown). An indication that the shear is beginning to strongly influence storm structure is the development of a pronounced convective asymmetry within the core region. Figure 11-3 illustrates this convective asymmetry at the time the shear threshold is reached (and the core begins to tilt). In this example, <u>the second P-3 mission would commence ~12 h after the first</u>.

Mission 2: A second P-3 will be prepared to sample the TC when the shear approaches a threshold value (~20 kts in the example). The objective is to document the initial development of shear-induced vertical tilt and the boundary layer response. The P-3 performs a single Figure-4 pattern (90-105 nmi legs) with TDR to obtain the TC core-region structure (Fig. 11-8). The P-3 then travels downwind to set up a rotated Figure-4 pattern with truncated radial legs. The radial legs should extend just outside the primary mesoscale region of convection radially beyond (~15-30 nmi) the eyewall. Dropsondes should be launched within and downwind of the convective region outside the eyewall in such a way as to sample low-θ_e air spiraling into the eyewall within the boundary layer.
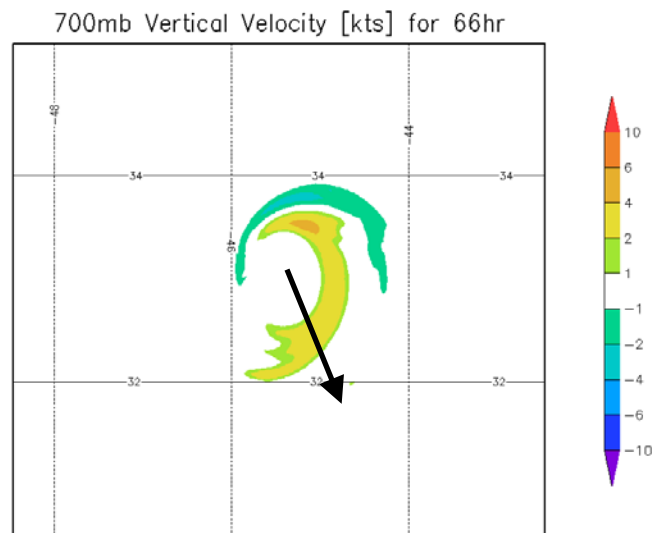
Figure 11-3: *Anticipated "threshold shear" convective asymmetry from HWRF.*

Figure 11-4 shows the tilted vorticity structure 12 h after the TC begins to develop a visible vertical tilt of the

core (i.e., through the displacement of circulation centers with height). By this time, the shear magnitude is 30-35 kts. The vortex tilts to the left of the large-scale, deep-layer shear vector, as expected based upon work cited in the **Background**. In this example, the upper-level vorticity of the TC ultimately weakens and merges with an upper-level, north-south oriented vorticity feature to its west (not shown). This behavior is closest to that in scenario 3).

Mission 3: The P-3 used in the "pre-shear" mission will be prepared to sample (at least 24 h after the pre-shear mission) the TC when the vertical tilt of the core has reached a large value. The P-3 repeats the "threshold shear" sampling of the previous mission (Fig. 11-8). At the same time the G-IV repeats the "pre-shear" sampling pattern (Fig. 11-6).
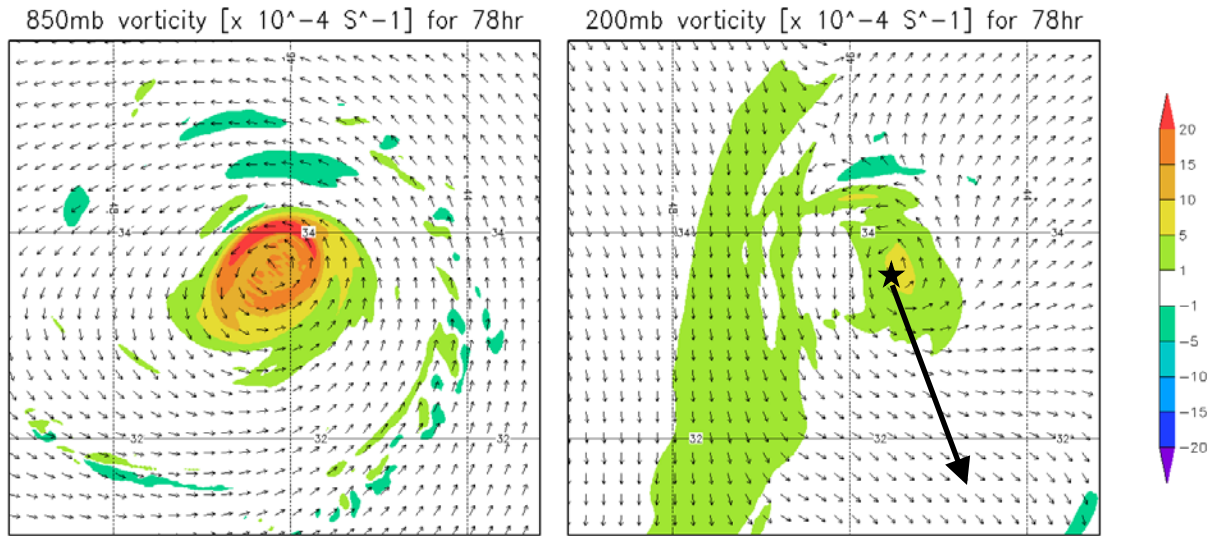
Figure 11-4: Anticipated "large-tilt" vortex structure from HWRF.

TC alignment and recovery sampling:

As discussed in the **Background**, some TCs are able to realign once tilted, even under sustained vertical wind shear. In the context of the intensity change Hypothesis 3, negative thermodynamic impacts on the TC should be reduced as the vortex aligns. In numerical simulations (e.g., Riemer et al. 2010), this is followed by re-intensification of the TC. In the example here, the vortex does not realign, and the primary circulation becomes increasingly shallow (not shown). The TC then continues to weaken (Figure 11-5). Whether the TC is resilient or is progressively sheared apart, a follow-up mission to investigate the continued evolution of the TC is important for a complete understanding of the life-cycle of a vertically-sheared storm.

Mission 4: The P-3 used in the "threshold shear" mission will be prepared to sample the TC after realignment has completed (or the vortex continues to be sheared apart). The objective is to verify vertical alignment in the kinematic field and the thermodynamic recovery of the boundary layer (or the continued deterioration of the circulation). The P-3 repeats the "threshold shear" and "large-tilt" sampling pattern (Fig. 11-8).
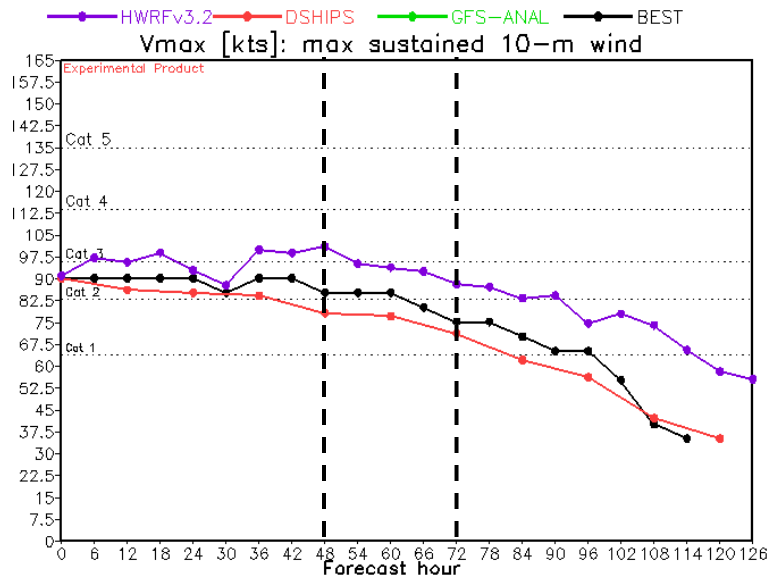
Figure 11-5: Anticipated weakening as shear-induced structure changes occur in HWRF (purple).

Analysis Strategy:

The basic analysis follows that presented in recent observational studies of the vertically sheared TC (Reasor et al. 2009; Reasor and Eastin 2012; Reasor et al. 2013; Rogers et al. 2013; Zhang et al. 2013). The analysis includes: low-wavenumber kinematic structure of the core region above the boundary layer, vortex tilt, and local VWS derived from airborne Doppler radar observations; low-wavenumber kinematic structure of the boundary layer derived from SFMR and dropsonde measurements; low-wavenumber thermodynamic structure within and above the boundary layer derived from dropsondes and flight-level measurements; and convective burst statistics derived from Doppler radar observations. New elements of the analysis will include: 3D kinematic structure out to at least 4-5xRMW using radar observations; low-wavenumber kinematic, thermodynamic, and moisture structures out to 150 nmi using G-IV radar and dropsonde observations; high azimuthal and radial representation of the inflow structure downwind of the mesoscale-organized convection radially outside the eyewall.

The above unprecedented dataset will be collected in the context of a TC encountering a large increase in VWS. We first document the basic kinematic evolution of the TC on both short (~1 h) and long (~12 h) timescales. For the optimal set of missions, the initial "pre-shear" vortex structure will be approximately axisymmetric and the vortex tilt should be a negligible fraction of the RMW. The core-region moisture envelope should also be approximately axisymmetric. The analysis may reveal horizontal inhomogeneities in θ_e at large distance from the core. Diagnostic analyses include: vertical tilt, local shear, 3D Doppler-derived vertical velocity and reflectivity, storm-relative streamline analyses out to 150 nmi, and 3D θ_e analyses below P-3 flight level within 4-5xRMW and below G-IV flight level between 60 and 150 nmi. These same diagnostics will also be computed at later stages of the sheared TC evolution.

Using the "threshold shear" mission data we document the development of tilt asymmetry out to 4-5xRMW, the distortion of the moist envelope, and the evolution of the near-core, storm-relative flow topology. Also at this stage, we document the development of convective asymmetry within and radially outside the eyewall, examine the shear-relative convective statistics (e.g., as in Eastin et al. 2005), and analyze changes in the boundary layer θ_e structure in relation to changes in convective organization outside the eyewall. At the "large tilt" stage, we anticipate asymmetric coverage of radar reflectors about the storm center. Where reflectors are, the analysis proceeds as above. Diagnostics relying on azimuthal coverage of the winds (e.g., the azimuthal-mean winds, tilt, and local shear) may be restricted to limited radial bands. If available, we will explore the benefits of Doppler Wind Lidar measurements in the echo-free regions of the storm. The objective at this

78

stage is to examine whether the tilt asymmetry organizes convection on the vortex scale, how and where low θ_e air is transported into the near-core region, whether low θ_e air is transported into the boundary layer outside the eyewall, the modification of θ_e as parcels move inward towards the eyewall (if they do; see Zhang et al. (2013) and Riemer et al. (2013) for examples where the storm-relative core-region flow within the boundary layer of a sheared storm is radially outward), and changes in azimuthal-mean θ_e within the eyewall region and its relation to intensity change.

At the "realignment and recovery" stage, the optimal experiment will reveal a core kinematic and thermodynamic structure that more closely resembles the "pre-shear" structure than observed during the intermediate missions. The moist envelope may still be distorted, but the mechanism for downward transport of the low θ_e air will be diminished due to the reduction in vortex tilt. If the vortex continues to shear apart during this mission, the analysis will focus on the development of boundary layer "cold pools" using the dropsonde measurements, and, to the extent possible, the deterioration of the vertical structure of the TC's primary circulation (e.g., Reasor et al. 2000; Sec. 4 of Riemer et al. (2013)).

Modules:

1) *Boundary layer inflow*

   Summary: This module is designed to complement standard operationally-tasked P-3 Tail Doppler Radar (TDR) missions by obtaining near-surface wind vector data from GPS dropwindsondes where Doppler winds are not readily available.

   Background: The near-surface inflow is a crucial region of a tropical cyclone (TC), since it is the area of the storm in direct contact with the ocean moisture and heat sources which power the storm. Recent composite analysis of near-surface wind data has led to a more accurate description of general TC inflow characteristics, including asymmetries (Zhang and Uhlhorn 2012). However, it has also become clear that there are few individual cases that contain sufficient observations to develop an accurate synoptic view and comprehensive understanding of boundary layer inflow evolution as a TC intensifies or weakens, changes motion, experiences eyewall/rain-band cycles, and is impacted by shear to varying degrees. To fill this data gap, the proposed modular experiment is developed to augment wind vector observations from Doppler radar that are routinely obtained by NOAA WP-3D aircraft.

   Synopsis: The flight pattern is consistent with a typical rotated "alpha" (Figure-4) pattern flown for TDR missions (Fig. 11-9). The rotated pattern (as opposed to the repeated alpha pattern) is preferable to better resolve higher (than 1) wavenumber asymmetric wind field structure. In addition, it is requested to fly the pattern as orthogonal pairs of radials, rather than rotating radials by 45 deg. as the flight proceeds. The initial (IP) and final (FP) points of the pattern are arbitrary. Required instrumentation consists of expendable probes (34 dropwindsondes and 16 AXBTs) as depicted in Fig. 11-9. Note that in particular, high-resolution sampling (3 sondes spaced ~1 min apart) is requested across the radius of maximum wind (RMW) on a pair of orthogonal radii to help better estimate boundary layer gradient winds. Center drops are requested on the first and last pass through the eye.

   Research plan: The optimal successful experiment will yield a synoptic view of near surface inflow over a series of consecutive missions to document the evolution of boundary layer inflow as a TC progresses through its life cycle. Our research goal is to better understand details about environmental impacts on BL inflow which is not adequately described by the composite analysis constructed from data obtained from numerous independent cases. Specific questions we wish to answer are: 1) How might environmental shear modulate the expected, frictionally-induced inflow asymmetry? 2) What is the relationship between near- surface inflow and inflow above the BL as depicted by Doppler wind analysis? 3) How are near-surface inflow and thermodynamic fields (temperature and moisture and associated fluxes) inter-related?

2) *Extratropical Transition*

Significance: The poleward movement of a tropical cyclone (TC) initiates complex interactions with the midlatitude environment frequently leading to sharp declines in hemispheric predictive skill. In the Atlantic basin, such interactions frequently result in upstream cyclone development leading to high-impact weather events in the U. S. and Canada, as well as downstream ridge development associated with the TC outflow and the excitation of Rossby waves leading to downstream cyclone development. Such events have been shown to be precursors to extreme events in Europe, the Middle East, and may have led to subsequent TC development in the Pacific and Atlantic basins as the waves progress downstream. During this time, the TC structure begins changing rapidly: the symmetric distributions of winds, clouds, and precipitation concentrated about a mature TC circulation center develop asymmetries that expand. Frontal systems frequently develop, leading to heavy precipitation events, especially along the warm front well ahead of the TC. The asymmetric expansion of areas of high wind speeds and heavy precipitation may cause severe impacts over land without the TC center making landfall. The poleward movement of a TC also may produce large surface wave fields due to the high wind speeds and increased translation speed of the TC that results in a trapped-fetch phenomenon.

During this phase of development, hereafter referred to as extratropical transition (ET), the TC encounters increasing vertical wind shear and decreasing sea surface temperatures, factors that usually lead to weakening of the system. However, transitioning cyclones sometimes undergo explosive cyclogenesis as extratropical cyclones, though this process is poorly forecast. The small scale of the TC and the complex physical processes that occur during the interactions between the TC and the midlatitude environment make it very difficult to forecast the evolution of track, winds, waves, precipitation, and the environment. Due to sparse observations and the inability of numerical models to resolve the structure of the TC undergoing ET, diagnoses of the changes involved in the interaction are often inconclusive without direct observations. Observations obtained during this experiment will be used to assess to what extent improvements to TC structure analyses and the interaction with the midlatitude flow improve numerical forecasts and to develop techniques for forecasting these interactions. Improved understanding of the changes associated with ET will contribute to the development of conceptual and numerical models that will lead to improved warnings associated with these dangerous systems.

Objective: The objective is to gather data to study the physical processes associated with ET and the impact of extra observations in and around an ET event on the predictability of the cyclone undergoing transition and of the environment. To examine the relative roles of the TC and midlatitude circulation, aircraft will be used to monitor the changes in TC structure and the region of interaction between the TC and midlatitude circulation into which it is moving.

Specific goals are:
- To obtain a complete atmosphere/ocean data set of the TC undergoing ET and interacting with the midlatitude circulation, especially at the cyclone outflow and midlatitude jet stream interface.
- To examine the interface between the upper-level outflow from the TC and the midlatitude flow, and how the interaction between the two affects the predictability of both the downstream flow and the enhanced precipitation in the pre-storm environment.
- To understand the dynamical and physical processes that contribute to poor numerical weather forecasts of TC/midlatitude interaction, including validation of forecasts with observations.
- To track the thermal and moisture characteristics of the evolving system and assess their impact on the predictability of TC/midlatitude interaction.
- To measure the influence of the increased vertical wind shear associated with the midlatitude baroclinic environment on the structural characteristics of the TC circulation.
- To gather microphysical and oceanic measurements along aircraft flight paths.

Requirements:
- The TC and its environment must have been sampled continuously by NOAA aircraft for at least one day prior to the ET event. Regular sampling by the P3s to get structure information from the Airborne Doppler Radar is required. Previous environmental sampling by the G-IV is helpful, but not necessary.

- The TC must have been of at least hurricane intensity during the previous sampling.
- The TC must not have had major land interactions during the previous sampling, or during the proposed experimental missions.
- Concurrent P3 and G-IV missions are helpful, but not required. Solo P3 missions would address vortex resilience issues. No solo G-IV missions would occur.

Hypotheses and questions:
ET depends upon the survival of the TC as it penetrates into midlatitudes in regions of increasing vertical wind shear.

- How is the TC vortex maintained in regions of vertical wind shear exceeding 30 ms-1?
- How is the warm core maintained long after the TC encounters vertical wind shear exceeding 30 ms-1?
- How does vertical shear exceeding 30ms-1 alter the distribution of latent heating and rainfall?
- Does vortex resilience depend upon diabatic processes? On subsequent formation of new vortex centers, or by enlisting baroclinic cyclogenesis?
- Does the vertical mass flux increase during ET, as has been shown in numerical simulations?
- Is downstream error growth related to errors in TC structure during ET?
- Is ET sensitive to the sea-surface temperatures?

Description: The mission is designed to use multiple aircraft to monitor interactions between the TC and the midlatitude circulation. The ideal storm will be a poleward-moving hurricane that is offshore the United States mid-Atlantic coastline. The optimal mission is designed to examine the TC core and the TC/midlatitude interface (Fig. 11-10). Aircraft will participate in staggered (12-hourly) missions until out of range, because of the possible rapid changes in structure.

TC region: The WP-3D will fly figure-4 or butterfly patterns as high as possible to avoid hazards such as convective icing. The aircraft will make as many passes as possible through the center of the TC undergoing ET, with a minimum of two passes necessary (Fig. 11-11). Legs can be shortened to the south of the storm center if necessary to save time. Dropwindsondes will be deployed at each waypoint and at evenly spaced intervals along each leg with optimal spacing near 60 n mi. AXBTs will be deployed at each waypoint and at the midpoint of each leg only in the northern semicircle from the cyclone center.

Due to a trapped fetch phenomenon, the ocean surface wave heights can reach extreme levels ahead of a TC undergoing ET. Therefore, primary importance for the WP-3D in the northeast quadrant of the TC will be the scanning radar altimeter (WSRA) to observe the ocean surface wave spectra, if available. Flight level will be chosen to accommodate this instrument.

TC/Midlatitude interface and pre-storm precipitation region: Ahead of the TC, important interactions between the midlatitude jet stream and the outflow from the TC occur. This region will be investigated by the G-IV releasing dropwindsondes every 120 n mi during its pattern. The Airborne Doppler Radar aboard the G-IV will be very helpful in determining the structure of the rain shield in this region, but is not a requirement.

References:

Bender, M. A., 1997: The effect of relative flow on the asymmetric structure in the interior of hurricanes. *J. Atmos. Sci.*, **54**, 703–724.

Black, M. L., J. F. Gamache, F. D. Marks, C. E. Samsury, and H. E. Willoughby, 2002: Eastern Pacific Hurricanes Jimena of 1991 and Olivia of 1994: The effect of vertical shear on structure and intensity. *Mon. Wea. Rev.*, **130**, 2291–2312.

Braun, S. A., M. T. Montgomery, and Z. Pu, 2006: High-resolution simulation of Hurricane Bonnie (1998). Part I: The organization of eyewall vertical motion. *J. Atmos. Sci.*, **63**, 19–42.

Davis, C. A., S. C. Jones, and M. Riemer, 2008: Hurricane vortex dynamics during Atlantic extratropical transition. *J. Atmos. Sci.*, **65**, 714–736.

DeMaria, M., 1996: The effect of vertical shear on tropical cyclone intensity change. *J. Atmos. Sci.*, **53**, 2076–2088.

DeMaria, M., M. Mainelli, L. K. Shay, J. A. Knaff, and J. Kaplan, 2005: Further improvements to the Statistical Hurricane Intensity Prediction Scheme (SHIPS). *Wea. Forecasting*, **20**, 531–543.

Eastin, M. D., W. M. Gray, and P. G. Black, 2005: Buoyancy of convective vertical motions in the inner core of intense hurricanes. Part II: Case studies. *Mon. Wea. Rev.*, 133, 209–227.

Emanuel, K. A., 1986: An air-sea interaction theory for tropical cyclones. Part I: Steady-state maintenance. *J. Atmos. Sci.*, **43**, 585–605.

Emanuel, K. A., 1991: The theory of hurricanes. *Annu. Rev. Fluid Mech.*, **23**, 179–196.

Frank, W. M. and E. A. Ritchie, 2001: Effects of vertical wind shear on the intensity and structure of numerically simulated hurricanes. *Mon. Wea. Rev.*, **129**, 2249–2269.

Gray, W. M., 1968: Global view of the origin of tropical disturbances. *Mon. Wea. Rev.*, **96**, 669-700.

Jones, S. C., 1995: The evolution of vortices in vertical shear. I: Initially barotropic vortices. *Quart. J. Roy. Meteor. Soc.*, **121**, 821–851.

Jones, S. C., 2000: The evolution of vortices in vertical shear. III: Baroclinic vortices. *Quart. J. Roy. Meteor. Soc.*, **126**, 3161–3185.

Kaplan, J., and M. DeMaria, 2003: Large-scale characteristics of rapidly intensifying tropical cyclones in the North Atlantic basin. *Wea. Forecasting*, **18**, 1093–1108.

Molinari, J., D. Vollaro, K. L. Corbosiero, 2004: Tropical cyclone formation in a sheared environment: A case study. *J. Atmos. Sci.*, **61**, 2493-2509.

Molinari, J., P. Dodge, D. Vollaro, K. L. Corbosiero, F. D. Marks Jr., 2006: Mesoscale aspects of the downshear reformation of a tropical cyclone. *J. Atmos. Sci.*, **63**, 341-354.

Reasor, P. D., M. T. Montgomery, F. D. Marks Jr., and J. F. Gamache, 2000: Low-wavenumber structure and evolution of the hurricane inner core observed by airborne dual-Doppler radar. *Mon. Wea. Rev.*, **128**, 1653-1680.

Reasor, P. D., M. T. Montgomery, and L. D. Grasso, 2004: A new look at the problem of tropical cyclones in vertical shear flow: Vortex resiliency. *J. Atmos. Sci.*, **61**, 3–22.

Reasor, P. D., M. Eastin, and J. F. Gamache, 2009: Rapidly intensifying Hurricane Guillermo (1997). Part I: Low-wavenumber structure and evolution. *Mon. Wea. Rev.*, **137**, 603–631.

Reasor, P. D., and M. D. Eastin, 2012: Rapidly intensifying Hurricane Guillermo (1997). Part II: Resilience in shear. *Mon. Wea. Rev.*, **140**, 425–444.

Reasor, P. D., R. Rogers, and S. Lorsolo, 2013: Environmental flow impacts on tropical cyclone structure diagnosed from airborne Doppler radar composites. *Mon. Wea. Rev.*, **141**, 2949–2969.

Reasor, P. D., and M. T. Montgomery, 2015: Evaluation of a heuristic model for tropical cyclone resilience. *J. Atmos. Sci.*, **72**, 1765–1782.

Riemer, M., M. T. Montgomery, and M. E. Nicholls, 2010: A new paradigm for intensity modification of tropical cyclones: thermodynamic impact of vertical wind shear on the inflow layer. *Atmos. Chem. Phys.*, **10**, 3163–3188.

Riemer, M., and M. T. Montgomery, 2011: Simple kinematic models for the environmental interaction of tropical cyclones in vertical wind shear. *Atmos. Chem. Phys.*, **11**, 9395–9414.

Riemer, M., M. T. Montgomery, and M. E. Nicholls, 2013: Further examination of the thermodynamic modification of the inflow layer of tropical cyclones by vertical wind shear. *Atmos. Chem. Phys.*, **13**, 327–

346.

Rogers, R., and Coauthors, 2006: The Intensity Forecasting Experiment: A NOAA Multiyear Field Program for Improving Tropical Cyclone Intensity Forecasts. *Bull. Amer. Meteor. Soc.*, **87**, 1523–1537.

Rogers, R., P. Reasor, and S. Lorsolo, 2013: Airborne Doppler observations of the inner-core structural differences between intensifying and steady-state tropical cyclones. *Mon. Wea. Rev.*, **141**, 2970–2971.

Simpson, R. H. and H. Riehl, 1958: Mid-tropospheric ventilation as a constraint on hurricane development and maintenance. *Proc. Tech. Conf. on Hurricanes*, Miami, FL, Amer. Meteor. Soc., D4.1-D4.10.

Tang, B., K. Emanuel, 2012: Sensitivity of tropical cyclone intensity to ventilation in an axisymmetric model. *J. Atmos. Sci.*, **69**, 2394–2413.

Wang, Y., M. Montgomery, and B. Wang, 2004: How much vertical shear can a well-developed tropical cyclone resist? Preprints, *26th Conference on Hurricanes and Tropical Meteorology*, Miami, FL, Amer. Meteor. Soc., 100-101.

Wong, M. L. M. and J. C. L. Chan, 2004: Tropical cyclone intensity in vertical wind shear. *J. Atmos. Sci.*, **61**, 1859–1876.

Zhang, J. A., and E. Uhlhorn, 2012: Hurricane sea surface inflow angle and an observation-based parametric model. *Mon. Wea. Rev*., **140**, 3587-3605.

Zhang, J. A., R. F. Rogers, P. D. Reasor, E. W. Uhlhorn, and F. D. Marks Jr., 2013: Asymmetric hurricane boundary layer structure in relation to the environmental vertical wind shear from dropsonde composites. *Mon. Wea. Rev.*, **141**, 3968–3984.

Tropical Cyclone in Shear Experiment

Principal Investigator(s): Paul Reasor (lead), Sim Aberson, Jason Dunion, John Kaplan, Rob Rogers, Jun Zhang, Michael Riemer (Johannes Gutenberg-Universität)

Objective: Sample the wind, temperature and moisture fields within and around a TC experiencing a significant increase in environmental vertical wind shear.

What to Target: The *environment* of a TC experiencing a significant increase in environmental vertical wind shear, but with minimal land interaction and positioned away from a significant gradient of sea surface temperature.

When to Target: Before a significant increase in environmental vertical wind shear and during the period of maximum vortex tilt. The G-IV take-off should be coordinated with the corresponding P-3 mission such that the innermost G-IV circumnavigation coincides with the P-3 sampling.
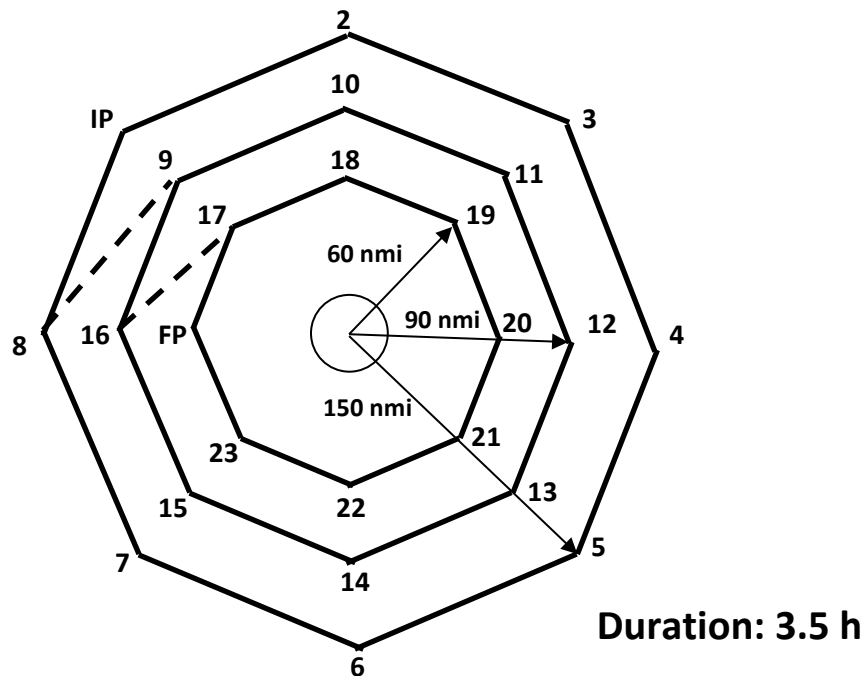
Figure 11-6: G-IV "pre-shear" and "large tilt" outer-core survey pattern

- Altitude: 40-45 kft
- Expendables: Deploy dropsondes at all turn points. No more than 24 GPS drops needed (18 if suboptimal hexagon pattern is flown).
- Pattern: The pattern is flown with respect to the surface storm center. Three concentric octagons (or suboptimal hexagons) are flown clockwise at decreasing radii of 150 nmi, 90 nmi, and 60 nmi. Dashed lines show transitions between rings. Time permitting, a fourth circumnavigation may be added. The vertices of the middle circumnavigation may be rotated to increase azimuthal resolution of the dropsonde observations.
- Instrumentation: Set airborne Doppler radar to scan F/AST on all legs.

Tropical Cyclone in Shear Experiment

Principal Investigator(s): Paul Reasor (lead), Sim Aberson, Jason Dunion, John Kaplan, Rob Rogers, Jun Zhang, Michael Riemer (Johannes Gutenberg-Universität)

Objective: Sample the wind, temperature and moisture fields within and around a tropical cyclone experiencing a significant increase in environmental vertical wind shear.

What to Target: The core region of a tropical cyclone experiencing a significant increase in environmental vertical wind shear, but with minimal land interaction and positioned away from a significant gradient of sea surface temperature.

When to Target: Before a significant increase in environmental vertical wind shear. The P-3 should be coordinated with the corresponding G-IV mission (see **Figure 7-1**).
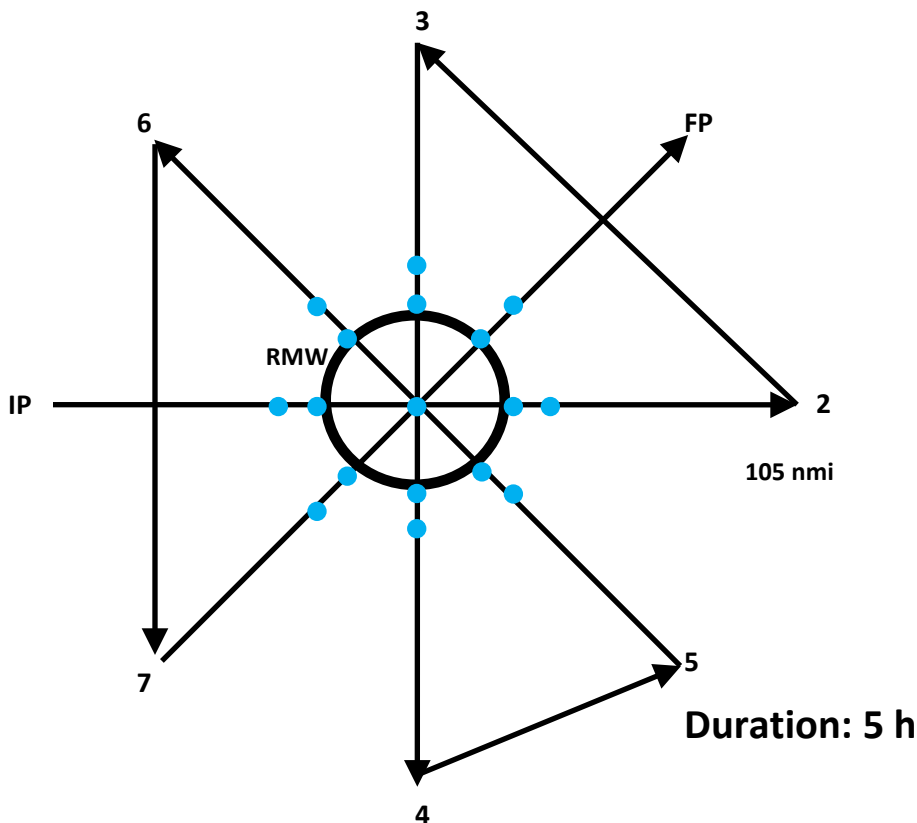
Figure 11-7: P-3 "pre-shear" core-region survey pattern

- Altitude: 12,000 ft (4 km) altitude preferable.
- Expendables: Deploy dropsondes at center of first and last pass, RMW, and 30 nmi (half distance to innermost G-IV circumnavigation) of Figure-4 legs. About 18 drops needed.
- Pattern: The pattern is flown with respect to the surface storm center. Radial legs of the rotated Figure-4 pattern extend 90-105 nmi.
- Instrumentation: Set airborne Doppler radar to scan F/AST on all legs.

Tropical Cyclone in Shear Experiment

Principal Investigator(s): Paul Reasor (lead), Sim Aberson, Jason Dunion, John Kaplan, Rob Rogers, Jun Zhang, Michael Riemer (Johannes Gutenberg-Universität)

Objective: Sample the wind, temperature and moisture fields within and around a tropical cyclone experiencing a significant increase in environmental vertical wind shear.

What to Target: The core region of a tropical cyclone experiencing a significant increase in environmental vertical wind shear, but with minimal land interaction and positioned away from a significant gradient of sea surface temperature.

When to Target: The large-scale, deep-layer shear reaches a critical threshold value and downshear convective asymmetry is evident; the TC core exhibits large vertical tilt (an intensifying TC may have reduced its rate of intensification or begun to weaken); and the TC core has realigned (a weakening or steady state TC may have begun to intensify).
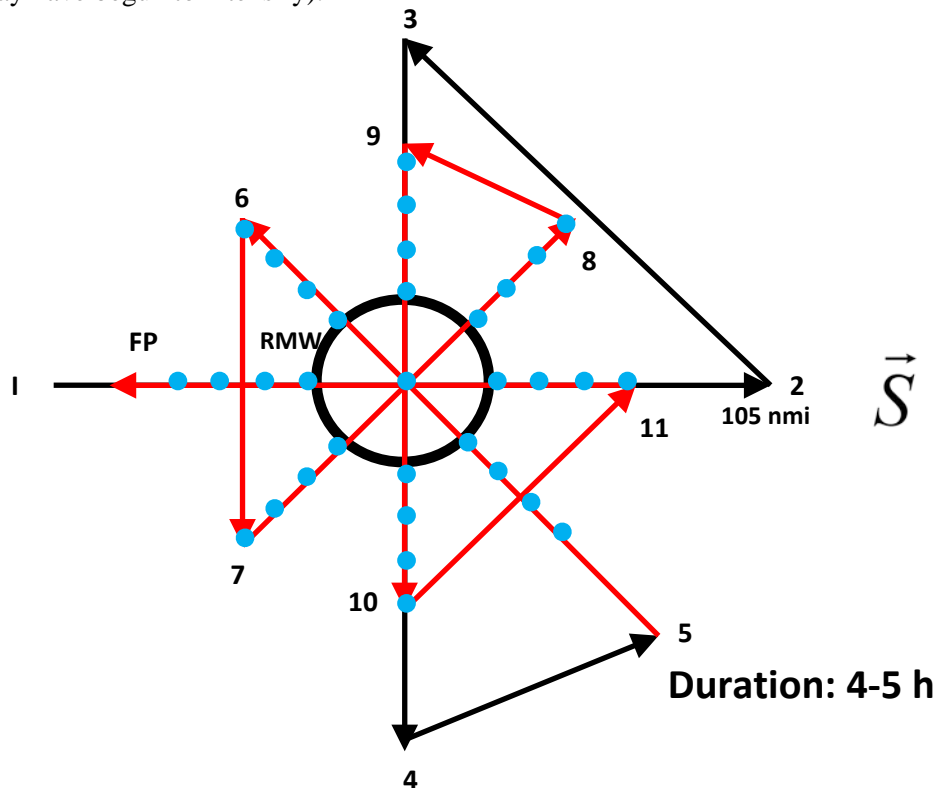
Figure 11-8: P-3 "threshold shear", "large-tilt", and "realignment and recovery" core-region survey pattern

- Altitude: 12,000 ft (4 km) altitude preferable.
- Expendables: Deploy dropsonde at center of first large-scale Figure-4 pass (if no G-IV, then also at IP and turn points). Deploy 4 equally-spaced dropsondes along each radial of the small-scale, rotated Figure-4 starting at the RMW and ending at turn point. About 33 drops needed (37 if G-IV not present).
- Pattern: The pattern is flown with respect to the surface storm center. The initial inbound leg falls along the large-scale, deep-layer shear vector. Radial legs of the initial Figure-4 pattern extend 90-105 nmi. Aircraft then flies 45 deg downwind (4 -> 5) to begin small-scale rotated Figure-4. Legs should extend just beyond the primary region of organized convection outside the eyewall (~15-30 nmi beyond RMW).
- Instrumentation: Set airborne Doppler radar to scan F/AST on all legs.
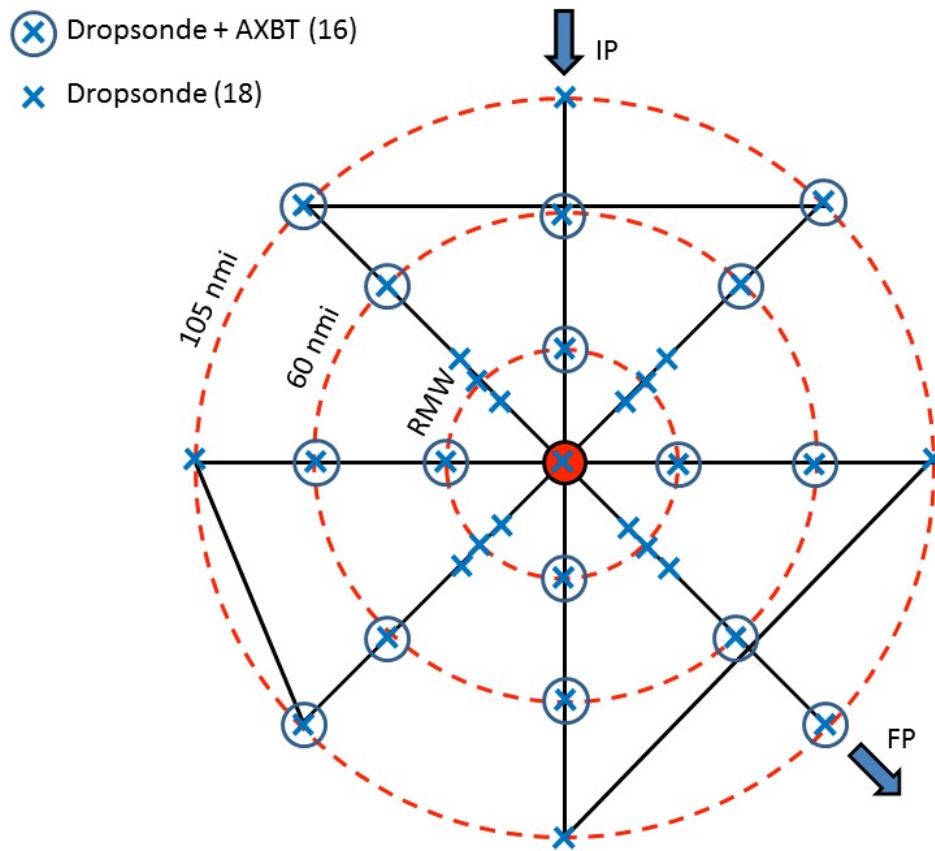
Figure 11-9: *Boundary Layer Inflow Module. GPS dropwindsondes (34 total) are deployed at 105 nmi and 60 nmi radii and at the radius of maximum wind along each of 8 radial legs (rotated alpha/Figure-4 pattern). On 4 of the 8 passes across the RMW, rapid deployment (~1 min spacing) of 3 sondes is requested. Center drops are requested on the initial and final pass through the eye. AXBT (16 total) deployments are paired with dropsondes at the indicated locations. Flight altitude is as required for the parent TDR mission, and initial and final points of the pattern are dictated by these same TDR mission requirements.*

Tropical Cyclone in Shear Experiment
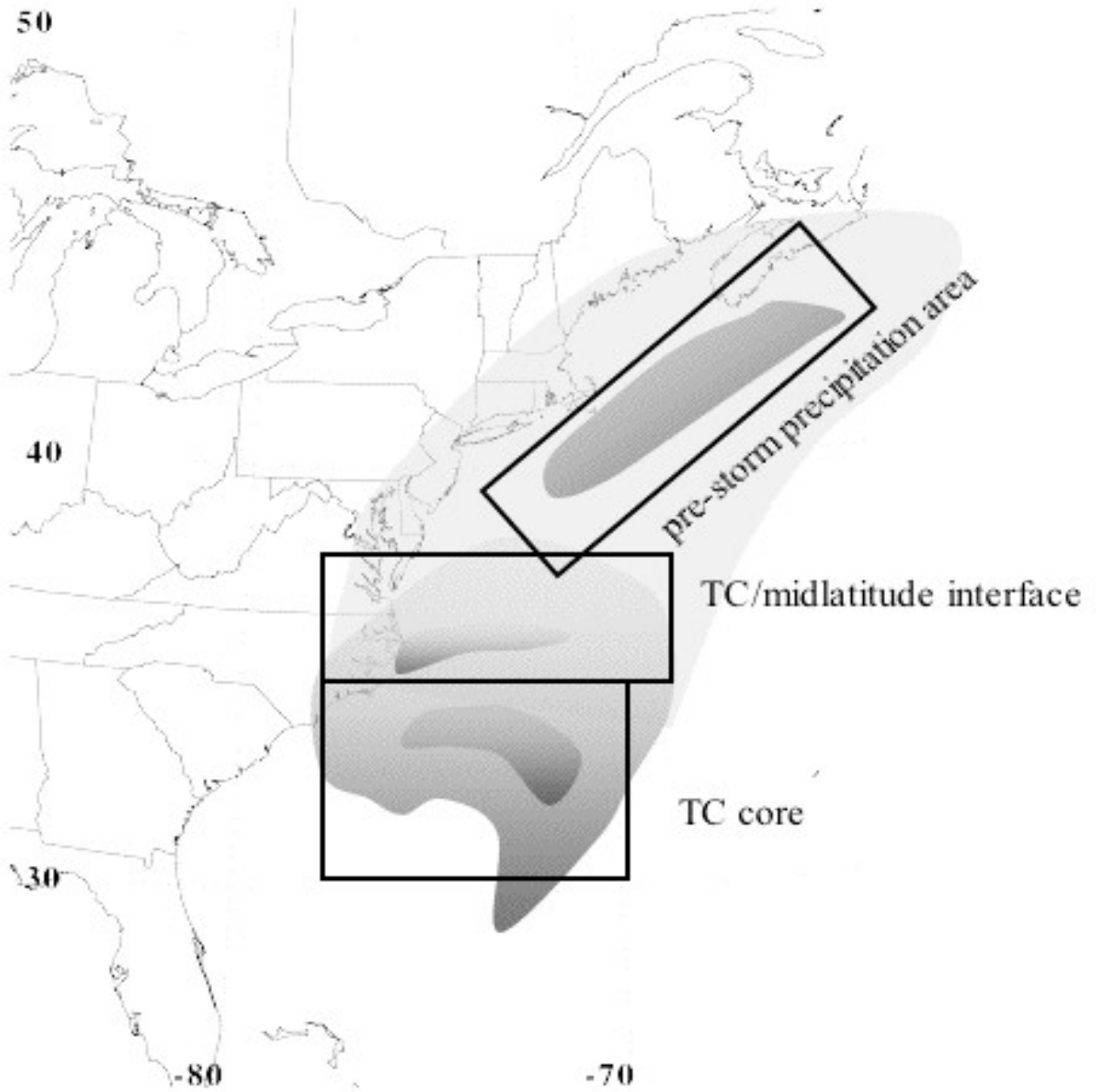
Figure 11-10: *Extra-tropical transition module. Schematic of Tropical Cyclone undergoing extra-tropical transition.*
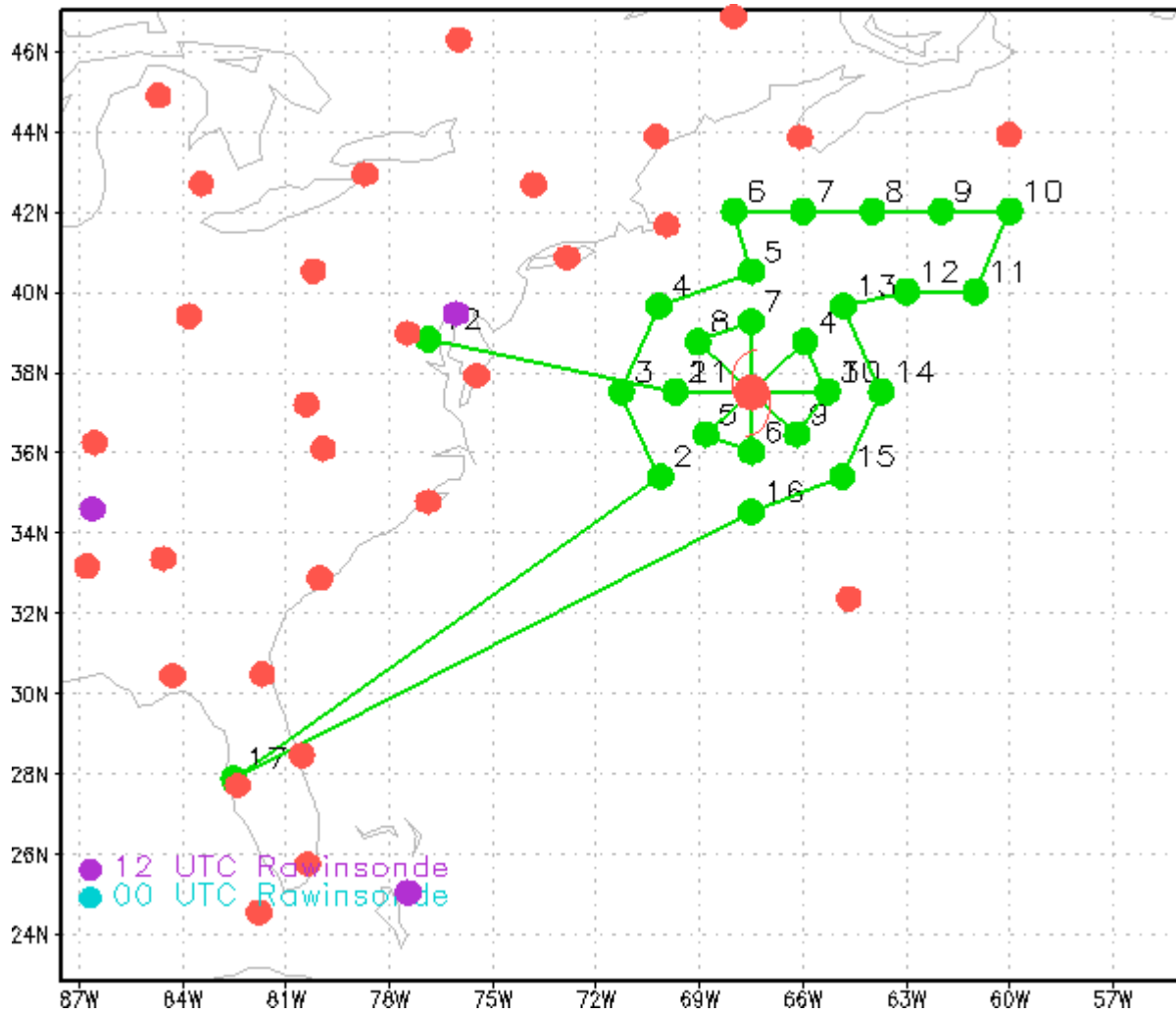
Figure 11-11: Extra-tropical transition module. Proposed flight tracks for G-IV and P3 aircraft.

12. Tropical Cyclone Diurnal Cycle Experiment

Principal Investigator: Jason Dunion (HRD)

Program Significance:

Numerous studies have documented the existence of diurnal maxima and minima associated with tropical convection. However, predicting the timing and extent of this variability remains a difficult challenge. Recent research using GOES satellite imagery has identified a robust signal of tropical cyclone diurnal pulsing. These pulses can be tracked using new GOES infrared satellite image differencing that reveals a "cool ring" (i.e. diurnal pulse) in the infrared that begins forming in the storm's inner core near local sunset each day. This diurnal pulse continues to propagate away from the storm overnight, reaching areas several hundred km from the storm center by the following afternoon. There appear to be significant structural changes to TCs [as indicated by GOES IR and microwave (37 and 85 GHz) satellite imagery] as diurnal pulses move out from the inner core each day and their timing/propagation also appears to be remarkably predictable. Although the relationships between the TC diurnal cycle and TC structure and intensity are unclear at this time, this phenomenon may be an important and fundamental TC process.

Objectives:

- The main goal of this experiment is to sample the thermodynamic and kinematic environment of diurnal pulses at various stages of their life cycles, including their initial formation and subsequent evolution, and to observe any corresponding fluctuations in TC structure and intensity during these events;
- Employ both NOAA P-3 and G-IV aircraft to collect kinematic and thermodynamic observations both within the inner-core (i.e., radius <~150 km) and in the surrounding large-scale environment (i.e., R=~150-400+ km) for systems that have exhibited signs of diurnal pulsing in the previous 24 hours;
- Employ the NOAA G-IV jet to sample the temperature, moisture, and winds at the TC cirrus canopy level before, during, and after the time of local sunset;
- Quantify the capabilities of the operational coupled model forecast system to accurately capture thermodynamic (e.g. cirrus canopy cooling at sunset) and kinematic (e.g. enhanced upper-level outflow) characteristics of the TC diurnal cycle and associated diurnal pulses;

Hypotheses:

- Although the exact nature of diurnal pulses is not yet clear, new GOES IR satellite imagery and recent model simulations indicate a diurnal process that may be driven by rapid changes in incoming shortwave radiation resulting in rapid cooling at the cirrus canopy level around sunset each day;
- Data from Caribbean rawinsondes and NASA HS3 Global Hawk GPS dropsondes suggests that there are two necessary conditions needed to initiate TC diurnal pulses: an established cirrus canopy over an area of deep convection and rapid cooling of the cloud tops (i.e. sunset cooling). These conditions appear create large (~2-5 C) temperature inversions near the cirrus canopy top that may be linked diurnal pulse formation;
- Diurnal pulses may be signatures of outwardly propagating gravity waves, harmonic oscillations of the CDO as it cools near the time of sunset, diurnally-driven changes in inertial stability in the upper-levels (i.e. cirrus canopy) of the storm, or temperature responses that lead to previously documented anvil expansion.

- Diurnal pulses may be associated with periods of enhanced upper-level outflow (as seen in GOES IR imagery) and may extend through a relatively deep layer of the low- to mid-level troposphere (suggested by 37/85 GHz microwave imagery and data from the P-3 lower fuselage radar);
- Observations of the TC diurnal cycle can be used to improve our understanding of this recently discovered phenomenon and test its observability in model simulations;

Links to IFEX goals:

- **Goal 1**: Collect observations that span the TC lifecycle in a variety of environments;
- **Goal 3**: Improve understanding of the physical processes important in intensity change for a TC at all stages of its lifecycle;

Model Evaluation Component: The TC diurnal cycle may be a fundamental TC process that initiates the formation of TC diurnal pulses near the time of local sunset each day. These TC diurnal pulses radially propagate from the TC inner core and reach peripheral radii (e.g. 300-400 km) the following morning and afternoon. Although the cirrus canopy is typically an under-sampled region of the storm, changes in the thermodynamic structure and outflow patterns in this region of the storm near the time of sunset will be sampled and may be a key component to the formation and evolution of TC diurnal pulses. The predictable propagation of TC diurnal pulses in both space and time each day makes them fairly easy to sample at various radii around the storm. Thermodynamic and kinematic observations will be made of the diurnal pulses from the surface to the cirrus canopy and will include outflow layer sampling, as well as areas of enhanced convergence, moisture, or vertical motions at various levels of the troposphere. Thermodynamic and kinematic observations that are collected during this module will be used to evaluate the robustness of the operational coupled model forecast system to represent the TC diurnal cycle.

Mission Description:

The experimental UW-CIMSS/HRD TC diurnal cycle web page (http://tropic.ssec.wisc.edu/real-time/tc_diurnal_cycle/tc_diurnal_cycle.php) will be used to monitor the development and propagation of TC diurnal pulses for storms of interest. The timing and propagation of diurnal pulses appears to be remarkably predictable: after its initial formation in the inner core region, it propagates outward at ~5-10 m s^{-1} and reaches peripheral radii (e.g. 200-500 km) at very specific times of day (local time). Therefore, a 24-hr conceptual clock describing the evolution of this phenomenon has been developed. Figure 12-1 shows the TC diurnal cycle clock that predicts the approximate times that diurnal pulse passes various radii and will be used in concert with the UW-CIMSS/HRD real-time diurnal pulsing imagery to plan aircraft sampling strategies and takeoff times.

The P-3 aircraft will dispense GPS dropsondes and collect Doppler radar data while flying a rotating figure-4 pattern (see sample pattern shown in Fig. 12-2) in the inner-core with leg lengths of 105-135 nm (~195-250 km) at the maximum safe altitude (~8k-12k feet) for avoiding graupel. The GPS dropsondes should be dispensed on each leg with a spacing of ~25 nm (45 km) to provide adequate coverage for sampling the radial gradients of kinematics and thermodynamics. The GPS dropsonde sampling density should be increased to ~15-20 nm (30-35 km) just ahead of, within, and behind the diurnal pulse that will be identified in real-time using the UW-CIMSS/HRD TC diurnal cycle satellite imagery P-3 lower fuselage (LF) radar imagery (Fig. 12-3). The circular outer band features depicted in Fig. 12-3 are in fact diurnal pulses and should be high priority targets. Since the diurnal pulse begins forming around local sunset (~1800-2100 LST) and typically passes the 200 km (105 nm) radius at ~0400-0800 LST the following morning, optimal P-3 sampling will occur from

~0000-1000 LST so that the aircraft can adequately sample the early-stage (inner core out to ~250 km (135 nm)) propagation of the diurnal pulse. The P-3 may also fly an arc cloud module or convective burst module as opportunities present. Since large arc cloud events have been noted to appear along the leading edge of diurnal pulses, the LPS should monitor TC diurnal cycle satellite imagery, visible satellite imagery, and the P-3 LF radar for opportunities to conduct the former module. The execution of these optional modules will be at the discretion of the LPS.

The NOAA G-IV (flying at ~175-200 hPa/~45,000-41,000 ft) GPS dropsonde drop points will be based on a star or star-circumnavigation pattern selected using real-time information from the UW-CIMSS/HRD TC diurnal cycle satellite imagery (Fig. 12-4). The star flight pattern will consist of several radial runs toward and away from the storm that will allow for sampling of radial gradients of winds and thermodynamics. GPS dropsondes will be deployed at the turn points in the pattern as well as at mid-points along each leg in the pattern. Additional GPS dropsondes will be deployed just ahead of, within, and behind the diurnal pulse (Fig. 4, yellow to pink shading) and will be determined by the LPS during the mission. Time permitting, a single hexagon circumnavigation of the storm will be made at a constant radius to provide tail Doppler radar coverage at/near the TC inner core region (Fig. 12-5). The radius will be selected based on safety considerations [typically 60-90 nm (110-165 km)] and GPS dropsondes will be deployed at each turnpoint. Since the diurnal pulse typically passes the TC outer radii (e.g. 300-400 km) later in the morning and early afternoon local time, the optimal G-IV sampling will occur slightly later than the optimal P-3 sampling. The TC diurnal cycle conceptual clock (Fig. 12-1) indicates that the cool ring passes the 300 (400) km radius at ~0800-1200 LST (~1200-1500 LST). Therefore, the optimal G-IV sampling will occur from ~0800-1500 LST and will target the later stages of the TC diurnal cycle evolution. The G-IV may also fly an arc cloud module as opportunities present. The G-IV ground-based LPS should monitor both TC diurnal cycle and visible satellite imagery, as well as real-time P-3 LF radar images that may be available on NASA's MTS aircraft tracking software) for signs of large arc cloud events along the leading edge of the diurnal pulse for opportunities to conduct the arc cloud module. The execution of this optional module will be at the discretion of the G-IV ground-based LPS.

When possible, TC Diurnal Cycle Experiment missions will be coordinated with the HRD Easterly Wave Genesis Experiment, TC in Shear Experiment, and Rapid Intensity Experiment (RAPX). This coordination will involve the WP-3D and G-IV and will be executed on a case-by-case basis.
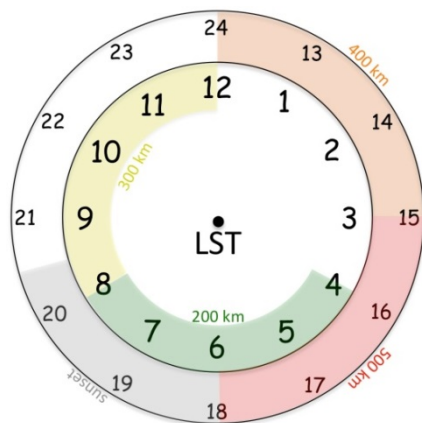
Figure 12-1. *Conceptual 24-hr TC diurnal cycle clock that outlines the lifecycle of diurnal pulses propagating away from the TC inner core. The diurnal pulse typically forms at local sunset (~1800-2030 LST, gray shading) and begins to propagate away form the inner core, passing the 200 km radius at ~0400-0800 LST (green shading) the following morning. It eventually reaches the 400 km radius at ~1200-1500 LST (orange shading) in the early afternoon.*
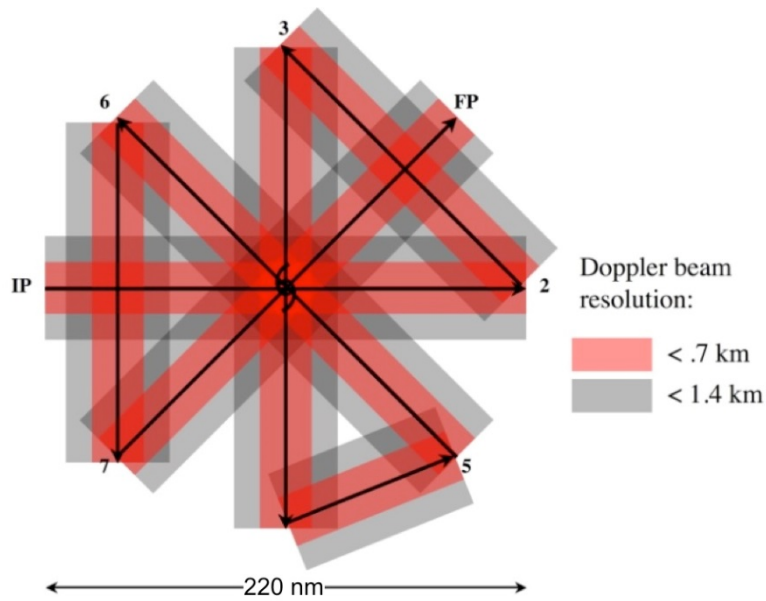
Figure 12-2. *Sample P-3 rotated figure-4 flight pattern. The red shading denotes locations where vertical spacing of Doppler beam < 0.7 km, grey shading where vertical spacing < 1.4 km. GPS dropsondes should be released at all turn points (past the turn after the aircraft has leveled), at midpoints of inbound/outbound legs, at the centers point between IP/2 and 5/6, and across the TC diurnal pulse.*
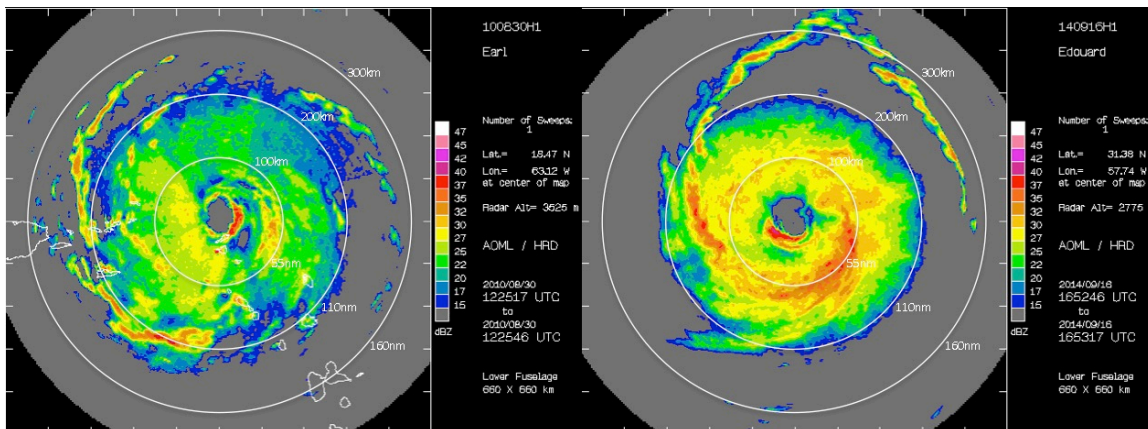
Figure 12-3. *P-3 lower fuselage radar showing 25-40 dBZ circular convective bands in the environments of (left) 2010 Hurricane Earl (R=~200-250 km) and (right) 2014 Hurricane Edouard (R=~200-300 km). These circular outer band features tend to be coincident with TC diurnal pulses and may be linked to the TC diurnal cycle.*
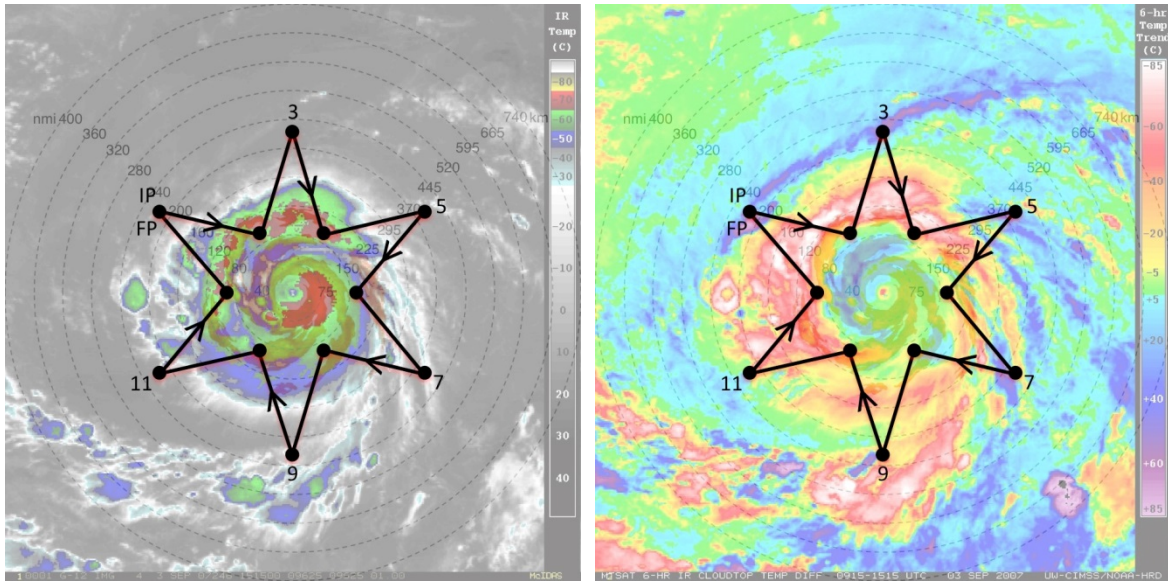
Figure 12-4. Sample G-IV star pattern with endpojnts that alternate between 90 and 216 nm (165 and 400 km). The endpoints can be adjusted inward or outward depending on the exact position of the outwardly propagating diurnal pulse and the size of the TC inner core. The pattern is overlaid on (left) GOES IR imagery and (right) UW-CIMSS IR diurnal cycle imagery. Yellow to pink shading in the latter image indicates a diurnal pulse propagating away from the storm during this time and shows its typical radial evolution at ~1100 LST when it has reached R=~300 km.
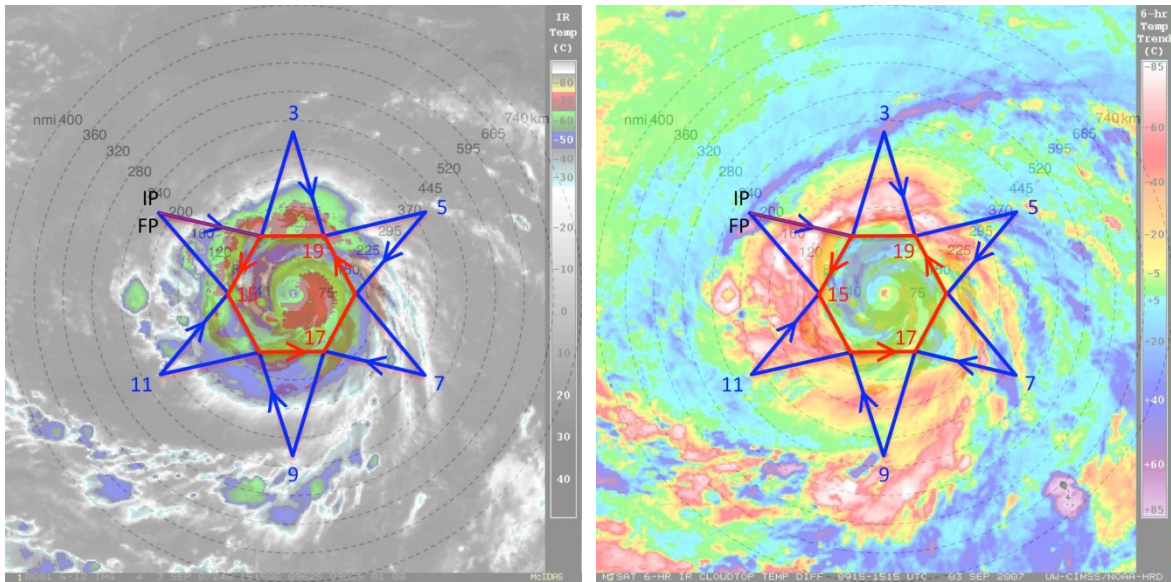
Figure 12-5. Same as in Fig. 12-4, except that a circumnavigation of the storm is performed after (or before) the star pattern is completed. The hexagon circumnavigation that is shown has points that are 90 nm (165 km) from the storm center, but can be adjusted outward for safety considerations depending on the strength and size of the TC.

Analysis Strategy

This experiment seeks to observe the formation and evolution of the TC diurnal cycle and associated diurnal pulses. Specifically, GPS dropsonde and radar observations will be used to analyze both the inner-core and environmental kinematics and thermodynamics that may lead to the formation of diurnal pulses and to document the kinematics and thermodynamics that are associated with TC diurnal pulses at various stages of their evolution.

Coordination with Supplemental Aircraft

NOAA will be conducting its Sensing Hazards with Operational Unmanned Technology (SHOUT) mission from 01 Aug – 30 Sep 2015. This field campaign will utilize one unmanned Global Hawk (GH) aircraft based from the NASA Wallops Flight Facility and will fly at approximately 55,000-60,000 ft altitude with mission durations of ~24 h. The GH will be used to sample both the TC inner core and surrounding environment. The primary science goals of SHOUT are to use adaptive GPS dropsonde sampling strategies to improve model forecasts of track and intensity, as well as to investigate processes in the TC inner core, boundary layer, and upper-level environment that impact intensity change and structure.

When possible, it will be desirable to fly P-3 and G-IV patterns that are coordinated with the GH (see Fig. 12-6 for sample flight patterns). "Coordinated" means a) designing tracks that provide enhanced spatial and/or temporal sampling between the different aircraft; b) flying radial penetrations where the P-3 and GH or WB-57 are vertically-stacked (the P-3 will be the low-altitude aircraft) for at least a portion of the flight leg, preferably when the aircraft are approaching the center of the TC; or c) coordinating missions that are flown on alternating days by the various aircraft. The across-track displacement during stacked coordination should be kept as small as practicable, e.g., no greater than 5-10 km. In practice, the NOAA P-3 will likely fly its planned figure-4/butterfly/rotating figure-4 patterns as indicated in Fig. 2. It should be noted that the GH can fly patterns that are similar in geometry to the NOAA P-3 patterns (Fig. 6). The G-IV pattern could either be designed/timed to supplement simultaneous coverage by the GH or could supplement storm environment coverage on days when the GH is not flying the storm.
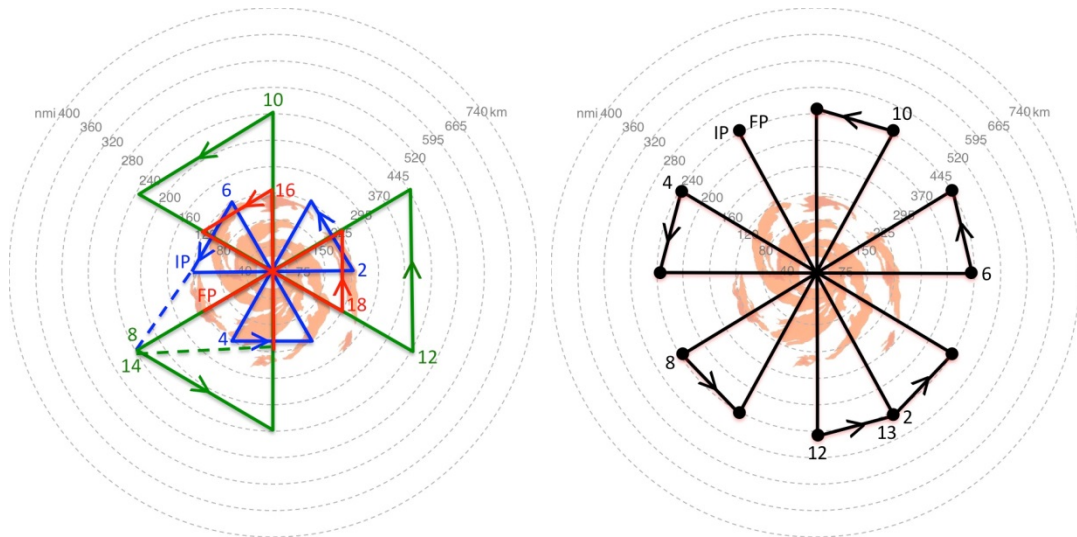
Figure 12-6. *Sample flight patterns for the NOAA SHOUT Global Hawk aircraft. (Left) Series of 3 alternating radial leg butterfly patterns and (right) rotated butterfly pattern with 30 degree rotated radial legs. On-station time for both patterns is ~15-20 hr and leg lengths are ~450 km.*

13. TC-Ocean Interaction Experiment

Principal Investigator(s): Rick Lumpkin (NOAA/PhOD), Gustavo Goni (NOAA/PhOD), George Halliwell (NOAA/PhOD), Luca Centurioni (SIO), and Nick Shay (U. Miami/RSMAS)

HRD Point of Contact: Jun Zhang

Primary IFEX Goal: 3 - Improve understanding of the physical processes important in intensity change for a TC at all stages of its lifecycle

Significance and Goals:

This component of the experiment broadly addresses improving understanding of the ocean's role in air-sea interaction and controlling TC intensity by making detailed measurements of these processes in storms. Specific science goals are in two categories:

Goal: To observe and improve our understanding of the upper-ocean response to the near-surface wind structure during TC passages. Specific objectives are to:

1.   Quantify the influence of the underlying ocean on atmospheric boundary layer thermodynamics and ultimately storm intensity.

2.   Quantify the capabilities of the operational coupled model forecast system to accurately capture and represent these processes

In addition, these ocean datasets fulfill needs for initializing ocean components of coupled TC Forecast systems at EMC and elsewhere.

Rationale:

Ocean effects on storm intensity. Upper ocean properties and dynamics play a key role in determining TC intensity. Modeling studies show that the effect of the ocean varies widely depending on storm size and speed and the preexisting ocean temperature and density structure. The overarching goal of these studies is to provide data on TC-ocean interaction with enough detail to rigorously test coupled TC models, specifically:

•   Measure the two-dimensional SST cooling, air temperature, humidity and wind fields beneath the storm and thereby deduce the effect of the ocean cooling on ocean enthalpy flux to the storm.
•   Measure the three-dimensional temperature, salinity and velocity structure of the ocean beneath the storm and use this to deduce the mechanisms and rates of ocean cooling.
•   Conduct the above measurements at several points along the storm evolution therefore investigating the role of pre-existing ocean variability.
•   Use these data to test the accuracy of the oceanic components coupled models.
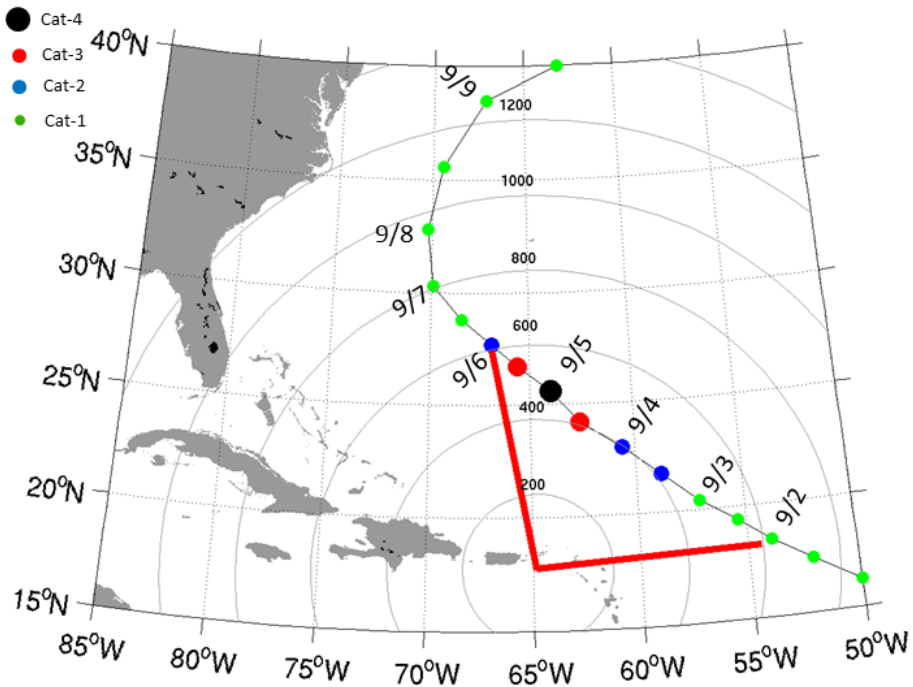
Figure 13-1: *Storm track with locations plotted every 12 hours. of Range rings are 200 nmi relative to forward operating base at St. Croix, USVI (STX/TISX), and red line delineates storm locations within 600 nmi of STX. In this example, the storm center remains within 600 nmi for 4 days.*

This multi-aircraft experiment is ideally conducted in geographical locales that avoid conflict with other operational requirements, for example, at a forward/eastward-deployed base targeting a storm not imminently threating the U.S. coastline. As an example, an optimal situation is shown in Fig. 13-1, with missions operating from St. Croix, USVI. A TC of at least minimal hurricane intensity is desired. In this example, the hypothetical storm remains within 600 nmi (a reasonable maximum distance) for four days, and at no time is forecasted to be a threat to land, including the U.S. coast.

a) Expendable profiler surveys from P-3 aircraft

Flight sequence:

Pre-storm: To establish the pre-storm upper ocean thermal and mass structure prior to a storm's arrival, a pre-storm expendable survey will be conducted. This mission will consist of deploying a large grid of AXCTDs/AXBTs to measure the three-dimensional temperature and salinity fields (Fig. 13-2). This flight would occur **48 hours prior to storm arrival**, based primarily on the forecasted track, and optimally covers the forecast cone-of-error. A total of **50-60 probes** would be deployed, depending on mission duration, and spaced approximate 0.5 deg. apart. The experiment is optimally conducted where horizontal gradients are relatively small, but AXCP probes may be included if significant gradients (and thus currents) are expected to be observed. Either P-3 aircraft may be used as long as it is equipped with ocean expendable data acquisition hardware.
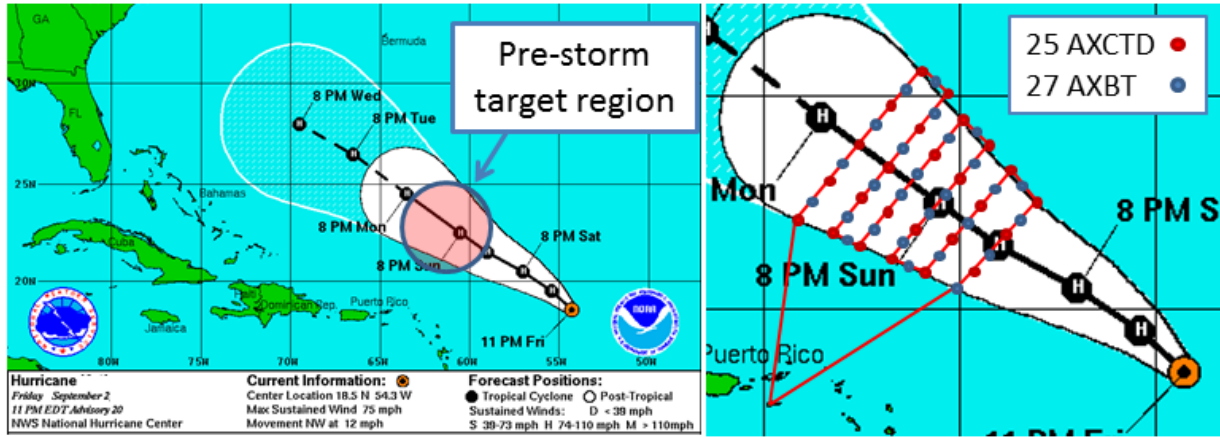
Figure 13-2: *Left: NHC official forecast track, which pre-storm ocean sampling region highlighted. Target region is centered ~48 hours prior to forecast arrival of storm. Right: P-3 flight track (red line) and ocean sampling pattern consisting of a grid of AXCTD/AXBT probes Probes are deployed at ~0.5 deg. intervals. Total time for this pattern is estimated to be ~9 hours.*

In-storm: Next, a mission is executed within the storm over the ocean location previously sampled (Fig. 13-3). This flight shall by conducted by the **P-3 carrying the Wide-swath Radar Altimeter (WSRA)** for purposes of mapping the two-dimensional wave field. The flight pattern should be a **rotated Figure-4**, and up to **20 AXBTs** should be deployed in combination with GPS dropwindsondes. Note that other experimental goals can and should be addressed during this mission, and a multi-plane mission coordinated with the other P-3, as well as G-IV, is desirable.
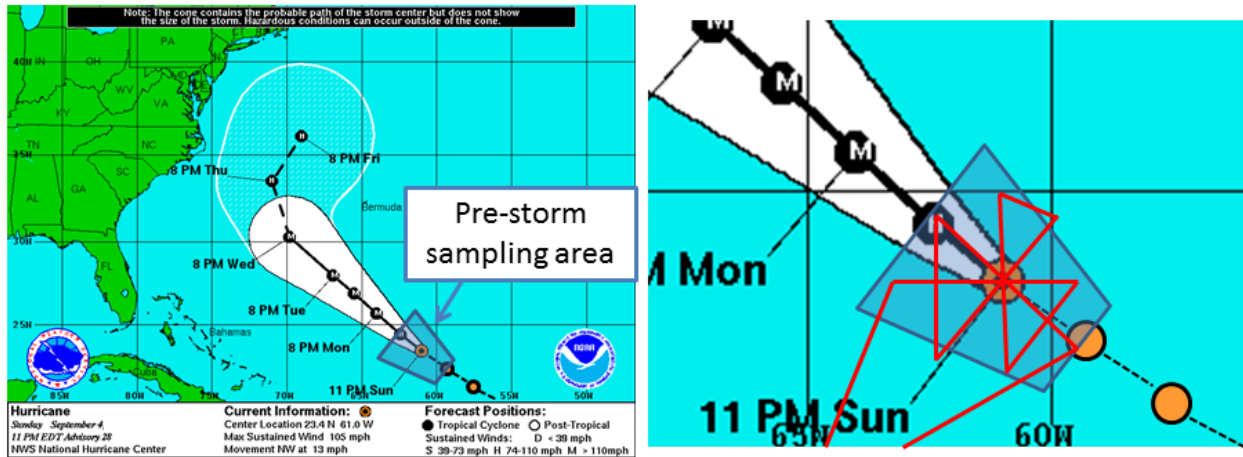
Figure 13-3: *Left: NHC official forecast track at time of in-storm mission, with pre-storm sampled region highlighted. Right: P-3 in-storm flight pattern centered on storm and over previously-sampled ocean area. Typical pattern is expected to be a rotated Fig-4. Total flight time ~8 hrs.*

Post-storm: Finally, a post-storm expendable survey shall be conducted over the same geographical location to assess ocean response, with slight pattern adjustments made based on the known storm track (Fig. 13-4). Approximately **60-70 probes** would be deployed (depending on duration limits), consisting mainly of **AXBTs/AXCPs** to map the three-dimensional temperature and currents, ideally 1-2 days after storm passage. In the Fig. 3-8 example, the pattern extends 470 km along the storm track, which in this example is ~0.75Λ, where

$\Lambda = 2\pi V/f$ is the inertial wavelength. Ideally, the pattern should extend up to 1Λ to resolve a full ocean response cycle. The storm speed *V* and flight duration limits will dictate whether this is possible. As for the pre-storm survey, either P-3 may be used.
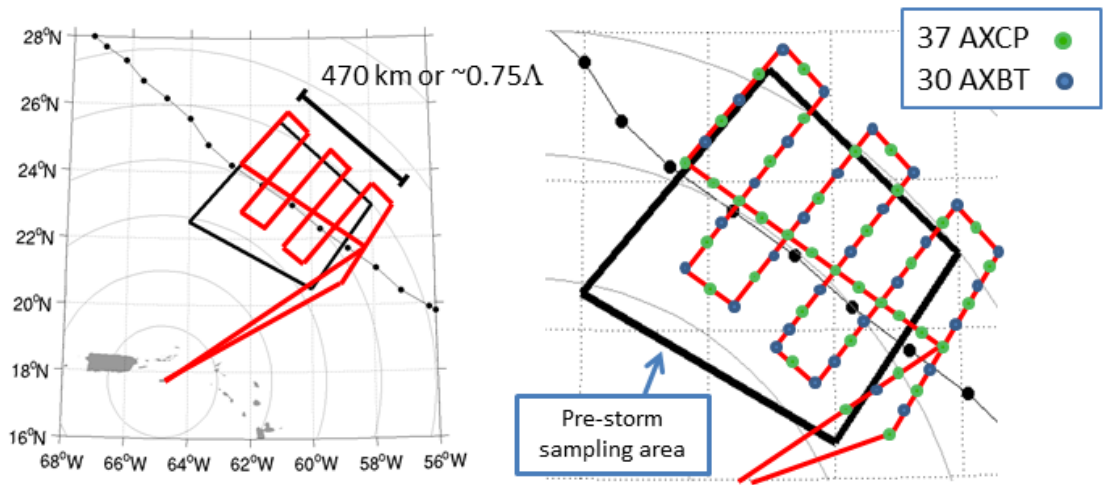
Figure 13-4: *Left: Post-storm ocean sampling flight pattern (red line), over previously-sampled area (black box). In this example, the pattern extends around 470 km in the along-track dimension, or around 0.75 of a near-inertial wavelength. Right: Flight pattern with expendable drop locations, consisting of a combination of AXCP and AXBT probes.*

b) Coordinated float/driftedeployment by AF C-130

Measurements will be made using arrays of drifters deployed by AFRC WC-130J aircraft in a manner similar to that used in the 2003 and 2004 CBLAST program. Additional deployments have since refined the instruments and the deployment strategies. This work will be coordinated with P-3 deployments of AXBTs, AXCTDs and AXCPs to obtain a more complete picture of the ocean response to storms.

MiniMet drifters measure SST, sea level air pressure and wind velocity. Thermistor chain Autonomous Drifting Ocean Station (ADOS) drifters add ocean temperature measurements to 150m. All drifter data are reported in real time through the Global Telecommunications System (GTS) of the World Weather Watch. An additional stream of real-time, quality controlled data is also provided by a server located at the Scripps Institution of Oceanography. A number of E-M APEX Lagrangian floats will measure temperature, salinity and velocity profiles to 200m. Float profile data will be reported in real time on GTS.

Coordination and Communications

Alerts - Alerts of possible deployments will be sent to the 53rd AWRO up to 5 days before deployment, with a copy to CARCAH, in order to help with preparations. Luca Centurioni (SIO) and Rick Lumpkin (PhOD) will be the primary point of contact for coordination with the 53rd WRS and CARCAH.

Flights:
Coordinated drifter deployments would nominally consist of 2 flights, the first deployment mission by AFRC WC-130J and the second overflight by NOAA WP-3D. An option for follow-on missions would depend upon available resources.

Day 1- WC-130J Float and drifter array deployment- Figure 13-5 shows a possible nominal deployment pattern for the float and drifter array. It consists of two lines, A and B, set across the storm path with 8 and 4

elements respectively. The line length is chosen to be long enough to span the storm and anticipate the errors in forecast track, and the lines are approximately in the same location as the pre-storm P-3 expendable probe survey. Instrumentation should be deployed 24-48 hours prior to storm arrival. The element spacing is chosen to be approximately the RMW. In case of large uncertainties of the forecast track a single 10 node line is deployed instead. The thermistor chain drifters (ADOS) are deployed near the center of the array to maximize their likelihood of seeing the maximum wind speeds and ocean response. The Minimet drifters are deployed in the outer regions of the storm to obtain a full section of storm pressure and wind speeds. The drifter array is skewed one element to the right of the track in order to sample the stronger ocean response on the right side (cold wake).

Day 2. P-3 In-storm mission- The in-storm mission will be conducted by the P-3 as previously described. Efforts will be made to deploy AXBTs during the mission near the locations of drifters/floats as reported in real time. It is highly desirable that this survey be combined with an SRA surface wave survey because high quality surface wave measurements are essential to properly interpret and parameterize the air-sea fluxes and boundary layer dynamics, and so that intercomparisons between the float wave measurements and the SRA wave measurements can be made.
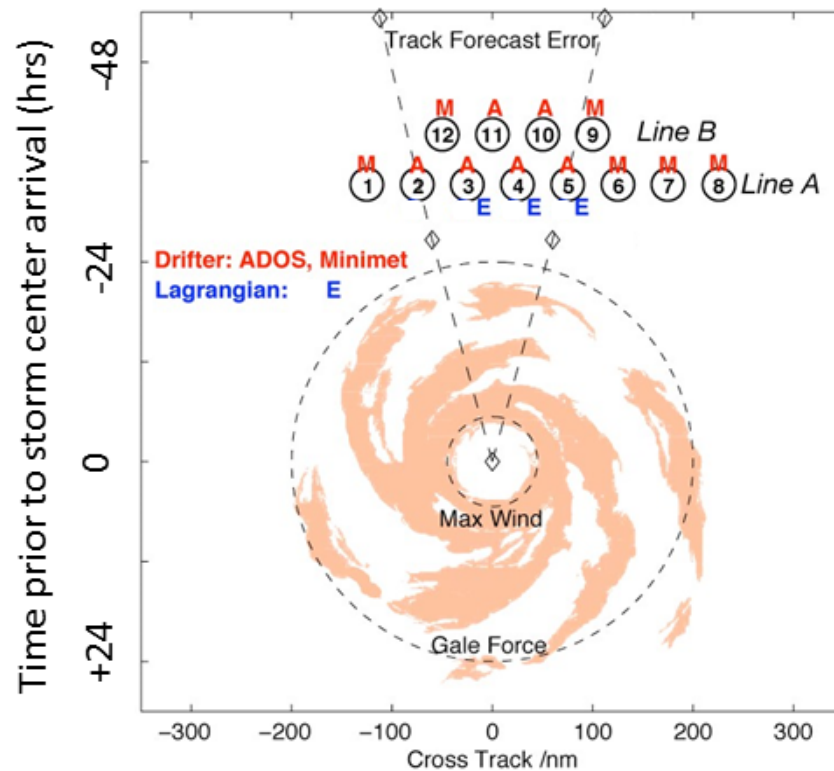
Figure 13-5: *Drifter array deployed by AFRC WC-130J aircraft. The array is deployed ahead of the storm with the exact array location and spacing determined by the storm speed, size and the uncertainty in the storm track. The array consists of ADOS thermistor chain (A) and minimet (M) drifters, and EM-APEX Lagrangian floats (E). Two items are deployed at locations 3, 4 and 5, and one item elsewhere.*

c) Underwater glider operations

To complement the aircraft-based experiments, underwater glider operations that started during the 2014 hurricane season will continue. Underwater gliders are cost-effective observational platforms used for targeted and sustained upper-ocean T, S observations, they operate easily in open waters, even under hurricane strength

winds, and can be navigated across moderately strong currents. The main objectives of the proposed work are to maintain upper ocean observations from underwater gliders, to evaluate their impact on and to improve understanding of ocean response to hurricane wind forcing and to help improve hurricane intensity forecasts. Of critical importance will be the joint analysis of the data collected through this project with those obtained through other targeted observations, WP-3D and WC-130J flights that deploy a suite of atmospheric sensors, and sustained ocean observations, such as surface drifters, Argo floats, eXpandable BathyThermographs (XBTs), etc.

3.1. Ocean Observations

The first two hurricane underwater glider missions were carried during the 2014 and 2015 Atlantic hurricane seasons (Fig. 13-6). In each mission, two gliders, one in the Caribbean Sea and one in the tropical North Atlantic Ocean, off Puerto Rico, were used and collected approximately 14,000 temperature, salinity, and oxygen profiles in regions that are severely undersampled. Gliders can navigate approximately 4,000 km during one mission and collect and transmit thousands of profiles during a 5-month deployment. While surfaced, they can also download any new instructions for altering the navigation route. Data are transmitted in real-time into the GTS and submitted to data centers for assimilation in forecast models.

During the previous hurricane missions, gliders were piloted to obtain repeated upper ocean sections of temperature and salinity before, during, and after the passage of a hurricane. These data allows to analyze the response of the ocean to the passage of a hurricane and to assess the recovery of the ocean.

Starting in the 2016 Atlantic hurricane season, the network will be expanded to four gliders, with two deployed in the Caribbean Sea and two in the tropical North Atlantic Ocean. These gliders will also include additional sensors, such as CDOM, chlorophyll-a, and backscatter.
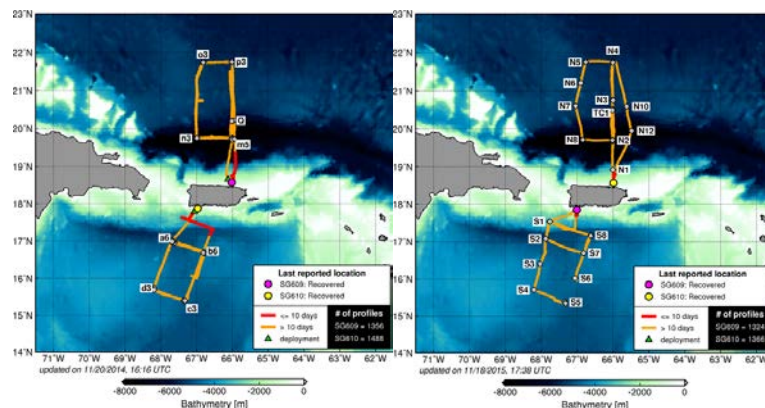
Figure 13-6. *Location of underwater glider observations during the 2014 (left) and 2015 (right) Atlantic hurricane seasons.*

d) AXBT deployments by TROPIC on AF C-130

In addition to the P-3 expendable ocean probe deployments described above, additional ocean temperature profiles will be obtained by AFRC WC-130J aircraft as part of the Training and Research in Oceanic and Atmospheric Processes in Tropical Cyclones (TROPIC) program under the direction of CDR Elizabeth Sanabia, Ph.D. (USNA). Several overlapping mission goals have been identified providing an additional opportunity for collaboration and enhancing observational data coverage. See www.onr.navy.mil/reports/FY11/mmsanabi.pdf for details.

e) Loop current experiment

Goal: To observe and improve our understanding of the upper-ocean response to the near-surface wind structure during TC passages. Specific objectives are:
1. The oceanic response of the Loop Current (LC) to TC forcing; and,
2. Influence of the ocean response on the atmospheric boundary layer and intensity

Rationale:
Ocean boundary layer and air-sea flux parameterizations. TC intensity is highly sensitive to air-sea fluxes. Recent improvement in flux parameterizations has led to significant improvements in the accuracy of TC simulations. These parameterizations, however, are based on a relatively small number of direct flux measurements. The overriding goal of these studies is to make additional flux measurements under a sufficiently wide range of conditions to improve flux parameterizations, specifically:
- Measure the air-sea fluxes of enthalpy and momentum using ocean-side budget and covariance measurements and thereby verify and improve parameterizations of these fluxes.
- Measure the air-sea fluxes of oxygen and nitrogen using ocean-side budget and covariance measurements and use these to verify newly developed gas flux parameterizations.
- Measure profiles of ocean boundary layer turbulence, its energy, dissipation rate and skewness and use these to investigate the unique properties of hurricane boundary layers.
- Conduct the above flux and turbulence measurements in all four quadrants of a TC so as investigate a wide range of wind and wave conditions.

The variability of the Gulf of Mexico Loop Current system and associated eddies have been shown to exert an influence on TC intensity. This has particular relevance for forecasting landfalling hurricanes, as many TCs in the Gulf of Mexico make landfall on the U.S. coastline. To help better understand the LC variability and improve predictions for coupled model forecasts, upper-ocean temperature and salinity fields in the vicinity of the LC will be sampled using expendable ocean profilers (see Fig. 13-7).

Pre- and post-storm expendable profiler surveys

Flight description:
Feature-dependent survey. Each survey consists of deploying 60-80 expendable probes, with take-off and recovery at KMCF. Pre-storm missions are to be flown one to three days prior to the TC's passage in the LC (Fig. 9-1). Post-storm missions are to be flown one to three days after storm passage, over the same area as the pre-storm survey. Since the number of deployed expendables exceeds the number of external sonobuoy launch tubes, profilers must be launched via the free-fall chute inside the cabin. Therefore the flight is conducted un-pressurized at a safe altitude. In-storm missions, when the TC is passing directly over the observation region, will typically be coordinated with other operational or research missions (e.g. Doppler Winds missions). These flights will require 10-20 AXBTs deployed for measuring sea surface temperatures within the storm.
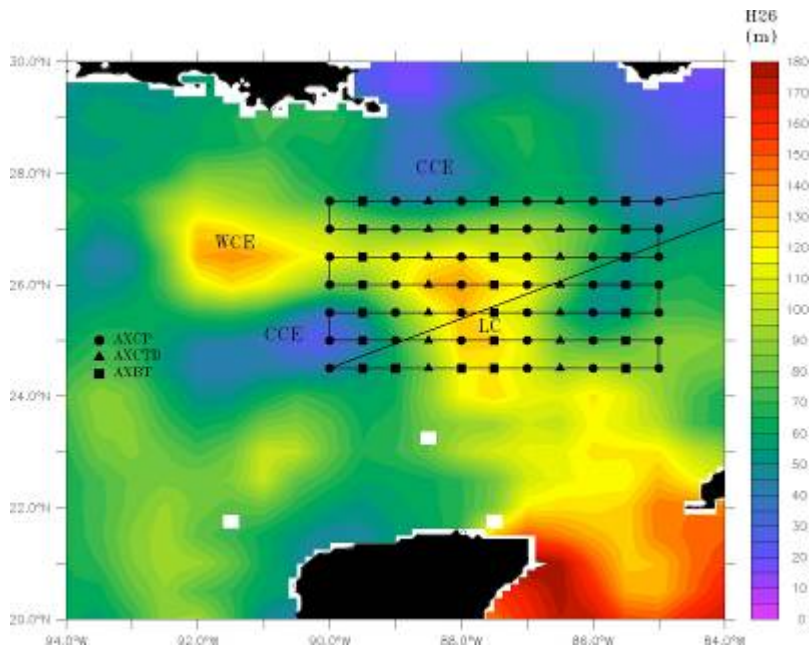
Figure 13-7: Typical pre- or post-storm pattern with ocean expendable deployment locations relative to the Loop Current. Specific patterns will be adjusted based on actual and forecasted storm tracks and Loop Current locations. Missions generally are expected to originate and terminate at KMCF.

Track-dependent survey. For situations that arise in which a TC is forecast to travel outside of the immediate Loop Current region, a pre- and post-storm ocean survey focused on the official track forecast is necessary. The pre-storm mission consists of deploying AXBTs/AXCTDs on a regularly spaced grid, considering the uncertainty associated with the track forecast. A follow-on post-storm mission would then be executed in the same general area as the pre-storm grid, possibly adjusting for the actual storm motion. Figure 13-8 shows a scenario for a pre-storm survey, centered on the 48 hour forecast position. This sampling strategy covers the historical "cone of uncertainty" for this forecast period.

Figure 13-8: *Track-dependent AXBT/AXCTD ocean survey. As for the Loop Current survey, a total of 60-80 probes would be deployed on a grid (blue dots).*

Coordinated float/drifter deployment overflights:

Measurements will be made using arrays of drifters deployed by AFRC WC-130J aircraft in a manner similar to that used in the 2003 and 2004 CBLAST program. Additional deployments have since refined the instruments and the deployment strategies. MiniMet drifters measure SST, sea level air pressure and wind velocity. Thermistor chain Autonomous Drifting Ocean Station (ADOS) drifters add ocean temperature measurements to 150m. All drifter data are reported in real time through the Global Telecommunications System (GTS) of the World Weather Watch. An additional stream of real-time, quality controlled data is also provided by a server located at the Scripps Institution of Oceanography.

If resources are available from other Principal Investigators, flux Lagrangian floats will measure temperature, salinity, oxygen and nitrogen profiles to 200 m, boundary layer evolution and covariance fluxes of most of these quantities, wind speed and scalar surface wave spectra, while E-M APEX Lagrangian floats will measure temperature, salinity and velocity profiles to 200m. Float profile data will be reported in real time on GTS.

This drifter effort is supported by the Global Drifter Program. The HRD contribution consists of coordination with the operational components of the NHC and the 53rd AFRC squadron and P-3 survey flights over the array with SFMR and SRA wave measurements and dropwindsondes. If the deployments occur in the Gulf of Mexico, Loop Current area, this work will be coordinated with P-3 deployments of AXBTs, AXCTDs and AXCPs to obtain a more complete picture of the ocean response to storms in this complex region.

Coordination and Communications:
Alerts - Alerts of possible deployments will be sent to the 53rd AWRO up to 5 days before deployment, with a copy to CARCAH, in order to help with preparations. Luca Centurioni (SIO) and Rick Lumpkin (PhOD) will be the primary point of contact for coordination with the 53rd WRS and CARCAH.

Flights:
Coordinated drifter deployments would nominally consist of 2 flights, the first deployment mission by AFRC WC-130J and the second overflight by NOAA WP-3D. An option for follow-on missions would depend upon available resources.

Day 1- WC-130J Float and drifter array deployment- Figure 13-9 shows a possible nominal deployment pattern for the float and drifter array. It consists of two lines, A and B, set across the storm path with 8 and 4 elements respectively. The line length is chosen to be long enough to span the storm and anticipate the errors in forecast track. The element spacing is chosen to be approximately the RMW. In case of large uncertainties of the forecast track a single 10 node line is deployed instead. The thermistor chain drifters (ADOS) are deployed near the center of the array to maximize their likelihood of seeing the maximum wind speeds and ocean response. The Minimet drifters are deployed in the outer regions of the storm to obtain a full section of storm pressure and wind speeds. The drifter array is skewed one element to the right of the track in order to sample the stronger ocean response on the right side (cold wake).

Day 2. P-3 In-storm mission- Figure 13-10 shows the nominal P-3 flight path and dropwindsonde locations during the storm passage over the float and drifter array. The survey should ideally be timed so that it occurs as the storm is passing over the drifter array.

The survey includes legs that follow the elements of float/drifter line 'A' at the start and near the end. The survey anticipates that the floats and drifters will have moved from their initial position since deployment and will move relative to the storm during the survey. Waypoints 1-6 and 13-18 will therefore be determined from the real-time positions of the array elements. Each line uses 10 dropwindsondes, one at each end of the line; and two at each of the 4 floats, the double deployments are done to increase the odds of getting a 10m data.

The rest of the survey consists of 8 radial lines from the storm center. Dropwindsondes are deployed at the eye, at half R_{max}, at R_{max}, at twice R_{max} and at the end of the line, for a total of 36 releases. AXBTs are deployed from the sonobuoy launch tubes at the eye, at R_{max} and at 2 R_{max}. This AXBT array is focused at the storm core where the strongest air-sea fluxes occur; the buoy array will fill in the SST field in the outer parts of the storm. In this particular example, the final two radials have been moved after the second float survey to avoid upwind transits. For other float drift patterns, this order might be reversed.

It is highly desirable that this survey be combined with an SRA surface wave survey because high quality surface wave measurements are essential to properly interpret and parameterize the air-sea fluxes and boundary layer dynamics, and so that intercomparisons between the float wave measurements and the SRA wave measurements can be made.

Extended Mission Description:
If the storm remains strong and its track remains over water, a second or possibly third oceanographic array may be deployed, particularly if the predicted track lies over a warm ocean feature predicted to cause storm intensification (Fig. 13-11). The extended arrays will consist entirely of thermistor chain and minimet drifters, with 7-10 elements in a single line. As with the main mission, the spacing and length of the line will be set by the size of the storm and the uncertainty in the forecast track.

Mission timing and coordination will be similar to that described above. P-3 overflights would be highly desirable.
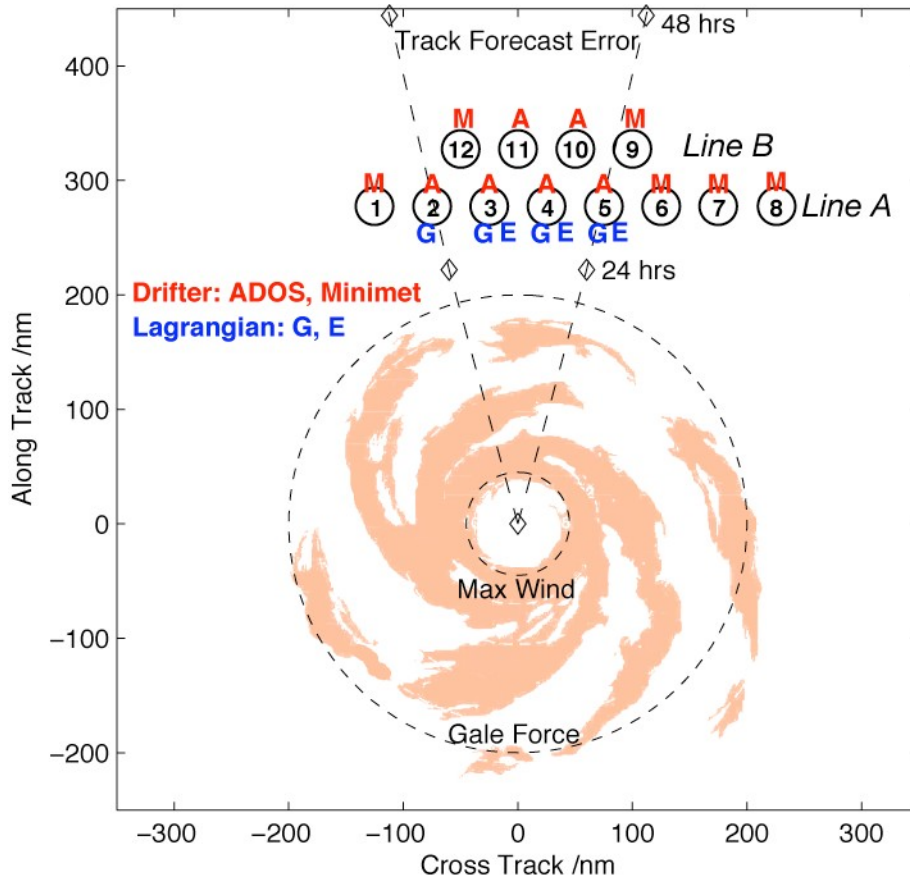
Figure 13-9: *Drifter array deployed by AFRC WC-130J aircraft. The array is deployed ahead of the storm with the exact array location and spacing determined by the storm speed, size and the uncertainty in the storm track. The array consists of ADOS thermistor chain (A) and minimet (M) drifters. Gas (G) and EM (E) Lagrangian floats could be added if available. Three items are deployed at locations 3, 4 and 5, two items at location 3 and one item elsewhere.*

Storm Motion

X AXBT
● GPS Dropsonde

Rmax

Nominal ~175km

At Survey Start

Array Line A

At Survey End

Floats and Drifters
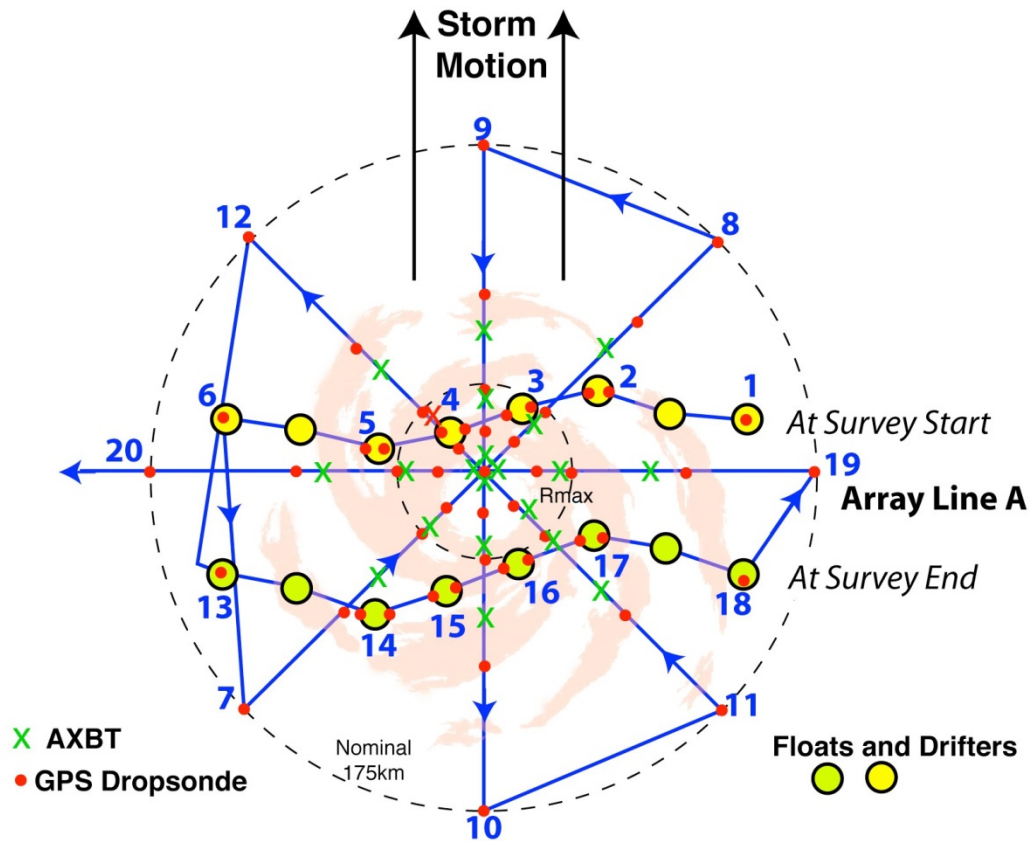
Notes:
4 diameter lines through eye each with
      9 dropsondes.   At eye, 0.5 Rmax, Rmax, 2 Rmax, Line end.
      5 AXBT.   At eye, Rmax, 2 Rmax
2 float array lines each with
      10 dropsondes. 2 at each of 4 floats, 2 Line ends.
Total: 56 dropsondes, 20 AXBT

Figure 13-10*: P-3 pattern over float and drifter array. The array has been distorted since its deployment on the previous day and moves relative to the storm during the survey. The pattern includes two legs along the array (waypoints 1-6 and 13-18) and an 8 radial line survey. Dropwindsondes are deployed along all legs, with double deployments at the floats. AXBTs are deployed in the storm core.*
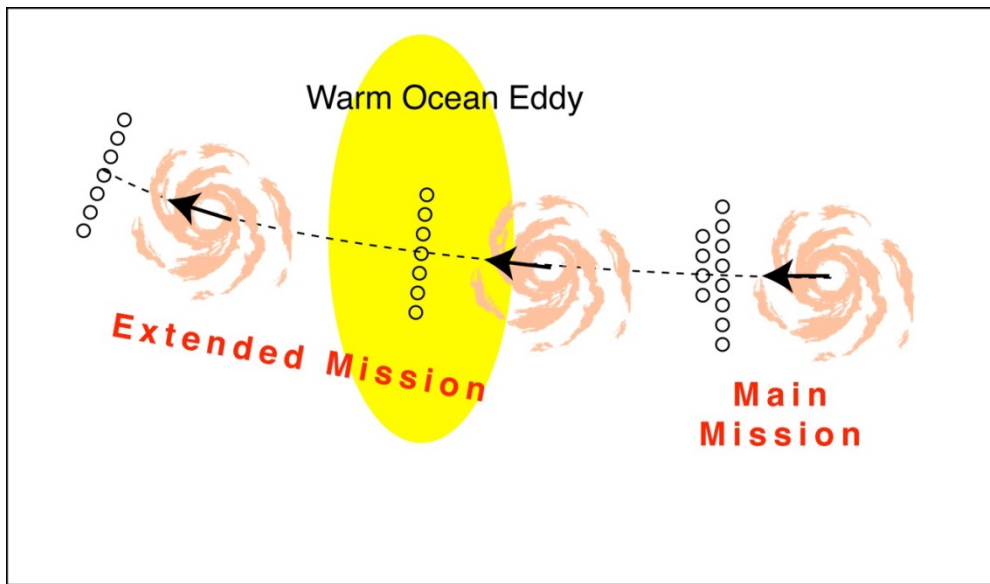
Figure 13-11: *Extended Mission. Two additional drifter arrays will be deployed along the storm track.*

14. Tropical Cyclone Landfall Experiment

Principal Investigators: John Kaplan, Peter Dodge, Ghassan Alaka, Hua Chen, Frank Marks, Jun Zhang, and Matt Eastin

Supported NOAA IFEX Goals:

☐   **Goal 1**: Collect observations that span the TC lifecycle in a variety of environments for model initialization and evaluation;

☐   **Goal 3**: Improve our understanding of the physical processes important in intensity change for a TC at all stages of its lifecycle.

Program Significance:

The lifecycle of a TC often ends when it makes landfall and decays as it moves inland. During a hurricane threat, an average of 300 nm (550 km) of coastline is placed under a hurricane warning, which costs approximately $150-300 million in preparation per event. The size of the warned area depends on the extent of hurricane and tropical storm- force wind speeds at the surface, evacuation lead-times, and the storm track forecast. Research has helped reduce uncertainties in the track and landfall forecasts, and now one of the goals of the IFEX is to improve the accuracy of the surface wind fields in TCs, especially near and after landfall. Improvements in track forecasts and surface wind field analyses could produce more accurate hurricane warning areas thereby optimizing the cost of hurricane landfall preparations. In addition to the surface wind field, the forecast of severe weather embedded within a landfalling TC is particularly difficult. Recent studies have highlighted the front-right quadrant of a landfalling TC as a region of increased severe weather risk, particularly TC tornadoes (e.g., Schultz and Cecil 2009). However, some landfalling TCs are associated with more severe weather than others, which has prompted the HRD to explore how numerical modeling (e.g., the HWRF model) can improve severe weather forecasts issued by the NHC and the SPC prior to, during, and after TC landfall.   This experiment can help guide research at the HRD by providing real-time observations of severe weather to verify the HWRF model.

There are still uncertainties in deriving surface wind estimates from flight-level and SFMR wind speeds collected near the coast. Changing bathymetry could alter the breaking wave field, which could change the roughness length at higher wind speeds and microwave emissions. Evaluation of these effects may lead to adjustments to the operational surface wind speed algorithms.

Analysis of Doppler radar, GPS dropwindsonde, SFMR, flight-level and WSRA or AWRAP data collected during hurricane flights can help achieve the IFEX goals for the 2015 Hurricane Field Program. A major goal of the IFEX is to capture the lifecycle of a TC and, while landfall typically occurs at the end of the TC lifecycle, the same data collection strategies developed for mature hurricanes over the open ocean can also be applied at landfall. Subsets of the collected data can be transmitted to the NHC and to the EMC, for assimilation into the HWRF model. Doppler and GPS dropwindsonde data can be analyzed to derive three-dimensional wind fields to compare with the HWRF output and data from the SRA can be compared to the HWRF wave fields. In addition to shear and heat flux from the ocean, landfalling hurricanes experience other conditions that may affect intensity change. These include changes in ocean wave action in shallow waters, change in surface roughness, drier and/or cooler inflow from the land, and topographical impacts. Radar, dropwindsonde, and SFMR data can help observe and analyze those conditions. Decay over land is also important, and data collected during and shortly after landfall should help refine both operational statistical models (such as the Kaplan/DeMaria decay model) and numerical

models like the HWRF.

The HRD has developed a real-time surface-wind analysis system to aid the NHC in the preparation of warnings and advisories in TCs. In the past, the wind analyses produced using the HRD analysis package have been used both for post-storm damage assessment by emergency management officials and by researchers seeking to validate their model analyses and forecasts. In addition, these wind analyses also have the potential to be employed for use in the initialization of real-time storm surge models.

As a TC approaches the coast, surface marine wind observations are normally only available in real time from National Data Buoy Center moored buoys, Coastal-Marine Automated Network (C-MAN) platforms, and a few ships. Surface wind estimates must therefore be based primarily on aircraft measurements. Low-level (<5,000 ft. [1.5 km] altitude) NOAA and AFRES aircraft flight-level wind speeds are adjusted to estimate surface wind speeds. These adjusted wind speeds, along with C-SCAT and SFMR wind estimates, are combined with actual surface observations to produce surface wind analyses. These surface wind analyses were initially completed after the landfall of Hurricane Hugo in South Carolina and of Hurricane Andrew in South Florida in support of post-landfall damage surveys conducted by FEMA. In recent years, these analyses have been produced in real time for use by the NHC for many of the TCs that have affected the Western Atlantic basin, including such notable landfalling storms as Opal (1995), Fran (1996), Georges (1998), Bret (1999), Floyd (1999), Isidore (2003), Frances (2004), Ivan (2004), Jeanne (2004), Dennis (2005), Katrina (2005), Rita (2005), Wilma (2005), Ike (2008), Irene (2011) and Isaac (2012). Dual-Doppler analysis provides a complete description of the wind field in the core and, recently, the analysis techniques have been streamlined so that these real-time wind analyses can be computed aboard the aircraft and wind fields at selected levels transmitted from the aircraft to the NHC and the NCEP. These wind fields are also quite useful for post-storm analysis.

Severe weather, including the potential for tornadoes, is often associated with landfalling TCs. The basic dynamic and thermodynamic structures found in TC supercells are not well-understood. While some studies have found that TC tornadoes rely on some of the same factors as Great Plains tornadoes, some key differences exist, such as the height and amplitude of these vortices. Most TC tornadoes occur in the front-right quadrant of the TC primarily from 12 hours prior to 48 hours after landfall (Schultz and Cecil 2009). Additionally, the most damaging TC tornadoes occur in rain bands outside of the TC inner core (> 95 nm [150 km]). While TC tornadoes are typically weaker than their Great Plains counterparts, these TC tornadoes account for at least 10% of all tornado records from Louisiana to Maryland (Schultz and Cecil 2009). Unlike Great Plains tornadoes, TC tornadoes are typically associated with smaller values of CAPE. Instead of relying on high CAPE, TC tornadoes owe some of their existence to the friction-induced convergence that accompanies landfalling TCs. The sudden deceleration of the wind as it encounters the rougher land surface helps drive vertical motion, which promotes embedded mesovortices and severe weather.

Recent research efforts in coordination with the NHC and the SPC are focused on improving the prediction of TC tornadoes based on the HWRF model output prior to and during TC landfall. Unfortunately, the HWRF model does not possess a resolution fine enough to capture tornadoes. Instead, *signatures* of tornadoes (e.g., helicity, wind shear, vorticity, radar hook echoes) will be sought out in the flight data (e.g., Doppler, GPS dropwindsondes) and will be used to verify the HWRF model output. Since some landfalling TCs produce more tornadoes than others, one goal of this experiment is to better understand the structure and thermodynamical properties of tornado-inducing rainbands in landfalling TCs.

Recent GPS dropwindsonde data from near and inside the flight-level radius of maximum wind speeds (RMW) in strong hurricanes have shown remarkable variations of the wind with height. A common feature is a wind speed maximum at 300-500 m altitude. Theoretical and numerical modeling of the

hurricane boundary layer suggests that the low-level jets are common features. The height of the jet varies by storm quadrant, and modeling indicates that this variation can be enhanced as a TC crosses land. In addition, GPS dropwindsonde data will provide critical observations of temperature and moisture associated with severe weather embedded within TC outer rain bands, which will help to provide a better picture of supercell structures within landfalling TCs.

While collection of dual-Doppler radar data by aircraft alone requires two P-3 aircraft flying in well-coordinated patterns, time series of dual-Doppler data sets have been collected by flying a single P-3 toward or away from a ground-based Doppler radar. In that pattern, the aircraft Doppler radar rays are approximately orthogonal to the ground-based Doppler radar rays, yielding true Dual-Doppler coverage. Starting in 1997, the Atlantic and Gulf coasts were covered by a network of Doppler radars (Weather Surveillance Radar 88 Doppler [WSR-88D]) deployed by the National Weather Service (NWS), Department of Defense, and Federal Aviation Administration. Each radar site transmits the base data (Level II) in near real time to a central site. These data are subsequently archived at the National Climatic Data Center. In precipitation or severe weather mode, the radars collect volume scans every 5-6 min.

If a significant TC moves within 215 nm (440 km) of the coast of the eastern or southern United States, then (resources permitting) a P-3 will obtain Doppler radar data to be combined with data from the closest WSR-88D radars in dual- Doppler analyses. The tail radar is tilted to point 20 degrees forward and aft from the track during successive sweeps (the fore-aft scanning technique [F/AST]). These analyses could resolve phenomena with time scales < 10 min, the time spanned by two WSR-88D volume scans. This time series of dual-Doppler analyses will be used to describe the storm core wind field and its evolution. The flight pattern is designed to obtain dual-Doppler analyses at intervals of 10-20 min in the core. Deploying dropwindsondes near the coast will augment the Doppler data, where knowledge of the boundary-layer structure is crucial for determining what happens to the wind field as a strong storm moves inland. Dropwindsondes will also be deployed in the eyewall in different quadrants of the TC. To augment the core analyses, dual-Doppler data can also be collected in the outer portions of the storm, beyond the range of the WSR-88D, because the alternating forward and aft scans in F/AST mode intersect at 40 degrees, sufficient for dual-Doppler synthesis of wind observations.

Objectives:

☐ Collect NOAA P-3 Doppler, flight-level, and SFMR surface wind data both within the inner-core (radius < 120 nm) and near storm (120 nm < radius < 240 nm) environment to help improve and validate real- time and post- storm surface wind estimates in tropical cyclones.

☐ Document the thermodynamic and kinematic changes in storm structure during and after landfall and improve our understanding of the factors that modulate changes in tropical cyclone intensity near the time of landfall.

☐ Collect observations that will aid in the evaluation of the current operational coupled model forecast system's ability to predict the three-dimensional structure of tropical cyclones both at the time of landfall as well as after the cyclone has moved inland.

☐ Collect dynamic and thermodynamic data in outer rainbands (> 90 nm [150 km] from TC center) of tropical cyclones that are either likely to make landfall or to make a close enough approach to the coastline that they have the potential to produce tornadoes.

Hypotheses:

☐ It is possible to improve real-time surface wind estimates for landfalling tropical cyclones by obtaining in-situ inner-core and near storm wind data collected utilizing NOAA P-3 aircraft.

☐ The above landfall datasets can be used to validate statistical and numerical model landfall surface wind forecasts.

☐ Our understanding and ability to forecast changes in the structure and intensity of landfalling tropical cyclones can be enhanced utilizing the high-resolution kinematic and thermodynamic data sets collected during the aforementioned landfall research missions.

☐ Traditional environmental parameters (e.g., CAPE, vertical shear, helicity) will distinguish sectors of the storm that are most supportive of supercell development. Thus, the area coverage of SPC-issued severe weather watches may be optimized and the HWRF output can be validated based on datasets produced via the modules described in this experiment.

Model Evaluation Component:

Recent tropical cyclones (e.g., Irene [2011], Sandy [2012]) have produced over-land wind gusts that have often exceeded the values expected based upon both the simulated and observed maximum sustained wind. Thus, it is hypothesized that the collection of landfalling datasets such as those proposed for this experiment will help researchers evaluate the capability of the HWRF model to accurately predict both the maximum sustained wind and wind gusts of landfalling TCs. In addition, forecasts of TC tornadoes have generally depended on climatology even though some numerical models have the capability to resolve tornadic signatures within TCs. Thus, a goal of this experiment is to evaluate how accurately the HWRF model simulates the mesoscale convective features that are capable of producing tornadoes. Since the HWRF model resolution is currently too coarse to explicitly simulate TC tornadoes, the *signatures* of TC tornadoes will be analyzed in the landfalling datasets and compared with the HWRF output. This includes traditional environmental fields that are indicative of tornadoes, such as CAPE, vertical shear, and helicity.

Mission Description:

This is a ***multi-option, single-aircraft*** experiment designed to study the changes in TC surface wind structure and to document TC supercell characteristics near and after landfall. All three modules described here could also be incorporated into operational surveillance or reconnaissance missions. It is designed for one or two single-aircraft missions with a P-3 when a hurricane or tropical storm moves within 215 nm (400 km) of the U.S. coastline. The first of these two flights will typically consist of the Offshore Intense Convective module followed by either the Coastal Survey or Real-time modules. While the storm location relative to the coastline will dictate which combination of these modules will be flown, the Offshore Intense Convection module will generally precede all of the others.

Landfall flights may be coordinated with mobile observing systems that are sometimes deployed ahead of landfalling tropical cyclones. These additional observations could be particularly useful for: 1) documenting the inland decay of surface winds associated with TC landfall and 2) for identifying the location of any tornadoes that might be generated by the landfalling tropical cyclone.

The aircraft must have working lower fuselage and tail radars. The HRD should have access to a workstation on board, so radar and GPS dropwindsonde data can be analyzed and transmitted to the NHC.

The SFMR should be operated, to provide estimates of wind speed at the surface. If the AWRAP or C-SCAT is on the aircraft then it should also be operated to provide another estimate of the surface wind speeds. If the WSRA is working it also should collect wave and sweep heights to characterize the storm surge and breaking wave field near the coast. If the scanning LIDAR is available, then it should be operated to obtain wind profiles in the clear air regions, especially in the offshore flow. If the portable Doppler radars (Shared Mobile Atmospheric Research and Teaching Radar [SMART- R] and/or Doppler on Wheels [DOW]) and the portable wind towers are deployed, they should be placed ~35-80 nm (65-130 km) inland in the onshore flow regime as depicted in Fig. 14-3, if possible, to document the decay of the tropical cyclone wind field and to help identify any tornadoes that the landfalling tropical cyclone may produce. If possible, one of the DOWs should be positioned relative to the nearest WSR-88D such that the dual-Doppler lobes cover the largest area of onshore flow possible. In the schematic shown in Fig. 14-3, one of the DOWs is positioned north-west of the Melbourne WSR-88D so that one dual- Doppler lobe is over the coastal waters and the other covers the inland region. The profiler is positioned within the inland dual-Doppler lobe to provide independent observations of the boundary layer to anchor the dual-Doppler analysis.

All modules support real-time and post-storm surface wind analyses and the identification/verification of potential tornadoes produced by the landfalling tropical cyclone. The flight patterns will depend on the location and strength of the storm relative to surface observing platforms and coastal radars. The three modules can be easily incorporated into a tasked operational mission. In the case of the Offshore Intense Convection module, different legs of this module may be incorporated into legs of a figure-4 pattern if supercells are encountered (Fig. 14-1).

1. Offshore Intense Convection Module

Description
This module focuses on the collection of dual-Doppler radar and vertical profiles of the lower atmosphere near intense convective cells (>35 dBZ on the LF radar) located in an offshore outer rainband (>90 nm [150 km] from the storm center) but embedded within the onshore flow. This module can be easily incorporated during either operational TD-R flights or the other two modules (i.e., Coastal Survey or Real-time modules) when a suitable outer rainband is encountered. Fig. 14-1 shows an example flight pattern along the Carolina coast. In order to provide adequate estimates of low-level vertical shear and instability, the aircraft should fly this module at an altitude of 10,000 ft. (3.0 km) or higher. The Doppler radar should operate in F/AST mode to provide wind estimates on each side of the aircraft track. **A minimum of 6 GPS dropwindsondes should be deployed**, although ideally ≥10 GPS dropwindsondes will be deployed if resources allow. If less than 10 GPS dropwindsondes are deployed in total, then at least 2 GPS sondes should be deployed on either side of the intense convection and at least 1 GPS dropwindsonde should be deployed each time the band-axis is crossed (at least 6 GPS dropwindsondes in total). For GPS dropwindsondes deployed in or near intense convection, getting as close as comfortably possible to the convection is preferred. The first flight leg should cross the target band ~10-13 nm (20-25 km) downwind of the intense convective cells and proceed until the aircraft is 13 nm (25 km) outside the rainband axis, deploying a GPS dropwindsonde at the band axis and end point. The aircraft then turns upwind and proceeds along a straight track parallel to the rain band axis, ideally deploying GPS dropwindsondes every 10-13 nm. The length of this leg can be adjusted as needed, but should be a minimum of 40 nm (75 km). When the aircraft is ~10-13 nm upwind of the target cells, the aircraft turns and proceeds along a track orthogonal to the band axis until the aircraft is 13 nm (25 km) inside the rainband axis. GPS dropwindsondes should be deployed at the initial and endpoints of this leg as well as at the band axis. Finally, the aircraft turns downwind and proceeds along a straight path parallel to the rain band axis, deploying GPS dropwindsondes every 10-13 nm. The end point of this final leg should be 10-13 nm downwind of the initial target cell to ensure adequate dual-Doppler radar coverage of all cells.

From here other modules can be resumed. The total time to complete this module should not exceed 60 minutes, and in most case can be completed in less time.

Note: This module's flight pattern can be reversed depending either on the location of the intense cells relative to the aircraft's initial approach vector or the need for flight safety. This module could also be easily incorporate into any tasked operational or research missions in which an outer rainband (> 90 nm [150 km] from the storm center) with embedded intense convective cells (>35 dBZ on the LF radar) is encountered during ferry to or from the storm core. **In other words, this module is _not_ strictly limited to the Landfall and Inland Decay Experiment.**

Significance

As tropical cyclones move inland and weaken, tornadoes also become a significant threat to society and one of
the most difficult forecast problems. Since 2004, over 650 tornadoes have been spawned by 26 tropical cyclones impacting the U.S. coastline, resulting in 24 deaths, over 300 injuries, and more than $400 million in damage. Many of these tornadoes are spawned by *miniature supercells*. Much of the forecast challenge is due to significant differences in structure, organization, and environment from the classic midlatitude supercell: the miniature supercells are shallower, weaker, shorter-lived, and less buoyant, but occur in a very moist, high-wind, high- rotation environment with more vertical wind shear. Furthermore, individual miniature supercells often occur in close proximity to one another along organized outer rain bands, whereas their midlatitude counterparts often occur in relative isolation. As a result, midlatitude conceptual models have shown very limited success when applied to tornado forecasting in tropical cyclones. Numerous studies have documented the onshore environmental conditions and evolution of miniature supercells associated with TC tornado outbreaks, but little is known about the *offshore environment and cell evolution* just prior to tornado outbreaks. The goal of the "Offshore Intense Convection" module is to document the structure, evolution, and low-level environment of the stronger convective cells (>35 dBZ) located offshore in an outer rainband (> 90 nm [150 km] from the TC center) that will soon move onshore and potentially spawn tornadoes. This goal is consistent with the three primary goals of the IFEX.

Analysis Strategy

The P-3 Doppler radar data will be carefully edited and then synthesized into a three-dimensional wind field. Dropsonde and flight-level data will be analyzed and combined with an available rawinsonde and surface (e.g. buoys, CMAN, etc.) observations to establish the dynamic and thermodynamic environment of the targeted cells.

Any available land-based radar will be used to augment the cell evolution documented by the airborne radars. Observations of TC supercells will be used to validate HWRF output and will assess the HWRF model's ability to predict signatures of tornadic activity. The supercell's environment and structure will be used to verify the HWRF model output and will allow for a direct comparison with mid-latitude supercells.

2. Coastal Survey module:

Description

When a TC is making landfall, the Coastal Survey module will provide information about the boundary layer in
the onshore and offshore flow regimes. Fig. 14-2 shows an example of this pattern for a hurricane landfall near Melbourne, Florida. On the first coastal pass the P-3 would fly parallel 6-10 nm (10-15) km offshore to obtain SFMR surface wind speeds (leg 1-2 in Fig. 14-2). The track should be adjusted so that the SFMR footprint is out of the surf zone. The second pass should be as close to the coast as safety

permits, to sample the boundary layer transitions at the coast in onshore and offshore flow (leg 3-4 in Fig. 14-2). The first pass should be at 5,000 ft. (1.5 km) or less, and the aircraft could climb to higher altitudes for the second pass. On both of these passes the aircraft should fly to 150 km or the radius of gale-force wind speeds and release GPS dropwindsondes at the RMW and at intervals of 7.5, 15, 30, 45, and 60 or 75 nm (12.5, 25, 50, 75, and 100 or 125 km) on either side of the storm track, to sample both onshore and offshore flow regimes. Three to four GPS dropwindsondes would be deployed quite near the coast, followed by 3-4 GPS dropwindsondes spaced every 20-30 km along the trajectory. The Doppler radar will be in F/AST mode, to provide wind estimates on either side of the aircraft track. This module could be flown when the hurricane is making landfall or just after the storm has moved inland. The pattern could be flown in ~2 h.

Analysis Strategy
In addition to the data processing described in modules 1 and 3, the Doppler radar swath data will be edited and synthesized into wind fields. The winds will be compared with GPS dropwindsondes and SFMR, AWRAP, and/or LIDAR data to characterize the differences between the onshore and offshore flow.

3. Real-time module:

Description
The Real-time module combines passes over marine surface platforms with one or more figure-4 patterns in the core of the hurricane (Fig. 14-3). The aircraft flies at or below 5,000 ft. (1.5 km) (or the lowest level deemed to be safe by aircraft flight personnel), so that flight-level wind speeds can be adjusted to 30 ft. (10 m) to combine with measurements from marine surface platforms. Flight-level and GPS dropwindsonde data obtained near the platforms will be used to validate the adjustment method. Note that if the storm is outside of WSR-88D Doppler range then the figure-4 pattern could be repeated before returning home.

The landfall flight pattern should take advantage of buoys or C-MAN sites nearby, if those platforms are expected to experience wind speeds > 25 m s^{-1}. The aircraft descends at the initial point and begins a low-level figure-4 pattern, possibly modifying the legs to fly over the buoys (Fig. 14-3). The radar will be in F/AST mode. If time permits, the aircraft would make one more pass through the eye and then fly the Dual-Doppler option. In this example, the pattern would be completed in about 2.5 h. Dropwindsondes would be deployed near the buoys or C-MAN sites and at or just inside the flight-level RMW.

Note that the optimal volume scans for this pattern will be obtained when the storm is 35-80 nm (60-150 km) from the radar, because beyond 80 nm (150 km) the lowest WSR-88D scan will be above 5,000 ft. (1.5 km) which is too high to resolve the low-level wind field. Within 35 nm (60 km) the volume scan will be incomplete, because the WSR-88D does not scan above 19.5 degrees. It is essential that these passes be flown as straight as possible, because turns to fix the eye will degrade the Doppler radar coverage.

Analysis Strategy
Flight level, Doppler radar, GPS dropwindsonde, and SFMR data transmitted in real time will be ingested into the HRD wind-analysis system archive, where the observations are standardized to average 1 minute data at a standard height of 10 m in an open exposure. These data, in addition to other surface observations could then be combined to produce analyses of surface wind speed and provided to forecasters and/or emergency manager in real-time. The quality-controlled data will also be available for assimilation into models such as the HWRF model and to validate surface wind field forecasts produced by both the statistical Kaplan/DeMaria decay model as well as the operational HWRF model.
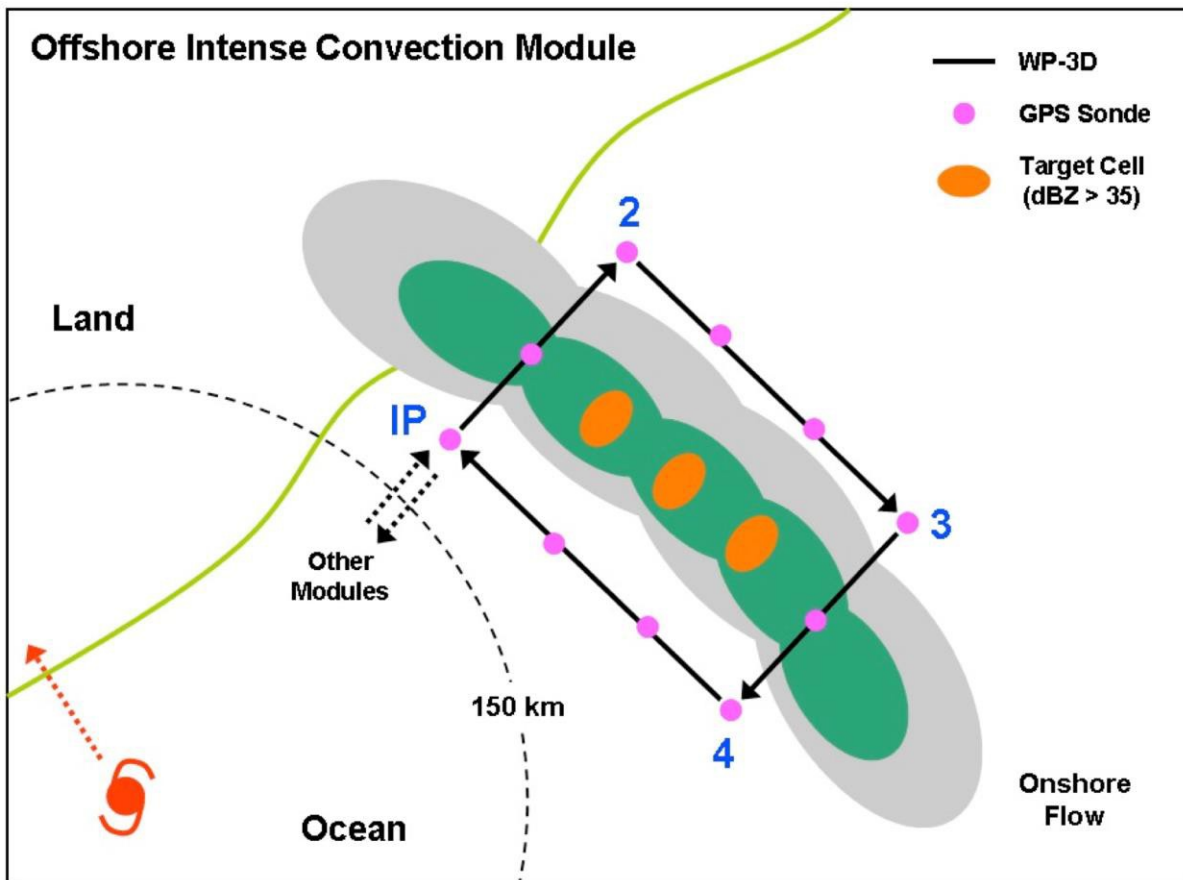
Fig. 14-1. *Offshore Intense convection module.*

Notes:

☐ The **IP** should be a minimum of 90 nm (150 km) from the storm center. The first leg (**IP-2**) starts 13 km (25 km) inside the rain band axis. Legs **IP-2** and **3-4** should be ~10-13 (20-25 km) downwind and upwind of the target cells to ensure adequate Doppler coverage. Legs **2-3** and **4-IP** should be 13 nm inside and outside the rain band axis. The length of legs **2-3** and **4-IP** can be adjusted but should be 40 nm (75 km) at a minimum.

☐ Deploy GPS dropwindsondes at the start or end points of each leg, at the band axis crossing points, and at ~10-13 nm intervals along each leg parallel to the band. The interval at which GPS dropwindsondes are deployed depends on how many are available, but **at least 2 GPS dropwindsondes should be deployed on either side of the convection and at least 1 dropwindsonde should be deployed each time the band-axis is crossed (for a minimum of 6 GPS dropwindsondes)**.

☐ Aircraft altitude should be at 10,000 ft. (3.0 km) or higher. Set airborne Doppler to scan in F/AST mode on all legs. Aircraft should avoid penetration of intense reflectivity regions (particularly over land).
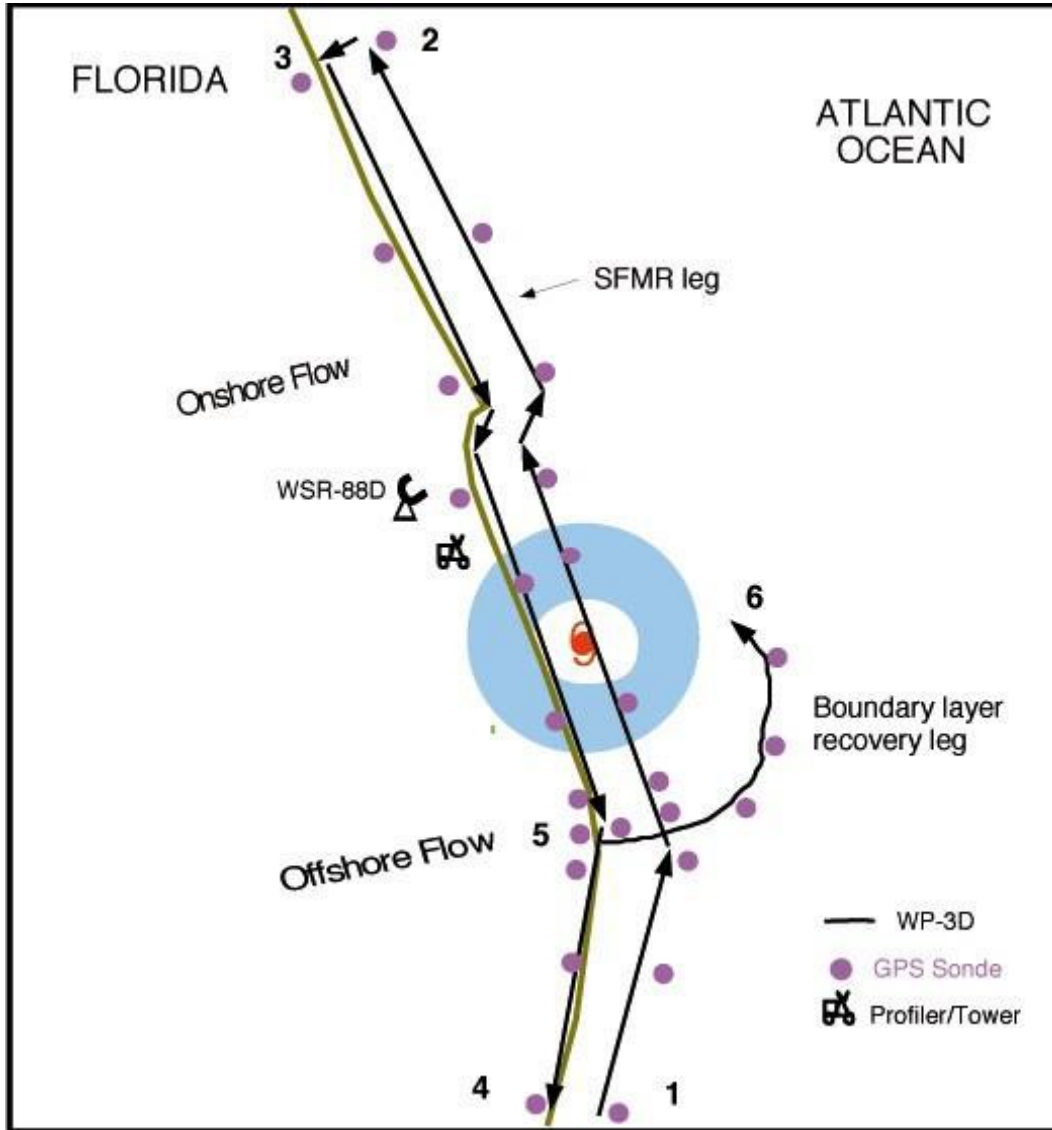
Fig. 14-2. *Coastal Survey module.*

Notes:

☐ First pass starts 80 nm (150 km) from center or at radius of gale-force wind speeds, whichever is closer. Pass from
1-2 should be 6-10 nm (10-15 km) offshore for optimum SFMR measurements. Release GPS dropwindsondes at RMW, and 7.5, 15, 30, 45, and 60 or 75 nm (12.5, 25, 50, 75, and 100 or 125 km) from RMW on either side of storm in legs **1-2** and **3-4**. GPS dropwindsondes should be deployed quickly at start of leg **5-6**, and then every 6-10 nm hereafter.

☐ Set airborne Doppler on all legs with single PRF > 2400 and 20% tilt. Aircraft should avoid penetration of intense reflectivity regions (particularly those over land)
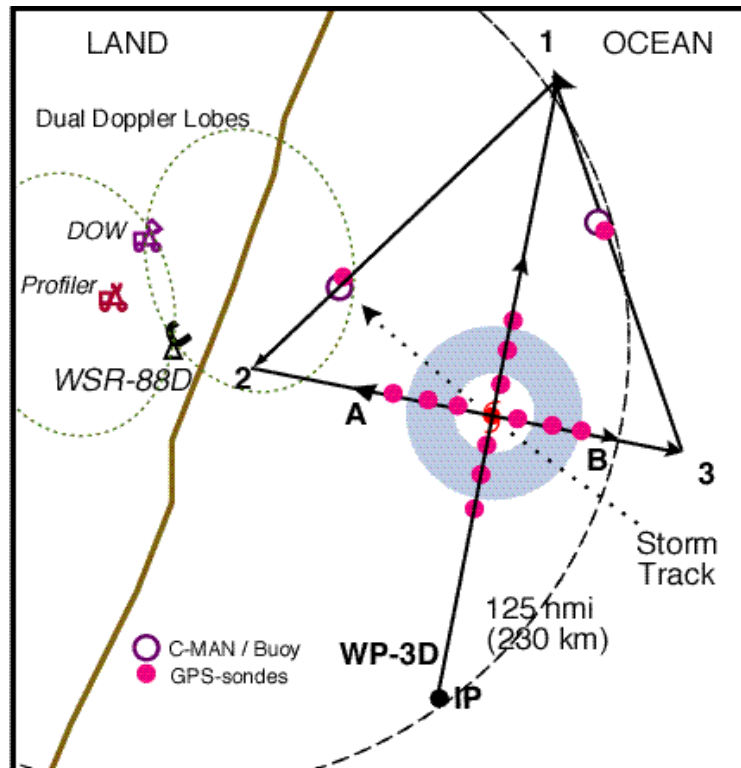
Fig. 14-3. *Real-time module.*

Notes:

☐   TAS calibration required. The legs through the eye may be flown along any compass heading along a radial from the ground-based radar. The **IP** is approximately 100 nm (185 km) from the storm center. Downwind legs may be adjusted to pass over buoys.

☐   P-3 should fly legs along the WSR-88D radials.

Aircraft should avoid penetration of intense reflectivity regions (particularly those over land).

☐   Wind center penetrations are optional.

15. Rapid Weakening Experiment (RWEX)

Principal investigators: Kimberly Wood (Mississippi State), Kelly Ryan (HRD)

Significance and background

Though operational tropical cyclone (TC) intensity forecasting has improved in recent years (DeMaria et al. 2014), predicting rapid changes in the 1-minute maximum sustained wind (hereafter referred to as intensity) remains prone to error. While strides have been made to reduce error in forecasts of rapid intensification (RI; an intensity change of at least 30 kt in 24 h), little work has been done on over-water rapid weakening (RW; an intensity change of at least -30 kt in 24 h [Wood and Ritchie 2015]). Accurate forecasts of rapid changes in TC intensity near land and/or prior to landfall can significantly impact preparations made by marine interests and coastal communities. However, few RW events have been measured by aircraft, limiting observations to geostationary and infrequent polar satellite measurements.

Vertical wind shear is a major factor in weakening as shown by numerous studies (e.g., DeMaria 1996; Frank and Ritchie 2001; Wong and Chan 2004). Its role in RW is less obvious, as composite shear only marginally increased during RW in both the North Atlantic and eastern North Pacific (Wood and Ritchie 2015). Decreasing sea surface temperatures (SSTs) have also played a role in RW (Wood and Ritchie 2015), and a study that included Hurricane Rita (2005) demonstrated the need for better representation of the oceanic mixed layer for intensity forecasting (Jaimes and Shay 2009).

Other case studies of RW are limited: the examination of Hurricane Earl (Jaimes et al. 2015) focused on ocean and near-surface properties and the TC's response to changes in them, and an evaluation of Hurricane Lili (2002; Frederick 2003) placed the TC's RW in the context of historical events but not in the context of its environment. Zhang et al. (2007) explored the usefulness of satellite data in improving model forecasts of Hurricane Lili's RW, also suggesting that dry air intrusion contributed to RW. It is notable that both Lili and Rita rapidly intensified prior to rapidly weakening, and both TCs made landfall post-RW.

The RW of Hurricane Earl (2010; Jaimes et al. 2015) and Hurricane Patricia (2015) were sampled, but more data in more environments are needed to improve our understanding of the structural changes that occur during RW as well as the relationship of the rate of weakening to environmental factors such as dry air intrusion and decreasing SSTs (see Figures 15-1-15-2 for more examples). Better understanding of the physical processes and environments involved in RW should subsequently improve forecasting models such as the Statistical Hurricane Intensity Prediction Scheme (SHIPS; DeMaria and Kaplan 1999).

Aircraft observations of multiple weakening events are needed to better characterize the contribution of different negative environmental factors to the likelihood of RW and the overall rate of weakening in 24 h. Contrasting slower weakening with RW should highlight the differences in both TC structural evolution and the environment that contribute to weakening rates.
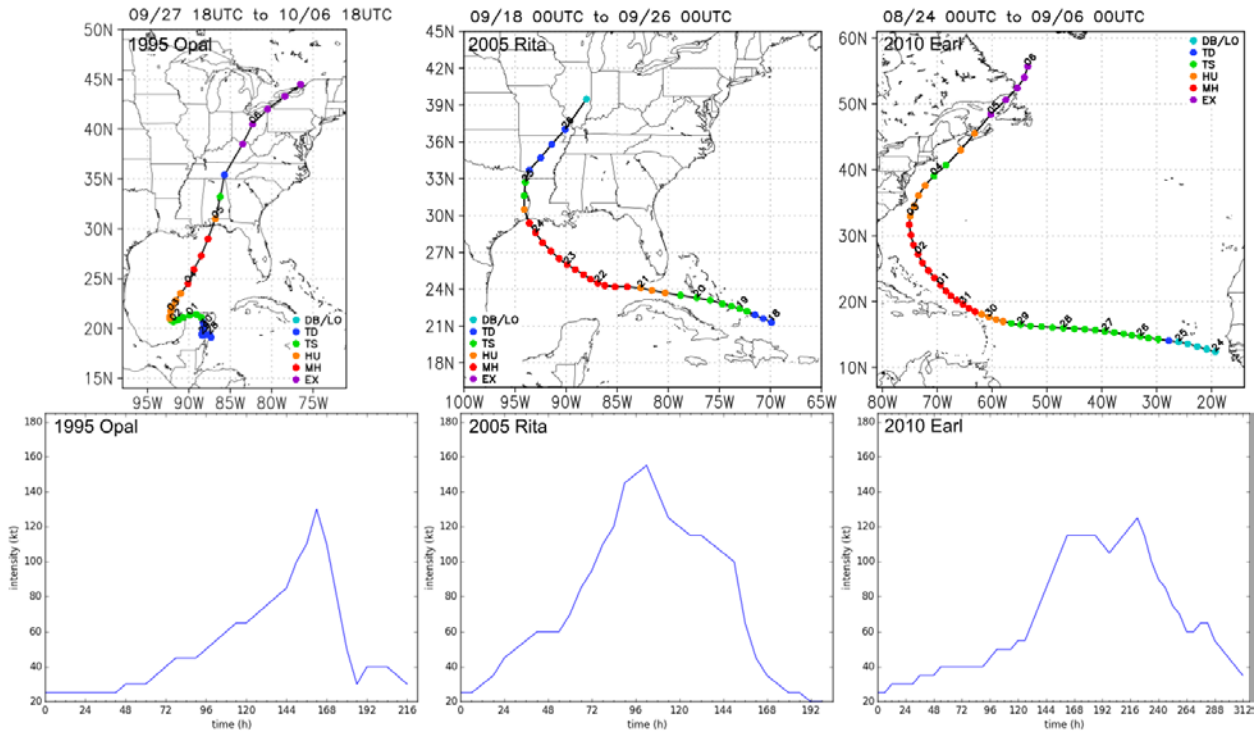
Figure 15-1. *Three examples of rapid weakening near land in the North Atlantic.*
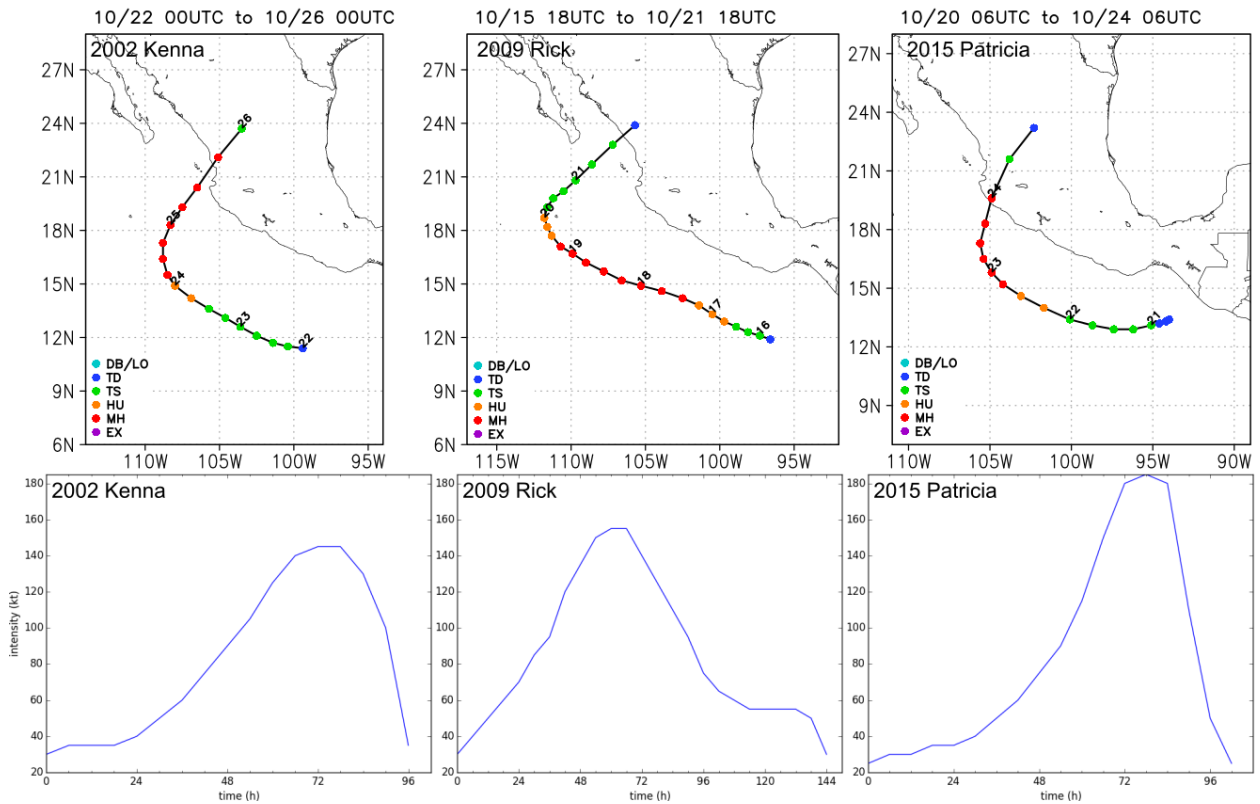
Figure 15-2. *Three examples of rapid weakening near land in the eastern North Pacific.*

Objectives

The main objective of this experiment is to examine the characteristics of both the TC and its environment prior to and during weakening, particularly RW. These observations will be analyzed in order to improve understanding of the physical processes and environmental factors involved in these events and explore avenues for improved forecast accuracy.

Observations of the ocean, of winds, and of thermodynamic variables taken by the G-IV and NOAA P-3 aircraft within the core of weakening and rapidly weakening TCs and their large-scale environments will enable the achievement of this objective. The best candidates for sampling will be TCs moving over cooler SSTs as well as increasing vertical wind shear. TCs that begin to entrain dry air as they move over cooler SSTs should also be sampled.

Hypotheses

- The three leading factors that cause RW are cooling SSTs, dry air intrusion, and increasing vertical wind shear.
- Of these three leading factors, cooling SSTs dominate due to their impact on inner core convection, making the storm more vulnerable to dry air intrusion and/or vertical wind shear.
- Observations spanning the core of the TC and its environment will improve our understanding of conditions that precede RW as well as occur during it, allowing us to investigate impacts such as the rate of erosion of the warm core and the role of core tilt.

Links to IFEX goals

- Goal 1: Collect observations that span the TC life cycle in a variety of environments for model initialization and evaluation
- Goal 3: Improve understanding of the physical processes important in intensity change for a TC at all stages of its lifecycle

Model evaluation component

Zhang et al. (2007) showed utility in adding satellite observations to improve model forecasts of RW. However, little work has been done that tests the addition of aircraft observations to model representation of these TCs that rapidly weaken over open ocean, both for intensity and structural evolution. Also, more oceanic observations, particularly for weakening TCs, may improve the capability of models to capture oceanic features that influence intensity (e.g., Jaimes and Shay 2009). The range of spatial scales at which data will be collected for weakening TCs in this experiment should provide a sufficient dataset by which to evaluate operational modeling systems, such as the ability of the models to capture changes in the TC structure.

Mission description

Systems expected to weaken over open-ocean will be targeted, such as those forecast to move over cooler SSTs. The best-case scenario would be to sample a TC that is also expected to entrain dry air and encounter increasing vertical wind shear beginning 24 h prior to the forecast onset of RW. Eastern Pacific TCs are of particular interest since many cases of RW occur in this basin. If missions are flown up to every 12 h from this point until the

completion of RW (24 h after onset), the structural evolution leading up to and during the entire process should be captured. As many of these systems appear to undergo RI prior to RW, coordination with RAPX would be optimal.

To enable all of the desired observations, the NOAA P-3 and G-IV are required to fly simultaneously. Eye penetration is needed to obtain accurate samples of the current intensity as well as the structure of the inner core and the ocean below the center. Both AXBTs (if available) and dropsondes from the NOAA P-3 should be used every ~40 km for adequate sampling coverage. Larger intervals may not properly capture the variability in the storm's structure. An example flight pattern is provided in Figure 15-3.

The G-IV should follow the pattern shown in Figure 15-4 above 40000 ft. with dropsondes launched at 4 RMW, 5 RMW and 6 RMW (~200-500km) to measure characteristics of the near-storm environment. A secondary pattern for the G-IV is displayed in Figure 15-5 where dropsondes are deployed in each quadrant at those radii. Since it is a long flight (~9 hours), this pattern is ideal when the TC is within 1 hour of the deployment location. Using either pattern, these radii will enable the derivation of vertical wind shear and upper-level divergence, both having shown a relationship to RW. The use of dropsondes in this manner should also highlight the location and magnitude of any dry air entrainment that is occurring.

This experiment can also make use of observations from the NASA Global Hawk. If the G-IV is unavailable, tandem flights of the NASA Global Hawk and NOAA P-3 should capture much of the structural evolution during RW, especially if all instrumentation on board the Global Hawk can be utilized simultaneously within 600 km of the TC center (dropsondes, S-HIS, HIRAD, HIWRAP, and HAMSR).

Analysis strategy

This experiment is intended to support a multi-dimensional, multi-scale analysis of the conditions leading up to and during RW. Satellite observations will be used to evaluate the environmental conditions of the atmosphere and ocean surface during the experiment, as well as *in situ* observations such as ocean buoys when available. Examination of data measured in the inner core (Doppler radar reflectivity and vertical velocity) will show structural evolution as the TC weakens. Dropsonde data from the inner core and the environment will highlight the influence of environmental factors on the structure of the TC as it weakens, and ocean data will demonstrate the influence of changes in oceanic properties. Results from these analyses will be used to assess predictors that may improve the SHIPS model for rapidly weakening TCs.

References

- DeMaria, M., 1996: The effect of vertical shear on tropical cyclone intensity change. *J. Atmos. Sci.*, **53**, 2076-2087.
- DeMaria, M., and J. Kaplan, 1999: An updated Statistical Hurricane Intensity Prediction Scheme (SHIPS) for the Atlantic and eastern North Pacific basins. *Wea. Forecasting*, **14**, 326–337.
- DeMaria, M., C. R. Sampson, J. A. Knaff, and K. D. Musgrave, 2014: Is Tropical Cyclone Intensity Guidance Improving? *Bull. Amer. Meteor. Soc.*, **95**, 287-398.
- Frank, W. M., and E. A. Ritchie, 2001: The effects of vertical wind shear on the intensity and structure of numerically simulated hurricanes. *Mon. Wea. Rev.*, **129**, 2249-2269.
- Jaimes, B., and L. K. Shay, 2009: Mixed layer cooling in mesoscale oceanic eddies during Hurricanes Katrina and Rita. *Mon. Wea. Rev.*, **137**, 4188-4207.
- Jaimes, B., L. K. Shay, and E. W. Uhlhorn, 2015: Enthalpy and Momentum Fluxes during Hurricane Earl Relative to Underlying Ocean Features. *Mon. Wea. Rev.*, **143**, 111-131.

- Wong, M. L. M., and J. C. L. Chan, 2004: Tropical Cyclone Intensity in Vertical Wind Shear. *J. Atmos. Sci*, **61**, 1859-1876.
- Wood, K. M., and E. A. Ritchie, 2015: A definition for rapid weakening in the North Atlantic and eastern North Pacific. *Geophys. Res. Lett.*, **42**, 10091-10097.
- Zhang, X., Q. Xiao, and P. J. Fitzpatrick, 2007: The Impact of Multisatellite Data on the Initialization and Simulation of Hurricane Lili's (2002) Rapid Weakening Phase. *Mon. Wea. Rev.*, **135**, 526-548.
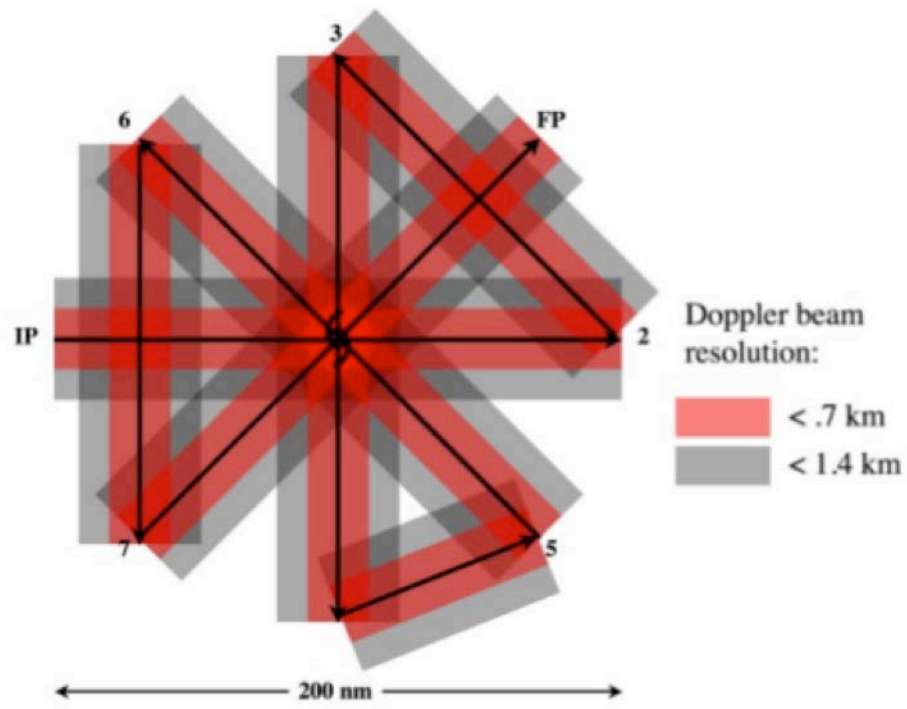
Figure 15-3. *Sample rotated figure 4 pattern designed for the RAPX mission. Shading indicates the Doppler beam resolution at each location along the flight path. Dropsondes should be released at the turning, mid, and center points. An additional dropsondes should be released between the turn and mid points for each radial pass. If possible, release AXBTs coincident with dropsonde locations. Duration ~ 4 hours*
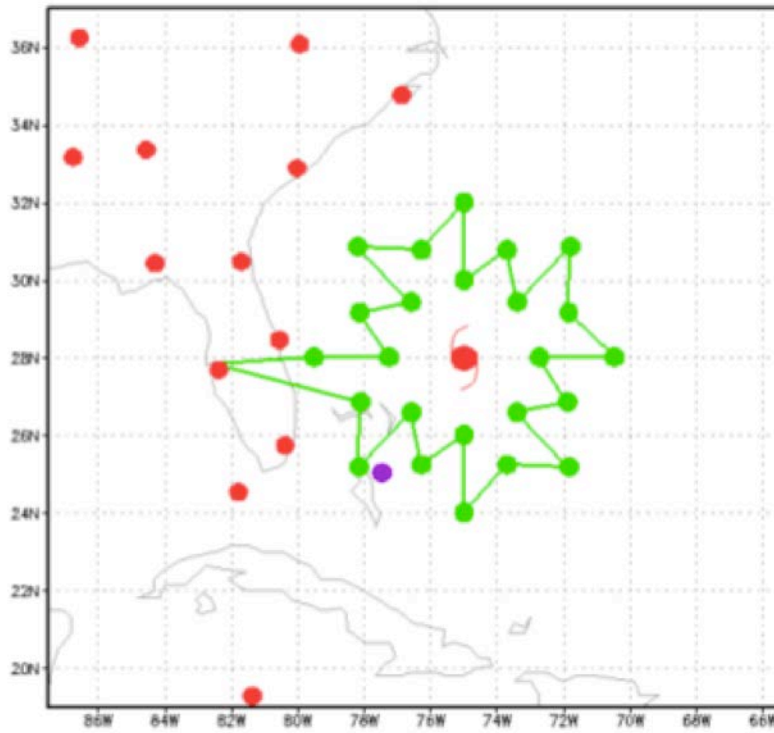
Figure 4. Sample G-IV flight pattern for the RAPX mission; Green dots indicate dropsonde release locations at radii of 220, 330, and 440 km relative to the TC center. Duration ~6 hours
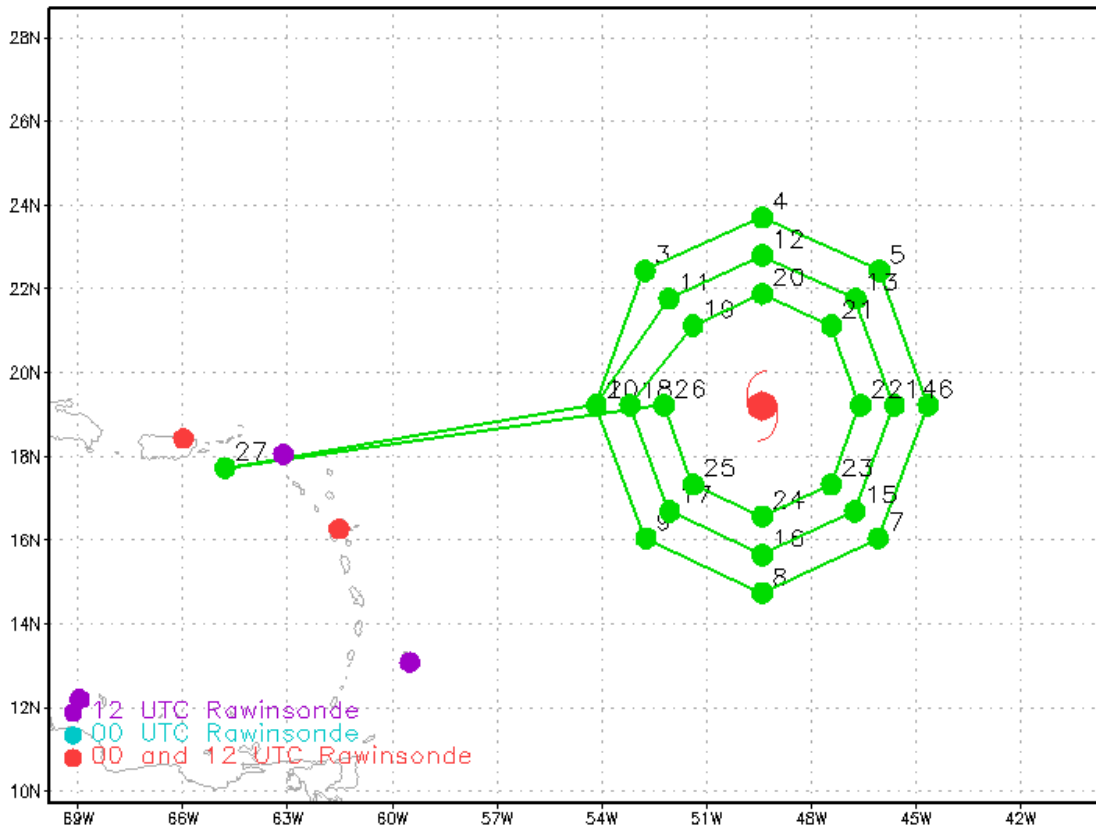
Figure 5. *Sample G-IV flight pattern when TC is within 1-hour proximity to deployment location. Dropsondes are released with 45 degree spacing at 4, 5, and 6 RMWs (~200-500 km). Duration ~9 hours*

16. Convective Burst Module

Principal Investigator(s): Robert Rogers (HRD), Altug Aksoy (HRD), Jon Zawislak (Florida International University)

Objective: To sample the wind, temperature, and moisture fields within and around an area of deep convection at high time frequency and to use them in high-resolution data assimilation experiments.

What to Target: An area of vigorous, deep convection occurring within the circulation of a tropical cyclone (tropical depression or stronger).

When to Target: When deep convection is identified either by radar or satellite during the execution of a survey pattern. Particular attention should be paid when a developing area of deep convection can be detected on the downshear (as inferred by real-time SHIPS analyses) side of the storm.

This is a stand-alone module that takes 1-2 h to complete. Execution is dependent on system attributes, aircraft fuel and weight restrictions, and proximity to operations base. The objectives are to obtain a quantitative description of the kinematic and thermodynamic structure and evolution of intense convective systems (convective bursts) and the nearby environment to examine their role in tropical cyclone genesis and intensity change. It can be flown separately within a mission designed to study local areas of convection or at the end of one of the survey patterns. Once a local area of intense convection is identified, the P-3 will transit at altitude (10-12,000 ft.) to the nearest point just outside of the convective cores and sample the convective area (Fig. 16-1). The sampling pattern will be either a circumnavigation (when sampling a burst within a TC of tropical depression strength or less or well-removed from the radius of maximum wind (RMW) of a tropical storm or stronger) or a series of inbound/outbound radial penetrations or bowtie patterns (when sampling a burst within the radius of maximum wind of a tropical storm or hurricane). If the convective burst is at or near the RMW, repeated sampling can allow for a following of the burst around the storm. This is especially useful to sample the structural evolution of the burst as it moves around the storm.

The high-resolution data collected in this module is planned to be embedded within the typical Hurricane Ensemble Data Assimilation System (HEDAS) framework to carry out storm-scale data assimilation that focuses specifically on the high-resolution analysis of the identified intense convective region. With current technology, a smaller domain with 1-km grid spacing will be nested within the HEDAS 3-km analysis domain, where the data will be assimilated for the duration of its collection (1-2 hours, at 5-10 min intervals). This is a typical setup that has been traditionally used in continental storm-scale radar data assimilation applications and has been shown to be effective to obtain realistic storm structures in analyses and short-range forecasts. With such high-resolution analyses, we hope to be able to obtain fully three-dimensional model representations of the observed convective regions for more detailed investigation, as well as investigate their short-range predictability. In an observing system experiment (OSE) mode, various assimilation experiments can also be devised to investigate hypothetical scenarios for how an observed convective region could interact with the surrounding vortex and impact its evolution.

For circumnavigation patterns, the aircraft should fly a series of straight legs just outside of the main convection, with every effort made to fly the aircraft level for optimal Doppler radar sampling. The tail radar should optimally be operated in F/AST sector scan and regularly spaced dropwindsondes (10-20 km apart) will be released during this time. While flying parallel to the leading convective line, dropwinsonde deployment should occur as close to the leading line as is safely possible. Once the circumnavigation is completed, and the P-3 is near the original IP, two straight-line crossings of the convective area should be performed with the P-3 avoiding the strongest cores, as necessary for safety considerations. The P-3 should fly at a constant altitude of 10-12,000 ft – radar or pressure altitude is fine. When a high-altitude (i.e., above the flight-level of the P-3) aircraft is present, efforts should be made to coordinate this portion of the pattern with the high-altitude aircraft, so that the two aircraft are as close to vertically-stacked as possible. The P-3 should perform as many circumnavigations (or partial ones) of the convective burst as time permits within the 1-2 h window.

For bowtie (radial penetration) patterns, the tail radar should be operated in F/AST full-scan mode. Dropsondes should be released ~10-20 km apart on all passes. Repeat penetrations as long as time permits within the 1-2 h window. When a high-altitude aircraft is present, efforts should be made to coordinate the pattern with the high-altitude aircraft, so that the two aircraft are as close to vertically-stacked as possible.
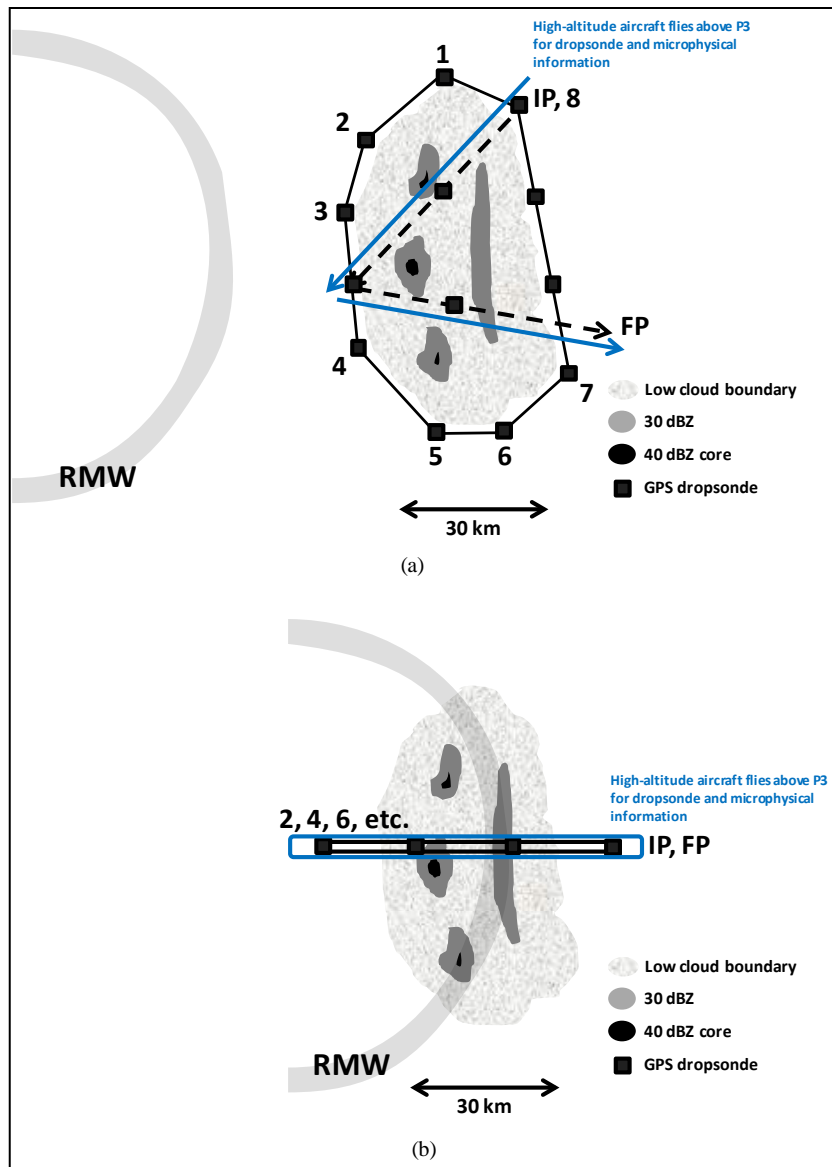
Figure 16-1: *P-3 Convective burst module. (a) circumnavigation for when burst is well outside RMW or within a TC of tropical depression strength or less; (b) bowtie pattern for when burst is within or near RMW of tropical storm or hurricane.*

- **Altitude**: 12,000 ft (4 km) altitude preferable.
- **Expendables**: Release dropsondes at turn points and at intermediate points as indicated in Figure. Additionally, release 1-2 drops during penetration of convective system. No more than 15 dropsondes needed for this module.
- **Pattern**: Circumnavigation (IP to point 6) by single P-3 when burst is outside RMW or in weak system. Then fly convective crossing (6-7-FP). Repeat circumnavigation (time permitting). If available, high-altitude aircraft (e.g., ER-2 or Global Hawk) flies either racetrack or bowtie pattern during P-3 circumnavigation, flies vertically aligned with P-3 during convective crossing. Repeated radial penetration (i.e. bowtie) when burst is inside or near RMW of tropical storm or hurricane.
- **Instrumentation**: Set airborne Doppler radar to scan F/AST on all legs.

17. Eye-eyewall Mixing Module

Principal Investigator: Sim Aberson (HRD)

Significance: Eyewall mesovortices have been hypothesized to mix high entropy air from the eye into the eyewall, thus increasing the amount of energy available to the hurricane. Signatures of such mesovortices have been seen in cloud formations within the eyes of strong TCs, in radar reflectivity signatures (Hurricane Fabian), and from above during aircraft penetrations (Hurricanes Hugo and Felix). Doppler radar was able to sample such features in Hurricanes Hugo and Felix, though interpretation with sparse observations through the small features has been difficult. Dropwindsondes released in very intense tropical cyclones, in conjunction with large-eddy simulations, have provided some thermodynamic data. However, the kinematic and thermodynamic structures of these features have never been directly observed. Observations within the eye near or below the inversion can allow for the study of the these mesovortices and improve knowledge of small-scale features and intensity changes in very strong TCs.

Objective: The objective is to directly observe the three-dimensional kinematic and thermodynamic structures of eyewall mesovortices for the first time. This would allow research into the impact these features have on subsequent intensity changes.

Requirements: A TC with a clearly defined visible eye, eyewall, and inversion and an eye diameter of at least 25 nm is needed. This should only be done during daytime missions. The inversion level is defined as the interface between cloudy air below and clear air above inside the eye. This can be done as a module during any other experiment.

Hypothesis: Eyewall mesovortices play an important role in tropical cyclone intensity change.

Description: Although this is not a standalone experiment in itself, it could be included within any missions during aircraft passage through the eye (Fig. 17-1). The P-3 will penetrate the eyewall at the altitude proposed for the remainder of the flight. Once inside the eye, the P-3 will descend from that altitude to a safe altitude below the inversion while performing a figure-4 pattern. The leg lengths will be determined by the eye diameter, with the ends of the legs at least 2 nm from the edge of the eyewall. Upon completion of the descent, the P-3 will circumnavigate the eye about 2 nm from the edge of the eyewall in the shape of a pentagon or hexagon. Time permitting; another figure-4 will be performed during ascent to the original flight level. Depending upon the size of the eye, this pattern should take between 0.5 and 1 h.
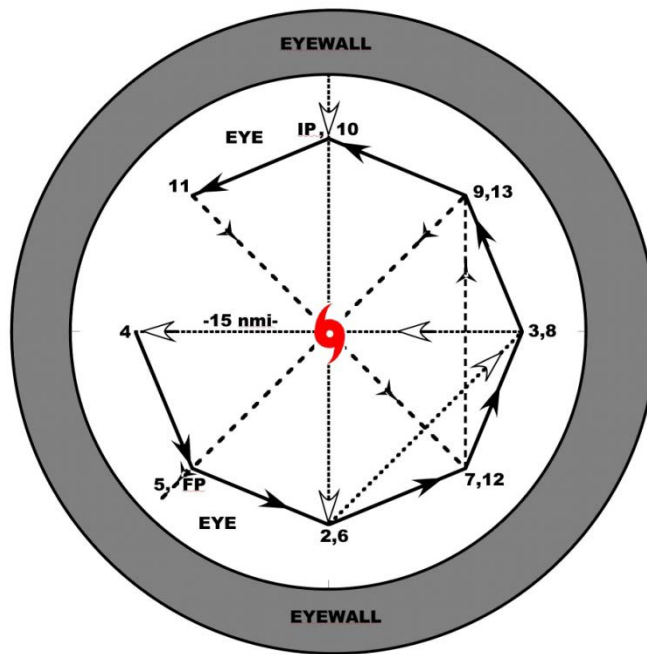
Figure 17-1. *The P-3 approaches from the north, penetrates the eyewall into the eye, and descends below the inversion while performing a figure-4 (dotted line) in the eye. The P-3 circumnavigates the eye in an octagon or pentagon (solid line), and then ascends while conducting another figure-4 (time permitting) rotated 45 degrees from the original (dashed line).*

18. Secondary Eyewall Formation and Eyewall Replacement Cycle Module

Principal Investigators: Hui Christophersen, Robert Rogers, Jason Dunion, Jun Zhang

Collaborators: Jeff Kepert, Kristen Corbosiero, Anthony Didlake, Yuqing Wang, David Nolan and Sergio Abarca

Primary IFEX Goals:

1- Collect observations primarily for mature hurricanes that may undergo a secondary eyewall formation (SEF) and eyewall replacement cycles (ERCs) based on radar, dropsonde, flight-level, Doppler Wind Lidar (DWL), and Coyote PBL measurements;
2- Test utility of new observing platforms (Coyote UAS) and instruments (DWL) in diagnosing physical processes responsible for SEF/ERC, and use data to optimize sampling strategies for improving TC structure predictions in an OSE/OSSE framework;
3- Improve understanding of the dynamic and physical processes that are responsible for SEF/ERC.

Significance & Background:

Secondary eyewall formation (SEF) and eyewall replacement cycles (ERCs) frequently occur during the mature phase of the tropical cyclone (TC) lifecycle. These processes typically result in a halting of the intensification of a TC, and occasionally lead to a temporary weakening as the secondary eyewall becomes the dominant eyewall (Sitkowski et al., 2011). Additionally, they typically lead to a significant broadening of the wind field, increasing the total kinetic energy of the storm and thus the risks from storm surge. Statistical analysis of a 10-year (1997-2007) dataset shows that 77% of major hurricanes (120 knots or higher) in the Atlantic Ocean, 56% in the eastern Pacific, 81% in the western Pacific, and 50% in the Southern Hemisphere underwent at least one ERC (Hawkins and Helveston, 2008). Despite the relative frequency of their occurrence, operational forecasting of SEF/ERCs remains a great challenge, partly since there is no consensus on the mechanisms responsible for SEF or ERC.

There are a wide variety of studies that aim to understand SEF and ERC with different emphases on the internal dynamics and external environmental forcing. The axisymmetric balanced flow, constrained by heat and tangential momentum forcing, generally satisfies gradient wind and hydrostatic balance above the boundary layer (BL) (Abarca and Montgomery, 2013). From the perspective of diabatic forcing, Rozoff et al. (2012) proposed that a sustained azimuthal-mean latent heating outside of the primary eyewall could lead to SEF. This hypothesis was supported by the numerical simulations given by Zhu and Zhu (2014). In a similar sense, diabatic heating/cooling associated with rainbands plays an important role in the structure and intensity change of the storm (Wang 2009; Li et al 2014; Moon and Nolan 2010; Didlake and Houze, 2013a, b) and thus they may also contribute to the SEF/ERC. Didlake and Houze (2013a) proposed that there exists a critical zone where sufficiently high vertical shear of the radial wind can limit the altitude of the convectively induced supergradient flow, leading to low-level convergence in this radial zone and allowing the convection to develop into a secondary eyewall. Corbosiero and Torn (2016) proposed a hypothesis that an increase of convergence induced by the cold pool that formed from convectively-driven downdrafts and low-level radial inflow could enhance rainband convection and lead to SEF. The roles of convective and stratiform heating profiles in rainbands in modifying hurricane structure and intensity, and potentially SEF, is an area of ongoing research.

Montgomery and Kallenbach (1997) proposed that vortex Rossby wave (VRW) interaction with the mean flow may contribute to SEF. VRWs, supported by the radial vorticity gradient outside of the radius of the maximum wind (RMW), propagate from the primary eyewall radially outward until they reach their stagnation radius. At this stagnation radius, inward-moving cyclonic eddy momentum may contribute to SEF. The role of VRWs in SEF is further examined in high-resolution hurricane simulations by Abarca and Corbosiero (2011). Judt and Chen (2010), by contrast, downplayed the importance of VRWs, and instead attributed the large accumulation of convectively generated PV through eddy heating in the rainband region as an essential factor for SEF.

In contrast to the balanced arguments discussed above, unbalanced dynamics in the BL have also been recognized as an important element in SEF. In this framework, the axisymmetric flow in the BL does not satisfy gradient wind and thermal wind balance. Several studies (Wu et al., 2011; Huang et al., 2012; Abarca and Montgomery, 2013) have pointed out that the precursors of SEF include the broadening of the tangential wind field and the

intensification of inflow in the BL, followed by development of supergradient winds and an enhanced horizontal convergence. In-situ observations also demonstrated this existence of supergradient flow (Didlake and Houze, 2011; Bell et al. 2012). Kepert (2013) specifically examined the role of the BL in a balanced vortex framework. He proposed that the BL contributed to the SEF and ERC through a positive feedback mechanism that involves a local enhancement of the radial gradient of vorticity, frictionally forced updraft and convection. Moon et al. (2010) attributed the local vorticity enhancement from processes such as rainband convection.

To test the varying mechanisms proposed to explain SEF and ERC, it is important to obtain kinematic and thermodynamic observations near the eyewall and rainbands. In particular, since most previous analyses focus on azimuthally averaged quantities, it is important to obtain adequate azimuthal and radial sampling both near the primary eyewall and a potentially-developing secondary eyewall. For example, Abarca et al. (2016) pointed out the lack of data particularly at radial distance between 120-200 km in Hurricane Edouard (2014). Additionally, some measure of kinematic and thermodynamic structures along a rainband/developing secondary eyewall can be used to evaluate the along-band structures (Wang 2009; Moon and Nolan 2010; Didlake and Houze 2011, 2013a,b). Observations sampled through this module can be used to evaluate the different proposed mechanisms of SEF and ERC. Data-impact studies on TC analyses and forecasts can also be conducted using the OSSE approach to find optimal sampling strategies for the prediction of SEF/ERC. If this module is flown every 12 h (e.g., in conjunction with the TDR experiment), then the temporal resolution will provide an opportunity to evaluate the importance of the various proposed mechanisms at different stages in the evolution of the secondary eyewall. The dataset from this module eventually will benefit our understanding of the dynamic and physical processes that are responsible for SEF/ERC.

Objectives:

The main objectives of the SEF/ERC module are:

- Perform analyses with sampled observations to examine key factors that are responsible for SEF/ERCs;
- Validate key features linked with different hypotheses of SEF/ERCs using observations;
- Conduct OSE/OSSE studies to optimize sampling strategies for improving SEF/ERC predictions;
- Improve understanding of the dynamic and physical processes of SEF/ERCs.

Hypotheses:

There are many hypotheses for the formation of the secondary eyewall and subsequent ERCs. The sampling strategy proposed here is intended to allow for a testing of as many of these hypotheses as possible. This experiment aims to investigate the following hypotheses:

- Unbalanced boundary layer (BL) spinup paradigm. Processes potentially linked to SEF/ERCs will be examined, including: the generation of supergradient winds in boundary layer, increases in boundary layer inflow, and the emergence of deep convection originating from the boundary layer.
- A feedback mechanism for SEF/ERCs that consists of a local enhancement of the radial vorticity gradient outside of the primary eyewall, with induced frictional updrafts and convection. This feedback mechanism is linked to a combination of both balanced (e.g. vorticity generation and initiation of upward motion) with unbalanced theory (e.g. the development of enhanced and potentially supergradient flow in the BL).
- Enhanced convergence between cold pools that form from convectively-driven downdrafts and low-level inflow. This convergence invigorates rainband convection that eventually becomes the secondary eyewall.

We note that the above hypotheses place a decidedly different importance on the role of balanced vs. unbalanced processes in SEF/ERC. The first hypothesis states that unbalanced BL processes alone can develop secondary wind maxima without prescribed heat sources and/or inertially constrained swirling flow either within or above the boundary layer. The development of the supergradient winds near the top of the boundary layer coincides with horizontal convergence and the eruption of deep convection out of the BL. The second hypothesis states that the BL process is a 'slave' to the SEF. The local enhancement of the vorticity gradient *causes* the local frictional updraft, while the existence of the supergradient flow is a by-product of this frictional convergence. Though the last tested hypothesis lies in the overall framework of the unbalanced BL spinup paradigm, it emphasizes the role of low moist static energy air within the boundary layer that are associated with the convergence.

Modeling Evaluation:

- Examine the hallmarks of the proposed hypotheses through OSE studies by using the sampled observations
- Further validate proposed hypotheses through a series of OSSE studies

Mission Description:

This module focuses on mature hurricanes (e.g. category 2 or stronger) with a well-defined eye as seen in visible, infrared, and microwave satellite imagery. Sampling can be achieved in combination with the P-3 Doppler Wind Lidar, Coyote UAS and P-3, G-IV or Global Hawk dropsondes. This module can generally be flown in conjunction with TDR Experiment survey patterns, with the addition of either a spiral pattern (pre-SEF) or moat circumnavigation (post-SEF) added onto the survey. The module can also be flown during the TC Diurnal Cycle Experiment and DWL Experiment.

Module Option 1 (PRE-SEF): Mature hurricane that has pronounced rainband activity, and possibly a secondary eyewall forming. Proposed flight pattern (Fig. 18-1) should take place when microwave satellite imagery indicates the presence of asymmetric rainbands occurring in the storm environment.

(a)

(b)
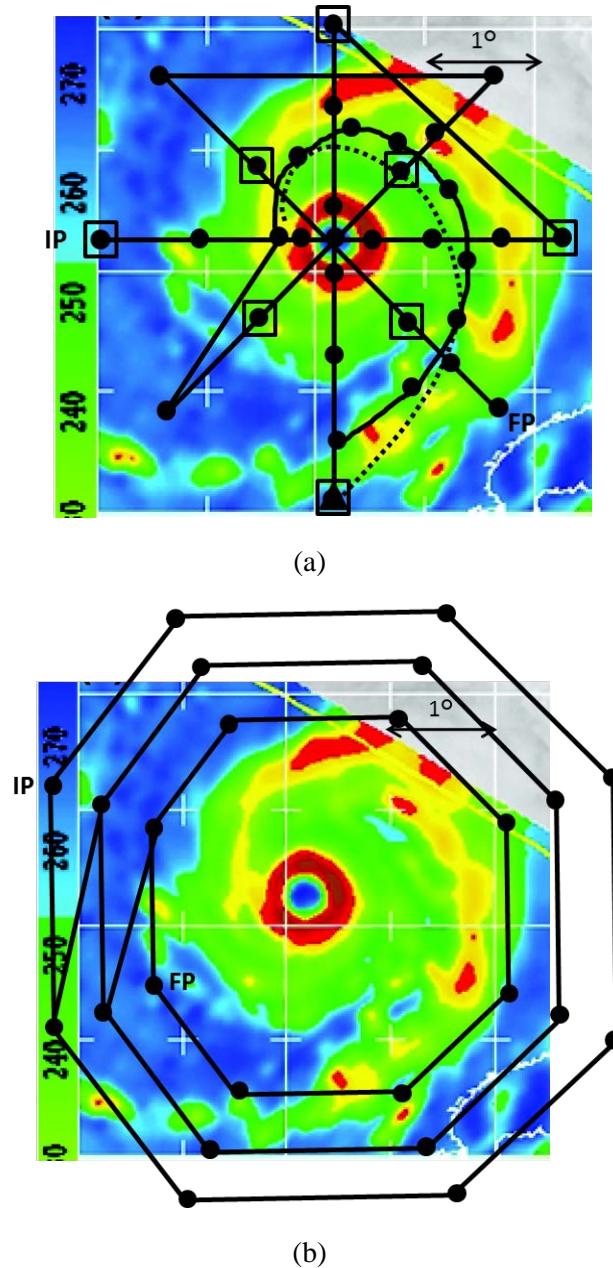
Figure 18-1: *(a) P-3 Rotating figure-four pattern with Coyote deployed inflow path (dashed line; proposed launch point for Coyote Inflow Module indicated by triangle) overlain on a sample 85 GHz satellite image, showing pre-SEF, to depict features to target. Circles indicate dropsonde locations; open squares indicate AXBT deployment locations. Alternatively, the use of IR sondes would be preferred. This scenario may be combined with DWL Experiment. (b) G-IV circumnavigation pattern.*

- Altitude: 10,000-12,000ft (3-4 km) altitude preferable for P-3
- Expendables: For P-3, deploy dropsondes at all turn and mid-points in Figure 4 survey pattern, first center pass, four locations in primary eyewall, and in middle of rainband precipitation feature. Also release dropsonde at ~50 nm spacing along rainband spiral. If Coyote is available, deploy it following the inflow path where it will collect observations that can be used to calculate BL characteristics outside, within, and inside rainband. For G-IV, release dropsondes at all turn points.
- Pattern: For P-3, fly a combination of a rotated Figure-4 and a rainband spiral along the inside edge of the rainband, within ~5-10 nm of the inner edge of the rainband. Fly the spiral pattern straight and level as long as possible, i.e., keeping aircraft bank angle at a minimum, to minimize loss of radar data due to aircraft banking. Ferry time may preclude the second Figure-4. For G-IV, fly pattern such that the innermost circumnavigation is as close to outer edge of rainband as is safely allowed.

Module Option 2 (POST-SEF): Mature hurricanes that are expected to have a secondary eyewall already formed or are undergoing an ERC. These concentric rings can be easily detected based on radar or microwave satellite imagery. For storms that are already undergoing these ERCs and repeated ERCs are forecast, sampling patterns as indicated in Fig. 18-2 are proposed.
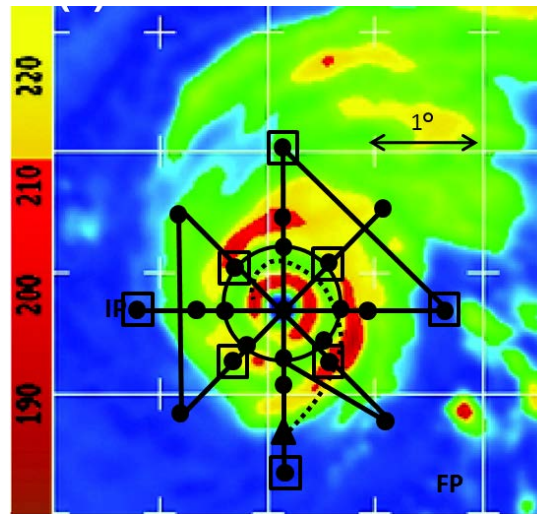
(a)
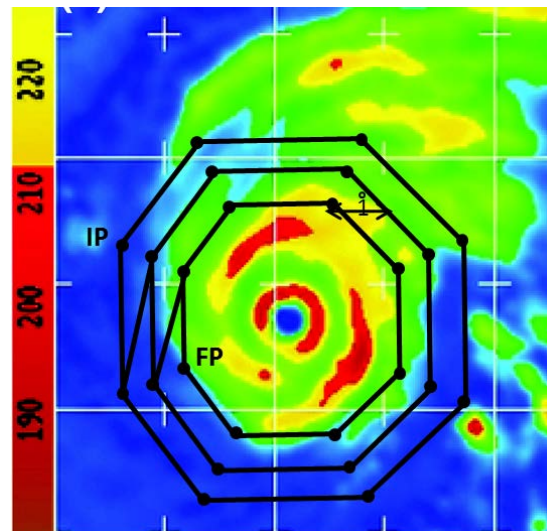
(b)

Figure 18-2: (a) P-3 Rotating figure-four pattern with Coyote deployed inflow path (dashed line; proposed launch point for Coyote inflow module indicated by triangle) overlain on a sample 85 GHz satellite image, showing post-SEF, to depict features to target. Circles indicate dropsonde locations; open squares indicate AXBT deployment locations. Alternatively, the use of IR sondes would be preferred. This scenario may be combined with DWL module. (b) G-IV circumnavigation pattern.

- Altitude: 10,000-12,000ft (3-4 km) altitude preferable for P-3
- Expendables: For P-3, Deploy dropsondes at all turn and mid-points in Figure 4 survey pattern, plus first center pass, at four locations in primary eyewall. Also release dropsonde at ~50 nm spacing along circumnavigation in moat region. If Coyote is available, deploy it following the inflow path where it will collect observations that can be used to calculate BL characteristics outside, within, and inside outer eyewall. For G-IV, release dropsondes at all turn points.
- Pattern: For P-3, fly a combination of a rotated Figure-4 and a circumnavigation in the moat region, within ~5-10 nm of the inner edge of the outer eyewall. Fly the circumnavigation straight and level as long as possible, i.e., keeping aircraft bank angle at a minimum, to minimize loss of radar data due to aircraft banking. Ferry time may preclude the second Figure-4. For G-IV, fly pattern such that the innermost circumnavigation is as close to outer edge of outer eyewall as is safely allowed.

Module Option 3 (PRE-SEF/ POST-SEF): When available, Global Hawk aircraft dropsondes can provide complementary observations compared to P-3 and G-IV (Fig. 18-3). Global Hawk flies at approximately 55,000-60,000 ft altitude with mission durations of ~24 hour. It will provide excellet temporal coverage that might be critical to analyze the evolution of the secondary eyewall.
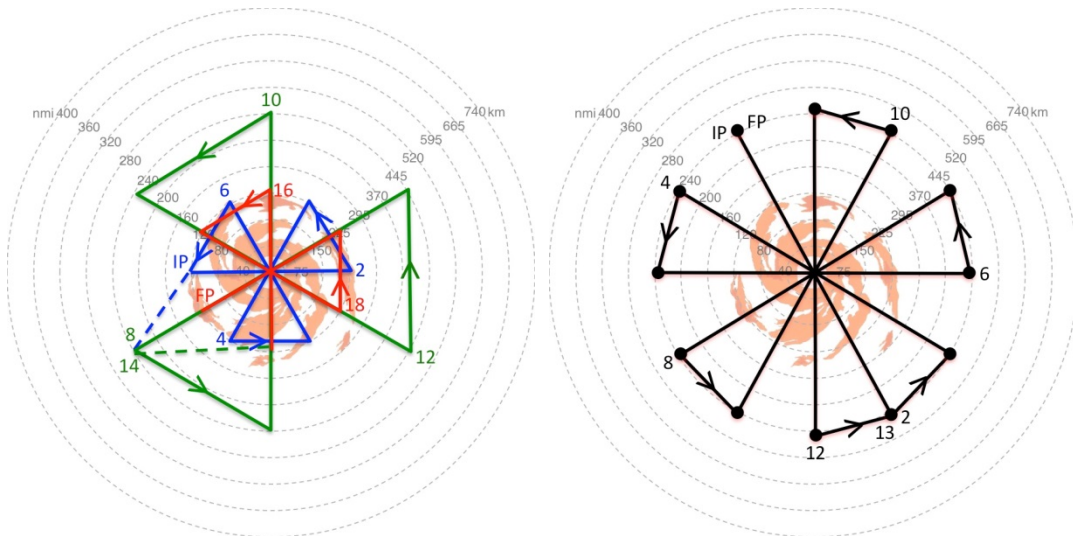
Figure 18-3: Sample flight patterns for the NOAA SHOUT Global Hawk aircraft. (Left) Series of 3 alternating radial leg butterfly patterns shown by the green line and (right) rotated butterfly pattern with 30 degree rotated radial legs. On-station time for both patterns is ~15-20 hr and leg lengths are ~450 km.

- Altitude: 55-60,000 ft
- Expendables: Deploy dropsondes at all turn points, RMW, 2*RMW. If the storm shows one concentric ring, left flight pattern preferable. Deploy dropwonds at the eye, first eyewall, secondary eyewall (if shown), and all turn points. If only one primary rainband with no clear-defined eye, perform right flight pattern.
- Instrumentation: Dropsondes.

Analysis Strategy:

Data collected by option 1 can be used to diagnose different roles in SEF. Specifically, gradient wind (and departures thereof) within and above the BL can be calculated from dropsondes; tangential winds and vorticity can be calculated from dropsonde, Doppler radar, flight-level, and DWL measurements; and moist static energy calculation, can be calculated from dropsondes. Observations that are collected can also be used to conduct data impact studies as well as provide insights for OSSE studies.

Data measured by option 2 would be useful to diagnose the formation and characteristics of the moat region and its role in ERC. Azimuthal coverage of the data would be particularly important to carry out analysis to validate different hypotheses of SEF/ERC. Data collected by module option 3 can provide longer temporal coverage than option 1 and 2 that will be useful to diagnose the temporal evolution of the SEF/ERC.

References:

Abarca, S. F., and K. L. Corbosiero, 2011: Secondary eyewall formation in WRF simulations of Hurricanes Rita and Katrina (2005). *Geophys. Res. Lett.*, **38**, 1-5.

Abarca, S. F., and M. T. Montgomery, 2013: Essential Dynamics of Secondary Eyewall Formation. *J. Atmos. Sci.*, **70**, 3216-3230.

Abarca, S. F., M. T. Montgomery, S. Braun, and J. Dunion, 2016: Secondary Eyewall Dynamics as Captured by an Unprecedented Array of GPS Dropsondes Deployed into Edouard 2014, 32nd Conf. on Hurricanes and Tropical Meteorology, San Juan, PR.

Bell, M. M., M. T. Montgomery, and W.-C. Lee, 2012: An Axisymmetric View of Concentric Eyewall Evolution in Hurricane Rita (2005). *J. Atmos. Sci.*, **69**, 2414-2432.

Corbosiero K. L., and R. D. Torn, 2016: Diagnosis of Secondary Eyewall Formation Mechanisms in Hurricane Igor (2010), 32nd Conf. on Hurricanes and Tropical Meteorology, San Juan, PR.

Didlake Jr., A. C., and R. A. Houze, 2011: Kinematics of the Secondary Eyewall Observed in Hurricane Rita (2005). *J. Atmos. Sci.*, **68**, 1620–1636.

Didlake, Jr., A. C., and R. A. Houze, 2013a: Convective-Scale Variations in the Inner-Core Rainbands of a Tropical Cyclone. *J. Atmos. Sci.,* 70, 504-523.

Didlake, A. C., and R. A. Houze, 2013b: Dynamics of the Stratiform Sector of a Tropical Cyclone Rainband. *J. Atmos. Sci.*, 70, 1891-1911.

Hawkins, J. D., and M. Helveston, 2008: Tropical cyclone multiple eyewall characteristics. Preprints, 28th Conf. on Hurricanes and Tropical Meteorology, Amer. Meteor. Soc., Orlando, FL.

Huang, Y.-H., M. T. Montgomery, and C.-C. Wu, 2012: Concentric Eyewall Formation in Typhoon Sinlaku (2008). Part II: Axisymmetric Dynamical Processes. *J. Atmos. Sci.*, 69, 662-674.

Judt, F., and S. S. Chen, 2010: Convectively Generated Potential Vorticity in Rainbands and Formation of the Secondary Eyewall in Hurricane Rita of 2005. *J. Atmos. Sci.*, 67, 3581-3599.

Kepert, J. D., 2013: How does the boundary layer contribute to eyewall replacement cycles in axisymmetric tropical cyclones? *J. Atmos. Sci.*, 70, 2808-2830.

Li, Q., Y. Wang, and Y. Duan, 2014: Effects of Diabatic Heating and Cooling in the Rapid Filamentation Zone on Structure and Intensity of a Simulated Tropical Cyclone. *J. Atmos. Sci.,* 71, 3144-3163.

Montgomery, M. T., and R. J. Kallenbach, 1997: A theory for vortex Rossby-waves and its application to spiral bands and intensity changes in hurricanes. *Quart. J. Roy. Meteor. Soc.,* 123, 435-465.

Moon, Y., and D. S. Nolan, 2010: The Dynamic Response of the Hurricane Wind Field to Spiral Rainband Heating. *J. Atmos. Sci.*, 67, 1779-1805.

Moon, Y., D. S. Nolan, and M. Iskandarani, 2010: On the Use of Two-Dimensional Incompressible Flow to Study Secondary Eyewall Formation in Tropical Cyclones. *J. Atmos. Sci.*, **67**, 3765-3773.

Rozoff, C. M., D. S. Nolan, J. P. Kossin, F. Zhang, and J. Fang, 2012: The Roles of an Expanding Wind Field and Inertial Stability in Tropical Cyclone Secondary Eyewall Formation. *J. Atmos. Sci.,* 69, 2621–2643.

Sitkowski, M., J. P. Kossin, and C. M. Rozoff, 2011: Intensity and Structure Changes during Hurricane Eyewall Replacement Cycles. *Mon. Wea. Rev.,* 139, 3829-3847.

Wang, Y., 2009: How Do Outer Spiral Rainbands Affect Tropical Cyclone Structure and Intensity?. *J. Atmos. Sci.*, 66, 1250-1273.

Wu, C.-C., Y.-H. Huang, and G.-Y. Lien, 2012: Concentric Eyewall Formation in Typhoon Sinlaku (2008). Part I: Assimilation of T-PARC Data Based on the Ensemble Kalman Filter (EnKF). *Mon. Wea. Rev.*, 140, 506–527.

Zhu, Z.-D., and P. Zhu (2014), The role of outer rainband convection in governing the eyewall replacement cycle in numerical simulations of tropical cyclones*, J. Geophys. Res. Atmos*., 119, 8049–8072

19. TC Warm Core Module

Principal Investigators: Kelly Ryan (HRD), Jason Dunion (HRD), and Klaus Dolling (MDC)

Significance and Background:

Forecasting TC intensity continues to be a challenge, and analyzing the thermodynamic structure of TCs is shown to be important in understanding intensity changes. Despite the significance in understanding the structure of the maximum perturbation temperature, the relationship between the warm core and intensity is not fully understood. The wind-induced-surface-heat-exchange (WISHE) theory explains how a TC intensifies and suggests that the maximum perturbation temperature is located in the upper level troposphere (Emanuel 1986). However, recent modeling studies propose a variety of distinctive warm core heights in their TC simulations. Stern and Nolan (2012), Stern and Zhang (2013), and Wang and Wang (2014) found that a maximum perturbation temperature exists in the mid-level troposphere due to mean descent and a mid-level static stability maximum. They claim that the scarcity of observations inhibits the ability to determine a typical TC warm core structure. Therefore, a higher resolution of thermodynamic quantities is desired to determine standard warm core characteristics.

The evolution of the warm core throughout a TCs life cycle is not well documented, though some modeling studies have investigated the relationship between the maximum perturbation temperature and rapid intensification. During the RI process in their idealized simulations, Stern and Zhang (2013) found the greatest warming at the mid-level troposphere. They determined that the warm core is maximized at this height due to eddy radial advection as indicated by upward motion in the mid-level eye region. In later stages of RI, they deduced that mean vertical advection warms the eye. Wang and Wang (2014) found that in addition to the mid-level maximum in their simulation of Super Typhoon Megi, an upper-level warm core developed during the onset of RI, which dominated over the mid-level maximum throughout the rapid intensification process due to detrainment and downdrafts from convective bursts. Chen et al 2011 and Chen and Zhang (2013) also suggest that descent and detrainment from convective bursts cause an upper-level warm core to form, and claims this triggers RI in their simulation of Hurricane Wilma.

Both Stern and Nolan (2012) and Stern and Zhang (2013) concluded that there was no relationship between the TC intensity and the height of the warm core in their simulations. However, observational analyses of TC soundings in Durden (2013) indicate that there is a tendency for the height of the TC warm core to increase with increasing intensity. The study explains that a large variability in the height of the maximum perturbation temperature is exhibited ranging from 760 to 250 mb. Durden discovered a positive correlation between the maximum warm core height and TC size, environmental instability, and upper-level divergence. In an analysis on the evolution of Hurricane Humberto, Dolling and Barnes (2012, 2014) discovered a low-level warm core in the early stages of development.   Similar to Durden (2013), the height of the maximum temperature perturbation in Humberto rises and falls as Humberto intensifies and then weakens. The warm core structure depends on the stage of Humberto's life cycle, the physical processes creating the warm core, and the environmental shear and moisture.

The effects of VWS on TC intensity are known to be detrimental (DeMaria 1996), yet the influence of shear on the warm core is not well known. Frank and Ritchie (2001) observed a weakening of the maximum perturbation temperature from the top down due to radially outward eddy fluxes of entropy influenced by VWS at upper levels in their TC simulation. Riemer et al. 2010 and Riemer and Montgomery (2011) propose that VWS reduces the moist entropy into the eyewall, therefore decreasing the overall magnitude of the warm core. However, in Stern and Zhang (2013), the presence of shear in their simulations does not affect the structure or evolution of the TC warm core. Dolling and Barnes (2012, 2014) determined that Hurricane Humberto intensified under increasing vertical shear, and the maximum perturbation temperature remained in the lower troposphere through intensification and dissipation stages. The discrepancy between studies gives rise to the need for additional

observational analyses that focus on how shear influences the development and evolution of the TC warm core.

The data collected from the P-3 and G-IV dropsondes, TDR, SFMR, and flight level data will be used to study the characteristics and evolution of the thermodynamic structure throughout the lifecycle of a TC. In collaboration with NOAA missions, NASA will be conducting its SHOUT field campaign during the 2016 hurricane season and will utilize one Global Hawk (GH) aircraft, flying at ~55-60,000 feet and capable of mission durations of ~24 hr. The GH will be equipped with 3 additional instrument platforms that can be used to study the TC warm core:

i.   AVAPS dropsonde system: capable of deploying up to 88 dropsondes per mission; provides pressure, thermodynamic, and wind information at 2 Hz (~5 m, PTH) and 4 Hz (~2.5 m, winds) vertical resolution;
ii. The High Altitude Monolithic Microwave Integrated Circuit (MMIC) Sounding Radiometer (HAMSR): microwave sounder with 25 spectral channels in 3 bands (50-60 GHz, 118 GHz, and 183 GHz); provides 3-D distributions of temperature, water vapor, & cloud liquid water; 2 km vertical and 2 km horizontal (nadir) resolution; 40 km wide swath;
iii. High-Altitude Imaging Wind and Rain Airborne Profiler (HIWRAP): dual-frequency (Ka- & Ku-band), dual beam, conical scanning Doppler radar; provides 3-D winds, ocean vector winds, and precipitation; 60 m vertical and 1 km horizontal resolution.

Objectives:

- Sample and examine the thermodynamic structure of the TC inner core during formation, intensification, rapid intensification, dissipation, and re-intensification stages.
- Determine the height and 3D structure of the maximum perturbation temperature
- Determine the number of vertical local maxima that exist during each stage of the TC lifecycle.
- Explore the mechanisms affecting warm core formation and evolution in the TC inner core and environment.

Hypotheses:

- During the initial stages of warm core development, the maximum temperature perturbation is located underneath a light stratiform precipitation region free from any deep convection.
- As a TC strengthens, the maximum temperature perturbation increases (decreases) with height with increasing (decreasing) intensity.
- During rapid intensification, detrainment and descent of stratospheric air due strong convective bursts in the eyewall aids in the development of an upper-level warm core.
- The structure of the warm core in both the horizontal and vertical directions will be affected by environmental parameters (vertical wind shear, dry air, environmental stability, etc…)

IFEX Goals:

- Goal 1: Collect observations that span the TC lifecycle in a variety of environments;
- Goal 3: Improve understanding of the physical processes important in intensity change for a TC at all stages of its lifecycle.

Analysis Strategy:

This experiment focuses on observing the structure, formation, and evolution of the TC warm core in various environments. For all stages of the TC life cycle, composite depictions of the thermal structure will be created using thermodynamic inner core and environmental observations taken from dropsondes, HAMSR, TDR, and in situ aircraft observations. By analyzing the height and structure of the maximum perturbation temperature during formation, intensification, rapid intensification, dissipation, and re-intensification stages, a relationship between the warm core evolution and TC intensity can be investigated. Environmental observations during each stage of the TC life cycle will be used to explore the mechanisms that influence the warm core structure and its

relationship to intensity. This allows for the development of a database of typical warm core structures in various environments.

Modeling Component:

Understanding the evolution of the warm core during the various stages of a TC life cycle would expose similarities and differences between the thermal structure seen in real-time TCs and TC simulations. This leads to an evaluation of current model schemes and parameterizations and ideally will improve operational model intensity forecasts. Observations taken during formation of the warm core at early stages of the TC life cycle may provide an alternative approach to initializing TC simulations.

Mission Description:

The sampling strategy will depend on the lifecycle stage of the target TC and whether the Global Hawk (GH) is available.

Coordination Requirements**:**

This module can be conducted in concurrence with other experiments such as the Tail Doppler Radar, Doppler Wind LIDAR, TC Shear, Genesis, and Rapid Intensification (RAPX) Experiments, among others. Flight coordination among P-3, G-IV, and Global Hawk aircraft is ideal when possible. Missions conducted in a variety of shear environments and encompassing all TC life cycle stages is desirable. For the case of a rapidly intensifying TC, the GH is necessary to obtain the desired observations.

When Global Hawk is in use:

GPS dropsondes will be deployed from the GH over the low level circulation center (whether that is under convection, stratiform rain, or clear skies) including center drops and a high density of GPS dropsondes out to approximately 2 RMWs. GPS dropsondes will be deployed on each radial transect with a drop over the low level circulation center and a drop near 0.5 RMW.   Radially outward of 0.5 RMW, the GPS dropsondes will sample approximately every 0.25 RMW out to 2 RMW. Between 2 and 3 RMW (out to about 400 km), approximately 0.5 RMW intervals are required. Since SHOUT GH missions will typically include multiple eye crossings and extended radial legs from the storm center (~215-270; 400-500 km), GPS dropsonde, HAMSR, and HIWRAP observations can be used to observe the temporal and spatial variability of the TC warm core region (Fig. 19-1). GPS dropsondes, HAMSR, and HIWRAP will be utilized to retrieve higher time density observations of thermal structure and associated eyewall convective bursts, wind speeds, and reflectivity changes.

When possible, the P-3 and G-IV should coordinate with the GH to maximize sampling of the TC warm core. The P-3 will obtain TC center fixes to guide the upper-level GH flight pattern and fly at 4-5 km altitude (as high as safety permits). Any dropsondes used for the coordinated experiments can be utilized to study the low-level warm core structure, especially during early stages of the TC development. All stages of the TC life cycle under any shear environment are of interest. A direct center drop from the P-3 is required for this mission. If deep convection is present in the eyewall, GPS sondes may be deployed at smaller radial intervals (~5-10 km). This requires a drop just on the inner edge of the convective burst and at these higher intervals throughout the convective element. The G-IV will sample the environment from 300 to 500 km in a star shaped ring beginning (or finishing) with a circumnavigation around the inner core (Fig. 19-2). GPS dropsondes will be deployed at mid and turning points in the environment.

For genesis cases without a well-defined low-level circulation center, the GH will follow the path shown in Fig. 19-3 to sample the region of expected TC development. Dropsondes will be deployed at ~100 nautical miles

(North, South, East, and West directions) from the region of interest, and every ~40 nautical miles while crossing over the region itself. If the TC Genesis experiment is active, P-3 dropsondes should be deployed at the mid and turning points of a figure 4 pattern centered on the region of interest.

When Global Hawk is not in use:

GPS dropsondes will be deployed from the P-3 over the low level circulation center (whether that is under convection, stratiform rain, or clear skies) including typical mid-point, turning-point and center drops as well as a higher density of GPS dropsondes in the inner core. GPS dropsondes will be deployed on each radial transect with a drop over the low level circulation center and a drop near 0.5 RMW. Radially outward of 0.5 RMW, the GPS dropsondes will sample approximately every 0.25 RMW out to 2 RMW. Between 2 and 3 RMW (out to about 400 km), approximately 0.5 RMW intervals are required. The G-IV will sample the outer core to the environment in a star shaped ring beginning (or finishing) with a circumnavigation around the inner core (Fig. 2). GPS dropsondes will be deployed at typical mid and turning points in the environment, as well as 6 drops equally spaced along the circumnavigation at 60-degree intervals relative to storm center.

For genesis cases without a well-defined low-level circulation center, the G-IV will follow the path shown in Fig. 19-4 to sample the region of expected TC development. Dropsondes will be deployed at ~100 nautical miles (North, South, East, and West directions) from the region of interest, and every ~40 nautical miles while crossing over the region itself. If the TC genesis experiment is active, P-3 dropsondes should be deployed at the mid and turning points of a figure 4 pattern centered on the region of interest.
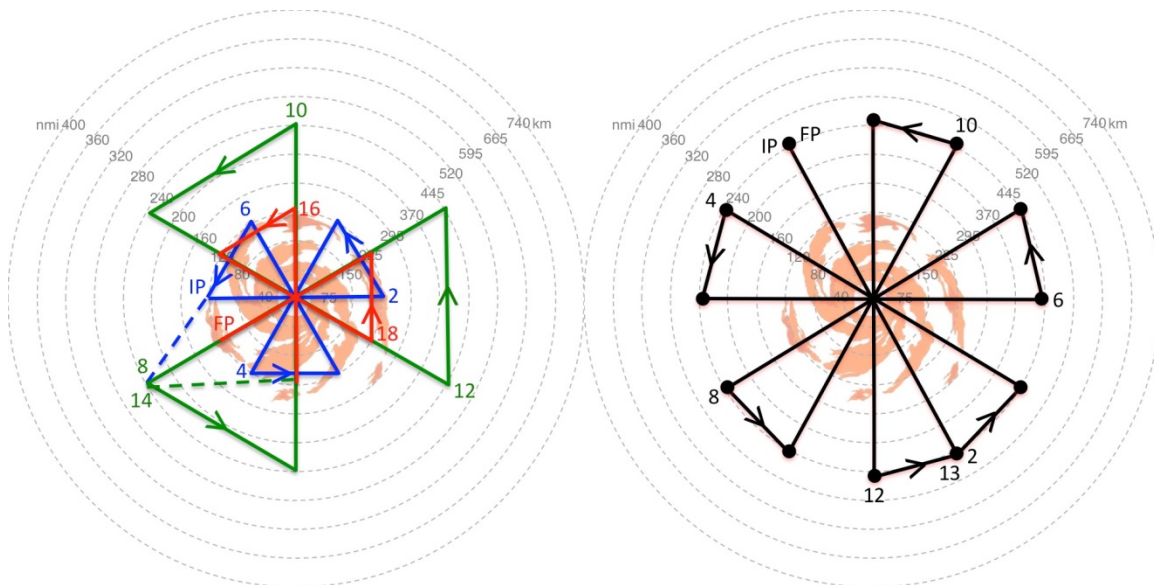
Figure. 19-1. Sample Global Hawk flight patterns that will be conducted during the 2015 NOAA SHOUT field campaign; (Left) Repeated butterfly pattern that includes a series of alternating small (blue curve)-large (green curve)-small (red curve) tracks. The small and large butterflies have radial legs that will range from ~80-160 nm (~150-300 km) and ~215-270 (400-500 km) respectively. (Right) rotated butterfly pattern with 30 degree rotated radials and ~215-270 (400-500 km) radial legs.
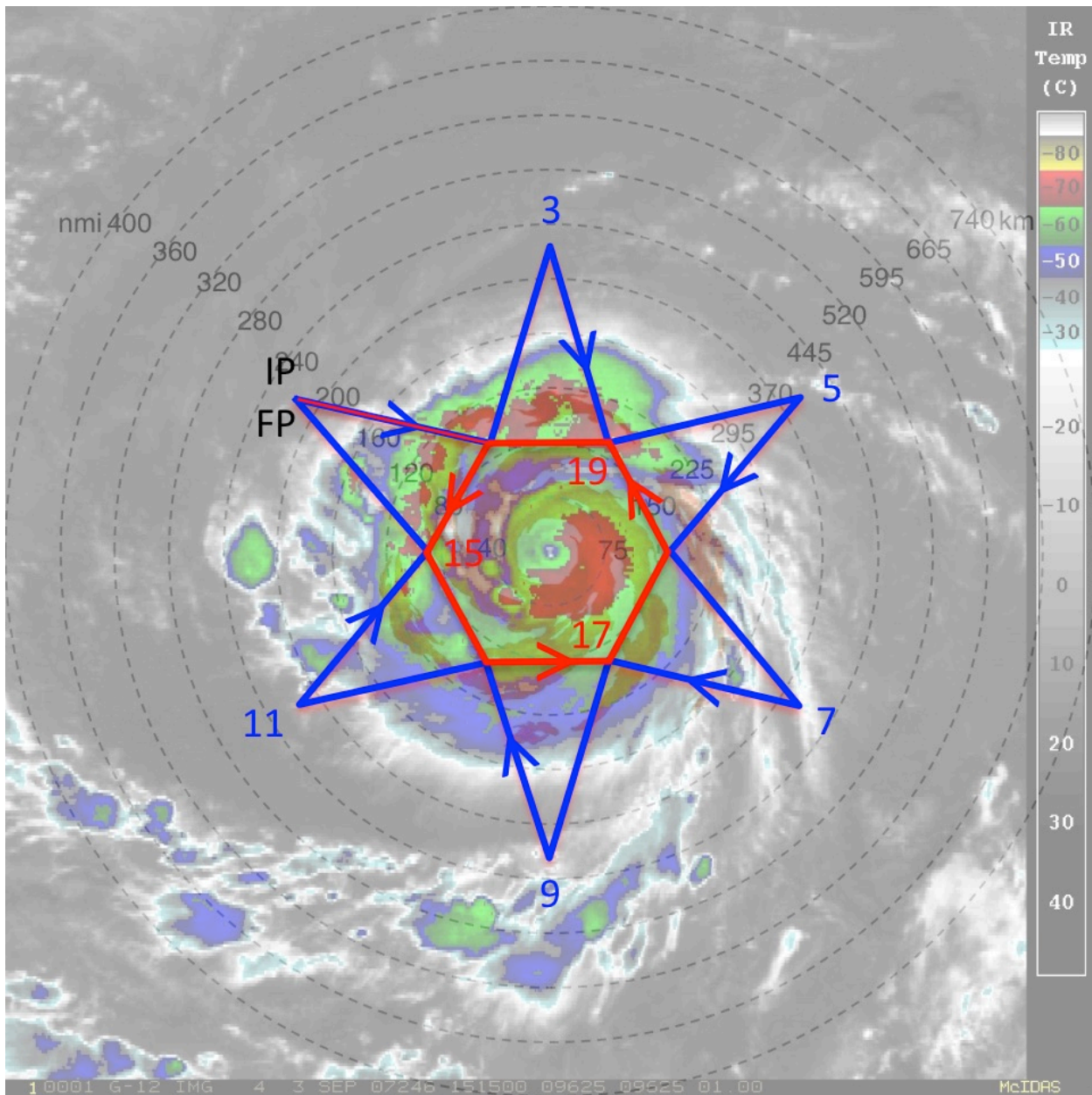
Figure 19-2. Sample G-IV star pattern with endpojnts that alternate between two radii; A circumnavigation of the storm is performed after (or before) the star pattern is completed. The hexagon circumnavigation that is shown has points that are 90 nm (165 km) from the storm center, but can be adjusted outward for safety considerations depending on the strength and size of the TC inner core.
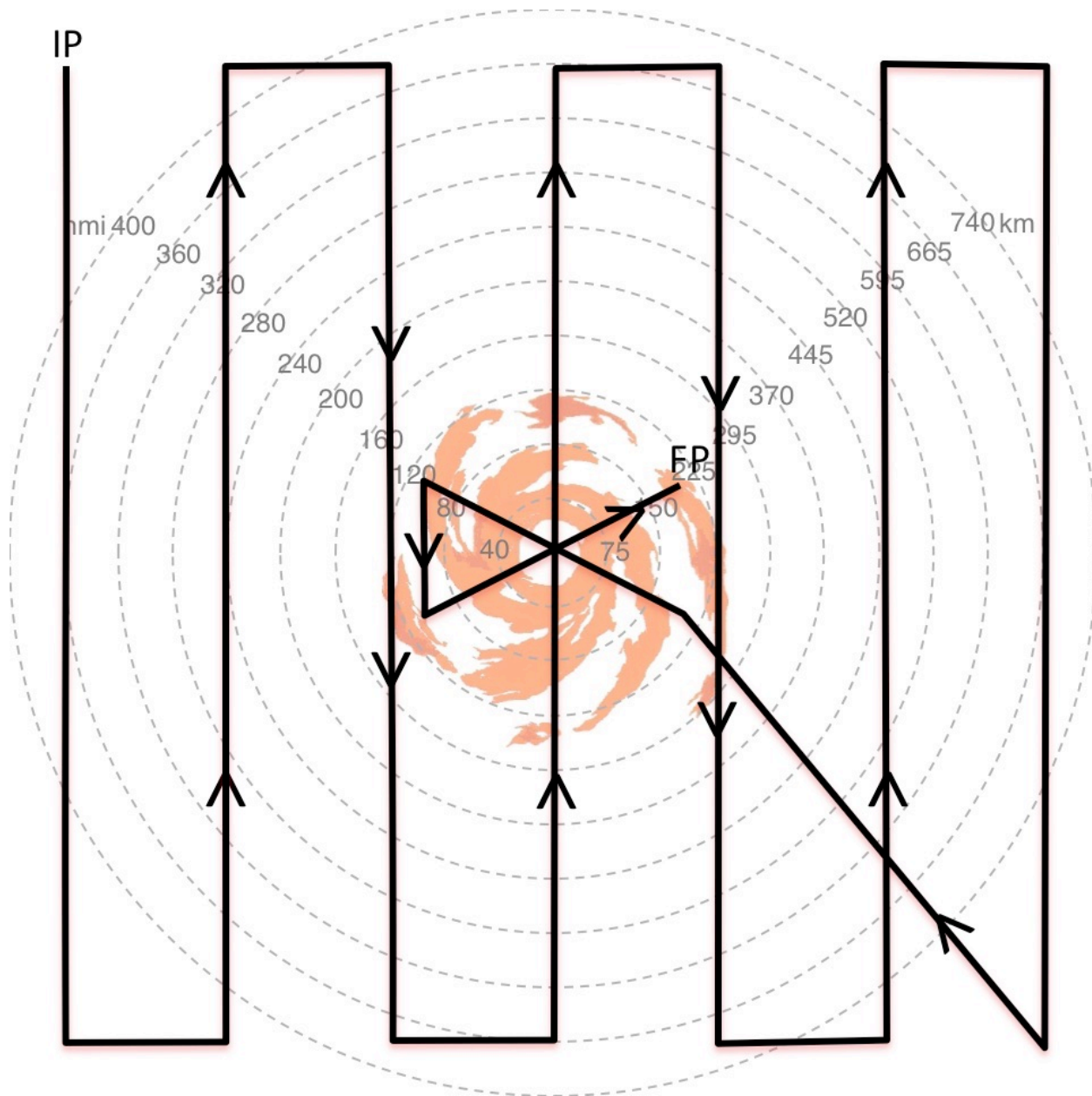
Figure 19-3. *Sample GH 12x12 degree lawn mower pattern with areal coverage of ~1300x1300 km (~700 x 700 nm), leg spacing of 2 degrees, 2 center crossings made during an alpha pattern at the end of the pattern, and an on-station time of ~20 hours.*
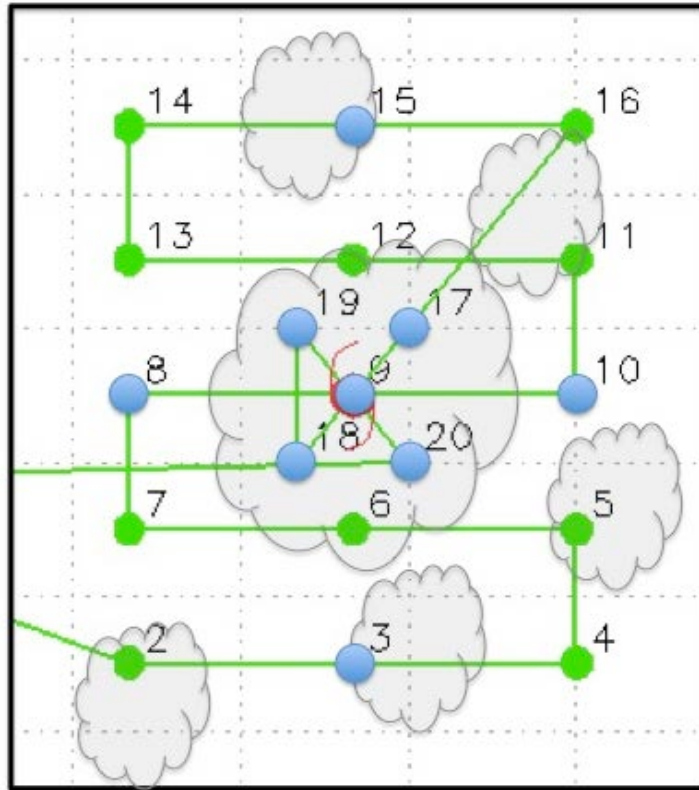
Figure 19-4. Sample G-IV 8x8 degree lawn mower pattern with areal coverage of ~900x900 km, leg spacing of 2 degrees, 2 center crossings made during figure 4 pattern at the end of the path, and a duration of ~8 hours. Blue dots are dropsonde deployment locations. The clouds represent the area of interest and the red symbol indicates the approximate location of the center of this region.

20. Hurricane Boundary Layer (HBL) Experiment

Principal Investigator: Jun Zhang (HRD)

Co-Investigators: Joe Cione (HRD), Robert Rogers (HRD), Lisa Bucci (HRD), Kelly Ryan (HRD), Jason Dunion (HRD), Robert Atlas (AOML), David Emmitt (SWA), Gary Barnes (UH)

Program Significance:
The near-surface inflow is a crucial region of a tropical cyclone (TC), since it is the area of the storm in direct contact with the ocean moisture and heat sources which power the storm (Zhang 2010; Wroe and Barnes 2003). The boundary layer has been identified in prior studies to be of critical importance to hurricane intensification (e.g., Emanuel 1997; Smith et al. 2009; Zhang and Marks 2015). Despite the critical nature of this environment, routine collection of kinematic and thermodynamic observations in the boundary layer remains elusive (Black et al. 2007). Currently, boundary layer observations, especially associated with turbulence, are very limited since the primary source of data is from point-source GPS dropsonde measurements (Zhang et al. 2013). The lack of data coverage at low levels is a primary reason why hurricane boundary layer structure and associated physical processes remain poorly represented in today's operational hurricane models (Zhang et al. 2012; Zhang et al. 2015).

Recent composite analysis of near-surface wind data has led to a more accurate description of general TC inflow characteristics, including asymmetries (Zhang and Uhlhorn 2012). However, it has also become clear that there are few individual cases that contain sufficient observations to develop an accurate synoptic view and comprehensive understanding of boundary layer inflow evolution as a TC intensifies or weakens, changes motion, experiences eyewall/rain-band cycles, and is impacted by shear to varying degrees. This experiment aims to fill this data gap.

Objectives:
The main objectives of the Hurricane Boundary Layer Experiment are to:
- Directly measure turbulent fluxes in the hurricane boundary layer;
- Characterize the distribution and variations of boundary layer heights in hurricanes;
- Identify and document the characteristics of organized eddy such as boundary-layer rolls;
- Quantify the capabilities of the operational hurricane models to accurately represent turbulent fluxes and boundary layer rolls.

Model Evaluation Component:
Turbulent fluxes are the key boundary layer conditions for numerical models. How energy is transported in the hurricane boundary layer is crucial to the hurricane maintenance and intensification. Boundary layer rolls are quasi-two dimensional features that can affect the surface flux transport and modulate the mean boundary layer structure. Observations that are collected during this experiment will be used to evaluate the robustness of the operational coupled model forecast system (e.g. HWRF) to represent turbulent mixing processes.

Mission Description:
This is a multi-option, single or multiple-aircraft experiment that is designed to measure both the mean and turbulent structure of the hurricane boundary layer. A combination of data sources from GPS sondes, AXBTs, high frequency turbulence sensors, Doppler Wind Lidar (DWL), on NOAA P3s and COYOTE unmanned aircraft are applied to determine the quantities listed in the above objectives. This experiment includes 3 modules: 1) stepped-descent module, 2) DWL boundary-layer module, 3) boundary layer inflow module. Turbulence sensors on P3s need to be calibrated at the start of the field season as described in the turbulence calibration module.

Module/Option 1a: Stepped-descent module (40 minutes):
The module is flown between the eyewall and an outer rainband by NOAA P3s or COYOTE. It does not require any penetration of convective cells, the eyewall or convective rainbands. Preference is for a region that is either rain-free or stratiform rain only. For the simplest experiment 5 legs would be flown, each about 40 km or 5 minutes in duration (Figs. 20-1 and 20-2). The pattern would begin with a pass at 3 to 4 km altitude rapidly jettisoning 4 GPS sondes spaced approximately 10-km apart. During this pass 2-3 AXBT's would also be deployed to determine the SST. Airborne radiometers (SFMR) would also provide an estimate of surface wind speeds, and if there are enough scatterers in the volume the Doppler radar can be used to determine mesoscale wind and divergence. The first leg (at ~ 3 km altitude) can be done in conjunction with the standard figure-4 patterns.

The GPS sondes and Doppler wind lidar (DWL) are used to estimate the boundary layer height to the eyewall and the mean conditions of the boundary layer and the lower portion of the layer above. Because it is difficult to determine the height of the inflow layer at real time, the height of the maximum wind speed is defined to be top of the boundary layer, which is around 500 – 1000 m. The inflow layer top is expected to be 1-2 km in height. We can use the dropsonde and DWL data at the end of outbound radar leg to diagnose the boundary layer height. Then we turn back into the storm to do the stair-step. The aircraft would descend to 600 m above the inflow top (about 2400 m) and fly toward the eyewall along an approximate radial. This leg will cover 40 km or require about 5 minutes. The aircraft will then turn and descend ~500 m and fly out-bound for 5 minutes. Two more legs will be completed, each another 500 m below the previous pass. The last pass will be 700 to 800 m above the sea. If the aircrew deems it safe a final pass could be flown 400 to 500 m above the sea. All legs will finish with a turn upwind to keep the legs nearly vertically aligned and in the same portion of the TC. Time to complete the module is about 40 min including descents and turns.

These five passes and the GPS sondes will allow for a determination of the sensible and latent heat fluxes (total enthalpy flux) as a function of height and radial distance adjacent to the eyewall or a convective rainband from the top of the inflow layer to 500 m altitude. The combination of the vertical profiles of equivalent potential temperature (θe) and the determination of the fluxes at the top of the inflow layer will allow an estimate of the air-sea fluxes as a residual and directly through the application of the bulk aerodynamic formulae applying AXBT, SFMR, and 10 m observations obtained from the GPS sondes. The scheme will allow us to infer the magnitude of the transfer coefficients necessary to achieve energy balance, provide insight to the role of dissipative heating, and determine the role of entrainment of warmer θe through the top of the inflow layer.

Module/Option 1b: DWL Boundary-Layer Module:
The DWL on NOAA P3 aircraft measures three-dimensional wind velocities with ~50 m vertical resolution and ~2 km horizontal resolution (Pu et al, 2010). In the stare mode, the horizontal resolution in the marine boundary layer is on the order of a few meters. This is a new tool for boundary layer observations in addition to the existing GPS dropsonde and Doppler radar. Airborne Doppler radars provide three-dimensional wind estimates only where there is precipitation, whereas a DWL can provide wind estimates wherever there are aerosols and broken cloudiness.

This module is designed to complement standard operationally-tasked P-3 Tail Doppler Radar (TDR) missions. This module will target sampling of the kinematic structure of the boundary layer with focus on investigating the characteristics of the boundary layer height and coherent structures. The module can be combined with other experiments or modules, as it does not necessarily require a specific flight track. The DWL will scan in the following modes with downward looking direction. The first is a full scan mode. The second mode follows a sector scanning strategy that allows an increase in the horizontal resolution of the wind retrieval.

Module/Option 1c: Boundary-layer inflow module:
This module is designed to complement standard operationally-tasked P-3 Tail Doppler Radar (TDR) missions by obtaining near-surface wind vector data from GPS dropwindsondes where Doppler winds are not readily available.

The flight pattern is consistent with a typical rotated "alpha" (Figure-4) pattern flown for TDR missions (Fig. 20-3). The rotated pattern (as opposed to the repeated alpha pattern) is preferable to better resolve higher (than 1) wavenumber asymmetric wind field structure. In addition, it is requested to fly the pattern as orthogonal pairs of radials, rather than rotating radials by 45 deg. as the flight proceeds. The initial (IP) and final (FP) points of the pattern are arbitrary. Required instrumentation consists of expendable probes (34 dropwindsondes and 16 AXBTs) as depicted in Fig. 20-3. Note that in particular, high-resolution sampling (3 sondes spaced ~1 min apart) is requested across the radius of maximum wind (RMW) on a pair of orthogonal radii to help better estimate boundary layer gradient winds. Center drops are requested on the first and last pass through the eye. The COYOTE can be flown along the inflow trajectory along with this module for P3 aircraft.

Turbulence Calibration Module (2-3 hours)
The calibration module only needs be executed on separate flights at beginning of the field season. The following maneuvers are requested for turbulence sensors calibration:
1). Dynamic Yaw--2 sets: First set, vary sideslip angle (beta) by +/- 4 degrees. This maneuver requires 5 full sinusoids, with one consisting of left 4 degrees, back through center, right 4 degrees, back to center--one sinusoid. Second set, set angle variation, and perform faster roughly +/- 2.5 degree variation with 25 sec period.
2). Acceleration/Deceleration (AC/DC) run--1 set: Start at normal flight speed, slow to minimum sustainable flight speed, increase to maximum flight speed, slow minimum flight speed, return to normal speed. Try to maintain constant altitude (vary angle of attack).
3). Wind Circles: Two 360° standard rate turns: first clockwise, then counter-clockwise. We need 360° of data to be in a coordinated turn, so after the pilot enters the turn and it is coordinated, only then 'start the clock'.
4). Wind box: Straight and level box, 2 min on each side, standard rate 90° turn on the corners. The box consists of 4 two-minute legs, with 90 degree standard rate turns after the completion of each leg. The box should be set up to fly one leg into, the next cross, the third out of, and the fourth cross wind direction. Indicated airspeed should be 210-220 kt.
5). Pitch (angle of attack) maneuvers--2 sets of 5: Five sinusoids with angle attack variations of +/-5 to 7 degrees. One complete sinusoid should have a period of 15 to 20 seconds. Upon completion of one set, fly straight and level roughly 2 minutes and begin second set.

All of these maneuvers should be aligned with the wind. The boxes should have legs parallel and perpendicular to the wind. The calibrations should be completed at the mean radar altitude where the measurements were conducted or roughly 1,500 ft (500 m). The maneuvers should be conducted in smooth air (as smooth as possible).

References:
Barnes, Gary M., Mark D. Powell, 1995: Evolution of the Inflow Boundary Layer of Hurricane Gilbert (1988). *Mon. Wea. Rev.*, 123, 2348–2368.
 Black, P. G., and coauthors, 2007: Air-sea exchange in hurricanes: Synthesis of observations from the Coupled Boundary Layer Air-Sea Transfer experiment. *Bull. Amer. Meteorol. Soc.,* **88**, 357-374.
 Emanuel, K.A., 1997: Some aspects of hurricane inner-core dynamics and energetics. J. Atmos. Sci., 54, 1014-1026.
Pu, Z., L. Zhang, and G. D. Emmitt, 2010: Impact of airborne Doppler wind lidar profiles on numerical simulations of a tropical cyclone, Geophys. Res. Lett., 37, L05801.
Smith, R. K., M. T. Montgomery, and S. V. Nguyen, 2009: Tropical cyclone spin-up revisited. *Quart. J. Roy Met. Soc.*, **135**, 1321–1335.
Wroe, D. R., and G. M. Barnes, 2003: Inflow Layer Energetics of Hurricane Bonnie (1998) near Landfall. *Mon. Wea. Rev.*, 131, 1600–1612.
Zhang, J. A., 2010: Estimation of dissipative heating using low-level in-situ aircraft observations in the hurricane boundary layer. J. Atmos. Sci., 67, 1853-1862.Zhang, J. A., and F. D. Marks, 2015: Effects of horizontal diffusion on tropical cyclone intensity change and structure in idealized three-dimensional numerical simulations. *Mon. Wea. Rev.*, **143**, 3981–3995.

Zhang, J. A., and E. W. Uhlhorn, 2012: Hurricane sea surface inflow angle and an observation-based parametric model. *Mon. Wea. Rev.*, **140**, 3587–3605.

Zhang, J.A., S.G. Gopalakrishnan, F.D. Marks, R.F. Rogers, and V. Tallapragada, 2012: A developmental framework for improving hurricane model physical parameterization using aircraft observations. Trop. Cycl. Res. Rev., 1 (4):419-429, doi:10.6057/2012TCRR04.01.

Zhang, J. A., R. F. Rogers, P. D. Reasor, E. W. Uhlhorn, F. D. Marks, 2013: Asymmetric Hurricane Boundary Layer Structure from Dropsonde Composites in Relation to the Environmental Vertical Wind Shear. *Mon. Wea. Rev.*, **141**, 3968–3984.

Zhang, J. A., D. S. Nolan, R. F. Rogers, and V. Tallapragada, 2015: Evaluating the impact of improvements in the boundary layer parameterizations on hurricane intensity and structure forecasts in HWRF. *Mon. Wea. Rev.*, **143**, 3136–3154.
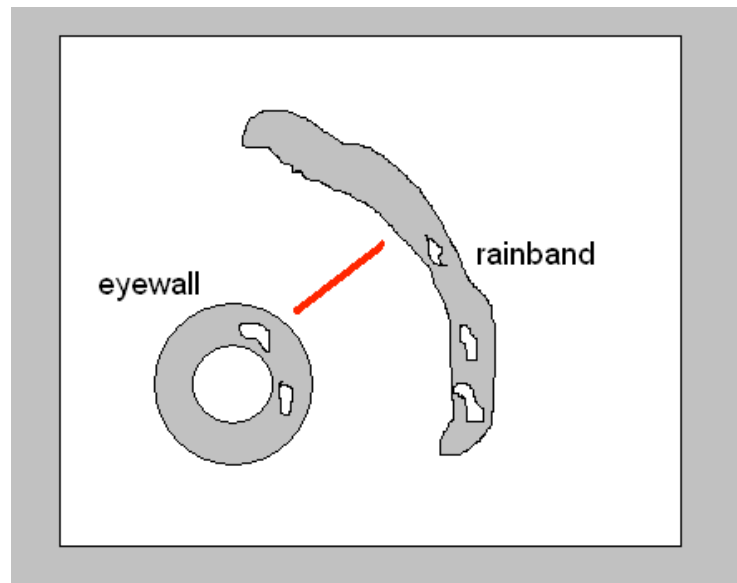
Figure 20-1: *Plan view of the preferred location for the stepped-descent module. Red line shows aircraft track.*
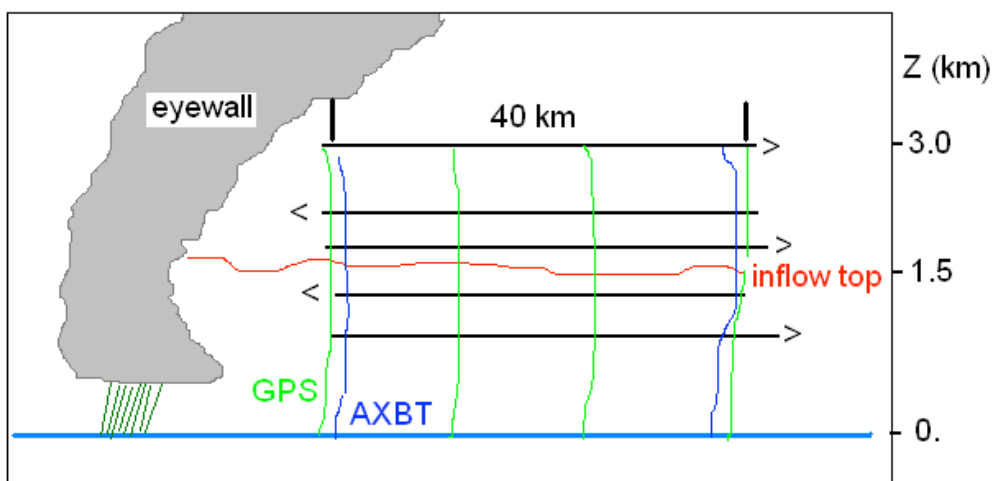
Figure 20-2: *Vertical cross-section of the stepped-descent module.*
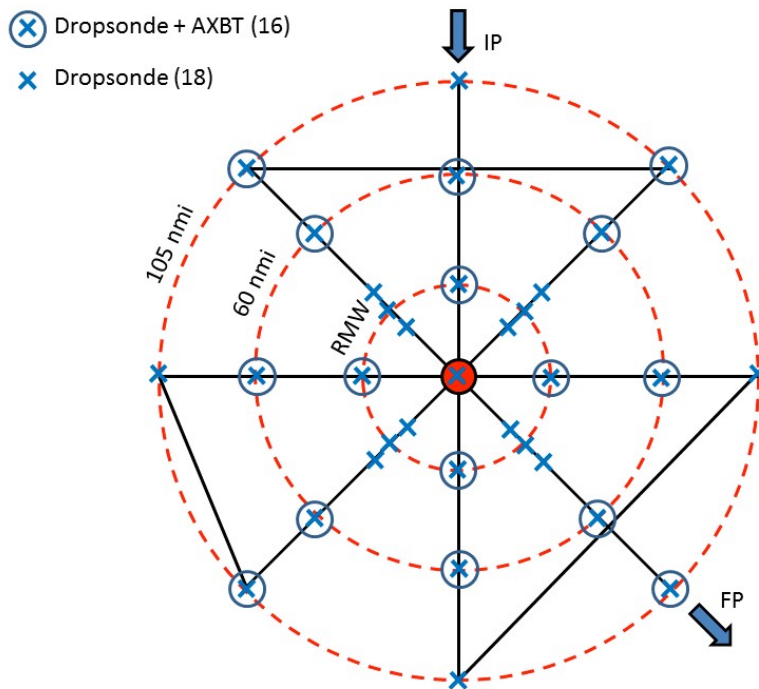
Figure 20-3: *Boundary Layer Inflow Module. GPS dropwindsondes (34 total) are deployed at 105 nmi and 60 nmi radii and at the radius of maximum wind along each of 8 radial legs (rotated alpha/Figure-4 pattern). On 4 of the 8 passes across the RMW, rapid deployment (~1 min spacing) of 3 sondes is requested. Center drops are requested on the initial and final pass through the eye. AXBT (16 total) deployments are paired with dropsondes at the indicated locations. Flight altitude is as required for the parent TDR mission, and initial and final points of the pattern are dictated by these same TDR mission requirements.*

21. Saharan Air Layer Experiment (SALEX): Arc Cloud Module

Principal Investigator: Jason Dunion (HRD)

Program Significance:
Arc clouds are common features in mid-latitude thunderstorms and mesoscale convective systems. They often denote the presence of a density current that forms when dry mid-level (~600-850 hPa) air has interacted with precipitation. The convectively-driven downdrafts that result reach the surface/near-surface and spread out from the convective core of the thunderstorm. Substantial arc clouds (i.e., >100 km in length and lasting for several hours) are also common features in the tropics (Figure 21-1), particularly on the periphery of African easterly waves (AEWs) and tropical cyclones (TCs). However, the physical processes responsible for such tropical arc clouds as well as their impacts on the short-term evolution of their parent disturbances are not well understood.

The mid-level moisture found in the *moist tropical* North Atlantic sounding described by Dunion (2011) is hypothesized to be insufficiently dry to generate extensive near-surface density currents around an African easterly wave (AEW) or tropical cyclone (TC). However, Dunion (2011) also described two additional air masses that are frequently found in the tropical North Atlantic and Caribbean during the summer months and could effectively initiate the formation of large arc clouds: (1) the Saharan Air Layer (*SAL*) and (2) *mid-latitude dry air intrusions*. Both of these air masses were found to contain substantially dry air (~50% less moisture than the *moist tropical* sounding) in the mid-levels that could support convectively-driven downdrafts and large density currents. Furthermore, outward-propagating arc clouds on the periphery of AEWs or TCs could be enhanced by near-surface super-gradient winds induced by the downward transport of high momentum air. Since most developing tropical disturbances in the North Atlantic are associated with a mid-level jet and/or mesoscale convective vortex near a state of gradient balance, any convectively-driven downdrafts would inject high momentum air into a near-surface environment that often contains a weaker horizontal pressure gradient. In such cases, density currents may be temporarily enhanced during local adjustments to gradient balance. Finally, tropical arc clouds may be further enhanced by outward-propagating diurnal pulses that originate from the convective core of the tropical disturbance (see HRD's TC Diurnal Cycle Experiment). New GOES IR TC diurnal cycle imagery indicates that arc clouds tend to form along the leading edge of outwardly propagating diurnal pulses that are associated with the TC diurnal cycle. The diurnal pulses reach peripheral radii where low to mid-level dry air is often located (e.g. R=300-500 km) at remarkably predictable times of day (e.g. 400 km at ~1200-1500 LST). Therefore, UW-CIMSS real-time TC diurnal cycle and visible satellite imagery, as well as P-3 lower fuselage (LF) radar data (where TC diurnal pulses are denoted by 25+ dBZ semi-circular convective bands propagating away from the storm) will be used to monitor the diurnal pulse propagation throughout the local morning hours and signs of arc cloud formation.

It is hypothesized that the processes leading to the formation of arc cloud events can significantly impact an AEW or TC (particularly smaller, less developed systems). Specifically, the cool, dry air associated with the convectively-driven downdrafts that form arc clouds can help stabilize the middle to lower troposphere and may even act to stabilize the boundary layer, thereby limiting subsequent convection. The arc clouds themselves may also act to disrupt the storm. As they race away from the convective core region, they create low-level outflow in the quadrant/semicircle of the AEW or TC in which they form. This outflow pattern counters the typical low-level inflow that is vital for TC formation and maintenance. As arc clouds propagate away from the tropical disturbance, they visibly emerge from underneath the central dense overcast that can obscure them from visible an infrared satellite view. Therefore, when arc clouds are identified using satellites, they are often in the middle to later stages of their lifecycles. Hence, the mechanism of enhanced low-level outflow is likely occurring at the time of satellite identification, while the mechanism of cooling/drying of the boundary layer has already occurred (though the effects may still be observable in the aircraft, GPS dropsonde and satellite data). This necessitates that the arc clouds be identified and sampled as early in their lifecycle as possible using available aircraft observations (e.g. flight-level, GPS dropsonde and P-3 LF radar, and P-3/G-IV Doppler radar data) and satellite imagery (e.g. TC diurnal cycle IR, visible, infrared, and microwave).

Objectives: The main objectives of the TC/AEW Arc Cloud Module are to:
- Collect observations in mid-level dry layers (e.g. the SAL) that are hypothesized to be a necessary ingredient for the formation of strong downdrafts and subsequent outflow boundaries & arc clouds;

- Collect observations across arc cloud features in the periphery of AEWs or TCs using aircraft flight-level data, tail Doppler radar data, and GPS dropsondes to improve our understanding of the physical processes responsible for their formation and evolution and how these features may limit short-term intensification;
- Target observations ahead of and behind arc cloud features to sample the horizontal gradients of temperature, moisture, and winds (e.g. outflow) from ~600 hPa to the surface;
- Quantify the capabilities of the operational coupled model forecast system to accurately capture and represent both mid-level dry air (e.g. the SAL) and thermodynamic and kinematic gradients across arc cloud features through direct comparison to observations as well as high-resolution analyses provided by HRD's state-of-the-art Hurricane Ensemble Data Assimilation System (HEDAS);

Links to IFEX: This experiment supports the following NOAA IFEX goals:
- **Goal 1**: Collect observations that span the TC lifecycle in a variety of environments;
- **Goal 3**: Improve our understanding of the physical processes important in intensity change for a TC at all stages of its lifecycle;

Model Evaluation Component: Arc clouds in the periphery of TCs represent the leading edge of large outflow boundaries that bring cool, dry air and enhanced outflow into the lower levels of the atmosphere. These rarely observed environments are formed in the presence of precipitation falling through mid-level dry air and are hypothesized to limit short-term TC intensification. Thermodynamic and kinematic observations that are collected during this module will be used to evaluate the robustness of the operational coupled model forecast system to represent the SAL and arc cloud environments. Data assimilation (DA) provides a natural platform to compare model output to observations by accounting for the underlying uncertainties of observations and model in a statistical framework. Normalization of model-observation differences by the total expected uncertainty allows for the identification of areas where lack of model performance is statistically the most significant. Furthermore, the high-resolution, three-dimensional analyses that DA produces provide the best estimate of the SAL structure within the modeling framework. Such analyses can be directly compared to operational model output to understand how well the SAL structure is represented in operational models and the consequences for subsequent model forecasts.

Mission Description:
This multi-option research module is designed to utilize the WP-3D [flight-level (flying at multiple levels above 1500 feet) and GPS dropsonde data] or G-IV (GPS dropsonde data) aircraft. Although this module is not a standalone experiment, it could be included as a module within any of the following HRD research missions: TC Diurnal Cycle Experiment, Easterly Wave Genesis Experiment, TC Rapid Intensity Experiment, or TC in Shear Experiment, or as part of operational G-IV Synoptic Surveillance and NHC-EMC-HRD Tail Doppler Radar (TDR) missions. Total precipitable water (TPW) satellite imagery will be used to identify mid-level dry air (≤45 mm TPW) in the periphery of the AEW or TC. These areas of mid-level dry air will be favorable locations for arc cloud formation, especially when TC diurnal pulses are passing radii where this low to mid-level dry air is located. Additionally, when this low- to mid-level dry air is located in the upshear quadrant or semicircle of the storm, arc cloud formation may be especially favorable. These favorable areas will be regions of preferred arc cloud formation and should be monitored closely using satellite imagery (e.g. UW-CIMSS TC diurnal cycle IR imagery, 1 km GOES visible, and 37 GHz microwave) and the P-3 LF radar during the mission. Depending on connection rates on the aircraft, supplemental communications via X-Chat with scientists on the ground would be desirable, especially given the unpredictability and rapid evolution of arc cloud features.

Option #1: G-IV aircraft. Once an arc cloud feature has been identified, a GPS dropsonde sequence (preferably running perpendicular to the arc cloud) should be made between the convective area where the arc cloud originated to at least 50 km beyond the leading edge of the arc cloud. Special attention should be paid to the transition zone across the leading edge of the arc cloud and to the environment adjacent to the convective core area where the arc cloud originated (behind the arc cloud). GPS dropsonde spacing should be ~35 km and the transect can be made inbound (sampling in front of, across, and then behind the arc cloud) or outbound (sampling behind, across, and then ahead of the arc cloud) relative to the convective core region of the AEW/TC. In addition to the more common arc cloud that propagates away from the AEW/TC, a second arc cloud has occasionally been observed propagating in toward the AEW/TC. This second arc cloud appears to spawn from the same convective region as the outbound arc cloud and simply moves toward the AEW/TC instead of away from it. If a second inward

propagating arc cloud is identified, the GPS dropsonde sequence should be extended to span the environments ahead of (relative to arc cloud motion) both arc clouds. Figures 21-2 and 21-3 provide example G-IV flight patterns across arc cloud candidates. This option can be easily incorporated into pre-existing flight patterns with minimal additional time requirements.

Option #2: WP-3D aircraft: After an arc cloud feature has been identified, a multi-level flight pattern running perpendicular to the arc cloud should be initiated. The Doppler radar should operate in F/AST mode to permit sampling of the three-dimensional winds throughout any precipitating arc clouds. The *initial* pass should extend between the convection where the arc cloud originated to at least 20 km beyond the leading edge of the arc cloud. Flight altitude should be >3000 m to permit the deployment of multiple GPS dropsondes. Special attention should be paid to the transition zone across the leading edge of the arc cloud and to the environment adjacent to the convection where the arc cloud originated (behind the arc cloud). GPS dropsonde spacing should be ~20 km [reduced to ~10 km spacing closer (≤20 km) to the arc cloud] and the transect can be made inbound (sampling in front of, across, and then behind the arc cloud) or outbound (sampling behind, across, and then ahead of the arc cloud) relative to the convective core region of the AEW/TC.   For the *second* pass, the aircraft should turn and descend to ~1000 m before proceeding back along the same transect extending from the originating convection to at least 20 km beyond the leading edge of the arc cloud. For the *final* pass, the aircraft should again turn and descend to ~500 m before again proceeding along a similar transect across the arc cloud. Flight altitudes for the second and final passes can be adjusted as needed for aircraft safety, but should sample as low as possible in order to capture any near-surface density current with the flight-level sensors. No dropsondes should be deployed on the second and final low-level passes. After the final low-level pass, the primary flight pattern can be resumed.   The total time to complete this option should not exceed 60 min, and in most cases can be completed in less time. Figures 21-2, 21-3, and 21-4 show sample fight patterns for this multi-level option.

Note: If other experiment goals, time constraints, and/or aircraft safety would prevent the low-level passes, this option could be altered to include only the initial pass with the dropsonde deployment sequence at altitudes >3000 m.
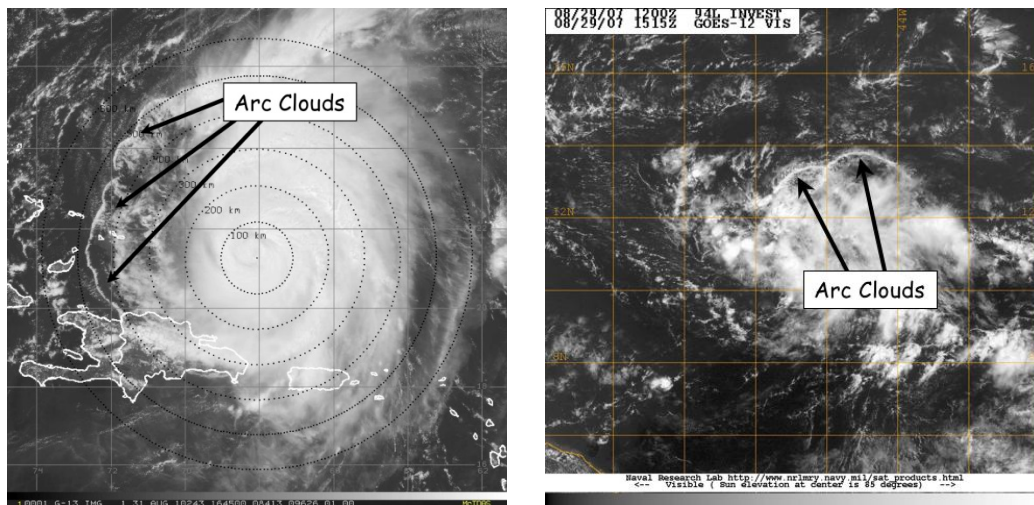
Figure 21-1: *GOES visible satellite imagery showing arc clouds racing away from the convective cores of (left) 2003 Hurricane Isabel and (right) 2007 Pre-Tropical Depression Felix.*
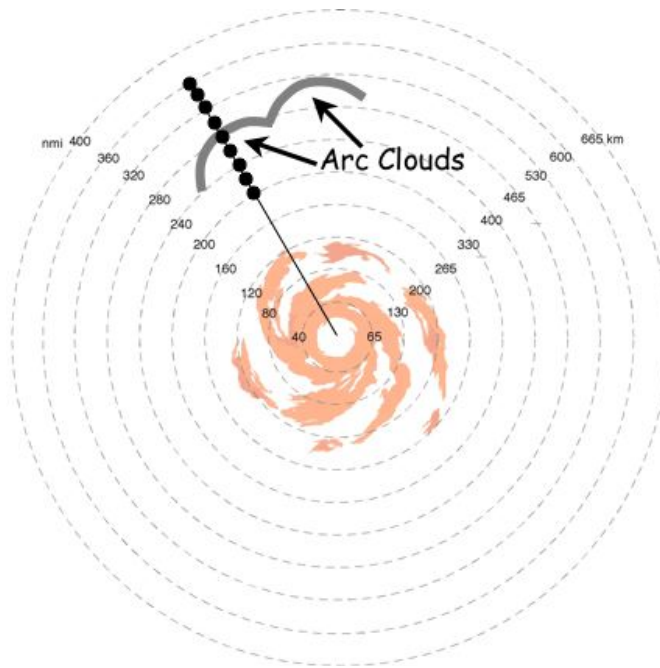
Figure 21-2: The G-IV (or WP-3D) flight track inbound or outbound to/from the TC/AEW. Azimuth and length of GPS dropsonde sequences during G-IV missions will be dictated by the pre-determined flight plan. For these cases, any G-IV flight legs that transect through the trailing and leading edges of the arc cloud are candidates for this module. When multiple arc clouds are present, the feature closest to the pre-determined flight track is desirable.
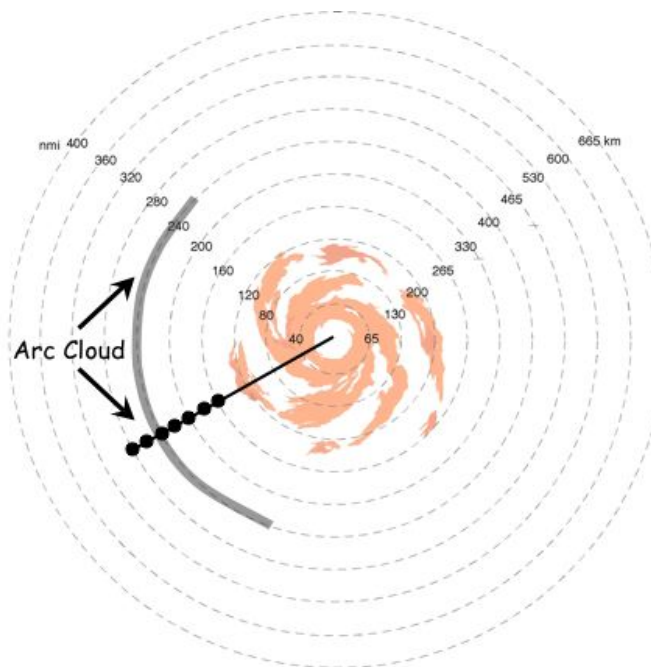
Figure 21-3: The G-IV (or WP-3D) flight track inbound or outbound to/from the TC/AEW. Azimuth and length of GPS dropsonde sequences during G-IV missions will be dictated by the pre-determined flight plan. For these cases, any G-IV flight legs that transect through the trailing and leading edges of the arc cloud are candidates for this module.
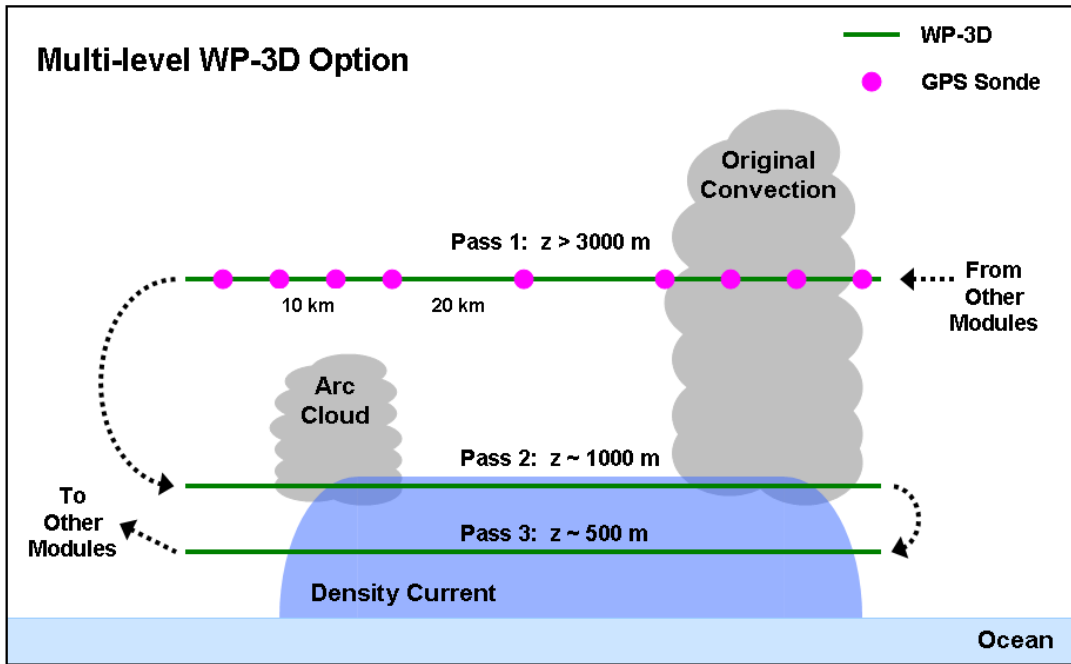
Figure 21-4: *The WP-3D flight track for the multi-level option. Azimuth and length of initial midlevel pass with GPS dropsonde sequence will be dictated by the pre-determined flight plan. Lengths of the low-level passes should span much of the distance between the arc cloud and its initiating convection, while flight altitudes should be near the top and middle of any near-surface density currents (adjusting for safe aircraft operation as needed).*

Analysis Strategy

This experiment seeks to collect observations across arc cloud features in the periphery of AEWs or TCs using aircraft flight-level data, Doppler data and GPS dropsondes to improve our understanding of the physical processes responsible for their formation and evolution, as well as how these features may affect TC structure and intensity in the short-term. The GPS dropsonde data will be used to calculate changes in static stability and possible impacts on surface fluxes both ahead of and behind the arc cloud (e.g. enhanced stability/reduced surface fluxes behind the arc cloud leading edge). Also, kinematics and thermodynamic associated with arc cloud events will also be compared to corresponding locations in model analysis fields (e.g. GFS and HWRF).
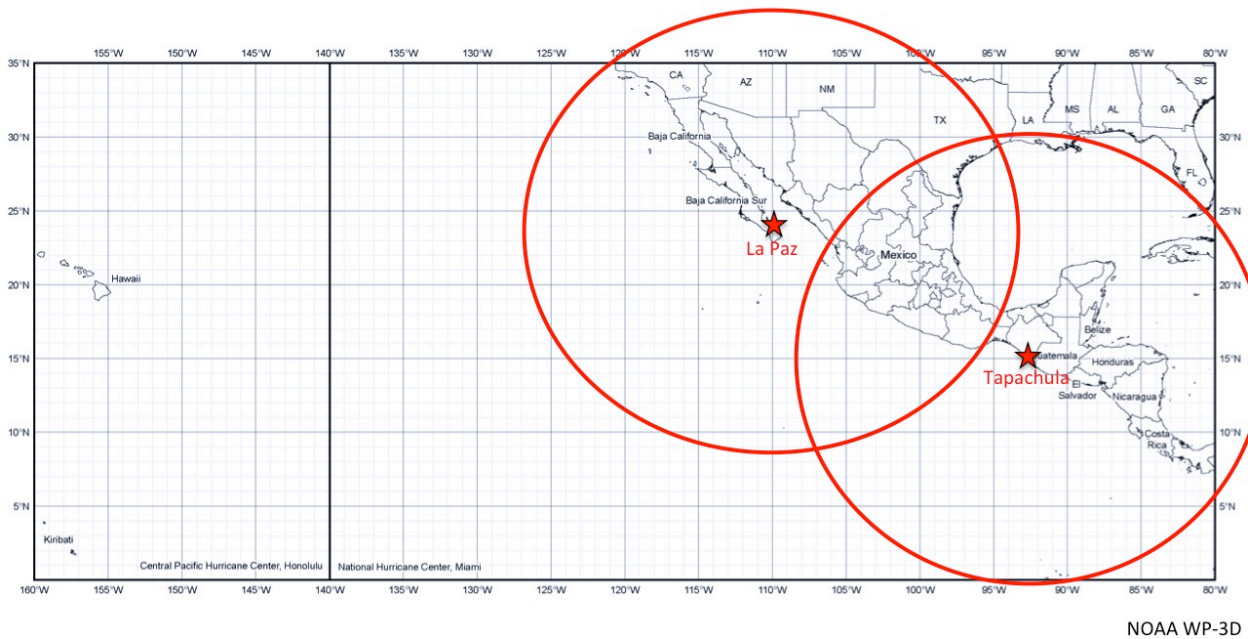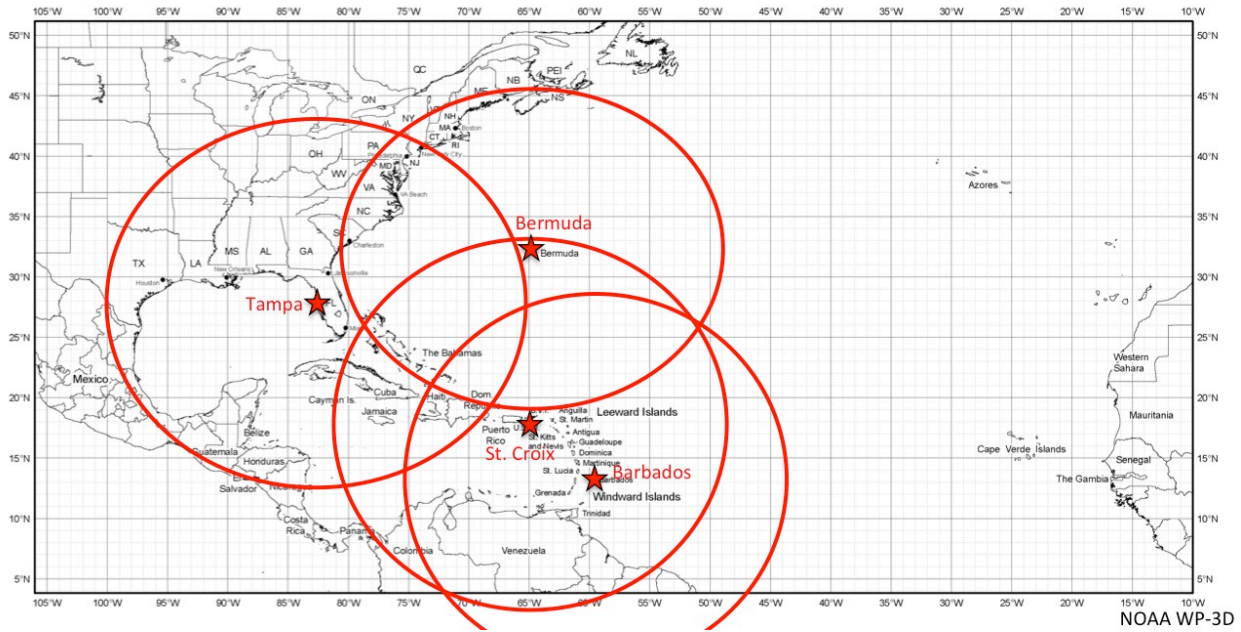
Map 1. Primary Atlantic and East Pacific operating bases and ranges (assuming ~2-h on-station time) for P-3.
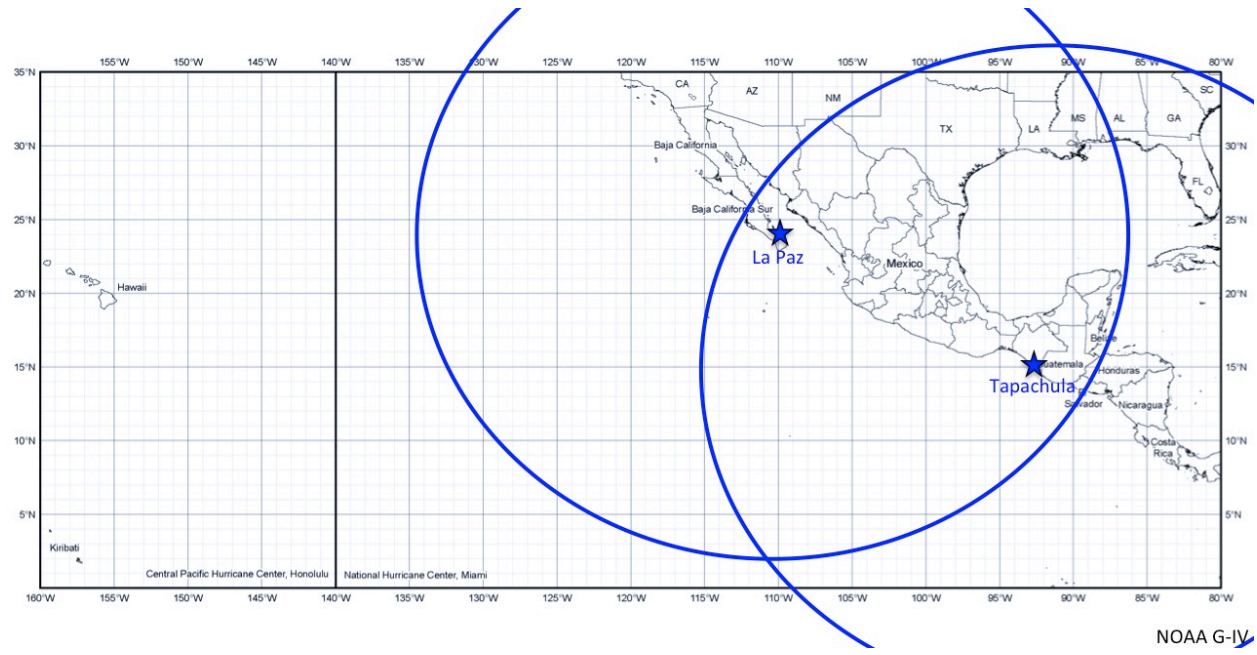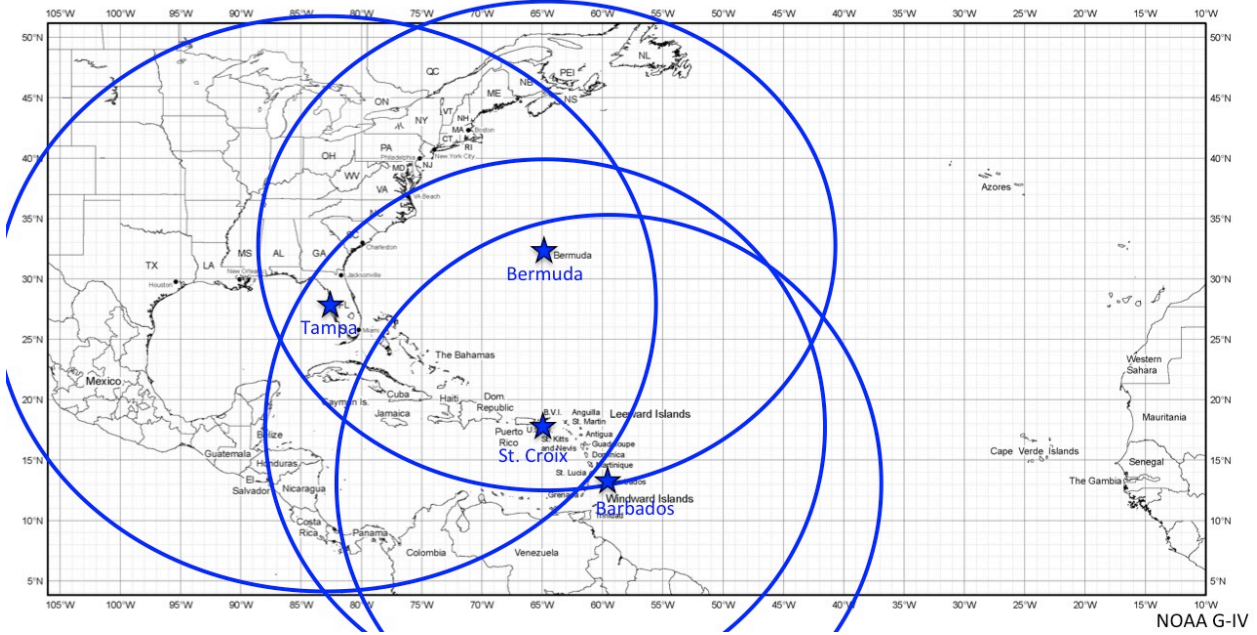
Map 2. Primary Atlantic and East Pacific operating bases and ranges (assuming ~2-h on-station time) for G-IV.
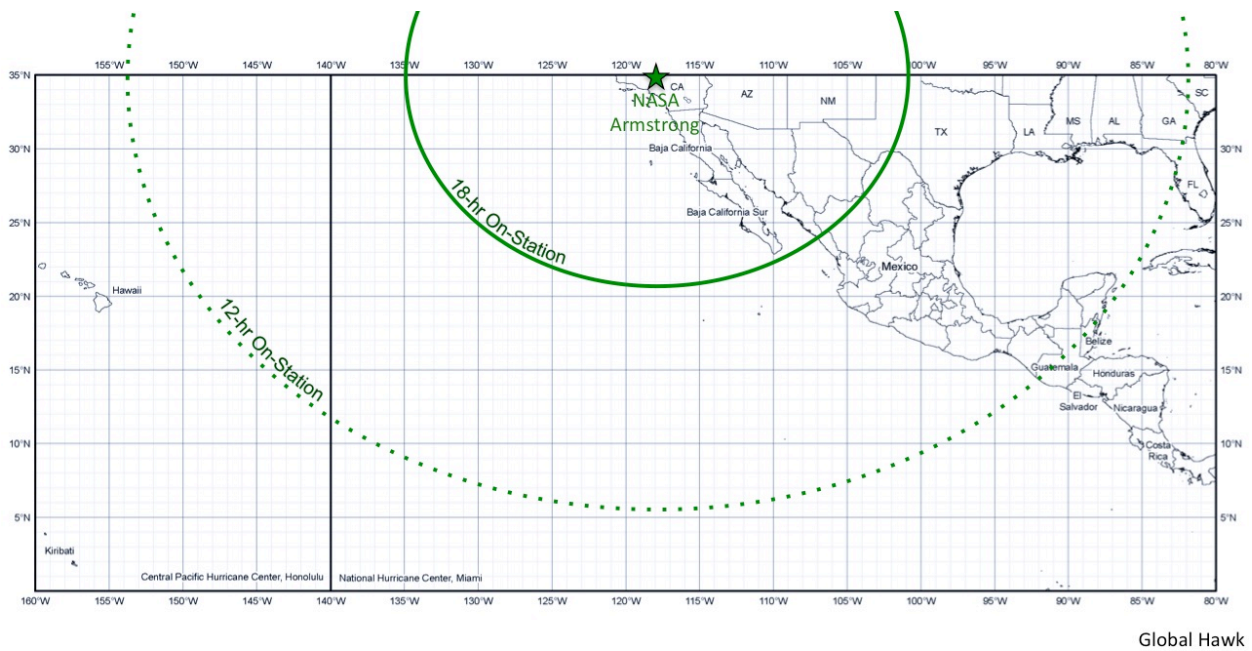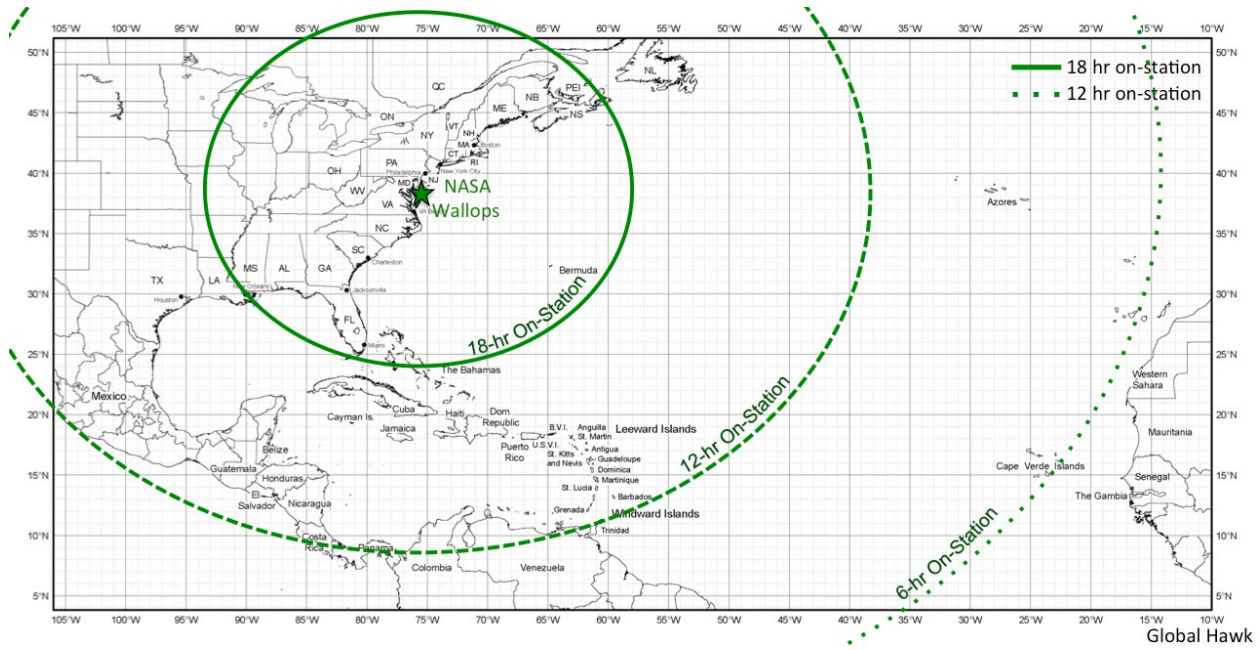
Map 3. Primary Atlantic and East Pacific operating bases and ranges for Global Hawk.